

Enhanced Moisture Sensitivity Study

Mansour Solaimanian
Scott Milander
Xuan Chen
Saman Barzegari
Shihui Shen

Larson Transportation
Institute Penn State University

WisDOT ID no. 092-18-06

September 2019



RESEARCH & LIBRARY UNIT



WISCONSIN HIGHWAY RESEARCH PROGRAM

WISCONSIN DOT
PUTTING RESEARCH TO WORK

TECHNICAL REPORT DOCUMENTATION PAGE

1. Report No. 0092-18-06		2. Government Accession No.		3. Recipient's Catalog No.	
4. Title and Subtitle Enhanced Moisture Sensitivity Study				5. Report Date September 2019	
				6. Performing Organization Code	
7. Author(s) Mansour Solaimanian, Scott Milander, Xuan Chen, Saman Barzegari, and Shihui Shen				8. Performing Organization Report No. LTI 2020-01	
9. Performing Organization Name and Address The Thomas D. Larson Transportation Institute, 201 Transportation Research Building Pennsylvania State University University Park, PA 16802				10. Work Unit No.	
				11. Contract or Grant No. 0092-18-06	
12. Sponsoring Agency Name and Address Wisconsin Department of Transportation Research & Library Unit 4822 Madison Yards Way Madison, WI 53705				13. Type of Report and Period Covered Final Report October 2017 – September 2019	
				14. Sponsoring Agency Code	
15. Supplementary Notes Project Oversight Committee Chair: Erik Lyngdal, Technical Oversight Committee Chair: Dan Kopacz, WisDOT Contact Specialist Senior: Heidi Noble					
16. Abstract The moisture damage susceptibility of four different asphalt concrete mixes from Wisconsin, two with dolomite aggregates and two with siliceous aggregate, was evaluated through laboratory and conditioning testing. One mix was considered a good performing mix and the other three with poor or marginal performance with respect to moisture damage resistance. Moisture conditioning followed existing standards and included freeze/thaw, suction/pressure through Moisture-induced Stress Tester (MiST), and simultaneous effect of water and loading using Hamburg Wheel Tracking Device. Wheel tracking was also conducted on specimens after conditioning with MiST as well as specimens maintained dry without water conditioning. The tests to measure mix properties followed existing standards or provisional standard protocols and included indirect tensile strength test, indirect tensile modulus test, Hamburg wheel tracking test, and ultrasonic pulse velocity test. Based on the results, the laboratory performance of the mixes was ranked with respect to moisture damage susceptibility, and a set of recommendations for establishing pass/fail criteria was developed and presented. MiST conditioning is recommended in case the intention is to evaluate the effect of moisture conditioning on engineering properties of the asphalt mix and when the changes in dynamic modulus of the asphalt mix is intended. Investigating the change in asphalt concrete modulus as a result of moisture damage is of interest as it is one of the major input parameters to the most recently developed performance prediction models. Recommendation is made to use Hamburg wheel tracking for at least medium to high traffic volume roads and continue using AASHTO T 283 for lower volume roads. Recommendation is also made to include criterion on minimum required wet strength in cases where AASHTO T 283 is utilized. This criterion is in addition to the existing criterion on minimum indirect tensile strength ratio (TSR) of the mix.					
17. Key Words Asphalt, moisture sensitivity, moisture damage, wheel tracking, modulus, strength, pulse velocity, indirect tensile strength, indirect tensile strength ratio, modulus ratio, HWTD, MiST			18. Distribution Statement No restrictions. This document is available through the National Technical Information Service. 5285 Port Royal Road Springfield, VA 22161		
19. Security Classif. (of this report) Unclassified		20. Security Classif. (of this page) Unclassified		21. No. of Pages 169	22. Price

Disclaimer

This research was funded through the Wisconsin Highway Research Program by the Wisconsin Department of Transportation and the Federal Highway Administration under Project 0092-18-06. The contents of this report reflect the views of the authors, who are responsible for the facts and accuracy of the data presented herein. The contents do not necessarily reflect the official views of the Wisconsin Department of Transportation or the Federal Highway Administration at the time of publication.

This document is disseminated under the sponsorship of the Department of Transportation in the interest of information exchange. The United States Government assumes no liability for its contents or use thereof. This report does not constitute a standard, specification or regulation.

The United States Government does not endorse products or manufacturers. Trade and manufacturers' names appear in this report only because they are considered essential to the object of the document.

Acknowledgements

This research became possible through financial sponsorship by the Wisconsin Department of Transportation. This financial support is greatly appreciated. We sincerely acknowledge the guidance provided to the research team by the Project Oversight Committee throughout the course of the project. Great assistance from undergraduate students Connor McNerny, Victor Cai, Zachariah Abbas, and Carly-Cliff Derosier is highly recognized with the tremendously demanding task of material processing. We would also like to thank Ms. Xue Wang from Penn State Altoona who helped with wheel tracking tests. Our appreciation is extended to Bloom Companies and Mr. Valbon Latifi for their valuable contribution in working with the aggregate producers with respect to procurement and shipment of materials from Wisconsin to Penn State. Finally, we would like to thank Advanced Asphalt Technologies for their assistance with dynamic modulus testing of specimens.

TABLE OF CONTENTS

1. INTRODUCTION	1
Background	1
Research Objectives	2
Scope of Research	2
2. EXPERIMENTAL PROGRAM	4
Overview	4
Selection of Materials	4
Aggregates	4
Binders	5
Material Processing	6
Mix Design Verification	6
Selection of Tests	8
Evaluation Using Boil Test	8
Evaluation Using AASHTO T 283 Standard and Tensile Strength Ratio	9
Testing with Hamburg Wheel Tracking Device	10
MiST Testing	12
Dynamic Modulus Test	13
Ultrasonic Pulse Velocity (UPV) Test	16
3. FINDINGS AND INTERPRETATION OF RESULTS	23
Boil Test	23
Tensile Strength Ratios	23
Wheel Tracking	25
Wheel Tracking under Wet Condition	25
Wheel Tracking under Dry Condition	26
Wheel Tracking of MiST Conditioned Specimens	27
Dynamic Modulus	28
Ultrasonic Pulse Velocity	32
Tests on unconditioned samples (Condition 1)	32
Tests on unconditioned samples, after measurement of G_{mb} (Condition 2)	33
Tests on unconditioned samples, after the first IDT DM test (Condition 3)	33
Tests on moisture-conditioned samples (Condition 4)	34
Tests on moisture-conditioned samples, after the second IDT DM (Condition 5)	35

Comparison of the results with IDT DM results.....	39
Moisture Damage Mitigation.....	41
Summary of Results.....	46
4. SUMMARY, CONCLUSIONS AND RECOMMENDATIONS	49
Summary	49
Conclusions	50
Recommendations.....	50
Selection of Test Protocol and Conditioning	50
Establishing Criteria.....	51
References	R-1
Appendix A - Gradations and JMF	A-1
Appendix B - Examination of Effect of Water on Asphalt Mix and Coated Aggregate	B-1
Appendix C - Results from Indirect Tensile Test	C-1
Appendix D - Results from Hamburg Wheel Tracking Test.....	D-1
Appendix E - Results from Dynamic Modulus Test.....	E-1
Appendix F - Results from Ultrasonic Pulse Velocity Test	F-1

LIST OF FIGURES

Figure 1 Wisconsin map: Locations of aggregate sources are shown in bold.	5
Figure 2 Different creep zones for a typical load-deformation test	11
Figure 3 Picture of MiST with lid secured ready for conditioning specimens	12
Figure 4 Specimen before MiST conditioning (L) and after MiST conditioning (R).....	13
Figure 5 Dynamic modulus test in IDT mode configuration: (a) front view and (b) side view (AASHTO TP 131-18).....	15
Figure 6 Average air void distribution for DM specimens	16
Figure 7 UPV test setup used in the study	17
Figure 8 Propagation of (a) compressional waves and (b) shear waves in a medium	18
Figure 9 Sample compressional wave signal output after a UPV test	18
Figure 10 Sample shear wave signal output after a UPV test.....	19
Figure 11 Location of measurements on test samples	20
Figure 12 Conducting UPV measurements on a 60-mm asphalt concrete sample: (a) compressional wave and (b) shear wave.....	20
Figure 13 Results from indirect tensile test, average of three replicates reported	24
Figure 14 Performance of Menasha mix tested in HWTD under submerged condition.....	26
Figure 15 Performance of Menasha mix in HWTD under dry testing condition.....	27
Figure 16 Performance of Menasha mix in HWTD tested dry after MiST conditioning	28
Figure 17 Average dynamic modulus of asphalt specimens before conditioning (25 °C).....	29
Figure 18 Indirect dynamic modulus and modulus ratio comparison for Rock Springs.....	30
Figure 19 Indirect dynamic modulus and modulus ratio comparison for Olsen.....	30
Figure 20 Indirect dynamic modulus and modulus ratio comparison for Waukesha.....	31
Figure 21 Indirect dynamic modulus and modulus ratio comparison for Menasha.....	31

Figure 22 Modulus ratio and tensile strength ratio comparison.....32

Figure 23 Comparison of moduli at different stages of UPV testing (stacked based on condition).....37

Figure 24 Comparison of moduli at different stages of UPV testing (stacked based on source).....37

Figure 25 Modulus after freeze/thaw conditioning (condition 5) versus initial modulus.....38

Figure 26 Modulus after MiST conditioning (condition 5) versus initial modulus38

Figure 27 Comparison between effect of freeze/thaw and MiST conditioning on moduli (Condition 5)39

Figure 28 Comparison of the modulus ratio of UPV and IDT DM based on the conditioning technique.....40

Figure 29 Comparison of modulus ratio from UPV and DM tests for MiST-conditioned specimens.....40

Figure 30 Comparison of modulus ratio from UPV and DM tests for freeze/thaw conditioned specimens.....41

Figure 31 Performance of Rock Springs mix after modification with P75 antistripping agent.....43

Figure 32 Results from HWTD for the Menasha source with PG 64-22.....44

Figure 33 Results from HWTD for the Waukesha source with PG 64-22.....44

Figure 34 Results of HWTD test under wet conditions with local limestone at 46 °C with PG 58-28WF
and PG 64-2245

LIST OF TABLES

Table 1 Aggregate Stockpiles Received for Each Source.....	5
Table 2 Data Related to Mixes Used in this Research.....	8
Table 3 Volumetric Parameters at Design for the Researched Mixes	8
Table 4 Tests Conducted on Asphalt Concrete Specimens.....	9
Table 5 Summary of conditioning methods used for asphalt concrete specimens.....	21
Table 6 Results from Conducting Moisture Damage Tests using three different procedures based on AASHTO Standard T-283.	24
Table 7 Test Results from HWTB Test.....	25
Table 8 Summary of modulus of elasticity for the four aggregate sources (dry and no water conditioning).....	33
Table 9 Summary of Modulus of Elasticity after <i>Gmb</i>	33
Table 10 Summary of modulus of elasticity for the four aggregate sources after the first IDT DM test	34
Table 11 Effect of different conditioning techniques on the estimated moduli after the first IDT DM Test	34
Table 12 Effect of different conditioning techniques on the estimated moduli after the second IDT DM Test	35
Table 13 Effect of water removal on the estimated moduli of MiST conditioned specimens.....	36
Table 14 Effect of water removal on the estimated moduli of freeze/thaw conditioned specimens.....	36
Table 15 Effect of Liquid Antistrip on Moisture Damage Resistance for Rock Springs Aggregate.....	42
Table 16 Effect of Binder Grade on HWTB Test Results	43
Table 17 HWTB Test Results with a Local Limestone Aggregate and Two Different Binders	45
Table 18 Results of HWTB Test with Menasha Aggregate under Different Conditions 46°C).....	46
Table 19 Ranking of Mixes with respect to Moisture Damage Susceptibility.....	47
Table 20 Summary of Materials, Tests, and Response Parameters in this Study	49
Table 21 Using Combination of TSR and Wet Strength as Pass/Fail Criteria.....	51
Table 22 Conceptual Criteria based on HWTB Test in Submerged Condition.....	52

This page intentionally left blank

CHAPTER ONE

Introduction

BACKGROUND

Asphalt pavements are inevitably subject to ingress of water. Prolonged exposure of these pavements to water, sometimes due to inadequate drainage, can result in premature failure of the pavement. Moisture damage occurs either through loss of adhesion between asphalt and aggregate (i.e., stripping of asphalt from aggregate) or due to cohesive failure of the binder itself (Hicks, 1991). Both phenomena contribute to reduction in strength or stiffness of the asphalt concrete layer. The reduction in stiffness contributes to the development of various forms of pavement distresses. An ongoing challenge exists with establishing proper testing protocols and specifications to minimize the potential for moisture damage of asphalt pavements.

Numerous laboratory tests have been investigated and developed over the years toward the design of moisture-damage-resistant asphalt mixes. The developed tests can be subdivided into two main categories: qualitative and quantitative. The qualitative tests include boil test, freeze/thaw and pedestal test, quick bottle test, rolling bottle method, and many others (Solaimanian et al. 2003). The quantitative tests include immersion compression tests, indirect tensile test, Marshall immersion test, double punch method, resilient modulus tests, Hamburg wheel tracking test, moisture-induced stress test, and several others (Solaimanian et al. 2003). The great number of different aggregate types and the numerous types of unmodified and modified asphalt binders used across the United States, coupled with varied environmental conditions, traffic, and construction practices, have made testing to accurately predict asphalt concrete moisture susceptibility a difficult task. It has remained a challenge to the pavement industry to improve the current moisture damage tests and enable better and more reliable distinction between poor and good performing asphalt mixes.

Review of the literature on moisture-induced damage tests indicates that a better alternative to the traditional AASHTO T 283 is deemed necessary by many state agencies and researchers. A number of different candidates have been researched during the past decade, including: dynamic modulus, tension-compression fatigue, Hamburg wheel tracking device (HWTD), Moisture-induced Stress Tester (MiST), flow number, and indirect tensile stiffness and strength tests. These studies generally featured a range of moisture-conditioning schemes, including dry, water bath, single freeze/thaw cycle, multiple freeze/thaw cycles, MiST, submersion during the test, long exposure to water (up to 70 days), and environmental conditioning. From the literature it can be concluded that the AASHTO T 283 cannot simulate the actual action of water as it happens during the service life of flexible pavements. The monotonic nature of loading in this test prevents obtaining sufficient information about the rate of moisture-induced damage progression

under cyclic loading. Under this literature review, the HWTD test and MiST were found to be among the most promising options to replace the current practice of moisture sensitivity evaluation. However, results of recent surveys indicate that DOTs and contractors are currently more inclined to use HWTD tests rather than MiST. A possible advantage of the HWTD test could be its applicability for rutting evaluation of the mixes at the same time the mix is exposed to water conditioning.

With regard to the tests on the mixture constituents, the surface free energy measurement technique seems to be an effective screening tool for determining the compatibility of binders and aggregates. Binder testing, especially when modified with an anti-strip additive, is always an effective way of identifying any adverse effect that the use of an additive might have on the rheological behavior and stability of the binders.

The Wisconsin Department of Transportation (WisDOT) has been among the most active state highway agencies in seeking improved testing protocols and specifications to address moisture damage of asphalt pavements. WisDOT's commitment in this respect is clearly manifested through the number of research projects it has funded with respect to various aspects of moisture damage of pavements. The research project discussed in this report is the most recent sponsored by the Department toward the improvement of existing test protocols and specifications.

RESEARCH OBJECTIVES

The overall goal of the project was to determine a reliable testing protocol for use by the Wisconsin Department of Transportation and develop recommendations regarding moisture sensitivity testing of asphalt concrete mixtures in Wisconsin. To achieve this goal, several objectives were pursued:

1. Identify the proper moisture sensitivity test method or suite of practical tests (along with the associated conditioning practices) that can be representative of the field performance of mixes.
2. Identify test methods capable of evaluating the effectiveness of moisture susceptibility treatments such as application of anti-stripping agents or modifications made to the mix design.
3. Correlate the laboratory evaluation results to the field performance in regard to moisture damage potential.
4. Revise the existing specifications or develop a guide specification if needed to reduce the risk of moisture damage.

SCOPE OF RESEARCH

The research was conducted for a period of 22 months, from October 2017 through August 2019, at the Northeast Center of Excellence for Pavement Technology (NECEPT) at Penn State. The initial task of the research included a comprehensive literature review of pertinent past research and specifications. This literature review was used to develop a laboratory testing plan and analysis to address the goal of the research. The laboratory work included a battery of moisture conditioning and mechanical tests to evaluate the moisture damage resistance of the selected research materials. Four different mixes were identified by

the Project Oversight Committee (POC) to be included in this research. The selection was based on laboratory test results as well as field performance. Two aggregates were dolomite based and two siliceous based.

Four different moisture conditioning schemes were exercised in this research following relevant AASHTO or ASTM standards: (1) vacuum saturation followed by freezing and hot water conditioning (AASHTO T 283), (2) vacuum saturation followed by hot water conditioning (AASHTO T 283), (3) MiST conditioning (ASTM D7870), and (4) submerged load-induced conditioning (AASHTO T 324). The effect of these conditioning schemes was assessed by measuring three properties: (1) indirect tensile strength, (2) indirect tensile dynamic modulus, and (3) rut depth under repeated wheel passes. A full matrix of testing was completed for all four aggregate sources. Based on the results from the full matrix comprehensive study, a moisture damage mitigation study was undertaken. Results were summarized, conclusions were drawn, and recommendations were made for improvement of specifications based on the findings.

CHAPTER TWO

Experimental Program

OVERVIEW

The core activity of this research was the selection and execution of a suitable set of conditioning and mechanical tests on specific materials selected to achieve the project objectives. The project required the development of an experimental plan for this purpose and approval of this plan by the Project Oversight Committee. The plan was developed based on the results from the literature review and submitted to the POC in March 2018. Execution of the plan began in April upon approval by the POC, even though because of time constraints, procurement and processing of materials as well as preliminary material characterization were initiated while the experimental plan was under development.

SELECTION OF MATERIALS

Materials for this research were selected based on discussions between the research team and the POC. The materials were selected by the POC in light of the project objectives.

Aggregates

Aggregates came from four different quarries known as the Menasha, Waukesha, Rock Springs, and Olsen quarries. The locations of the aggregate sources are presented in Figure 1. The Menasha and Waukesha aggregates are described as dolomite (dolostone) with some limestone. These two sources are in the central east and southeast of Wisconsin, respectively. The Menasha aggregate was selected because in the laboratory tests it had demonstrated a low tensile strength ratio (TSR) when tested to evaluate the moisture damage resistance, while the Waukesha aggregate was selected because it had exhibited high TSR. The aggregates from Rock Springs and Olsen, both siliceous based, were selected based on their field performance. The sources of these two aggregates were Rock Springs, centrally located, and Chippewa Falls and Downing, in the western part of the state, respectively. In at least one observation, these two aggregates had shown marginal or poor performance after 11 years of service.

The materials were received either in canvas bags or in 5-gallon plastic containers. Accompanying the material from each source was the asphalt binder, received either in 5-gallon containers or quart cans. The stockpiles received for each source are presented in Table 1. Containers of reclaimed asphalt pavement (RAP) and recycled asphalt shingles (RAS) were also shipped to the research facility in canvas bags or 5-gallon containers.

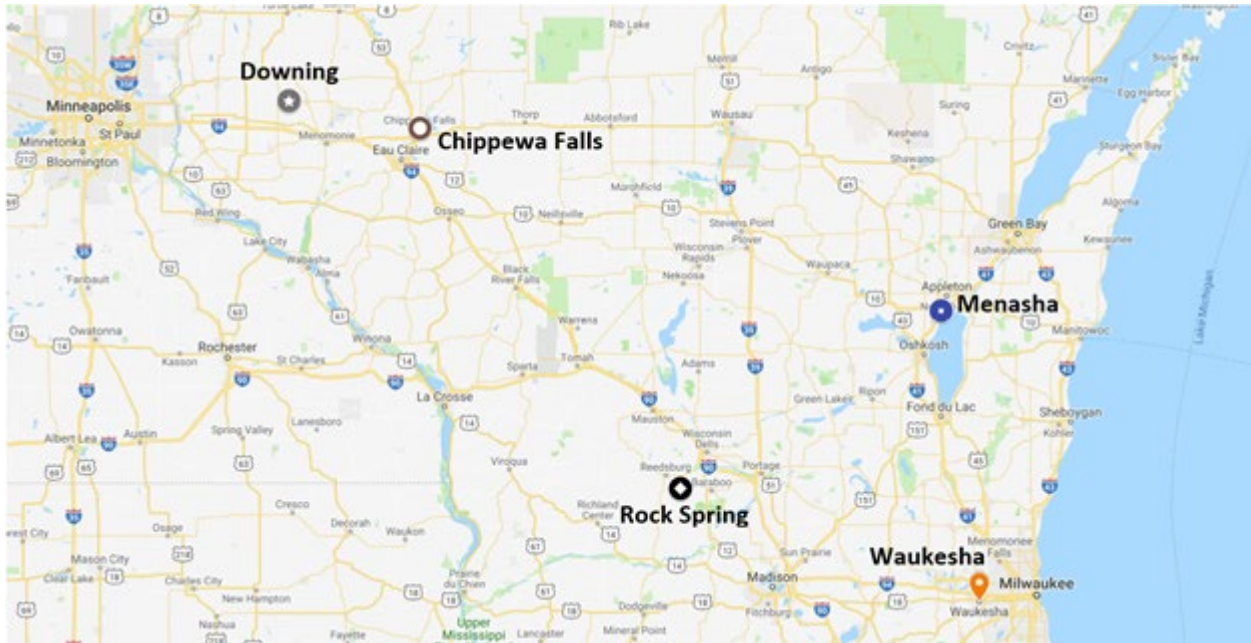


Figure 1 Wisconsin map: Locations of aggregate sources are shown in bold

Table 1 Aggregate stockpiles received for each source

		Stockpiles			
Aggregate Source	Menasha	Manufactured Sand	Natural Sand	1/2" Chip	5/8" Chip
	Waukesha	Manufactured Sand	Natural Sand	3/8" Chip	5/8" Chip
	Rock Springs	5/8" Screened Sand	1/4" & 3/16" Man. Sand Combined	3/8" Chip	3/4" Crushed Gravel
	Olsen	3/8" Screenings	3/8" Screened Sand	3/8" Bit	3/4" Bit

Binders

Four binder grades were received for this project. Binders designated as PG 58-28, 58-28F, and 58-28WF were received along with the aggregates from the Menasha and Waukesha sources. It must be noted that the designations “F” and “WF” at the end of the binder PG number are used to distinguish between the binders, as that is how the binders were labelled when received. These designations do not refer to specific grading of the binders the same way that the terms “S”, “H”, and “V” are used. Binders designated as 58S-28 accompanied aggregates received from the Olsen and Rock Springs sources. The boil test, discussed later,

was conducted as a screening test to choose one of the three binder sources for use with the Menasha and Waukesha aggregates.

Material Processing

A major activity of the research was processing of the materials received. Processing consisted of dry and washed sieve analysis of representative samples from each stockpile (AASHTO T 27 and T 11, respectively), sieving aggregates of each stockpile on individual sieves, and storing the materials for each sieve size in bins. Sieve analysis was conducted to determine the particle size distribution of each stockpile from each source through both wet and dry methods. Approximately 4,000 lb of materials were sieved and stockpiled, requiring a considerable level of time and resources. At times, a shortage of materials was noticed due to discrepancy between the gradation of as-received material and the JMF-reported gradation for all four sources. Under these conditions, through coordination with the source and the project subcontractor (Bloom Companies, LLC), additional material was received and processed.

Gradation of the RAP material for Menasha, Rock Springs, and Waukesha was determined using ignition oven (AASHTO 308) and solvent extraction. Among the four sources, Menasha was the only source indicating use of RAS along with RAP. Gradation of RAS particles was also determined using ignition oven.

Mix Design Verification

An important activity was verification of the designs as presented in the job mix formulas. The exception was the Olsen mix, for which adjustment to proportions of stockpiles was needed to establish a mix design with no RAP content. The gradations finalized for each mix are provided in Appendix A.

The research team noticed that the material received from the Olsen plant was significantly different from the gradation indicated in the original JMF received from WisDOT. Therefore, through coordination with the Project Oversight Committee, an updated version of the JMF was received. After comparing the results of sieve analysis performed in the lab with those from the old and new JMFs, it was concluded that the aggregates from Olsen complied better, but not completely, with the new JMF. However, the new JMF indicated the use of RAP, which was not part of the old JMF, and hence was not shipped to NECEPT. Although the material received as 3/4" bit, 3/8" bit, and 3/8" screened sand was generally in compliance with the new JMF, the gradation of the material designated as 5/16" in JMF was substantially different from the material received. To resolve this issue, the research team washed the materials retained on standard sieve #4 to obtain the desired gradation for the 5/16" for Olsen. Yet another issue with this source was the angularity and fractured face of the particles. Hence, the fractured face count was conducted according to ASTM D5821. For the coarse aggregate, combined from all stockpiles, the average percent of one face fractured was 81%, and for two or more faces fractured it was 72%. According to Superpave specification M 323, these values satisfy fractured face requirements for a surface mix for design traffic level of 0.3 to 3 million

ESALs (equivalent single axle loads). The level of fractured face does not satisfy the requirements for a surface mix at higher traffic levels. For example, for a traffic level of 3 to 10 million ESALs, the requirement is 85 and 80 percent, for one face and two or more faces fractured, respectively.

Since no RAP was received for the Olsen source (even though the JMF included RAP), several options were considered at the time: (1) request RAP from the source, (2) use RAP locally available at NECEPT, and (3) do not use RAP. After discussion with the POC, the decision was made to continue using the Olsen mix without inclusion of RAP, as that might provide a base in comparison with other sources for which RAP was part of the mix. Therefore, for the Olsen mix, the RAP material reported in the JMF was replaced by the aggregates received from this source. Attempts were made to proportion the aggregate stockpiles in a way to be close to the JMF gradation. For the Olsen aggregate, the original work was carried out with a finer mix, closer to the JMF gradation. To improve the design and volumetrics, a coarse gradation was adopted and used for further testing. For the Olsen aggregate, as the gradation and material were different from the JMF, the specific gravity of the aggregate was determined according to AASHTO T84 (fine aggregate) and AASHTO T85 (coarse aggregate), and the specific gravity of the combined gradation was used for further calculations. Comparison of bulk specific gravity (G_{mb}) from the aggregate tests and backcalculated effective specific gravity from mix maximum theoretical specific gravity (G_{mm}) indicated unreasonably large differences. The effective gravity, calculated from G_{mm} , was verified to be accurate, implying that the results from AASHTO T84 were heavily influenced by the material passing #200 sieve. As a result, the fine aggregate specific gravity test was repeated using the washed sieve material and after removing the material passing #200 sieve.

The approach for verification of mix design was through generating gyratory compacted specimens at design number of gyrations and design asphalt content as reported in the received job mix formula and using recommended mixing and compaction temperatures in the JMF (Table 2). Bulk specific gravity of compacted specimens was determined, paralleled with determination of G_{mm} of the loose mix for each for each source. Table 3 provides a summary of mix volumetrics at the design number of gyrations for each mix. Multilaboratory precision estimates provided in AASHTO T 312 for 12.5-mm mixes indicate a d2s limit of 1.7%. Difference "Two" Standard Deviation Limit (d2s), also known as 95% limit on the difference between two test results, indicates that approximately 95% of all pairs of test results from different laboratories can be expected to differ in absolute value by less than 2.77s, where "s" is standard deviation. Therefore, the air void levels obtained through the verification step were within the acceptable range in comparison with the values reported in the JMF.

Table 2 Data related to mixes used in this research

Source	NMAS mm	Binder PG	Total Binder Content %	Virgin Binder Content %	% RAP	% RAS	Mix Temp. °C	Comp. Temp. °C	Design No. of Gyations
Menasha	12.5	58S-28	6.0	4.6	23	2	148	140	40
Waukesha	12.5	58S-28	5.8	4.6	29	0	148	140	75
Rock S.	12.5	58-28WF	5.1	4.3	20	0	148	140	75
Olson	12.5	58-28WF	5.6	5.6	0	0	148	140	75

Table 3 Volumetric parameters at design for the researched mixes

		Menasha	Waukesha	Rock Springs	Olsen
Parameter	Design Gyations	40	75	75	75
	Virgin Binder, %	4.6	4.6	4.3	5.60
	Total Binder, %	6.0	5.8	5.1	5.6
	G _{mm}	2.468	2.500	2.470	2.515
	Air Void, %	3.6	3.2	3.4	3.9
	VMA, %	16.6	15.8	14.6	15.4
	VFA, %	78.6	79.7	76.7	75.2

Selection of Tests

Several test protocols were selected for this research. Selection was made based on the original proposal and results of the literature review (Task 1) and presented in the experimental program of Task 2. Table 4 presents a list of all asphalt concrete tests that were conducted for this research and the reason for their selection.

Evaluation Using Boil Test

Three different binders were received for the Menasha and Waukesha sources. Through coordination with the POC, it was decided to conduct a screening test to select the most appropriate binder for these two sources. A full matrix of boil testing was exercised using all four binders with materials from all four sources. Gradation closely matching job mix formula was applied for each case. Details of the boil test and the results are presented in Appendix B of this report. Final rating was assessed as an average value based on visual observation by three individuals. Bearing in mind that the results from the boil test are subjective in nature, no apparent incompatibility was found among the aggregates and binders, as the ratings averaged above 8 (out of 10) for all cases. A rating of 10 was considered an excellent adhesion. The results of this investigation were communicated with the POC chair. As a result of the discussion, it was decided to use 58-

28WF for the Menasha and Waukesha sources, as it is more readily available, and use the PG 58S-28 with the Olsen and Rock Springs sources, for which the binder was originally targeted. Additional boil tests were conducted at a later stage of the research using the coarse portion of the aggregates only (Appendix B). Results are discussed in the next chapter.

Table 4 Tests conducted on asphalt concrete specimens

Test	Standard	Purpose and Reason for Selection
Indirect Tensile Strength Test on Freeze/Thaw Conditioned Specimens	AASHTO T 283	Assess moisture damage resistance based on a widely used test protocol as the benchmark.
Hamburg Wheel Tracking Device (HWTD)	AASHTO T 324	The Hamburg Wheel Tracking test has been researched and is under serious consideration by several state highway agencies including Wisconsin.
Conditioning through Moisture Induced Stress Tester (MiST)	ASTM D 7870 plus Adhesion	MiST provides conditioning through suction/pressure of water into the specimen porous space, a process which simulates field conditions and is absent in the AASHTO T 283 protocol.
Dynamic Modulus	AASHTO TP 131	When tested on both dry and conditioned specimens, provides a measure of retained modulus, an engineering property which is an input to the <i>Mechanistic-Empirical Pavement Design Guide</i> .
Ultrasonic Pulse Velocity	ASTM C 597	Conducted on dry and conditioned specimens to determine if a quick nondestructive test such as UPV could provide reliable assessment of moisture damage in asphalt concrete.

Evaluation Using AASHTO T 283 Standard and Tensile Strength Ratio

AASHTO Standard T 283 was adopted as the reference testing system for moisture damage evaluation. This is the most widely used protocol by state highway agencies. Three different types of tests were conducted under this system. Two of the methods followed T 283 specimen preparation and testing procedures strictly, with one group undergoing one cycle of freeze at -18 °C followed by hot water conditioning at 60 °C, after vacuum saturation of specimens, and the other group was only subjected to hot water conditioning with no freeze, again after vacuum saturation. The original proposed plan for testing according to AASHTO T 283 included only the 95-mm-thick specimens with the freeze option. At the interim presentation of April 2018, the Project Oversight Committee recommended adding the no-freeze protocol, as that is the protocol used by Wisconsin DOT.

A modified version of the protocol was also conducted using the freeze option but using 60-mm-thick specimens. The 60-mm-thick specimen was used to make it possible for direct comparison of results with those obtained from disk-shaped specimens tested in dynamic modulus and Hamburg Wheel Tracking Device (HWTD). The disk-shaped dynamic modulus specimens and HWTD specimens were 60-mm thick.

Testing with Hamburg Wheel Tracking Device

Testing under Wet Conditions

AASHTO T 324 was followed for testing the specimen's resistance to moisture damage under wheel tracking. Testing was conducted on specimens when submerged in water at 46 °C and under 22,000 wheel passes. Replicate specimens were prepared using the gyratory compactor. The specimens were trimmed at the sides and were paired to deliver the required track. Two tracks were generated out of four compacted specimens.

Testing under Dry Conditions

The idea behind testing dry specimens using the HWTD was to determine how much of the damage could be attributed to the water effect, as some damage to the specimen is likely to occur simply because of loading, even in the absence of water. Such distinction is possible only through testing specimens under the same conditions but exposing one set to a dry testing environment and submerging another set in water while loading. The dry testing was completed for all four sources of material.

Investigating Temperature Control for Testing of HWTD under Dry Conditions

The major challenge faced was controlling temperature at 46 °C for dry testing. Dry testing was undertaken after modifications were made to the test equipment and temperature could be controlled within 46 ± 1 °C. The temperature control hood provided by the manufacturer was utilized and installed following the manufacturer's recommended installation guide. Originally, temperature fluctuation was within a range of 2 to 3 °C despite using the manufacturer's hood and the recommended procedure. The fluctuation was not believed to be the result of any manufacturing defect; rather it seemed to be an issue of the system's capability and accuracy.

Dummy specimens were prepared and subjected to HWTD loading under dry condition for a period of 5 hours. The machine temperature was set at 46 °C and a Campbell Scientific CR23X micrologger was utilized to record the temperature. Three thermocouples were used: one at the center of the device and the other two at the two ends, close to the specimens. Data were collected at a frequency of one data point per minute. Data collection was conducted while load tracking the specimens under dry conditions. This scheme of temperature measurement and testing provided data based on which adjustments were made to the machine to ensure temperature control within the target range. Adjustments included the addition of very small circulation fans inside the HWTD test chamber. Improvement was made to the machine temperature distribution by adding two small fans to the air circulation system. This effort helped bring the temperature fluctuation to within ± 1 °C. For reference, when testing under submerged conditions AASHTO T 324 requires temperature control within ± 1 °C. AASHTO T 324 does not provide any criteria for the temperature

range when testing under dry conditions. As no standard test protocol exists for testing specimens under dry conditions, the same temperature criteria used for wet conditions were applied to dry conditions.

Interpretation of HWTD Test Results

The graph of a typical deformation-time curve delivers three segments: initial (primary) creep, secondary creep, and tertiary creep (Figure 2). The initial creep defines the early stage of deformation, which typically occurs within a limited number of cycles. The secondary creep is a more stable part of deformation, which defines the progress of rutting with increasing number of passes linearly and typically carries a significantly larger number of cycles compared with the initial creep. Finally, the tertiary creep begins when the mix has become unstable and is showing a significant rate of deformation as time progresses. In this report, the point of intersection of the slopes from secondary and tertiary creeps is defined as the inflection point for tertiary creep. In case of testing under water, this point is defined as the stripping inflection point. There are several distinguishing parameters that can be derived from the HWTD test and used in this research: maximum rut depth (i.e., rut depth at the highest number of wheel passes), stripping or tertiary creep inflection point (SIP or TIP), ratio of stripping slope (or tertiary creep slope) to secondary creep slope, number of wheel passes to reach 10 mm of rut depth, rut depth after completion of 10,000 wheel passes, and finally the stripping slope in terms of rut depth for 1,000 wheel passes. All of these parameters have been extracted from the test results and presented in the next chapter.

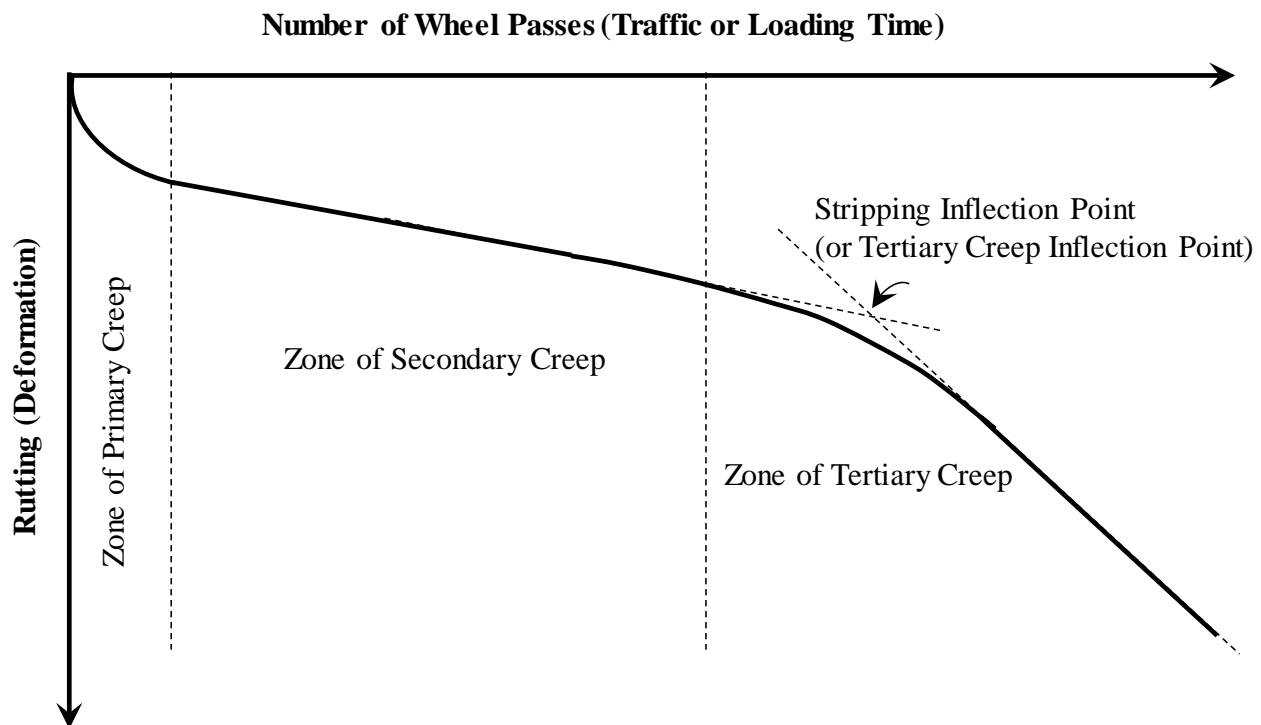


Figure 2 Different creep zones for a typical load-deformation test

MiST Testing

MiST was one of the main conditioning protocols utilized for this project (Figure 3). The standard protocol is covered under ASTM D7870. There is an AASHTO provisional test method, drafted in 2017, which had not yet been standardized at the time of this writing. The major difference is that the AASHTO version has an extra aspect of conditioning referred to as “adhesion conditioning.” This conditioning is for 20 hours at the same temperature as the cyclic conditioning and is done first. Previous work, as reported by the equipment manufacturer, has indicated that the pumping action is more suited to capture the cohesion effect (binder susceptibility to moisture damage) than the adhesion effect (the bond between the binder and the aggregate). Furthermore, parallel to this research, WisDOT has been conducting MiST with the adhesion conditioning. Therefore, MiST testing with the extra 20-hour conditioning time was selected for this research, as it makes it possible to compare the test results from this research with those from WisDOT, if needed. MiST testing was conducted at 46 °C so that the results could be compared with the test results from the HWTD tests.



Figure 3 Picture of MiST with lid secured ready for conditioning specimens

During this project a total of 28 specimens were conditioned using the MiST. Before conditioning, the bulk specific gravity of each specimen was measured.

Afterwards, sets of two or three specimens were placed inside the MiST chamber, each on a base plate separated by spacers (Figure 4). This step was followed by filling the chamber with water and securing the lid. After deairing the chamber, the 20-hour adhesion conditioning was started once the water temperature was within 10 °C of the setpoint (46 °C). Upon completion of adhesion conditioning, the cyclic conditioning was initiated under a pressure of 40 psi. It took roughly 3.5 hours to apply the required 3,500 suction/pressure cycles. Upon completion of the test, water was drained from the chamber into a clean bucket for visual observation of any material that may have been removed from the specimens during the conditioning cycles. The water for all sets of MiST-conditioned specimens for this project was clean and clear, indicating no loss of material during conditioning. After draining the warm water, cool water was poured inside the chamber to cool the specimens for several minutes before removal. After removing the specimens, each was tested immediately to determine the G_{mb} and G_{mb} swell index. The G_{mb} swell index is the percent change in bulk specific gravity before and after conditioning. The swell index was considerably low for all of the specimens tested in this research. The MiST-conditioned specimens were placed in front of fans to air dry after measuring their bulk specific gravities and before further testing. The specimens were

also subjected to CoreLok suction to remove water to the extent possible. It must be noted that drying specimens that have been subjected to MiST conditioning or vacuum saturation is very different from drying specimens that have been simply placed in water for a few minutes for the purpose of measuring specific gravity. In the former case, the amount of water filling the voids of the specimen is considerably higher than the amount of water in the latter, and cannot be easily removed from the specimen.



Figure 4 Specimen before MiST conditioning (L) and after MiST conditioning (R)

Dynamic Modulus Test

Dynamic Modulus as an Engineering Property

Dynamic modulus (E^*) is a linear viscoelastic material property. It is a performance-related property and a measure of time-dependent stiffness and response of the asphalt concrete under repeated loading at various loading frequencies. It is one of the main engineering properties used in the *Mechanistic-Empirical Pavement Design Guide* (MEPDG) to evaluate mix performance and in deciding the mix quality with respect to both rutting and fatigue cracking.

Test Protocols

The conventional test is conducted according to AASHTO T 342 using cylindrical specimens and the uniaxial mode of testing. Existing literature confirms that there is a strong correlation between the dynamic modulus values measured in uniaxial mode and the ones in indirect tension mode using disk-shaped specimens (Kim et al. 2004). In this research, indirect tension dynamic modulus testing of disk-shaped specimens was selected according to AASHTO T 131-18. The reason for this selection was to have dynamic modulus (DM) specimens with the same geometry as specimens used in the HWTD test and in the Moisture-induced Stress Tester.

Conditioning and Modulus Ratio

Dynamic modulus tests were conducted before and after exposure to different moisture-conditioning protocols. The objective was to investigate how different conditioning processes, namely, Moisture-induced Stress Tester and freeze/thaw conditioning, would affect modulus of asphalt concrete. MiST conditioning was conducted at 46 °C and included 20-hour static conditioning before application of suction pressure cycles. The modulus ratio (MR) is defined as the ratio of dynamic modulus after moisture conditioning (retained modulus) to that before conditioning of the same test specimen. Modulus ratios were also compared with tensile strength ratio measured following AASHTO T 283.

Testing and Computations

To conduct the DM test in the indirect tension (IDT) mode, a disk-shaped, 60-mm-thick specimen was subjected to controlled sinusoidal (haversine) compressive stress in the vertical direction and at different frequencies (0.1/0.5/1/5/10 Hz). A typical DM test is conducted at a range of temperatures. However, all testing for this research was conducted at 25 °C, since the goal was simply to determine the change in modulus as a result of moisture-induced conditioning. The applied stresses and resulting axial and transverse strains are measured as a function of time and used to calculate the dynamic modulus (AASHTO 2018). The test configuration is demonstrated in Figure 5. A set of four extensometers, two in the vertical direction and two in the transverse direction, were mounted at the vicinity of the center of the specimen. Each face of the specimen was instrumented with two extensometers (Figure 5). The extensometers capture displacement within the gauge length during the test. The gauge length of the extensometer used in this study was 38 mm.

All specimens were conditioned at a 25 °C environmental chamber overnight to ensure temperature uniformity within the specimen before the test. To minimize damage within the specimen, the test started at the highest frequency (10 Hz) and moved to lower frequencies in sequence. The stress level was chosen in a way to ensure that the maximum horizontal strain did not exceed 50 microstrains. The strain level should be sufficiently high to deliver reliable measurements and minimize noise effect but low enough to prevent any damage caused by mechanical loading.

Using the applied load amplitudes and measured vertical and horizontal displacement on the specimen, the dynamic modulus at each frequency is calculated as follows (AASHTO 2018):

$$|E^*(\omega)| = -\frac{2|P^*|}{\pi ad} \frac{\beta_1 \gamma_2 - \beta_2 \gamma_1}{\gamma_2 |V^*| - \beta_2 |U^*|} \quad (1)$$

Where:

$|E^*(\omega)|$ = Dynamic modulus, Pa

$|P^*|$ = Applied load amplitude, N

a = Loading strip width, m

d = Thickness of specimen, m

$\overline{|V^*|}$ = Average vertical displacement magnitude, m

$\overline{|U^*|}$ = Average horizontal displacement magnitude, m; and

$\beta_1, \beta_2, \gamma_1, \gamma_2$ = Geometric coefficients determined by extensometer gauge length.

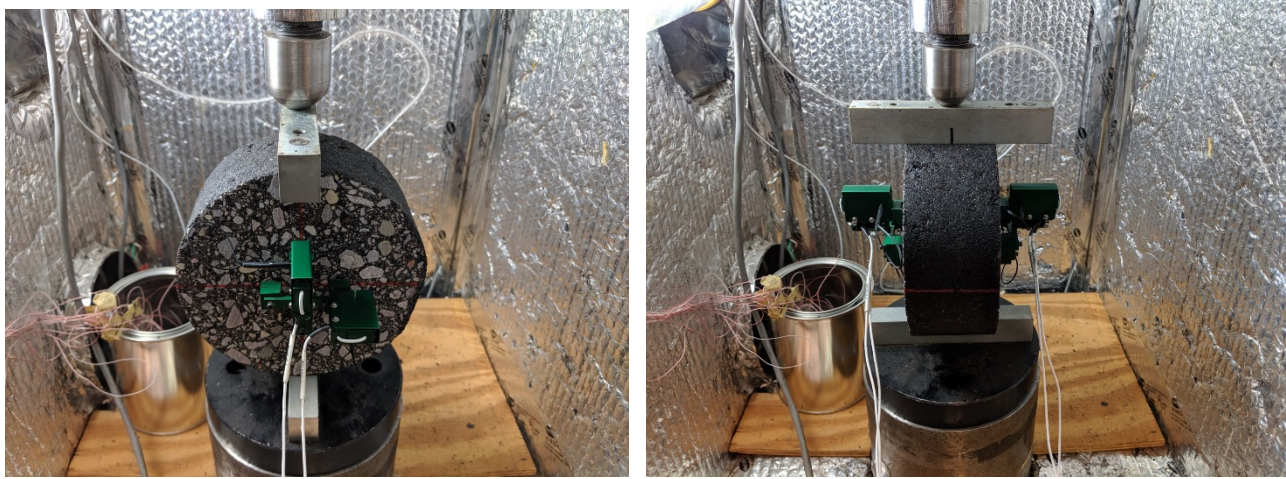


Figure 5 Dynamic modulus test in IDT mode configuration: (a) front view and (b) side view (AASHTO TP 131-18)

Specimen Preparation and Test Schedule

Specimens were prepared using a Superpave gyratory compactor. A 150-mm-tall specimen was compacted and cooled overnight. Subsequently, it was sawed to deliver two 60-mm-thick disk specimens. A total of six disk-shaped specimens were made through this process for each material source (total of 24 specimens). All specimens were marked so that specimens were loaded through the same axial direction before and after exposure to moisture conditioning.

The overall test schedule for each material source is illustrated in Appendix E. Scheduling the DM tests was somewhat challenging due to equipment limitations (for example, MiST can only process a maximum of three specimens at a time) and time constraints. To ensure consistency among all four material sources, a 21-day test cycle was designed and strictly applied to all material sources.

The bulk specific gravity of each test specimen (after trimming) was measured at several stages to closely monitor the changes in density at each stage, especially after testing and conditioning. On day 12, six specimens of each material source were split into two groups, each group subject to a different moisture conditioning process. The specimens were grouped via a random number generator to reduce bias. The air void comparison between the two groups and the overall average air void are presented in Figure 6. The average air voids of all groups were within the target of 7 to 8%, thus eliminating the effect of air void on moisture conditioning and mechanical tests.

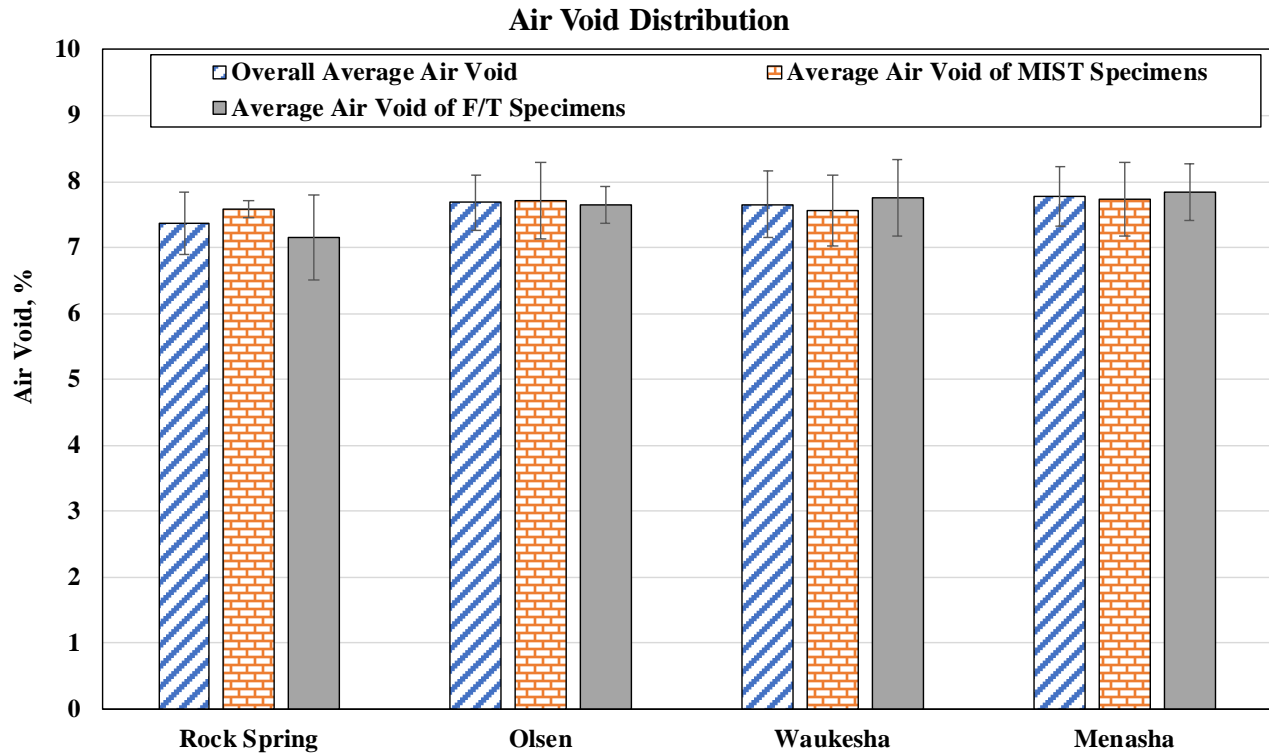


Figure 6 Average air void distribution for DM specimens

Ultrasonic Pulse Velocity (UPV) Test

Testing Asphalt Concrete with UPV

UPV utilizes the propagation speed of mechanical waves, mostly at frequencies in the range of about 50 to 150 KHZ within a medium, to determine the integrity and properties of samples. Propagation speed of mechanical waves is directly related to the density of the medium (the higher the density, the higher the wave speed), while the presence of voids and cracks reduces the wave speed. UPV has been widely used in the study of concrete samples and structures as, for example, discussed in studies by Tomsett (1980) and Panzera et al. (2011). The test method has been standardized in ASTM C597-16, but its application in asphalt mixtures is relatively new.

The potential of using ultrasonic technique to improve the testing and evaluation of asphalt mixture has been investigated by researchers such as Birgisson et al. (2003), Cheng et al. (2013), and Arabani and Tavassoti-Kheiry (2006). Cheng et al. (2013) used ultrasonic detection method (UDM) to determine the ultrasonic velocity of asphalt mixtures at different temperatures and water contents during the cycles of water temperature-radiations (W-T-R). The researchers reported that UDM can be used to quickly evaluate the damage state of asphalt mixture after the action of W-T-R cycles and it also effectively predicts the degree of damage.

UPV Test Setup

In this study, a Proceq® Pundit PL-2 UPV device with a pair of 150-kHz compressional transducers and a pair of 250-kHz shear wave transducers were used to conduct the UPV test (Figure 7). The test setup consists of a data acquisition and signal processing unit (a), a signal transducer (b), and a signal receiver (c). Depending on the type, the signal transducers can generate compressional waves (P-waves) or shear waves (S-waves), and the receivers are selected accordingly. Transducers with different frequencies can be used (e.g., 54 kHz, 150 kHz, etc.). In general, signals with higher frequencies can generate higher resolutions. However, the waves with higher frequency are more susceptible to attenuation. This issue becomes of concern

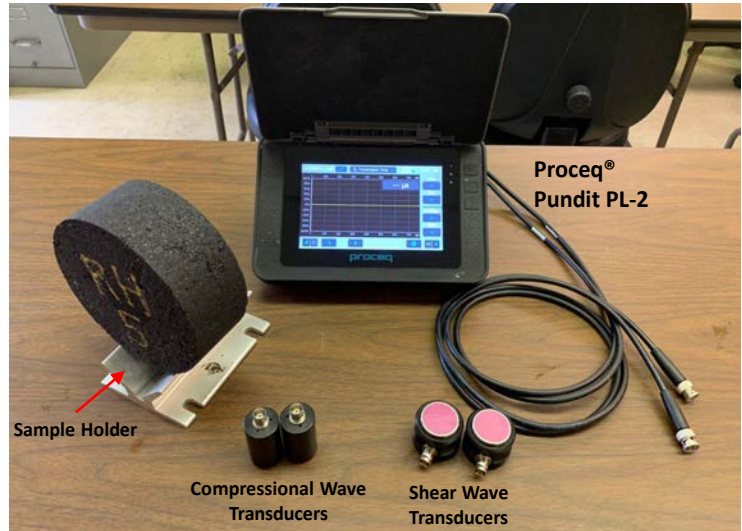


Figure 7 UPV test setup used in the study

in a material such as asphalt, which has high potential to attenuate signals due to its viscoelastic nature. Hence, the use of very-high-frequency signals should be avoided for asphalt concrete specimens to ensure that a high-quality signal can be collected for typical specimen sizes, shapes, and test conditions.

The most suitable combinations of gain-factor and excitation voltage were determined for testing 60-mm-thick, disk-shaped specimens to provide the average 80% signal amplitude for the transmitted pulses. The 80% threshold is a generally accepted criterion in UPV testing to ensure that the transmitted wave would be strong enough to provide an acceptable level of response but would not be so strong as to result in overshooting and failing to capture the actual oscillation peaks. To achieve this goal, one should consider attenuation characteristics of the medium (i.e., asphalt concrete in this case), geometry of the specimen, and microstructure of the material to be tested. The setup and target measurement locations were also determined according to the allowable margins for each type of transducer to be used.

Interpretation of UPV Test Results

Compressional and shear waves are inherently different in their properties. Compressional waves transmit through a material by reducing the molecular distance at parts of the material. Once the wave passes through a section of the material, the molecular distance returns to its original state (Figure 8-a). This process is energy-consuming, and the wave loses energy while propagating through a material. Compressional waves can transmit through all sorts of material (i.e., solid, liquid, or gas); however, they cannot transmit through a

discontinuity in a material (e.g., a crack or a large void). Hence, they can be used to determine the integrity of the medium. Shear waves, on the other hand, cause a disturbance in the medium (Figure 8-b). Based on the direction of the disturbance, shear waves can have different polarities. Shear waves cannot transmit through non-solid medium and cannot pick up the presence of water inside the material. A combination of compressional and shear waves can be used to determine the elastic properties of the material, including Poisson's ratio and elastic modulus.

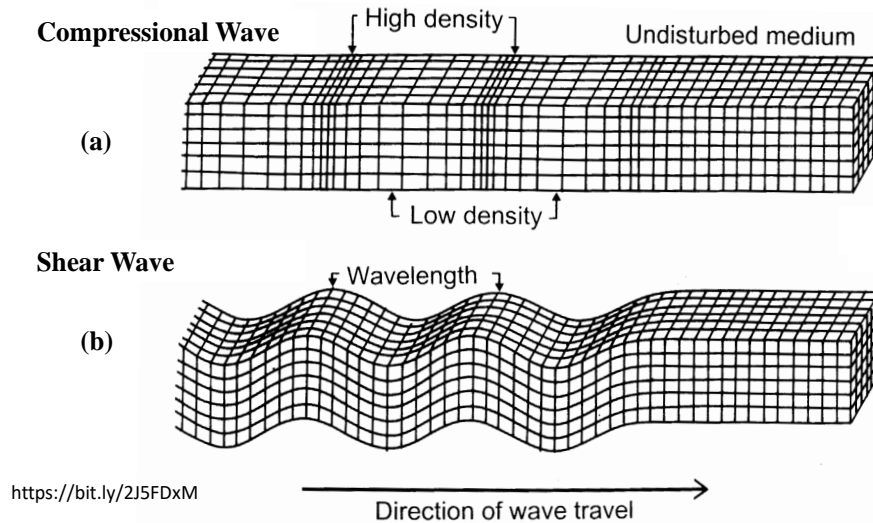


Figure 8 Propagation of (a) compressional waves and (b) shear waves in a medium

Figures 9 and 10 present signal outputs of a UPV test conducted on a sample of asphalt concrete in compressional and shear wave configurations, respectively.

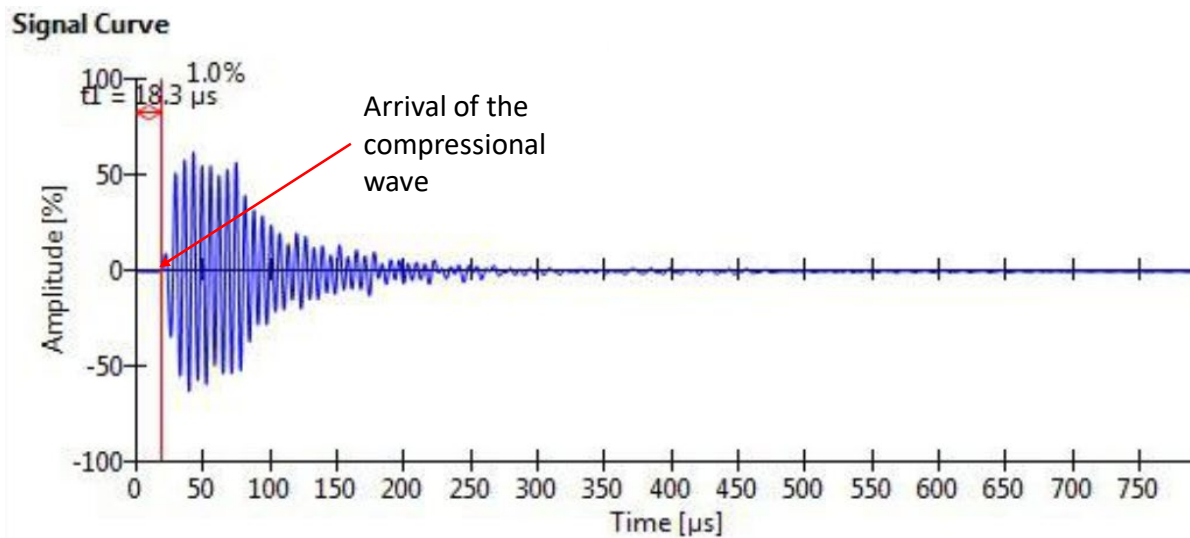


Figure 9 Sample compressional wave signal output after a UPV test

Signal Curve

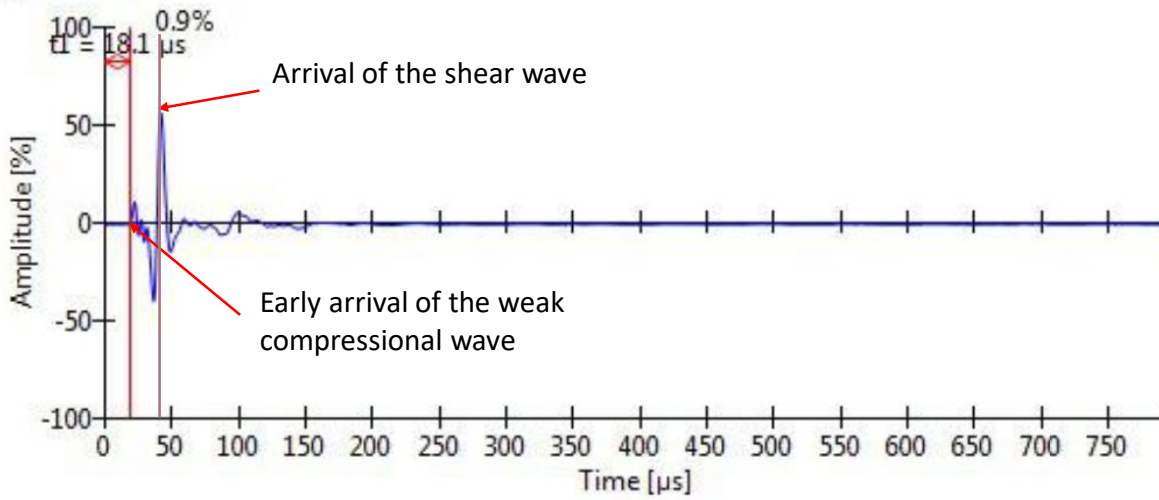


Figure 10 Sample shear wave signal output after a UPV test

The system starts the timer at the moment the first wave is generated in the transducers and records the time when the wave arrives at the receiver. In case of compressional waves (Figure 9), only p-waves are generated by the transducer, and the time when the front of this wave is received is reported as the propagation time. However, the shear wave transducers are known to generate both compressional and shear waves in the medium (Wong et al. 2008, Yurikov et al. 2019). These secondary p-waves are weaker than the compressional wave measurements, but they have higher transmission velocities than the shear waves and arrive at the receiving transducer earlier than the shear waves (Figure 10). The arrival time of the s-wave is the time associated with the maximum positive peak after the p-wave. For example, as shown in Figure 10, actual arrival time of the shear wave is 47 μs , and this time must be distinguished from the arrival time of the weak compressional wave, given by the device output as 18.1 μs . Hence, the correct time of arrival of the shear waves should be extracted manually from the raw waveform data. The travel time and the distance (height of sample) were used to calculate the velocity for both compression and shear wave (V_p and V_s , respectively). The estimated wave velocities for all of the samples from the four aggregate sources are provided in Appendix F.

In this study, the elastic modulus of asphalt concrete samples was calculated using Equation 2 (Kheiry et al. 2017).

$$E = \frac{\rho V_s^2 (3V_p^2 - 4V_s^2)}{V_p^2 - V_s^2} \quad (2)$$

Where: E = Elastic modulus of the material, ρ = density (kg/m^3), V_p = compressional wave velocity (m/s), and V_s = shear wave velocity (m/s).

Instrumentation of Specimens and Data Collection

All test samples had a diameter of 150 mm, with thickness of 60 mm or 95 mm, based on the purpose of the test. Measurements were conducted at different locations of the samples based on the type of the wave (Figure 11).

For compressional waves, five different measurements were conducted on each sample at points 1 through 5. The order of measurements was kept consistent at different stages of testing the same specimen so that a point-to-point comparison was possible from one stage of testing the specimen to the next. For shear waves, measurements were conducted only at the center of the specimen (i.e., point 5) to eliminate edge effects on the measurements. Wave reflection from the edges adds complexity to analysis and establishing arrival time of shear waves.

Both transducers were held in place firmly throughout the measurement. To improve the transmission of waves between the transducer and the specimen, a coupling agent was placed between the specimen and the transducers. The coupling agent is required to ensure proper contact between the transducer and the surface of the asphalt concrete specimen. For compressional wave measurements, a generic ultrasound gel was used, while for shear wave measurements, a specific shear coupling agent was used. This material has a very high viscosity, making the transmission of shear waves between the specimen and transducers possible.

Figure 12 demonstrates a typical UPV test on a 60-mm sample of asphalt concrete using both (a) compressional wave transducers and (b) shear wave transducers. Compressional wave transducers collect data regardless of the holding direction, whereas shear wave transducers are very sensitive to the polarity of the wave and must be held in the correct direction to maximize the quality of the collected data.

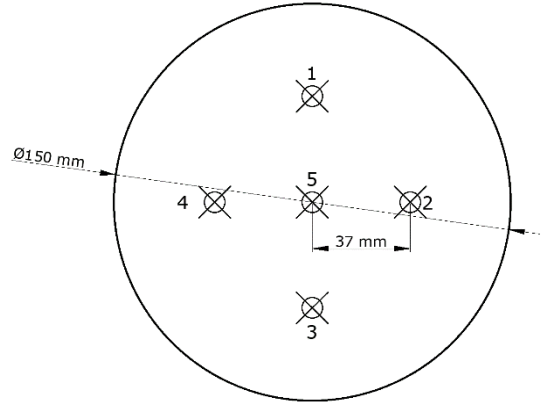


Figure 11 Location of measurements on test samples

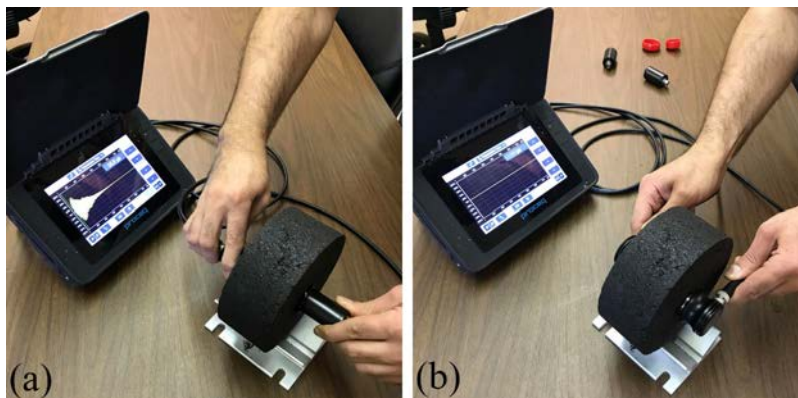


Figure 12 Conducting UPV measurements on a 60-mm asphalt concrete sample: (a) compressional wave and (b) shear wave

Testing Sequence

For each aggregate source, six replicate specimens were made using a Superpave gyratory compactor, followed by cooling to room temperature. The samples were then maintained at a 25 °C environmental chamber for 2 hours to achieve temperature equilibrium before conducting the baseline UPV measurements. Specimens were conditioned either through a cycle of freeze/thaw (AASHTO T 283-14) or using MiST. In summary, five sets of UPV measurements were conducted on samples at the following conditions:

1. On unconditioned samples
2. On unconditioned samples after measurement of bulk specific gravity (G_{mb})
3. On unconditioned samples after dynamic modulus test
4. On saturated conditioned samples after conditioning with MiST or AASHTO T 283
5. On dried and conditioned sample after dynamic modulus test

After the specimens were conditioned following DM testing (Table 5), three samples were conditioned for each aggregate source following AASHTO T 283 (with freeze/thaw) and three samples were conditioned using MiST. Conditioning was followed by storage in a 25 °C water bath for a minimum of two hours to achieve temperature equilibrium.

Table 5 Summary of conditioning methods used for asphalt concrete specimens

Menasha		Olson		Rock Springs		Waukesha	
ID	Conditioning	ID	Conditioning	ID	Conditioning	ID	Conditioning
MI1	MiST	OI1	MiST	RI1	MiST	WI1	Freeze/thaw
MI2	Freeze/Thaw	OI2	Freeze/Thaw	RI2	Freeze/Thaw	WI2	MiST
MI3	MiST	OI3	Freeze/Thaw	RI3	MiST	WI3	MiST
MI4	MiST	OI4	MiST	RI4	Freeze/Thaw	WI4	MiST
MI5	Freeze/Thaw	OI5	MiST	RI5	Freeze/Thaw	WI5	Freeze/thaw
MI6	Freeze/Thaw	OI6	Freeze/Thaw	RI6	MiST	WI6	Freeze/thaw

Condition 1 served as the baseline measurement (i.e., tests were conducted on dry specimens before any water conditioning). Furthermore, specimens were tested with UPV shortly after compaction, so that properties were not impacted by aging. Specimens in Condition 2 were soaked in water for 4 minutes for G_{mb} measurement and had therefore absorbed some water. Since the presence of water inside the specimen could potentially affect the compressional wave velocity in the specimens, compressional wave measurements were conducted immediately following removal of the specimens from the water bath. As shear wave velocity is not impacted by the presence of water, this velocity was measured after all of the compressional UPVs were finished. UPV measurements after the first IDT DM test (Condition 3) were conducted to assess any property change as a result of the IDT DM testing. Condition 4 measurements were conducted immediately after the end of water conditioning of the specimens that had been subjected to DM

testing. This stage of testing was intended to capture any potential moisture damage. However, as the samples at the end of the condition cycle were partially saturated, no direct comparison was possible with the previous measurements. Hence, UPV measurements of Condition 5 were conducted on specimens after they were allowed to dry to a good extent and before conducting the second IDT DM test. This drying period might have also contributed to some degree of healing in the specimens. As previously mentioned, at each stage, a total of five compressional measurements and one shear wave UPV measurement were conducted according to the layout shown in Figure 11. The average of the five compressional UPV measurements was used for determining the elastic modulus of the specimens using Equation 2.

CHAPTER THREE

Findings and Interpretation of Results

In this chapter, the results of the research project and the associated findings are presented. First, the results from each type of test are discussed, followed by overall interpretation of the results and recommendations for use of the results in specifications.

BOIL TEST

In general, when the boil test was conducted on specimens prepared using the design aggregate gradation, the level of binder stripping was relatively low. As the original results from the HWTD showed damage to the specimens, it was decided to rerun the boil tests using only the coarse aggregate portion for each source. Based on the testing on the coarse aggregate, the results indicated a higher level of stripping in the boil test when coarse aggregate was used compared to the mix aggregate gradation (see Appendix B for details).

TENSILE STRENGTH RATIOS

Results from testing specimens from all four sources of materials are presented in Table 6 and Figure 13. Details are provided in Appendix C. The results indicate susceptibility of all mixtures to moisture damage based on the AASHTO T 283 protocol when a freezing cycle is included in the conditioning. The results indicate a passing mix for Rock Springs, marginal performance for Menasha and Waukesha, and failing results for the Olsen mix when no freeze is applied and using TSR of 0.8 as the threshold. The no-freeze TSR results from this research closely or exactly match the no-freeze TSR results reported in JMF for two of the four mixes (Table 6). The two mixes showing a significant difference from the JMF TSR are the Waukesha and Olsen mixes. With no freeze cycle, the research results indicate these two mixes failing TSR, whereas the JMF presents passing mixes. This discrepancy could simply be the result of differences in binders used in the field versus those used in the research laboratory testing, even though one cannot reach this conclusion with a high level of certainty.

For all cases, the dry strength seems satisfactory, being in the range of 95 to 110 psi. This is a respectable level of dry strength because the binders are classified as PG 58-28. However, all specimens exhibited a noticeable amount of strength loss due to moisture damage when the freezing cycle was included, resulting in a poor to marginal tensile strength ratio.

Table 6 Results from conducting moisture damage tests using three different procedures based on AASHTO Standard T 283

		Factor	Source				
			Menasha	Waukesha	Rock Springs	Olsen	
Version of AASHTO T 283	95-mm Specimens, with Freeze	Dry Strength ⁽¹⁾	96.7	95.7	111.3	90.5	
		Wet Strength ⁽¹⁾	61.0	65.8	72.1	66.4	
		TSR ⁽²⁾	0.63	0.69	0.65	0.73	
	95-mm Specimens, No Freeze	Dry Strength	96.7	95.7	111.3	90.5	
		Wet Strength	73.0	70.7	91.8	63.6	
		TSR	0.75	0.74	0.83	0.70	
	60-mm Specimens, with Freeze	Dry Strength	108.2	109.2	120.9	94.5	
		Wet Strength	72.9	80.6	86.6	72.4	
		TSR	0.67	0.74	0.72	0.77	
	JFM Reported		TSR	0.78	0.97	0.83	0.86 ⁽³⁾

- (1) All strength values are reported in psi and represent average from three replicates.
- (2) TSR: Tensile strength ratio (average strength of conditioned specimens over that of dry specimens).
- (3) Not directly comparable with results from this research due to mix design differences.

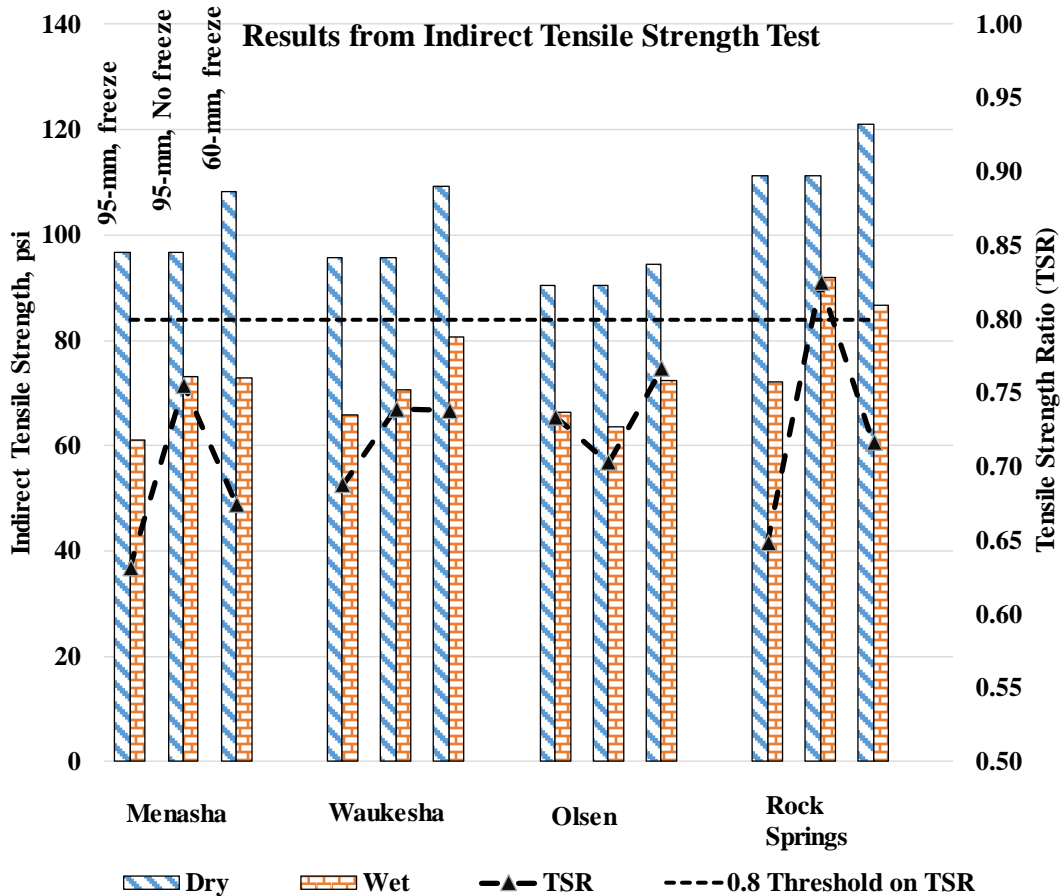


Figure 13 Results from indirect tensile test, average of three replicates reported

WHEEL TRACKING

Details of all HWTD test results for each source are presented in Appendix D. The appendix also includes the air void of specimens used in the right and left tracks for all HWTD tests (submerged, dry, and after MiST). A summary of test results is presented in Table 7. Six parameters were extracted from the test results, as presented in the table.

Table 7 Test results from HWTD test

Parameter	Condition	Aggregate Source			
		Menasha	Waukesha	Rock Springs	Olsen
Maximum Rut Depth, mm	Wet	22.0	17.4	18.8	21.6
	After MiST	9.1	10.9	8.1	9.4
	Dry	7.2	8.3	7.6	6.3
SIP	Wet	11,777	14,876	16,415	8,162
	After MiST	13,442	18,427	15,368	>22,000 ⁽¹⁾
	Dry	>22,000	>22,000	>22,000	>22,000
Stripping/Creep Slope Ratio	Wet	4.4	3.70	6.3	7.0
	After MiST	1.6	1.8	1.0	0.8
	Dry	0.9	0.9	0.6	0.6
Passes to 10 mm Rut	Wet	15,192	18,647	18,706	11,649
	After MiST	24,570 ⁽²⁾	23,837	36,379	26,815
	Dry	43,677	31,691	43,570	86,644
Rut Depth at 10,000 Passes, mm	Wet	6.0	4.9	4.8	7.6
	After MiST	6.0	5.9	6.0	6.6
	Dry	5.7	6.1	5.9	5.3
Stripping Slope (mm/1,000 passes)	Wet	1.36	1.03	1.58	2.05
	After MiST	0.31	0.47	0.19	0.23
	Dry	0.13	0.17	0.12	0.07

(1) Passes > 22,000 is not a direct measurement. It implies that, if an inflection point exists, it will be beyond the number of passes used in this research. The maximum number of wheel passes in this research was 22,000.

(2) Numbers shown larger than 22,000 are obtained through extrapolation and do not represent an actual number of cycles.

Wheel Tracking under Wet Conditions

An example of HWTD testing under submerged conditions is presented in Figure 14. All sources developed a stripping inflection point within the range of applied wheel passes. The ratio of stripping slope to creep slope is also noticeably high for all sources. The Olsen mix exhibited the poorest performance, reaching the stripping inflection point under 10,000 passes for both left and right tracks of the test and the highest stripping/creep slope ratio. It must be noted that the results from the HWTD test must be interpreted in the light of the fact that the test is highly severe and effective in terms of inducing damage to the mix under water. Therefore, a decision needs to be made with respect to establishing threshold values when using any of the parameters or a combination of them.

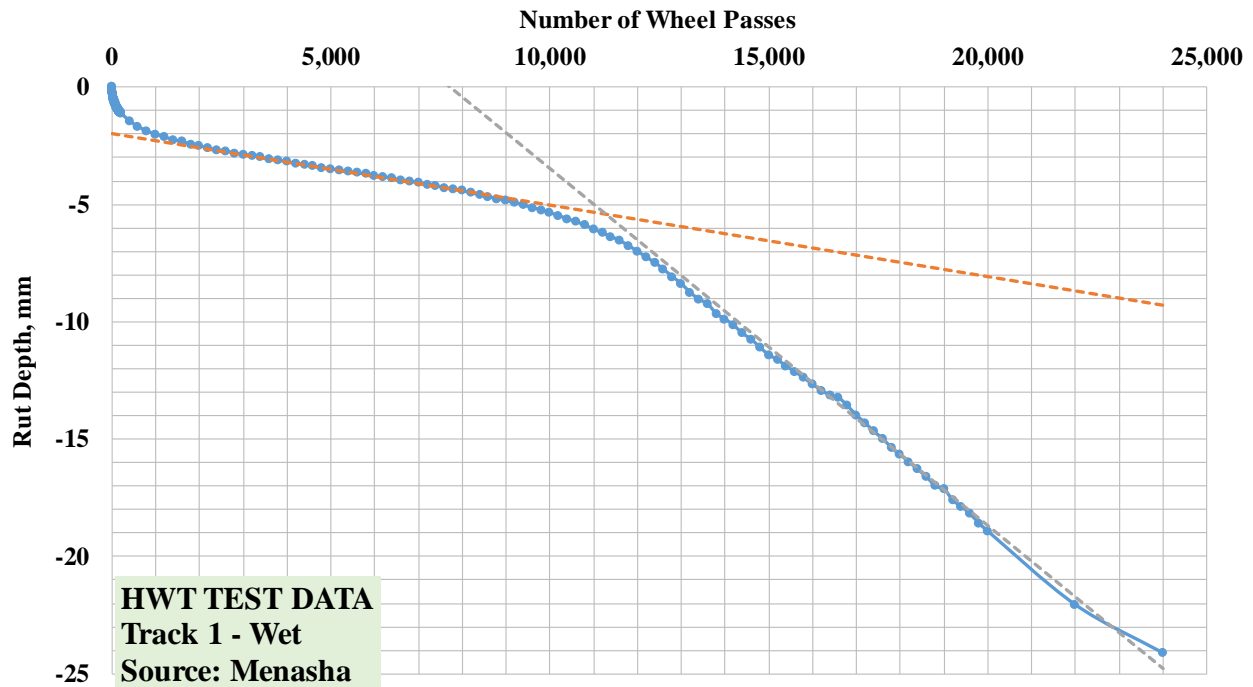


Figure 14 Performance of Menasha mix tested in HWT under submerged condition

Wheel Tracking under Dry Conditions

It was expected that HWT testing under dry conditions would be significantly less damaging to the tested materials. Indeed, this was the case as manifested in Table 7 for all sources, and in the example of the relationship between rut depth and number of passes as presented in Figure 15. The inflection point for tertiary creep was nonexistent. The creep slope ratio of less than 1 for all sources implies that the rate of rutting was decreasing with the increase in number of wheel passes within the range of applied passes. It can be clearly seen that there is a significant difference between the damage from wet tested specimens versus dry tested specimens. Therefore, the results clearly indicate that the major portion of damage for the tested mixes can be attributed to the water effect.

Sometimes, when a mix is tested dry, the slope of the curve showing the relationship between rut depth and number of wheel passes increases drastically at some point when the mix becomes unstable and develops tertiary creep. The curve of a tertiary creep failure under dry testing conditions resembles that of a stripping mix under submerged testing conditions. None of the four mixes tested dry developed tertiary creep under the applied testing conditions (i.e., temperature of 46 °C and 22,000 wheel passes).

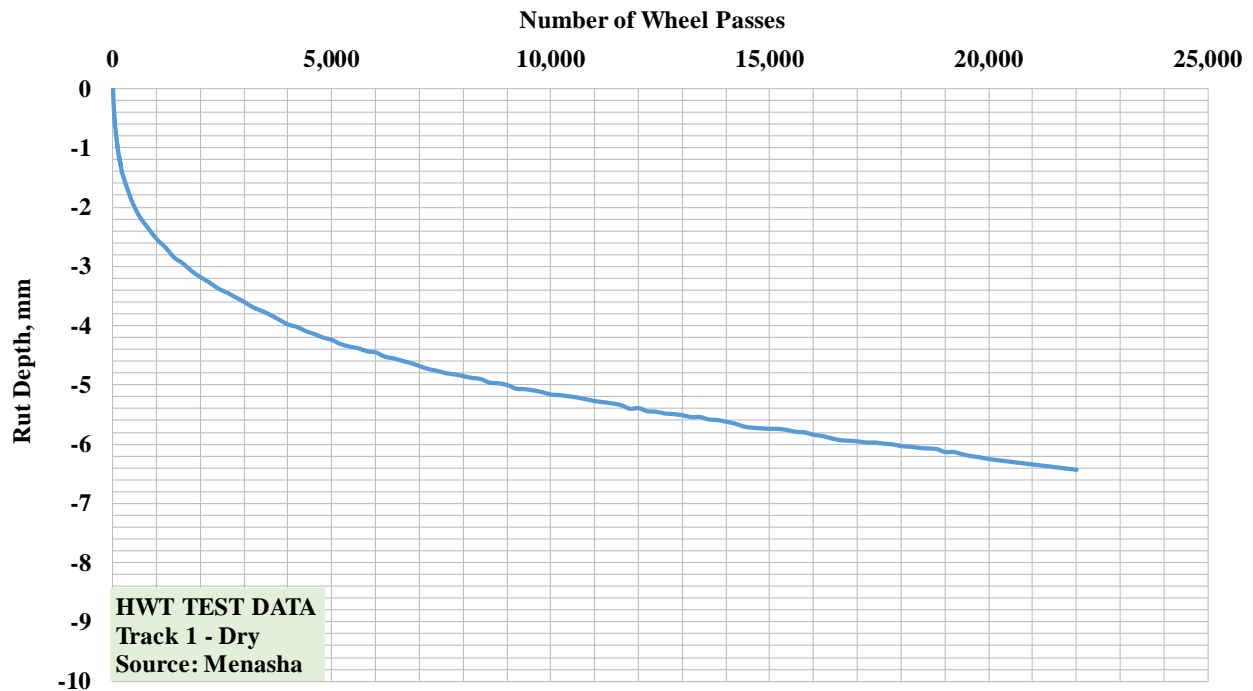


Figure 15 Performance of Menasha mix in HWTD under dry testing condition

Wheel Tracking of MiST-Conditioned Specimens

The last series of HWTD tests were conducted on the specimens which were subjected to MiST conditioning. Details of conditioning are explained in Chapter 2. After conditioning the specimens were processed for specific gravity measurement followed by the HWTD test. It should be noted that there was a time span of approximately 5 days between MiST conditioning and HWTD testing. This rest period might have contributed to some healing of specimens before HWTD testing. During rest periods healing can recover part of the damage caused to the specimen (Moreno-Navarro et al., 2015). The microdamage healing is real and measurable once the specimen is given enough time to rest (Little et al., 2001).

An example of results is presented in Figure 16. For all four sources and for all six parameters presented in Table 7 (except rut depth at 10,000 passes), the results for MiST-conditioned specimens consistently fall between those for dry and submerged tested specimens. The MiST-conditioned specimens suffered some level of damage, hence delivering results in the expected trend compared to dry specimens. The MiST-conditioned specimens, however, do not show the severity of damage seen in the submerged specimens.

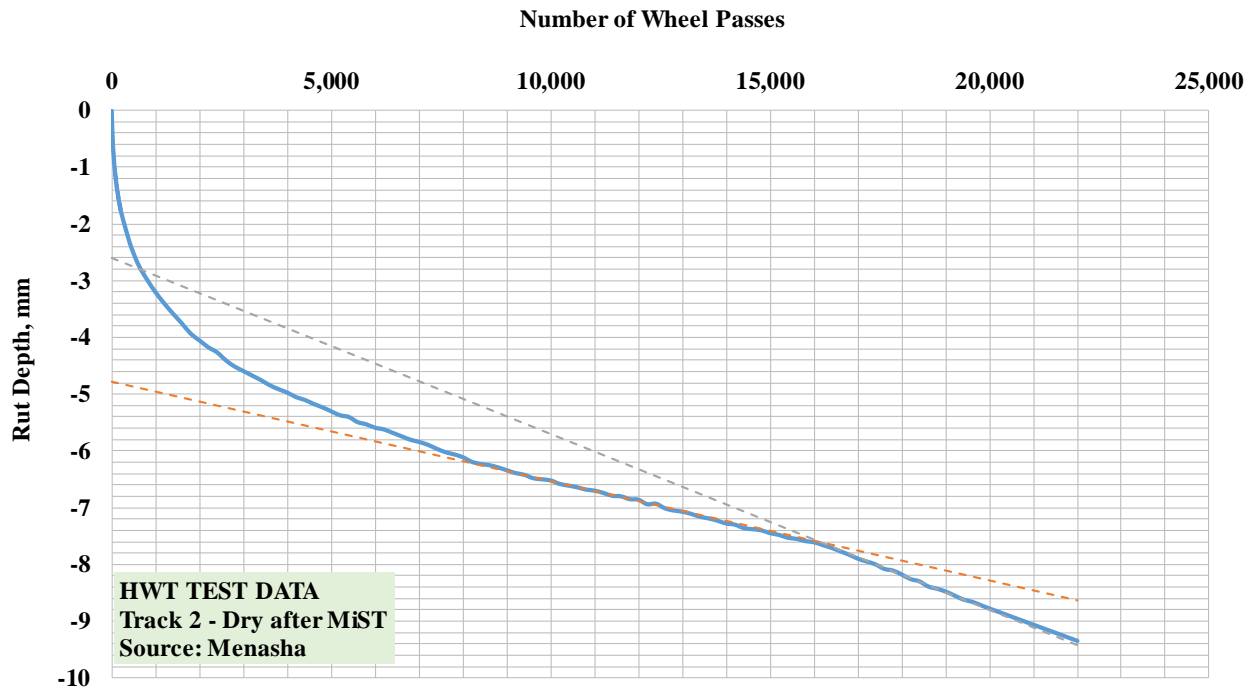


Figure 16 Performance of Menasha mix in HWT tested dry after MiST conditioning

DYNAMIC MODULUS

It was discussed in the previous chapter that dynamic modulus was measured on specimens before and after water conditioning. The purpose of this testing was to determine how the modulus (stiffness) of the mix is affected by moisture conditioning, as modulus is an important engineering property used in performance prediction models. The average dynamic modulus of all material sources under five test frequencies is shown in Figure 17. This plot depicts the dynamic modulus before moisture conditioning. The error bar stands for one standard deviation. As expected, modulus decreases as the loading frequency decreases. On average, higher values were obtained for the Waukesha and Rock Springs sources compared with the other two.

The comparison between dynamic modulus before and after moisture conditioning for each material source is presented in Figures 18 through 21 (individual test results are provided in Appendix E). As a reminder, conditioning was either through one cycle of freeze/thaw or through MiST. Modulus ratio refers to the dynamic modulus after moisture conditioning to the dynamic modulus before conditioning. For this research, there was a time span of 3 to 4 days after completion of conditioning (either MiST or freeze/thaw) and prior to the second IDT DM test. This time span was used to determine bulk specific gravity of specimens at different stages and to remove the water from the specimens to the extent possible so that IDT DM test results would be comparable with the original test results from dry specimens. Water reduction efforts included drying the samples in front of fans, as well as trying to remove excess moisture using a CoreLok[®] vacuum chamber.

For all mixes, with no exception, a drop in mix stiffness was observed after conditioning. Overall, the modulus ratio varies in the range of approximately 0.55 to 0.75. Lower dynamic modulus ratio is indicative of higher moisture damage effect. Except for the Rock Springs material, the general trend is that the freeze/thaw cycle has a more severe impact on reducing the modulus compared with the MiST conditioning. However, statistical student t-test analysis did not indicate any significant difference between the modulus ratio from MiST conditioning versus the modulus ratio from freeze/thaw conditioning for the sources used in this study.

Dynamic Modulus before Conditioning

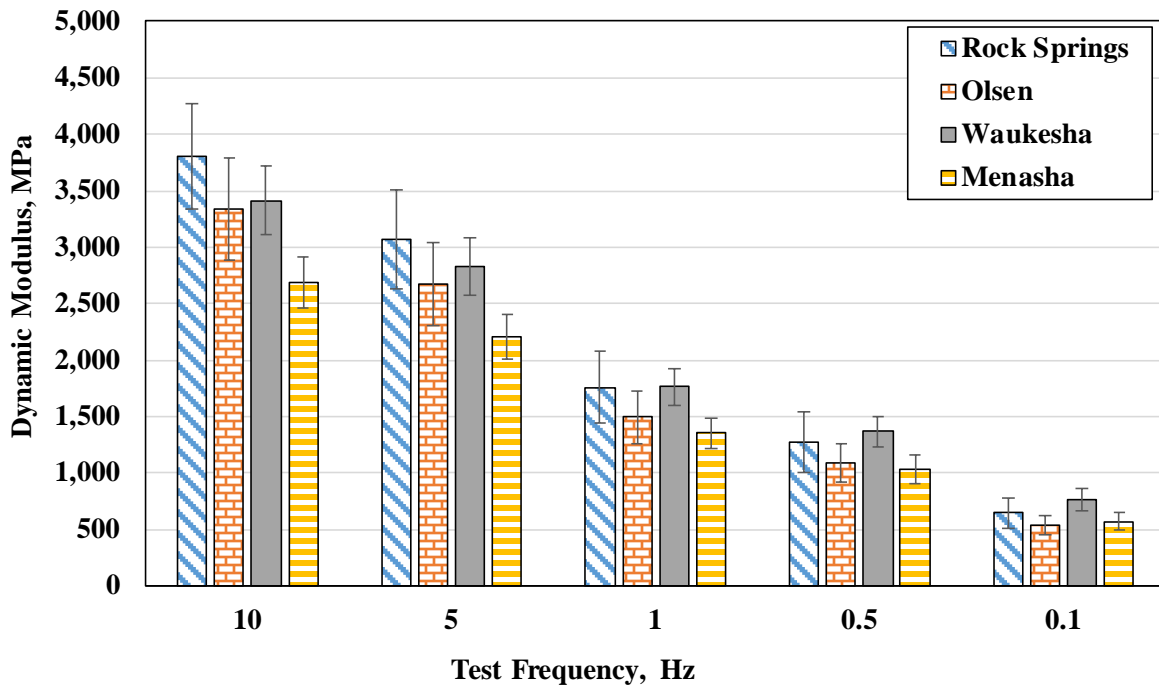
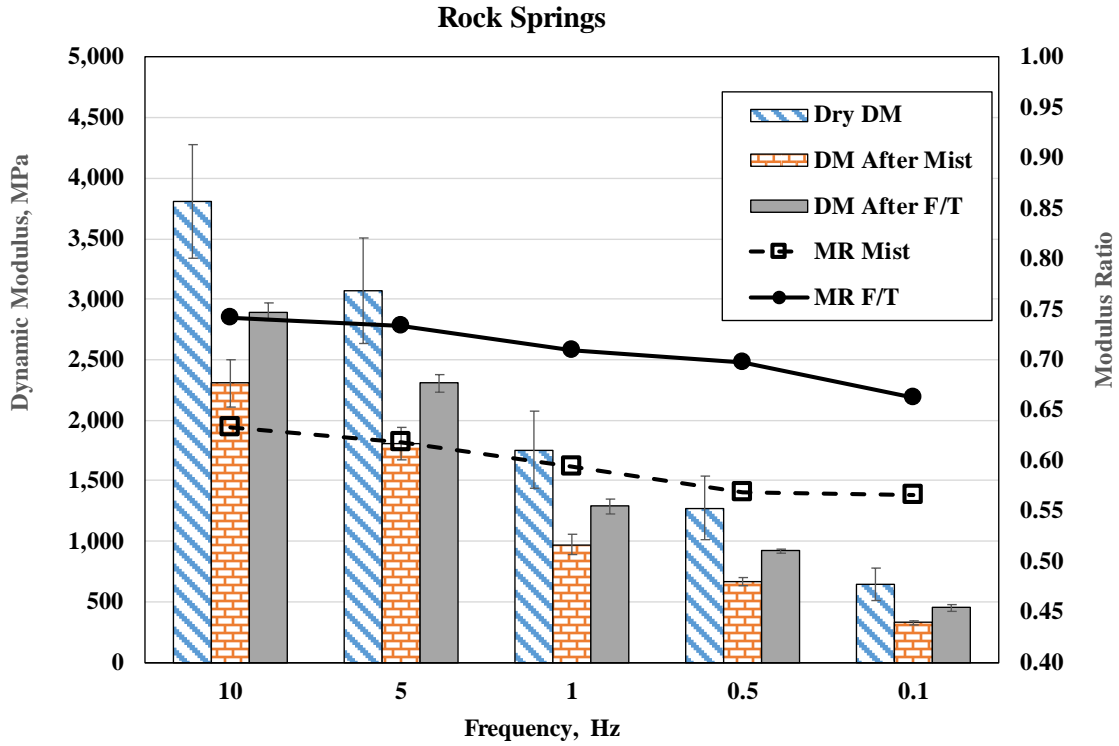


Figure 17 Average dynamic modulus of asphalt specimens before conditioning (25 °C)



Note: DM = Dynamic Modulus, F/T = Freeze/Thaw, MR = Modulus Ratio

Figure 18 Indirect dynamic modulus and modulus ratio comparison for Rock Springs

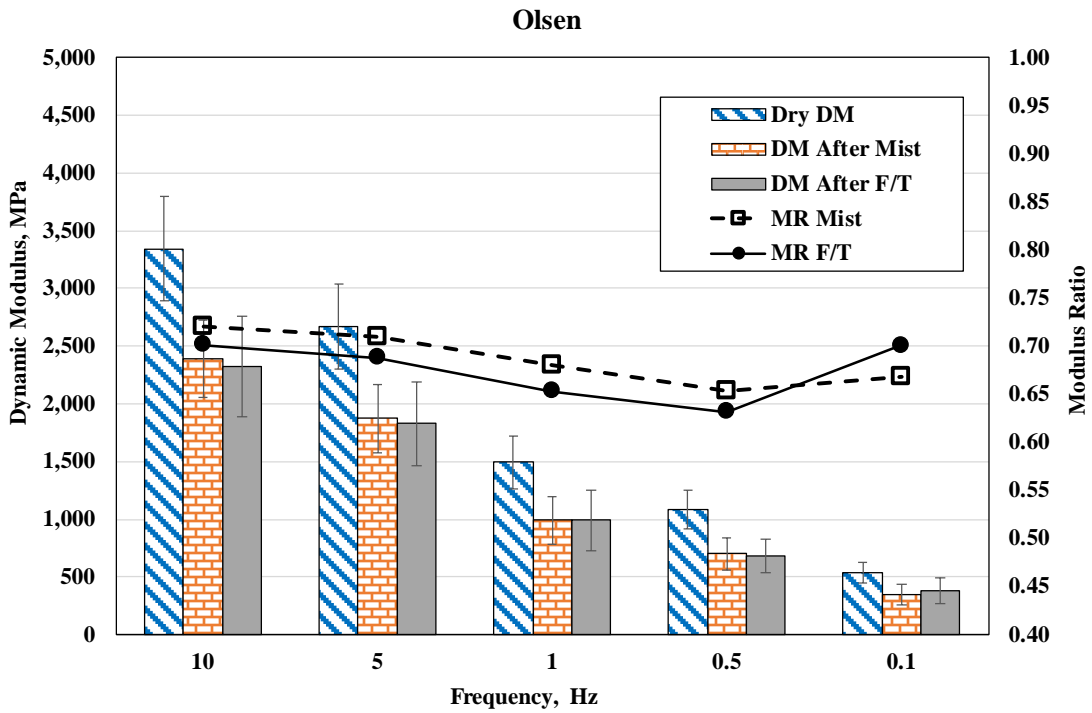


Figure 19 Indirect dynamic modulus and modulus ratio comparison for Olsen

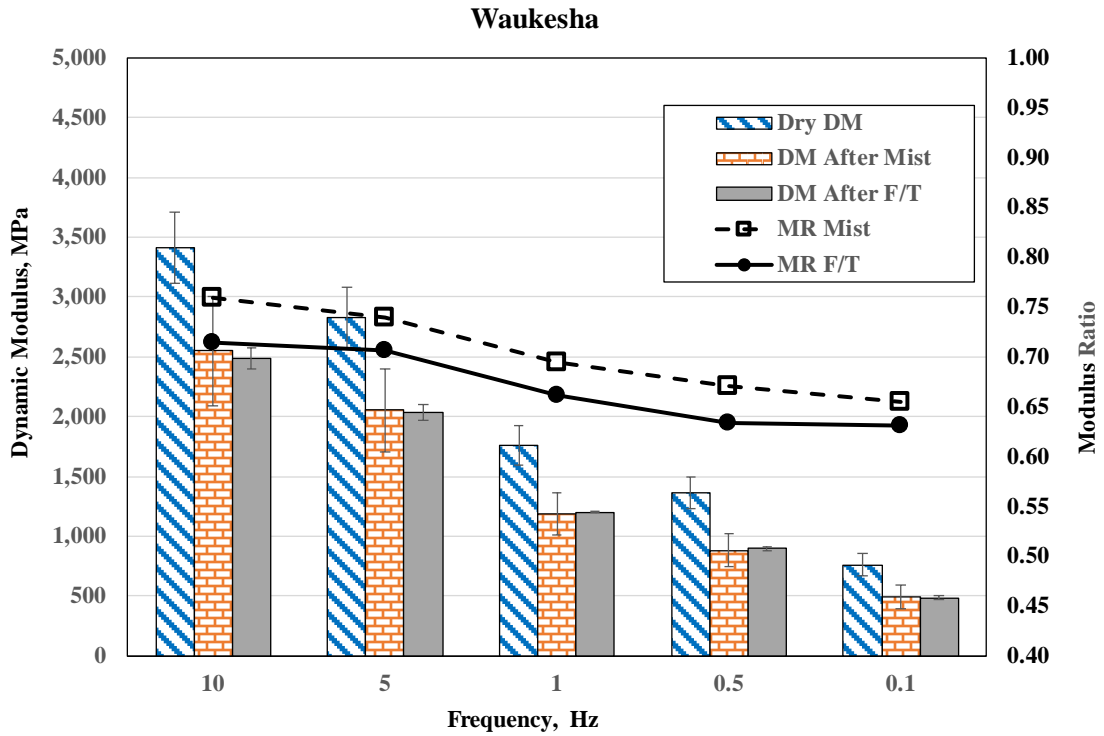


Figure 20 Indirect dynamic modulus and modulus ratio comparison for Waukesha

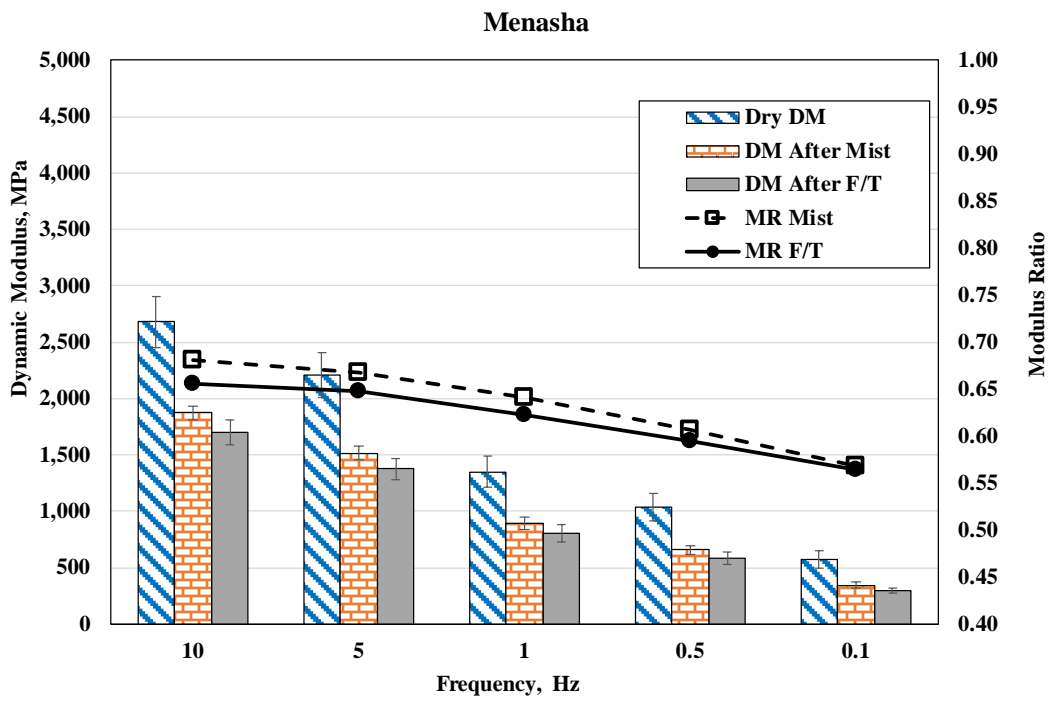


Figure 21 Indirect dynamic modulus and modulus ratio comparison for Menasha

It is of interest to know how the ranking of mixes based on the DM ratio compares with the ranking based on the tensile strength ratios. Such comparison is presented in Figure 22. In general, except for the Rock Springs mix, the DM ratio and TSR are roughly similar for the MiST DM ratio, freeze/thaw DM ratio, and TSR of 95-mm specimens with freeze. TSR with no freeze and TSR of 60-mm specimen appear to deliver the highest ratios. The implication of this finding is on deciding the threshold to be used as a pass/fail criterion in design specifications. Selection of the appropriate value depends on the type of conditioning and the engineering property to be considered (modulus versus strength). Note that the DM ratios presented in Figure 24 are the average of DM ratios from all testing frequencies.

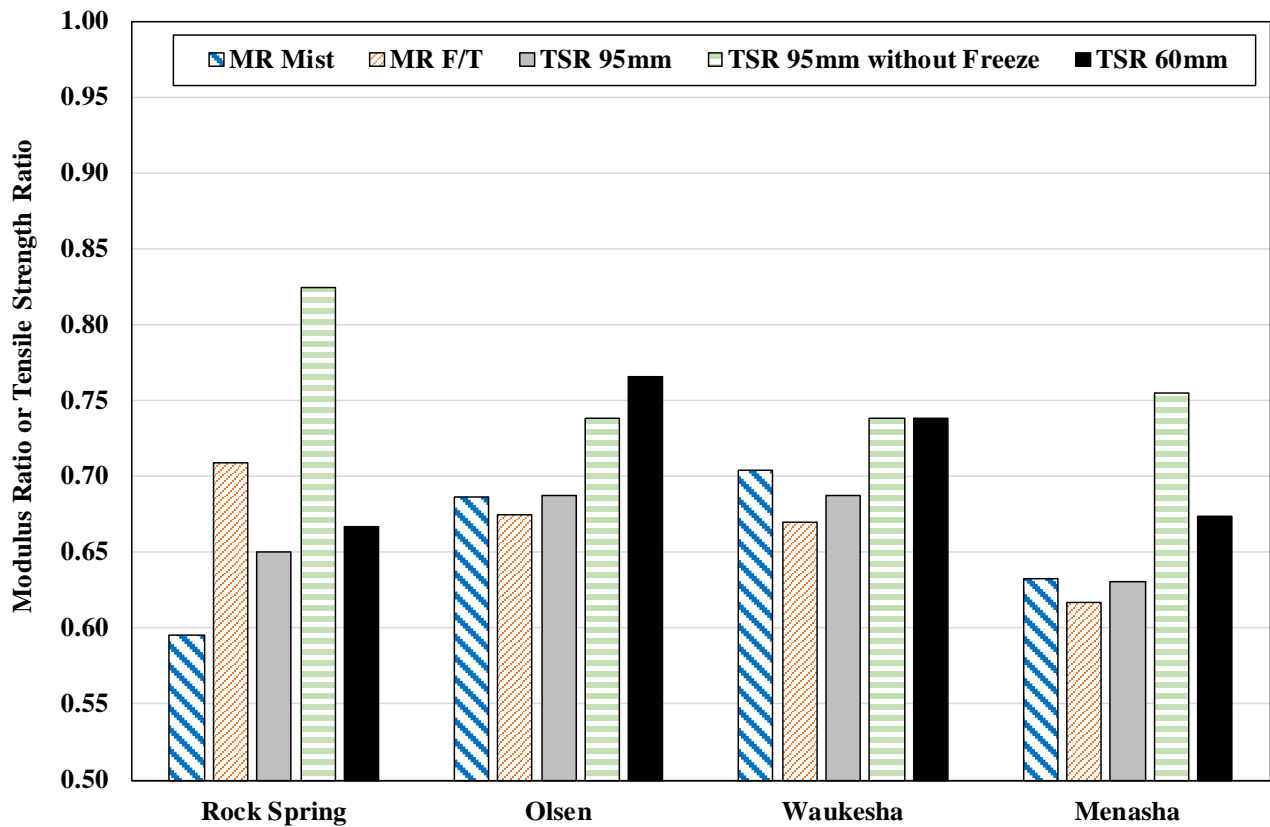


Figure 22 Modulus ratio and tensile strength ratio comparison

ULTRASONIC PULSE VELOCITY

Tests on Unconditioned Samples (Condition 1)

These measurements served as the baseline for comparison of the effect of conditioning and modulus testing on the properties of the specimens. Measured compressional wave velocities at the five points for each specimen were relatively consistent, with minimum coefficient of variation (COV) of 0.86% for specimen one of the Menasha specimens, and maximum COV of 6.93% for one of the Olsen specimens. Results are

summarized in Table 8. Figure 23 demonstrates the estimates of the elastic modulus of asphalt concrete specimens based on the results of the UPV test on unconditioned samples. The ranking of the mixes based on UPV modulus before conditioning almost matches the ranking of the mixes based on dynamic modulus, discussed previously. Rock Springs and Menasha demonstrate the highest and lowest modulus, respectively, like the results found from DM testing. Olsen and Waukesha fall between the two, as is also the case with the DM testing. Obviously, the numerical values from UPV testing are not directly comparable to those from DM testing because of significant difference in the frequency of testing.

Table 8 Summary of modulus of elasticity for the four aggregate sources (dry condition)

Aggregate Source	Average Modulus (MPa)	Standard Deviation (MPa)	COV (%)
Menasha	15935	219.6	1.38
Olsen	19261	1140.0	5.92
Rock Springs	19733	526.4	2.67
Waukesha	17598	689.3	3.92

Tests on Unconditioned Samples, after Measurement of G_{mb} (Condition 2)

These measurements were conducted to evaluate the effect of the absorbed water during the 4-minute submersion on the estimated moduli of specimens. On average, and except for the Olsen material, there was a slight increase in the compressive elastic modulus due to the intrusion of water into the specimen during density measurement (Table 9). The observed slight increase in moduli was expected, as the presence of water results in higher transmission velocity for compressional waves, hence higher modulus.

Table 9 Summary of modulus of eElasticity after G_{mb}

Aggregate Source	Average Modulus (MPa)	Standard Deviation (MPa)	COV (%)	% Change in Moduli from Condition 1
Menasha	16319	543.2	3.33	2.41
Olsen	19217	907.5	4.72	-0.23
Rock Springs	20232	992.9	4.91	2.53
Waukesha	17853	540.0	3.02	1.45

Tests on Unconditioned Samples, after First IDT DM Test (Condition 3)

Since the induced strain in IDT dynamic modulus testing was very small and the number of load repetitions was very limited, it was reasonable to assume that no damage would occur to the specimen as the result of this test. This is an important assumption because one of the methods used to assess moisture damage in this research was through comparison of specimen modulus before and after conditioning. If the impact of moisture damage were convoluted with the effect of damage from mechanical testing, then the results would not be conclusive and could not be used to truly assess the moisture damage effect. Hence, to ensure the

integrity of specimens after completion of the IDT DM test, UPV measurements were conducted on the specimens before and after completion of the modulus tests.

Table 10 presents the estimated modulus from the UPV test after completion of the first IDT DM test and its variation from the original UPV modulus estimate (Condition 1). As can be noticed, no significant change in average modulus for each of the four sources was observed at the end of the first IDT DM test, an indication of specimen integrity after completion of the DM test.

Table 10 Summary of modulus of elasticity for the four aggregate sources after the first IDT DM test

Aggregate Source	Average Modulus (MPa)	Standard Deviation (MPa)	COV (%)	% Change in Moduli from Condition 1
Menasha	15,716	1,001.9	6.38	-1.37
Olsen	19,162	730.9	3.81	-0.51
Rock Springs	19,733	469.2	2.38	0.00
Waukesha	17,866	418.6	2.34	1.52

Tests on Moisture-Conditioned Samples (Condition 4)

After completion of the IDT DM test, the specimens underwent freeze/thaw or MiST conditioning. A comparison of the estimated moduli at this stage with the original moduli (Condition 1) for all specimens is presented in Table 11. As expected, a drop in the estimated moduli in nearly all samples was observed.

Even with the noticeable presence of water in the conditioned specimens, the average moduli for the samples from all different sources decreased from those of Condition 1. The highest decrease of 9% belongs to the samples from Menasha, and the lowest decrease of 2% to the samples from Rock Springs. Statistical t-test analysis puts Menasha as the only mix with a significant drop in modulus for both conditioning systems. The t-test also shows the Olsen mix with a significant drop based on the freeze/thaw conditioning but not based on MiST conditioning. Moreover, the conditioning resulted in a significant increase in the variation between the moduli of the specimens compared with the moduli for Condition 1. This higher variability is most probably because of moisture conditioning.

Table 11 Effect of different conditioning techniques on the moduli after the first IDT DM test

Aggregate Source	After Freeze/Thaw				After MiST			
	Average Modulus (MPa)	Standard Deviation (MPa)	COV (%)	% Change	Average (MPa)	Standard Deviation (MPa)	COV (%)	% Change
Menasha	13,690	861.9	6.30	-14.09	15,257	246.6	1.62	-4.26
Olsen	16,529	806.2	4.88	-14.18	18,905	2,006.8	10.61	-1.85
Rock Springs	19,398	2,049.4	10.56	-1.69	19,209	177.1	0.92	-2.66
Waukesha	16,080	113.5	0.71	-8.62	17,143	270.6	1.58	-2.59

Tests on Moisture-conditioned Samples, Second IDT DM (Condition 5)

Mechanical testing of conditioned specimens can be conducted immediately after completion of conditioning or after some rest period and reduction of water content of the specimens. It was discussed previously that there was a time span of 3 to 4 days after completion of conditioning (either MiST or freeze/thaw) and prior to IDT dynamic modulus testing. Samples were dried during this time span to the extent possible so that UPV test results would be comparable with the original test results from dry specimens. In the previous sections it was demonstrated that IDT DM does not significantly affect the moduli of specimens. Hence, it is safe to assume that the moduli estimated using UPV after the second IDT DM can be effectively used to evaluate the effect of conditioning on the properties of samples. Note should be made that some level of healing might have occurred in the samples during the drying process, affecting the results.

A comparison of the estimated moduli for all samples is presented in Table 12. As can be noticed, in all sources the moduli have decreased compared with the moduli estimated from Condition 1 measurements. The amount of change is more pronounced from those reported in Table 11. The large scatter of the results in these samples is expected because of conditioning. It can also be noticed that, except for the Rock Springs samples, freeze/thaw conditioning caused larger changes in moduli compared with MiST conditioning.

Table 12 Effect of different conditioning techniques on the moduli after the second IDT DM test

Aggregate Source	After Freeze/Thaw				After MiST			
	Average Modulus (MPa)	Standard Deviation (MPa)	COV (%)	% Change	Average (MPa)	Standard Deviation (MPa)	COV (%)	% Change
Menasha	13,486	1,461.4	10.84	-15.37	14,564	265.9	1.83	-8.60
Olson	16,505	510.4	3.09	-14.31	17,949	1,675.5	9.33	-6.81
Rock Springs	19,882	2,433.9	12.24	0.76	17,998	337.7	1.88	-8.79
Waukesha	15,786	339.7	2.15	-10.29	16,592	341.3	2.06	-5.72

As can be clearly noticed, removal of the water from specimens resulted in reduction in the estimated moduli in almost all cases (Tables 13 and 14). A general comparison of all UPV test results for the five conditions discussed are presented in Figures 23 through 27.

Table 13 Effect of water removal on the moduli of MiST conditioned specimens

Aggregate Source	Partially Saturated Samples after Conditioning			Dried Conditioned Samples after Second IDT DM			
	Average Modulus (MPa)	Standard Deviation (MPa)	COV (%)	Average Modulus (MPa)	Standard Deviation (MPa)	COV (%)	% Change
Menasha	15,257	246.60	1.62	14,564	265.95	1.83	-4.54
Olson	18,905	2,006.79	10.61	17,949	1,675.51	9.33	-5.06
Rock Springs	19,209	177.15	0.92	17,998	337.75	1.88	-6.30
Waukesha	17,143	270.58	1.58	16,592	341.29	2.06	-3.21

Table 14 Effect of water removal on the moduli of freeze/thaw conditioned specimens

Aggregate Source	Saturated Samples after Conditioning			Dried Conditioned Samples after Second IDT DM			
	Average Modulus (MPa)	Standard Deviation (MPa)	COV (%)	Average Modulus (MPa)	Standard Deviation (MPa)	COV (%)	% Change
Menasha	13,690	861.86	6.30	13486	1,461.42	10.84	-1.49
Olson	16,529	806.25	4.88	16505	510.45	3.09	-0.15
Rock Springs	19,398	2,049.43	10.56	19882	2,433.92	12.24	2.49
Waukesha	16,080	113.47	0.71	15786	339.69	2.15	-1.83

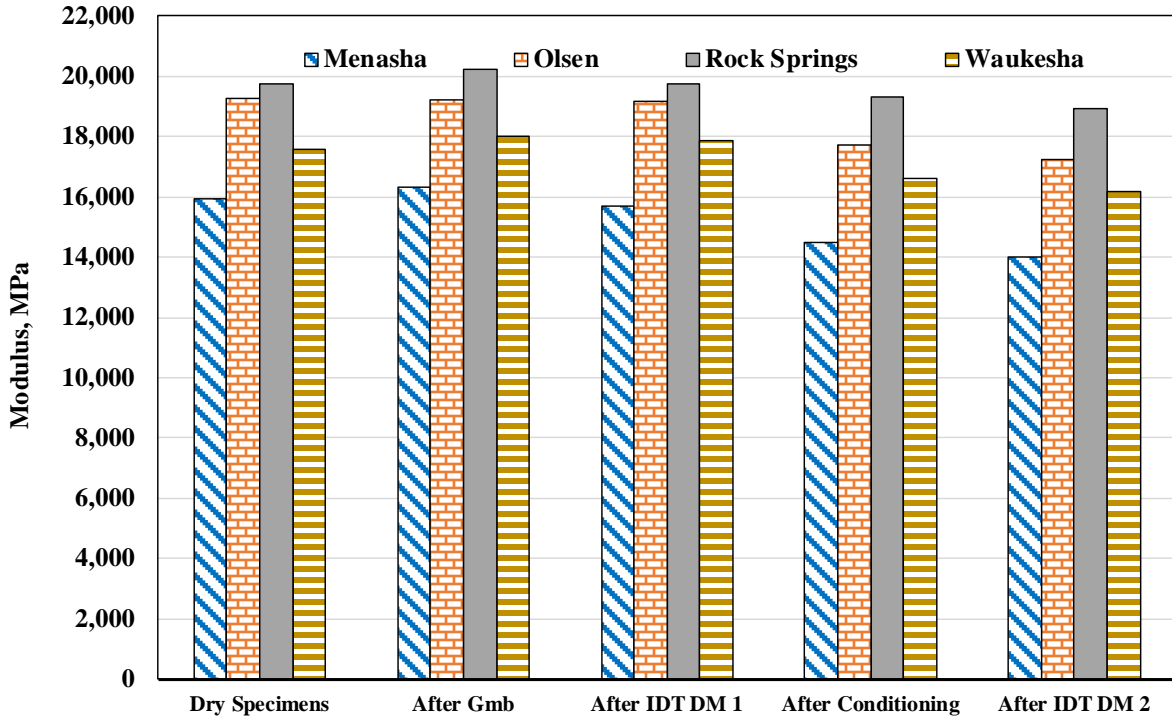


Figure 23 Comparison of moduli at different stages of UPV testing (stacked based on condition)

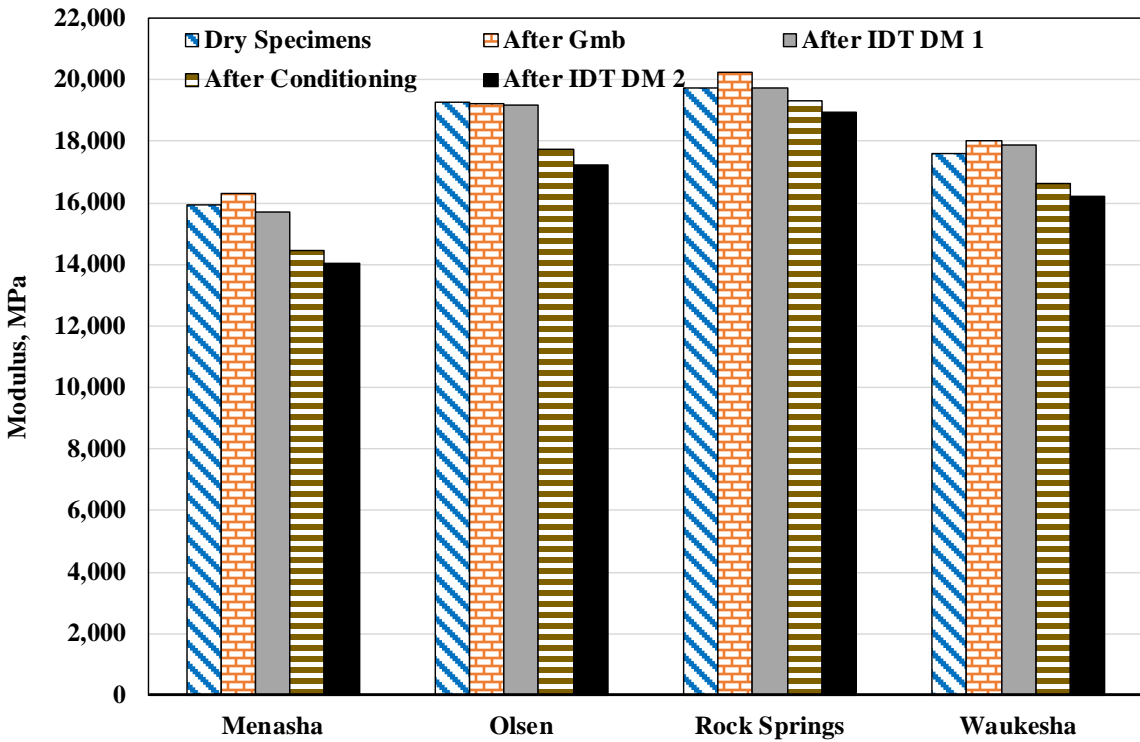


Figure 24 Comparison of moduli at different stages of UPV testing (stacked based on source)

Dried Samples

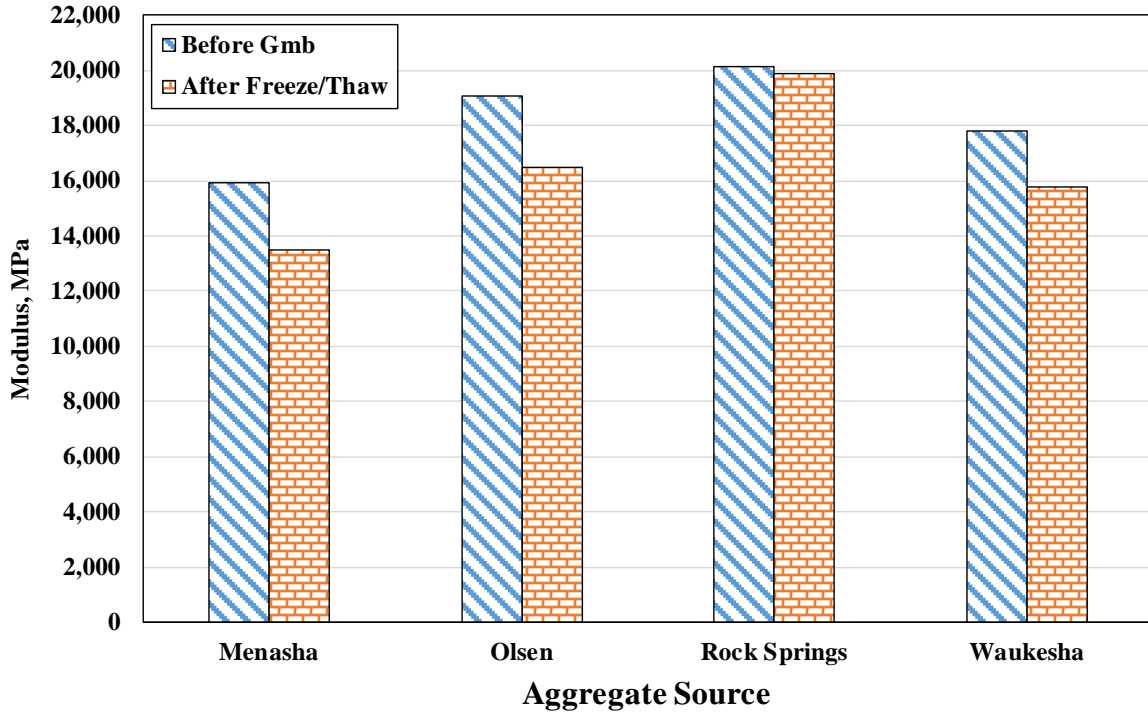


Figure 25 Modulus after freeze/thaw conditioning (condition 5) versus initial modulus

Dried Samples

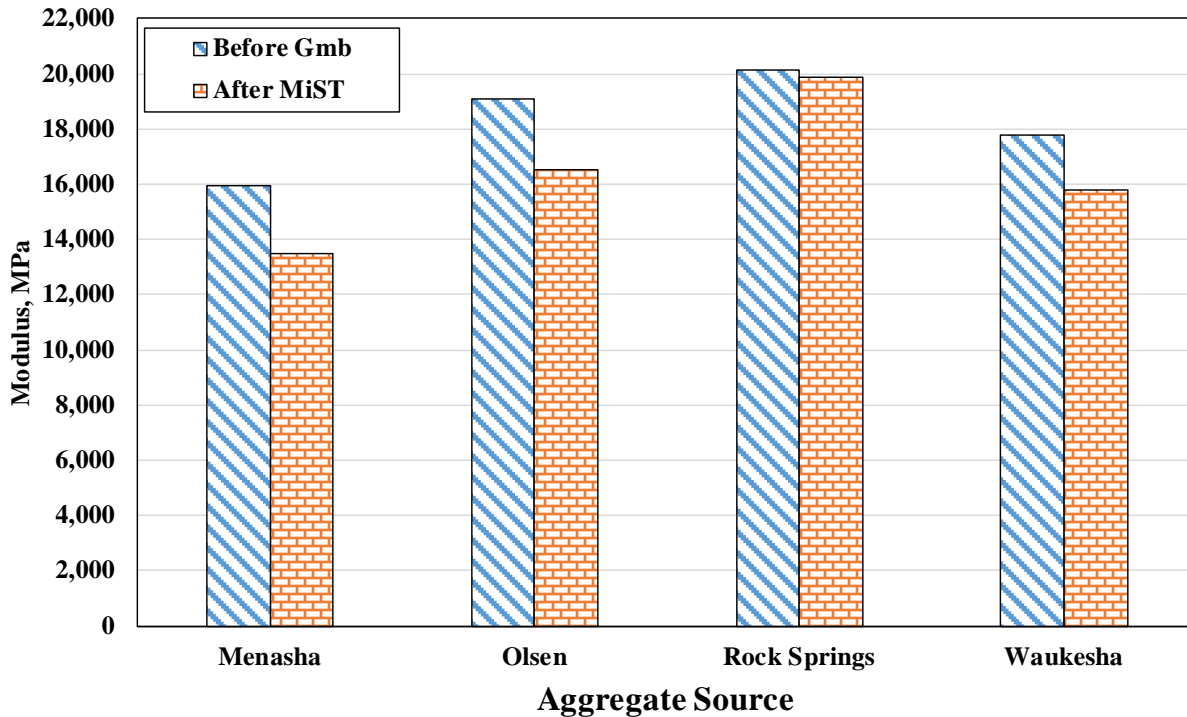


Figure 26 Modulus after MiST conditioning (condition 5) versus initial modulus

Dried Samples

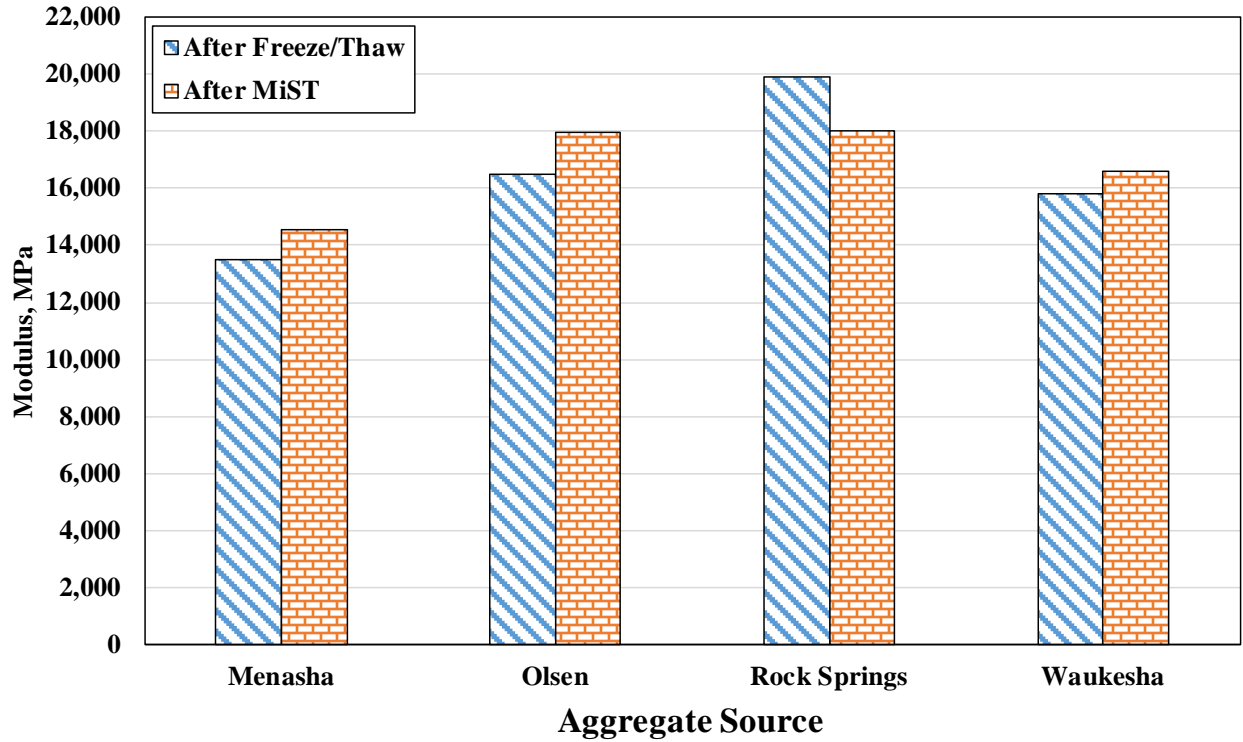


Figure 27 Comparison between effect of freeze/thaw and MiST conditioning on moduli (Condition 5)

COMPARISON OF THE RESULTS WITH IDT DM RESULTS

It was discussed that change of specimen modulus as a result of moisture conditioning was measured using both the IDT DM test and the UPV test. For each case, the term modulus ratio can be defined as presenting the ratio of retained modulus to the original modulus (Equation 3). A comparison of this modulus ratio is presented in Figure 28 for these two methods of testing. The scatter plots in Figures 29 and 30 indicate the strong correlation between the modulus ratio from the UPV test and the modulus ratio from the dynamic modulus test. Note should be made that the first graph presents the MiST-conditioned specimens and the second graph the freeze/thaw conditioned specimens. A detailed comparison for each source is presented in Appendix F.

$$\text{Modulus Ratio} = \frac{\text{Modulus after Conditioning}}{\text{Modulus before Conditioning}} \quad (3)$$

As can be noticed, the MR for UPV is significantly higher than the MR from IDT DM measurements, except for MiST conditioning on samples from the Waukesha aggregates source. For this case, both UPV and IDT DM result in the same MR. The fact that MR from UPV is higher than that of IDT DM is most probably the result of vastly different strain levels utilized in these two techniques of testing. Strain levels from UPV are significantly smaller and loading frequencies are much higher than those used in

IDT DM, resulting in significantly higher modulus values. The higher strain level of IDT DM and the lower loading frequency in this test can account for more of the induced damage.

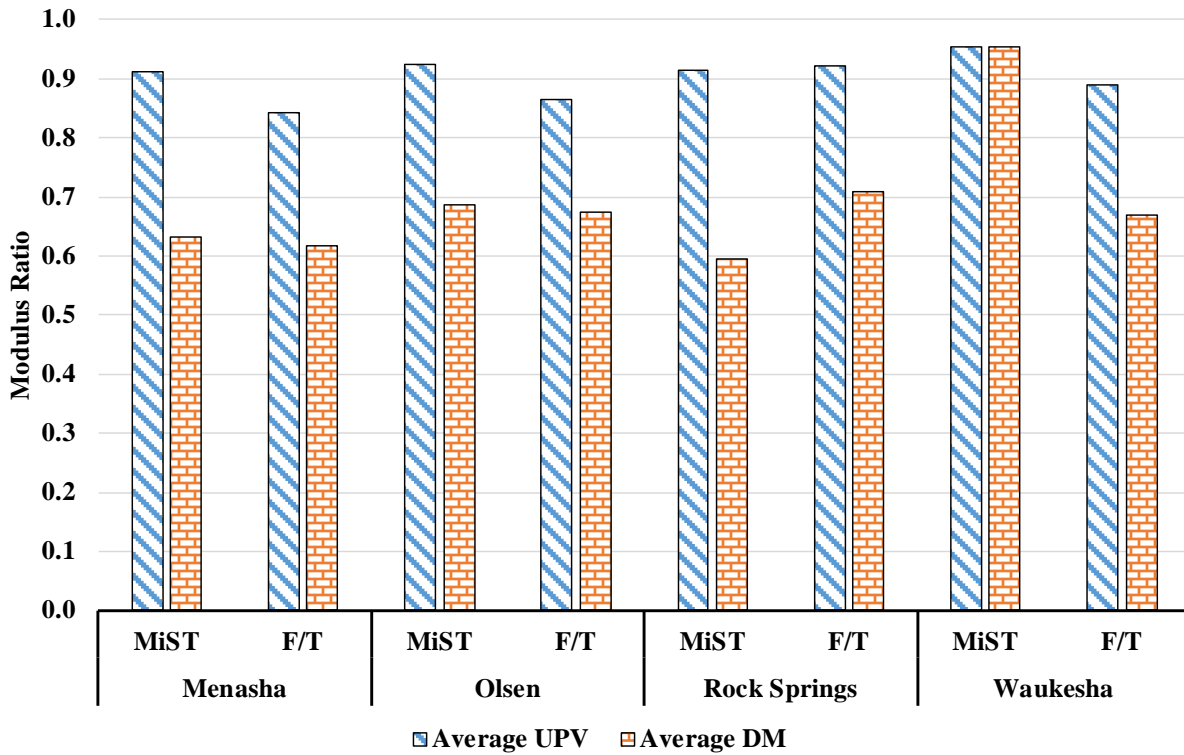


Figure 28 Comparison of the modulus ratio of UPV and IDT DM based on the conditioning technique

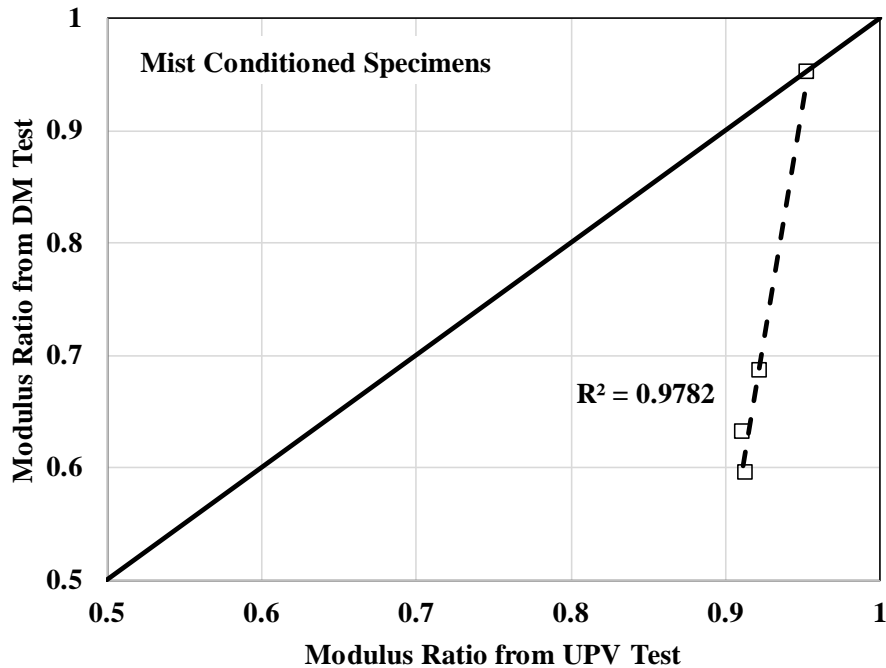


Figure 29 Comparison of modulus ratio from UPV and DM tests for MiST-conditioned specimens

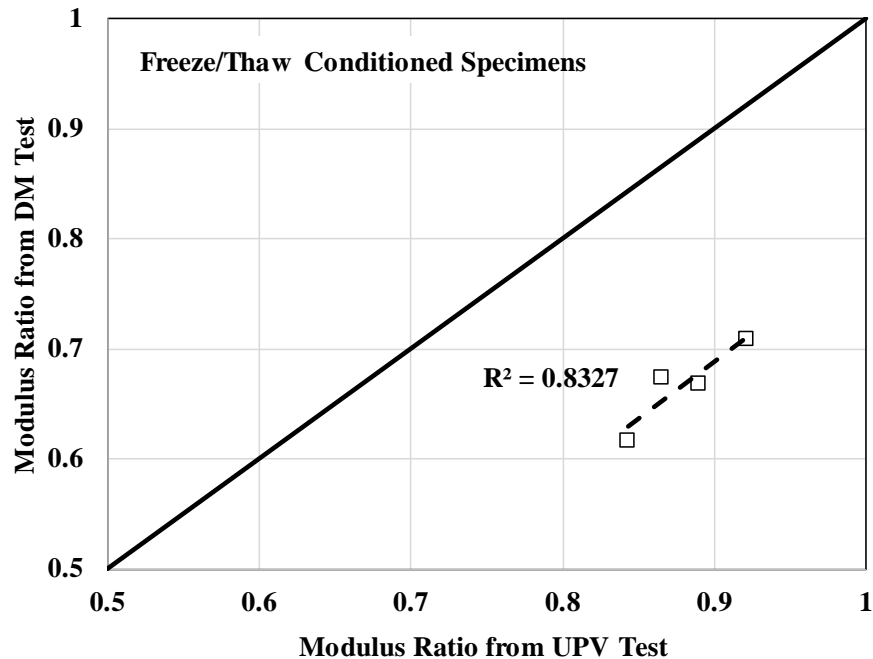


Figure 30 Comparison of modulus ratio from UPV and DM tests for freeze/thaw conditioned specimens

MOISTURE DAMAGE MITIGATION

An important part of this research was to investigate means of improving the moisture damage resistance of mixes in case the proposed testing protocols were indicative of poor performance. It was previously discussed that four different moisture conditioning schemes were utilized in this research. The plan for moisture damage mitigation was to change one or several mix parameters and subject the mix to a selected moisture conditioning and testing protocol to measure the effect of the change. The project time and budget constraints did not allow such sensitivity analysis for mixes from all four sources and using all conditioning and testing protocols that were employed during the full testing matrix. Therefore, the study was limited to three selected mixes and testing only with the Hamburg Wheel Tracking Device. The wheel tracking was selected for sensitivity analysis as one of the most reliable and conservative tests to evaluate the moisture damage effect. Furthermore, WisDOT has recently been utilizing wheel tracking for testing several mixes used in the state, and results from those tests could be used as reference in case there is future need for comparison.

The following measures were considered to study how the moisture damage could be reduced for the mixes studied in this research:

1. Binder Grade and Binder/Aggregate Compatibility
2. Aggregate Type Effect
3. Use of Liquid Antistripping Agent
4. Use of Hydrated Lime
5. Replacement of Material Passing #100 Sieve

The asphalt mixes selected for this part of the study included material from Menasha, Waukesha, and Rock Springs. Three liquid antistrip agents were considered: Ingevity P75, Ingevity P25, and PreTech Industries Pavegrip 300. The plan was to start with the P75 antistripping agent, and if not successful, continue using the next agent. The P75 antistripping agent is a warm-mix additive and has been specially formulated for one of the Wisconsin siliceous aggregate sources. The P25 agent is also a warm-mix asphalt additive and has been used in the Northeast region. The Pavegrip 300 has been promoted as a high-performance antistrip additive.

The experiment with the Rock Springs material only included using the P75 antistrip agent. The dosage rate was 0.4% by the mass of total binder. The antistrip agent was added to the virgin binder (PG 58S-28) following the manufacturer’s recommended blending process. Testing with HWTD was conducted and results indicated significant improvement in the outcome for all performance measures (Table 15 and Figure 31). Since the P75 additive resulted in significant improvement and excellent performance, no further modifications were made to the mix. Note should be made that calculation of stripping inflection point (SIP) is meaningful only if an inflection point exists and the slope of the second portion of the curve is larger than the first portion.

Table 15 Effect of liquid antistrip on moisture damage resistance for Rock Springs aggregate

Additive/Change	Maximum Rut Depth, mm	SIP	Strip/Creep Ratio	# of Passes to 10 mm Rut Depth	Rut Depth at 10,000 Passes, mm
None PG 58S-28	18.8	16,415	6.3	18,706	4.8
P75 Antistrip PG 58S-28	5.9	>22,000	0.8	63,144	3.9

The next set of experiments included materials from Menasha and Waukesha. Evaluation with the Waukesha aggregate was limited to the change of binder grade. However, evaluation with the Menasha aggregate was comprehensive, covering a range of changes to improve moisture damage resistance, as this was the mix showing the most level of susceptibility to moisture damage.

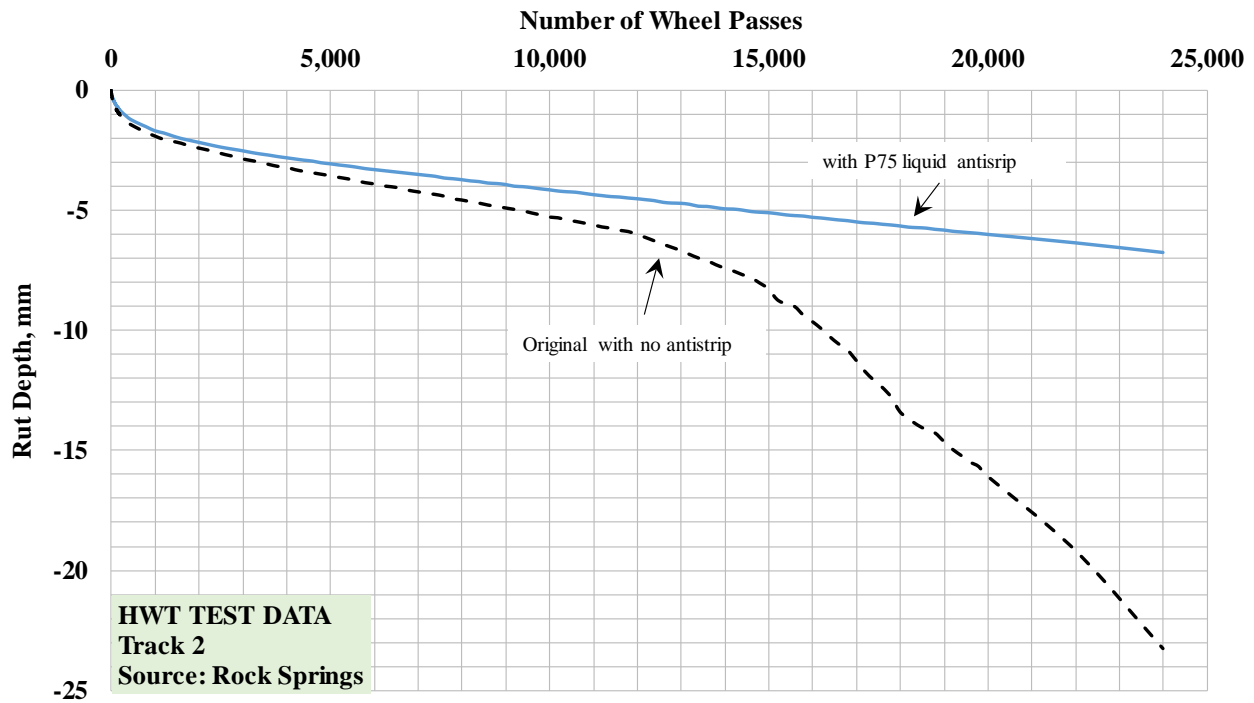


Figure 31 Performance of Rock Springs mix after modification with P75 antistripping agent

The first experiment with these two mixes consisted of replacement of the PG 58-28WF binder with a PG 64-22 binder, which is used as a standard binder at NECEPT. Specimens were made and subjected to testing under HWTD at 46 °C. Results manifested significant improvement in performance, an indication of the importance of binder in moisture damage resistance (Table 16 and Figures 32 and 33).

Table 16 Effect of binder grade on HWTD test results

Binder/Source	Rut Depth, mm	SIP	Strip/Creep Ratio	# of Passes to 10 mm Rut Depth	Rut Depth at 10,000 Passes, mm
PG 58-28WF Menasha	22.0	11,777	4.4	15,192	5.2
PG 64-22 Menasha	5.8	17,743	1.1	49,895	3.6
PG 58-28WF Waukesha	17.4	15,515	4.8	18,347	4.9
PG 64-22 Waukesha	7.3	15,635	1.5	33,300	3.65

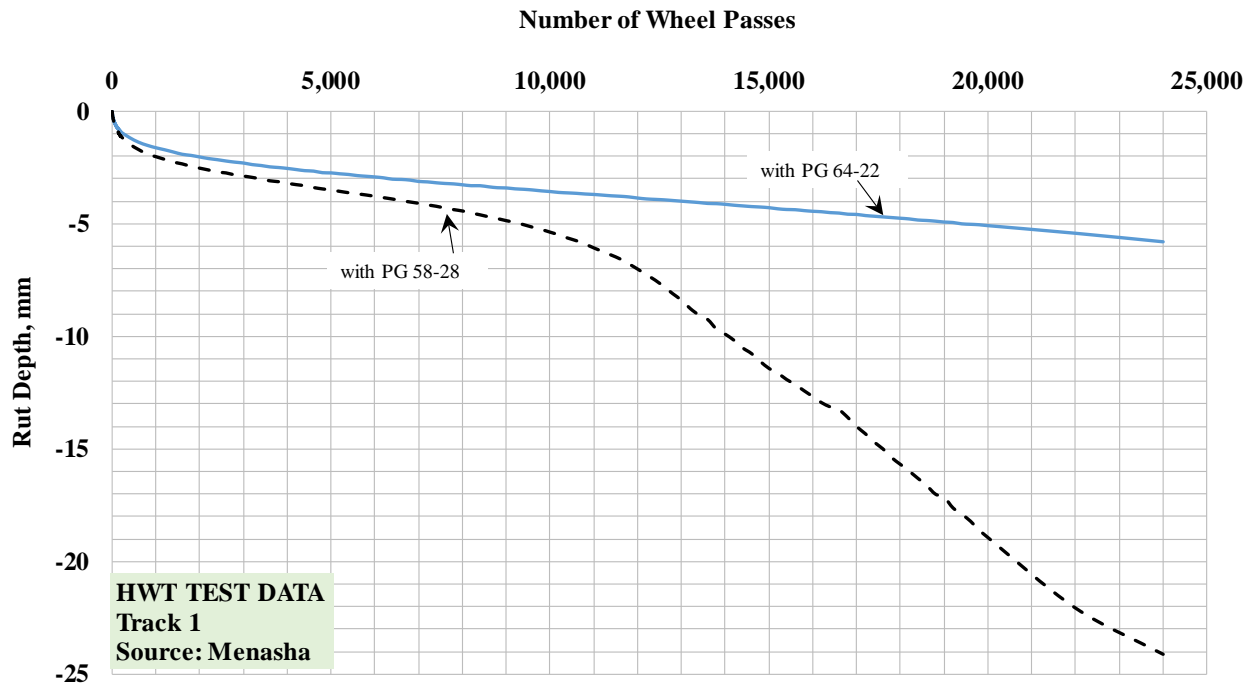


Figure 32 Results from HWT D for the Menasha source with PG 64-22

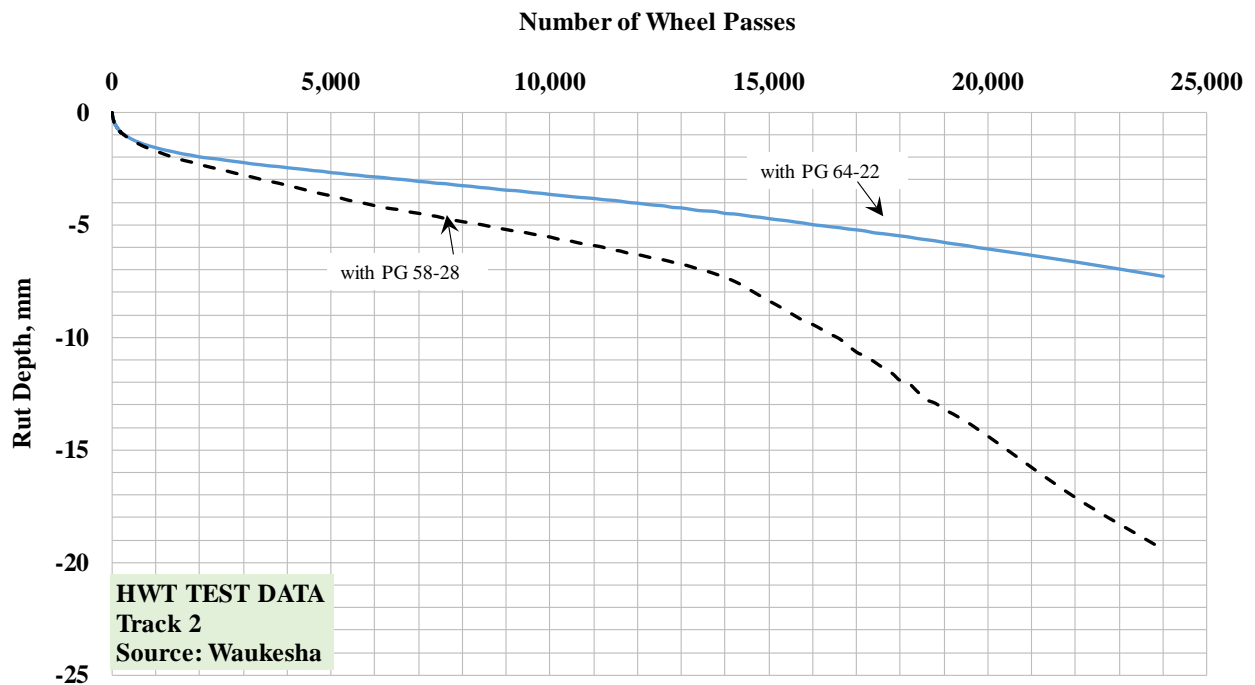


Figure 33 Results from HWT D for the Waukesha source with PG 64-22

For comparison, specimens were also made for a typical Superpave 9.5-mm mix with local aggregate (dolomite/limestone) using two different binders: the PG 64-22 binder and the PG 58-28WF binder that was received for use with the Menasha/Waukesha aggregates. These specimens were subjected to wheel tracking

at 46 °C. Results are presented in Table 17 and Figure 34. These two mixes performed better than the original mixes using Menasha/Waukesha aggregates and PG 58-28WF. One reason for such a significant improvement could be because of compatibility between the binder and the aggregate in the presence of water. However, one cannot ignore the fact that mix design and aggregate gradation might have contributed to the difference observed. It must also be noted that the mix with the local limestone aggregate and the PG 64-22 binder demonstrated better performance compared with the mix having the same aggregate but with the PG 58-28WF.

Table 17 HWTD test results with a local limestone aggregate and two different binders

Binder	Rut Depth, mm	SIP	Strip/Creep Ratio	# of Passes to 10 mm Rut Depth	Rut Depth at 10,000 Passes, mm
PG 58-28WF	5.6	19,907	10.7	23,571	3.7
PG 64-22	2.9	>22,000	1.0	171,762	2.2

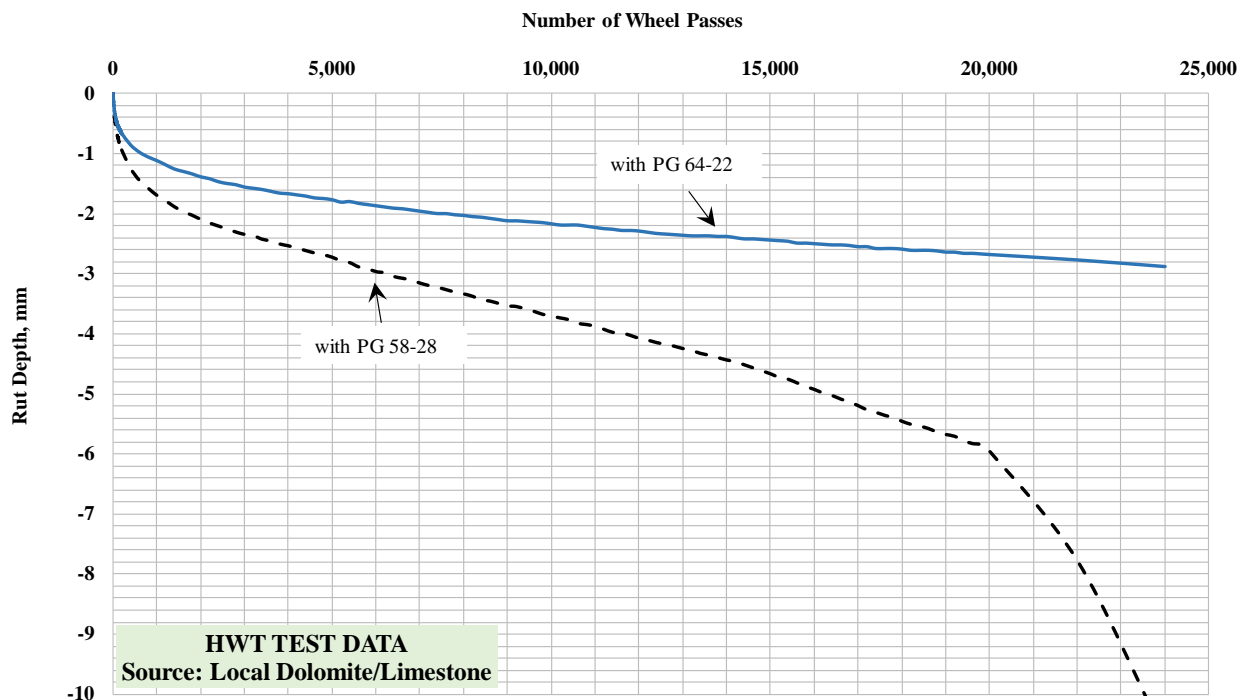


Figure 34 Results of HWTD test under wet conditions with local limestone at 46 °C with PG 58-28WF and PG 64-22

Attention was next placed on improving performance of the Menasha mix through several measures outlined previously. Results of different experiments using these measures are presented in Table 18. In

general, improvement was observed for all measures compared to the control mix even though not to a significant level. Associated graphs are presented in Appendix D due to space constraints.

Table 18 Results of HWTD test with Menasha aggregate under different conditions at 46 °C

Additive/Change	Maximum Rut Depth, mm	SIP	Strip/Creep Ratio	# of Passes to 10 mm rut depth	Rut depth at 10,000 passes, mm	Stripping Slope (mm/1,000 passes)
None PG 58-28WF	22.0	11,777	4.4	15,192	5.2	1.36
P75 PG 58-28WF	20.1	14,988	4.5	16,698	5.7	1.71
P25 PG 58-28WF	19.8	13,898	3.9	16,535	5.3	1.32
Lime PG 58-28WF	15.6	14,558	4.2	18,368	4.5	1.11
P75 PG 58S-28	15.8	15,171	3.7	18,674	5.0	1.02
Pavegrip™ 300 PG 58-28WF	19.9	12,345	4.1	16,129	5.2	1.21
P75 PG 58-28WF & Replacement of - #100	16.3	15,687	4.1	19,026	4.7	1.12

SUMMARY OF RESULTS

The amount of data generated in this research when combined with past data generated by WisDOT provides a strong database for deciding suitable tests and developing criteria to be used in the mix design stage and related specifications. Ranking of mixes based on different tests and parameters used in this research are presented in Table 19. Results from various tests and conditioning protocols do not necessarily rank the mixes in the same way with respect to moisture damage susceptibility. This is expected, as the mix response to different combinations of conditioning and testing processes will not be the same. In other words, the most likely reason for inconsistency in ranking is associated with the mechanism of inducing moisture damage in different tests and conditioning systems. The question to be answered is, which of the combinations provides the most reliable condition for predicting the mix performance in the field with respect to moisture damage.

A simple approach was developed to consider all rankings and combine them to deliver a final score for each mix, without consideration for severity of the damage for each case. In this approach, for a specific test result (for example, as ranked based on TSR), the mix with the least susceptibility to moisture damage among the four mixes was given a score of four, and the mix with the highest potential for moisture was given a score of one. Then, the scores from all ranking parameters were summed together. Based on this system of grading, scores of 93, 79, 75, and 53 were obtained for Rock Springs, Waukesha, Olsen, and Menasha, respectively. Such grading yields the following order from the least sensitive to the most sensitive with respect to moisture damage: Rock Springs, Waukesha, Olsen, and Menasha. This simple ranking sets the Rock Springs and Waukesha as better performing mixes compared with Olsen and Menasha. This grouping does not exactly match the JMF TSR, which sets all as passing mixes except Menasha. Nor does this ranking match the TSR findings of this research for both freeze and no-freeze options. While this ranking does not match the TSR of this research, it does correlate strongly with the ranking based on the wet strength of mixes from the indirect tensile test with the no-freeze cycle. This is an important conclusion and clarifies the reason for discrepancy between HWTD results and TSR results with the no-freeze cycle. TSR simply defines the ratio of strengths before and after conditioning and does not directly address the strength level of the mix. The HWTD test simulates load/water interaction with the mix under repeated loading, for which the results are heavily strength dependent.

It is worth exploring whether it makes more sense to base the moisture damage sensitivity of a mix on a combination of TSR and wet strength (or dry strength) rather than basing it solely on TSR. For example, when comparing wet strength and TSR of the Rock Springs mix with the other three mixes for the 60-mm specimens, TSR values are comparable, ranging between 0.67 to 0.77. However, the Rock Springs mix, despite having a comparable TSR to other mixes, has a significantly high wet strength and higher resistance to moisture damage.

The proposed ranking of these four mixes almost matches the ranking given by maximum rut depth from the HWTD test under submerged conditions. This ranking also almost matches the ranking based on the number of passes required to reach 10 mm of rut depth in the submerged HWTD test. The ranking also matches that based on stripping inflection point under submerged conditions. Finally, this ranking closely matches that given by dynamic modulus ratio and UPV modulus ratio based on the freeze/thaw conditioning.

Table 19 Ranking of mixes with respect to moisture damage susceptibility

	Parameter	Condition	1	2	3	4
Indirect Tensile Test	Indirect Tensile Strength	Wet No Freeze, 95 mm	R	M	W	O
		Wet Freeze, 95 mm	R	O & W same		M
		Wet Freeze, 60 mm	R	W	M & O same	
		MiST-IDT-DM	R	W	O	M
	Tensile Strength Ratio (TSR)	Wet No Freeze, 95 mm	R	M & W same		O
		Wet Freeze, 95 mm	O	W	R	M
		Wet Freeze, 60 mm	O	W	R	M
		Wet Freeze after IDT DM, 60 mm	O	W	R	M
		MiST after IDT DM, 60 mm	O	W	R	M
	HWTD Test	Max. Rut Depth, mm	Submerged	W	R	O
After MiST			R	M	O	W
Dry			O	M	R	W
SIP		Submerged	R	W	M	O
		After MiST	O	W	R	M
Strip/Creep Slope ratio		Submerged	W	M	R	O
		After MiST	O	R	M	W
Passes to 10 mm Rut		Submerged	R	W	M	O
		After MiST	R	O	M	W
		Dry	O	R	M	W
Rut Depth at 10,000 passes	Submerged	R	W	M	O	
	After MiST	R & W & M same			O	
IDT DM	Wet Modulus	After Freeze/Thaw	R	W	O	M
		After MiST	W	O	R	M
	Modulus Ratio	After Freeze/Thaw	R	W & O		M
		After MiST	W	O	M	R
UPV	Wet Modulus	After Freeze/Thaw	R	O	W	M
		After MiST	R	O	W	M
	Modulus Ratio	After Freeze/Thaw	R	W	O	M
		After MiST	W	M & R & O same		
Note on Acronyms: M (Menasha), O (Olsen), R (Rock Springs), and W (Waukesha)						

CHAPTER FOUR

Summary, Conclusions and Recommendations

SUMMARY

This research was undertaken with the goal of identifying suitable test protocols to assess the moisture damage potential of asphalt concrete mixes placed in the State of Wisconsin. To achieve this goal, specific mixes and materials were carefully selected by the Project Oversight Committee. Two of the mixes were from dolostone sources, one with high tensile strength ratio based on AASHTO T 283 and one with low tensile strength ratio. The other two were siliceous with marginal to poor field performance. A battery of conditioning procedures and tests were conducted on the selected mixes, and results were analyzed to determine the potential of the applied protocols for identifying the quality of tested mixes with respect to moisture damage resistance. Specific response parameters were analyzed from each conditioning and testing scheme. The response parameter after moisture conditioning was compared with that before conditioning with the objective of evaluating the capability of the procedure in manifesting the susceptibility of the mix to moisture damage. Table 20 shows response parameters, conditioning procedures, and mechanical tests investigated in this study.

Table 20 Summary of materials, tests, and response parameters in this study

Response Parameter	Conditioning	Test
Strength	Dry Hot Water/No Freeze, Freeze/Thaw, and MiST	Indirect Tensile
Modulus	Freeze/Thaw MiST	Indirect Tensile and UPV
Rutting	Dry, Hot Water/No Freeze, Freeze/Thaw, and MiST	HWT
Number of Cycles to Specified Rut Depth	Dry, Hot Water/No Freeze, Freeze/Thaw, and MiST	HWT
Ratio of Stripping Slope to Creep Slope	Dry, Hot Water/No Freeze, Freeze/Thaw, and MiST	HWT
Creep Slope for 1,000 Wheel Passes	Dry, Hot Water/No Freeze, Freeze/Thaw, and MiST	HWT

CONCLUSIONS

Based on the test results it was found that the conditioning and test protocols investigated in this research do not all rank the mixes in the same order with respect to moisture damage sensitivity. It is concluded that the most possible reason for inconsistency in ranking is associated with the mechanism of inducing moisture damage in different tests and conditioning systems. A simple approach was proposed to consider all rankings and combine them to deliver a final score for each mix, without consideration for severity of the damage for each case. Such grading yields the following order, from the least sensitive to the most sensitive with respect to moisture damage: Rock Springs, Waukesha, Olsen, and Menasha.

Results from AASHTO T 283 with the no-freeze group compare well with the values presented in the job mix formula for the Rock Springs and Menasha mixes, showing these two with good and marginal performance, respectively. However, the results do not compare well with the JMF TSR results for the Waukesha and Olsen mixes. Results also indicate that inclusion of the freeze cycle increases the level of damage and generally results in lower TSR.

The preceding ranking of the mixes almost matches the ranking given by the following parameters from HWTD testing under submerged test conditions: maximum rut depth, the number of passes required to reach 10 mm of rut depth, and the stripping inflection point. Finally, this ranking closely matches that given by dynamic modulus ratio and UPV modulus ratio based on the freeze/thaw conditioning.

The results from dynamic modulus testing indicated that both the MiST conditioning and freeze/thaw conditioning result in reduction of the mix modulus. However, it was generally found that the reduction was more severe when the freeze/thaw cycle was used. Similarly, the results from UPV testing also captured the effect of these two conditioning systems, as a reduction in UPV modulus was observed. It was also demonstrated that the presence of water in the specimens can affect the estimated moduli by UPV, resulting in higher moduli. The modulus ratio from the UPV tests was generally higher than that from dynamic modulus tests because the UPV testing was based on extremely small levels of strain and probably not capturing the induced damage to the same level as the dynamic modulus test is.

RECOMMENDATIONS

Selection of Test Protocol and Conditioning

Mix conditioning according to the AASHTO T 283 protocol, MiST, and Hamburg wheel tracking all are reasonable approaches to inducing moisture damage. However, attention must be paid to these methods with the respect to their ability to simulate field conditions. HWTD and MiST are better systems with respect to simulating the moisture damage in the field, as both induce suction and pressure into the mix under repeated cycles. The HWTD presents itself as the most severe in terms of inducing damage, and the results must be

interpreted accordingly. It may be appropriate to follow a tiered system of testing, for example to apply HWTD and MiST for roads with higher traffic volumes and AASHTO T 283 protocol for roads with lower traffic volumes. AASHTO T 282 is recommended for lower-volume roads, as the test requires simpler and less costly equipment compared with HWTD and is readily available in most laboratories of producers and state highway agencies. It is highly recommended that HWTD be included in the specifications for mix design, at least for heavy-duty projects. For those projects that require HWTD testing, there should not be any need for indirect tensile testing, as the results from HWTD are more reliable. It is also reasonable to explore the use of HWTD for the purpose of quality control during production. Current quality assurance/quality control procedures are widely based on mix design parameters (asphalt content, gradation, etc.) and compaction level, and the procedures lack any reliable performance test. HWTD is among the performance tests that should be investigated to fill this gap.

Finally, conditioning through MiST is very promising, and it has the potential to be included in specifications once further information is gathered on the system. It is recommended that work with this device should continue to collect more information. The process has great potential to be included in specifications.

In case performance prediction is considered using design guides such as AASHTO Pavement ME, consideration should be given to indirect tensile dynamic modulus testing, as it provides an essential engineering property which is an input to performance prediction models. The reduced modulus from moisture damage could be an input to the model to indicate possible increase in distress levels as a result of moisture damage. Finally, while ultrasonic pulse velocity proved capable of manifesting the modulus drop for both MiST-conditioned and freeze/thaw-conditioned specimens, the drops were not at the same level of modulus recorded from the indirect tensile test. Further research is needed to establish the UPV test for routine operation and inclusion in asphalt testing specifications.

Establishing Criteria

It was shown through comparison with HWTD test results that use of TSR by itself may be misleading. It is appropriate to consider TSR along with a minimum requirement on wet strength of the mix. Table 21 presents recommendations for consideration.

Table 21 Using combination of TSR and wet strength as pass/fail criteria

Conditioning (AASHTO T 283)	Minimum TSR	Minimum Tensile Strength (Wet), psi
No Freeze Cycle	0.80	70.0
With Freeze Cycle	0.75	65.0

In establishing criteria for accepting or rejecting a mix based on laboratory test results, one cannot ignore the impact of climate and traffic. A test protocol that might prove reliable in distinguishing between good and

poor performance of mixes in the field for certain climatic and traffic conditions may deliver false positive or negative results for an environment with different conditions. As the results presented in this report are provided for the State of Wisconsin, the impact of climate in connecting these results to field performance is accounted for to some extent. However, traffic should be factored into establishing design threshold values for moisture damage resistance of the mix. It is expected that a mix in a high-traffic location will be exposed to higher level of moisture-induced damage and distress compared to the same mix placed in a low-traffic environment, even under the same climatic conditions. Hence, it is warranted to tie the criteria for passing and failing a mix with respect to moisture damage to the expected traffic level. For example, the criteria presented in Table 22 could be used. It must be noted that the values presented in the table are examples based on the results obtained in this research. Comparison with field performance and validation of results is a definite need before implementing any criteria such as the ones presented in Table 22. As shown in this table, if the maximum rut depth does not exceed 10 mm after 20,000 cycles, there is little need to have any other check on the mix. If the maximum rut depth exceeds 10 mm, it will be wise to include further criteria such as SIP, strip/creep ratio, and number of passes to 10-mm rut depth. The results from HWTD tests in this research show that the strip/creep ratios for all mixes exceed 4.4. It is reasonable to use this criterion only if SIP is low. If SIP occurs at a very high number of wheel passes, then one wonders if the slope ratio should be included as a criterion even if it is excessively high. Inclusion of this ratio may lead to rejection of the mix despite high SIP and low rut depth. For example, for the Rock Springs and Waukesha mixes, the SIP is roughly 16,500 and 15,550, respectively, whereas the slope ratio is 6.3 for the former and 4.8 for the latter. At these high levels of SIP, even with high ratios of slope, the mix should not behave poorly.

Table 22 Conceptual criteria based on HWTD test in submerged condition

Traffic Level, (millions of ESALs)	Max. Rut Depth at 20,000 passes (mm)	SIP (minimum)	Strip/Creep Ratio (maximum)	Passes to 10-mm Rut (minimum)
≥ 8	10			
	15	16,000	2.0	15,000
≥ 2 and <8	10			
	15	14,000	2.0	12,000
	20	16,000	3.0	14,000
<2	15			
	20	14,000	3.0	10,000
	25	16,000	4.0	12,000

References

- AASHTO (2014), AASHTO T 283-14: Standard Method of Test for Resistance of Compacted Asphalt Mixtures to Moisture-Induced Damage. American Association of State Highway and Transportation Officials, Washington, D.C.
- AASHTO (2018), AASHTO TP 131-18: Proposed Standard Test Method for Determining the Dynamic Modulus of Asphalt Mixtures Using the Indirect Tension Test. American Association of State Highway and Transportation Officials, Washington, D.C.
- ASTM International (2016), ASTM C597-16: Standard Test Method for Pulse Velocity Through Concrete. ASTM International, West Conshohocken, PA.
- Arabani, M., & Kheiry T. P. (2006). A new method for determination of stiffness modulus of HMA mixtures, *ISSA world Congress and International seminar on Asphalt Pavement Maintenance Technologies*, Beijing, China.
- Birgisson, B., Roque, R., & Page, G. (2003). Ultrasonic pulse wave velocity test as a tool for monitoring changes in HMA mixture integrity due to exposure to moisture, *Journal of Transportation Research Record*, 1832, 173-181.
- Tomsett, H. N. (1980). The Practical Use of Ultrasonic Pulse Velocity Measurements in the Assessment of Concrete Quality, *Magazine of Concrete Research*, ISSN 0024-9831 | E-ISSN 1751-763X, Volume 32 Issue 30, 7-16.
- Cheng, Y. C., Zhang, P., Jiao, Y., Wang, Y., & Tao, J. (2013). Damage Simulation and Ultrasonic Detection of Asphalt Mixture under the Coupling Effects of Water-Temperature-Radiation, *Advances in Materials Science and Engineering*, <http://dx.doi.org/10.1155/2013/838943>, 9 pages.
- Hicks, R. G. (1991). "Moisture Damage in Asphaltic Concrete," *NCHRP Synthesis of Highway Practice 175*, Transportation Research Board, Washington, D.C.
- Kheiry, P. T., Boz, I., Chen, X., & Solaimanian, M. (2017). Application of Ultrasonic Pulse Velocity Testing of Asphalt Concrete Mixtures to Improve the Prediction Accuracy of Dynamic Modulus Master Curve. *Proceedings, Airfield and Highway Pavements*, 152-164.
- Kim, R.Y., Youngguk, S., King, M., & Momen M. (2004). Dynamic Modulus Testing of Asphalt Concrete in Indirect Tension Mode, *Journal of Transportation Research Record*, 1891, 163-173.
- Little, D.W., Lytton, R. L., Kim Y.R., & Kim, Y. (2001). Microdamage Healing in Asphalt and Asphalt Concrete, FHWA Final Report, Vol. 2, Report No. FHWA-RD-98-142, Texas Transportation Institute, Texas A & M University.
- Moreno-Navarro, F., Sol-Sánchez, M., & Rubio-Gámez, M.C. (2015). Exploring the recovery of fatigue damage in bituminous mixtures: the role of healing, *Journal of Road Materials and Pavement Design*, 16:sup1, 75-89, DOI: [10.1080/14680629.2015.1029706](https://doi.org/10.1080/14680629.2015.1029706).
- Panzer, A.L., F.P. Christoforo, F.P. Cota, P.H. R. Borges, & C.R. Brown (2011). Ultrasonic Pulse Evaluation of Cementitious Materials, *Advances in Composite Materials*, Analysis of Natural and Man-Made Materials, DOI: 10.5772/728, ISBN: 978-953-307-449-8.

- Solaimanian, M., Harvey, J. Tahmoressi, M. & Tandon, V. (2003). Test Methods to Predict Moisture Sensitivity of Hot-Mix Asphalt Pavements, *Proceedings, Symposium on Moisture Sensitivity of Asphalt Pavements*, San Diego, CA, Transportation Research Board, CD-ROM, pp. 77–110.
- Wong, R. C. K., Schmitt D. R., Collis, D. & Gautam, R. (2008). Inherent transversely isotropic elastic parameters of over-consolidated shale measured by ultrasonic waves and their comparison with static and acoustic in situ log measurements. *Journal of Geophysics and Engineering* 5(1): 103-117, DOI: 10.1088/1742-2132/5/1/011
- Yurikov, A., Nourifard, N., Pervukhina, M., & Lebedev, M. (2019). Laboratory ultrasonic measurements: Shear transducers for compressional waves. *The Leading Edge*, 38(5), 392-399.

APPENDIX A

Submitted Job Mix Formulas and Design Gradations

Table A-1 Gradation of Individual Stockpiles based on Dry Sieve Analysis - Menasha

		Menasha Plant - NECEPT - Before Wash					
Sieve Size		5/8"	1/2"	Mfg Sand	Nat Sand	RAP	RAS
1"	25mm	100	100	100	100	100	100
3/4"	19mm	100	100	100	100	100	100
1/2"	12.5mm	75.8	100	100	100	99.9	99.5
3/8"	9.5mm	10.6	94.4	100	100	96.8	98.6
#4	4.75mm	3.3	15.1	96.4	96.8	77.1	86.6
#8	2.36mm	1.0	2.1	64.6	86.5	54.5	74.3
#16	1.18mm	0.9	1.7	40.8	77.3	34.5	52.3
#30	0.6mm	0.9	1.6	27.6	62.2	19.8	31.8
#50	0.3mm	0.9	1.5	14.8	24.3	7.2	18.5
#100	0.15mm	0.9	1.4	4.8	3.0	2.6	7.6
#200	0.075mm	0.8	1.3	1.6	0.6	1.2	2.6

Table A-2 Gradation of Individual Stockpiles based on Washed Sieve Analysis - Menasha

		Menasha Plant - NECEPT - After Washing			
Sieve Size		5/8"	1/2"	Mfg Sand	Nat Sand
1"	25mm	100	100	100	100
3/4"	19mm	100	100	100	100
1/2"	12.5mm	75.2	100	100	100
3/8"	9.5mm	11.8	94.5	100	100
#4	4.75mm	4.0	15.8	95.1	97.0
#8	2.36mm	3.8	3.5	64.4	86.7
#16	1.18mm	3.7	3.1	41.3	77.1
#30	0.6mm	3.7	3.0	26.7	60.4
#50	0.3mm	3.7	2.8	13.6	22.5
#100	0.15mm	3.7	2.7	5.2	2.9
#200	0.075mm	3.7	2.6	2.7	0.9

Table A-3 Gradation of Individual Stockpiles based on Dry Sieve Analysis - Waukesha

Sieve Size		Waukesha - NECEPT - Before Wash				
		5/8"	3/8"	Mfg Sand	Nat Sand	RAP
1"	25mm	100	100	100	100	100
3/4"	19mm	100	100	100	100	100
1/2"	12.5mm	92.0	100	100	100	100
3/8"	9.5mm	21.1	93.3	100.0	100.0	95.2
#4	4.75mm	1.4	5.3	86.0	95.7	65.9
#8	2.36mm	1.1	2.3	55.3	88.9	43.4
#16	1.18mm	1.1	1.6	34.2	82.2	26.7
#30	0.6mm	1.0	1.5	20.9	66.6	14.2
#50	0.3mm	1.0	1.4	11.2	19.1	4.4
#100	0.15mm	0.9	1.4	5.2	2.2	1.5
#200	0.075mm	0.8	1.3	2.7	0.8	0.6

Table A-4 Gradation of Individual Stockpiles based on Washed Sieve Analysis - Waukesha

Waukesha - NECEPT - After Washing					
Sieve Size		5/8"	3/8"	Mfg Sand	Nat Sand
1"	25mm	100	100	100	100
3/4"	19mm	100	100	100	100
1/2"	12.5mm	93.5	100	100	100
3/8"	9.5mm	24.6	93.9	100	100
#4	4.75mm	2.4	6.5	86.7	95.7
#8	2.36mm	2.1	3.3	56.0	88.9
#16	1.18mm	2.0	2.6	34.8	82.2
#30	0.6mm	2.0	2.5	21.6	66.7
#50	0.3mm	2.0	2.5	11.9	19.7
#100	0.15mm	2.0	2.4	6.1	2.2
#200	0.075mm	1.9	2.4	3.7	0.8

Table A-5 Gradation of Individual Stockpiles based on Dry Sieve Analysis – Rock Springs

		Rock Springs - NECEPT - Before Wash					
Sieve Size		3/4"	3/8"	3/16" Manf. Sand	1/4" Manf. Sand	5/8" Screened Sand	RAP
1"	25mm	100	100	100	100	100	100.0
3/4"	19mm	100	100	100	100	100	100.0
1/2"	12.5mm	86.3	100	100	100	98.8	100.0
3/8"	9.5mm	59.5	100	100	100	97.0	85.1
#4	4.75mm	18.3	20.3	100.0	97.2	93.4	62.5
#8	2.36mm	8.2	3.2	79.8	81.3	90.9	45.3
#16	1.18mm	5.0	0.8	51.0	62.8	88.8	32.6
#30	0.6mm	3.9	0.5	30.1	47.2	82.4	20.5
#50	0.3mm	3.3	0.4	12.8	26.8	39.6	7.7
#100	0.15mm	2.5	0.3	2.9	3.5	4.4	2.5
#200	0.075mm	1.8	0.3	1.2	1.3	1.1	1.0

Table A-6 Gradation of Individual Stockpiles based on Washed Sieve Analysis – Rock Springs

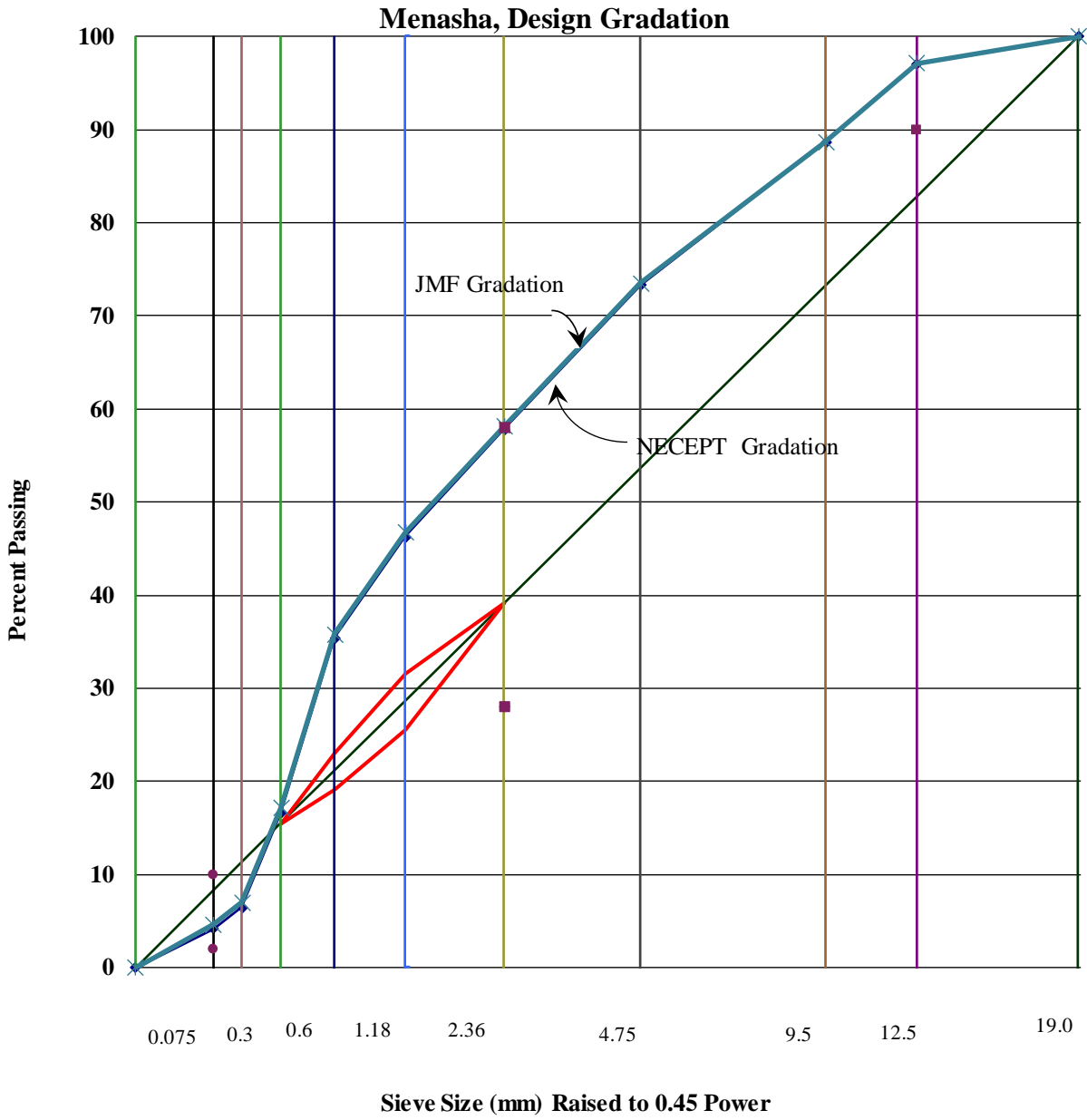
		Rock Springs - NECEPT - After Washing				
Sieve Size		3/4"	3/8"	3/16" Manf. Sand	1/4" Manf. Sand	5/8" Screened Sand
1"	25mm	100.0	100.0	100.0	100.0	100.0
3/4"	19mm	100.0	100.0	100.0	100.0	100.0
1/2"	12.5mm	91.0	100.0	100.0	100.0	98.8
3/8"	9.5mm	61.7	100.0	100.0	100.0	97.0
#4	4.75mm	20.6	24.9	99.9	97.4	93.4
#8	2.36mm	8.6	3.4	79.7	81.5	91.0
#16	1.18mm	5.3	1.0	51.0	63.1	88.8
#30	0.6mm	4.3	0.6	30.2	47.7	82.4
#50	0.3mm	3.7	0.5	12.9	27.6	38.3
#100	0.15mm	3.0	0.5	3.4	4.7	5.1
#200	0.075mm	2.3	0.4	1.7	2.3	1.6

Table A-7 Gradation of Individual Stockpiles based on Dry Sieve Analysis - Olsen

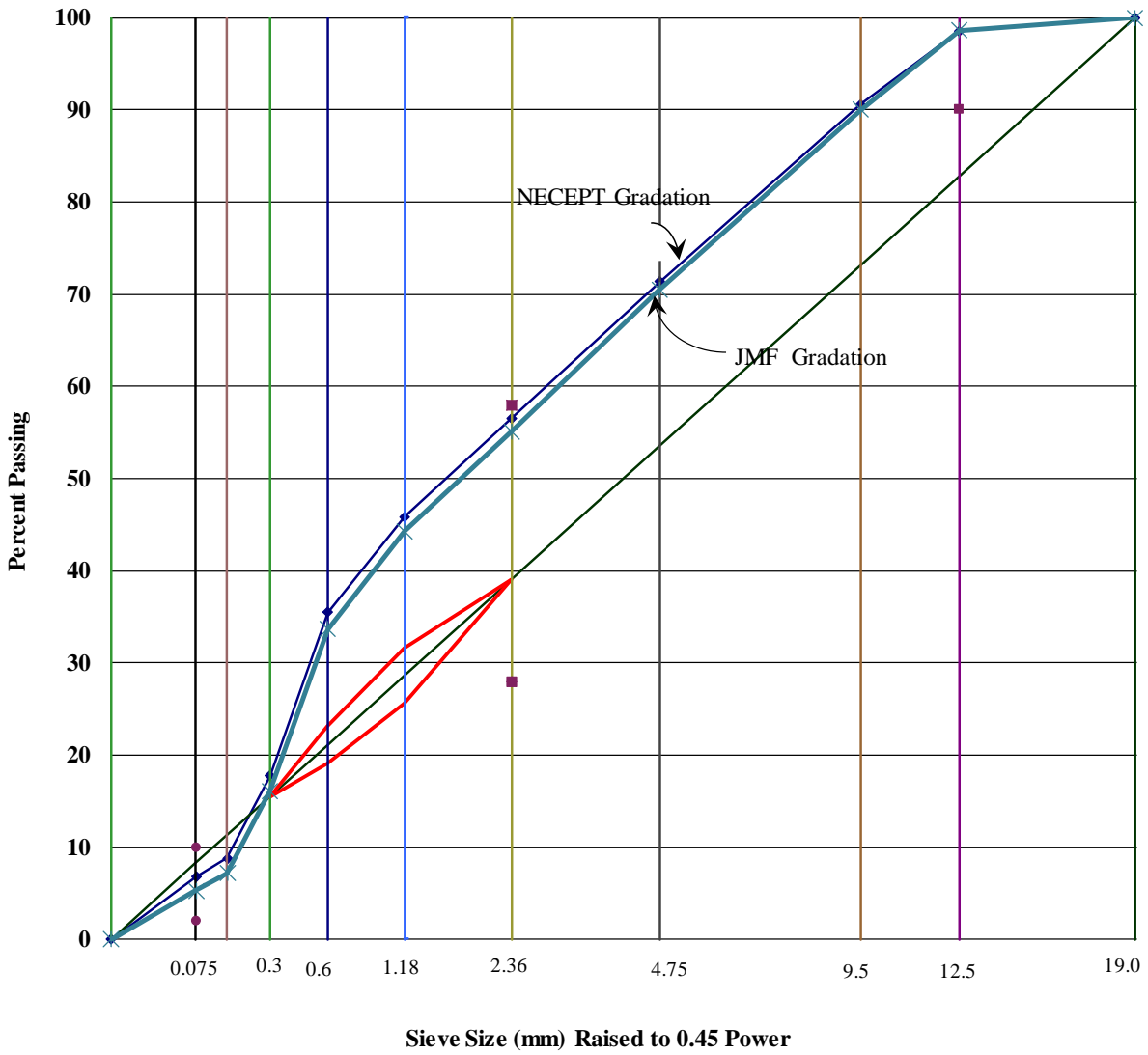
Sieve Size		Olsen - NECEPT - Before Washing			
		3/4" Bit	3/8" Bit	3/8" Screened Sand	3/8" Screenings
1"	25mm	100.0	100.0	100.0	100.0
3/4"	19mm	98.9	100.0	100.0	100.0
1/2"	12.5mm	58.5	100.0	100.0	100.0
3/8"	9.5mm	35.4	99.6	98.1	100.0
#4	4.75mm	19.3	75.1	83.9	91.7
#8	2.36mm	14.0	51.8	70.6	80.2
#16	1.18mm	10.7	36.1	54.1	71.7
#30	0.6mm	8.5	26.4	31.7	66.7
#50	0.3mm	5.4	17.1	9.1	58.8
#100	0.15mm	2.9	10.1	2.0	38.1
#200	0.075mm	1.7	6.1	0.9	17.2

Table A-8 Gradation of Individual Stockpiles based on Washed Sieve Analysis - Olsen

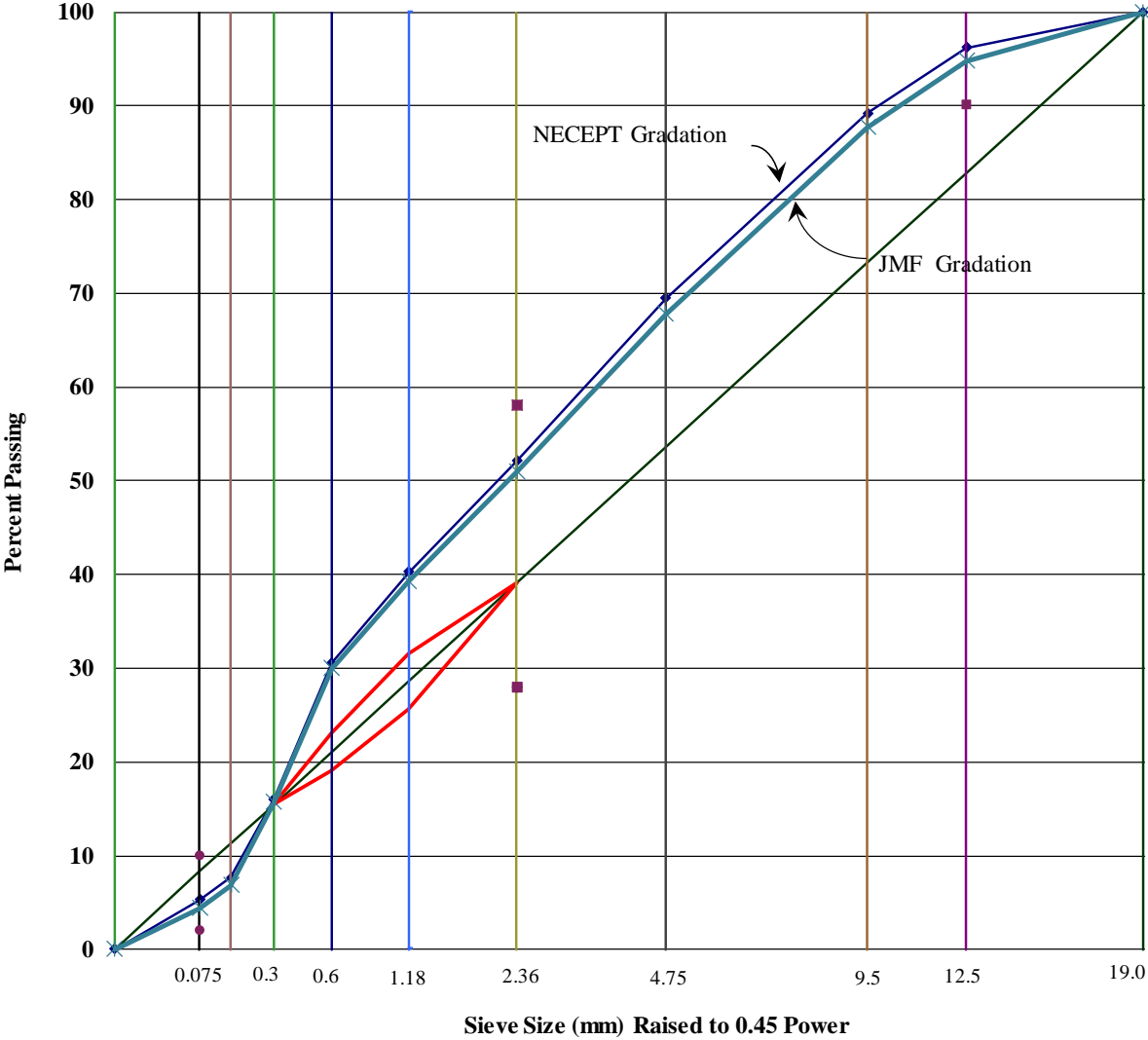
Sieve Size		Olsen - NECEPT - After Washing			
		3/4" Bit	3/8" Bit	3/8" Screened Sand	3/8" Screenings
1"	25mm	100.0	100.0	100.0	100.0
3/4"	19mm	96.8	100.0	100.0	100.0
1/2"	12.5mm	54.3	100.0	99.8	100.0
3/8"	9.5mm	30.9	100.0	97.5	100.0
#4	4.75mm	14.0	77.1	84.0	92.5
#8	2.36mm	9.3	53.8	70.6	81.4
#16	1.18mm	7.2	38.2	55.0	73.3
#30	0.6mm	6.2	28.7	33.8	68.7
#50	0.3mm	4.8	20.0	10.8	62.1
#100	0.15mm	3.4	13.2	3.8	44.7
#200	0.075mm	2.6	9.3	2.6	24.3



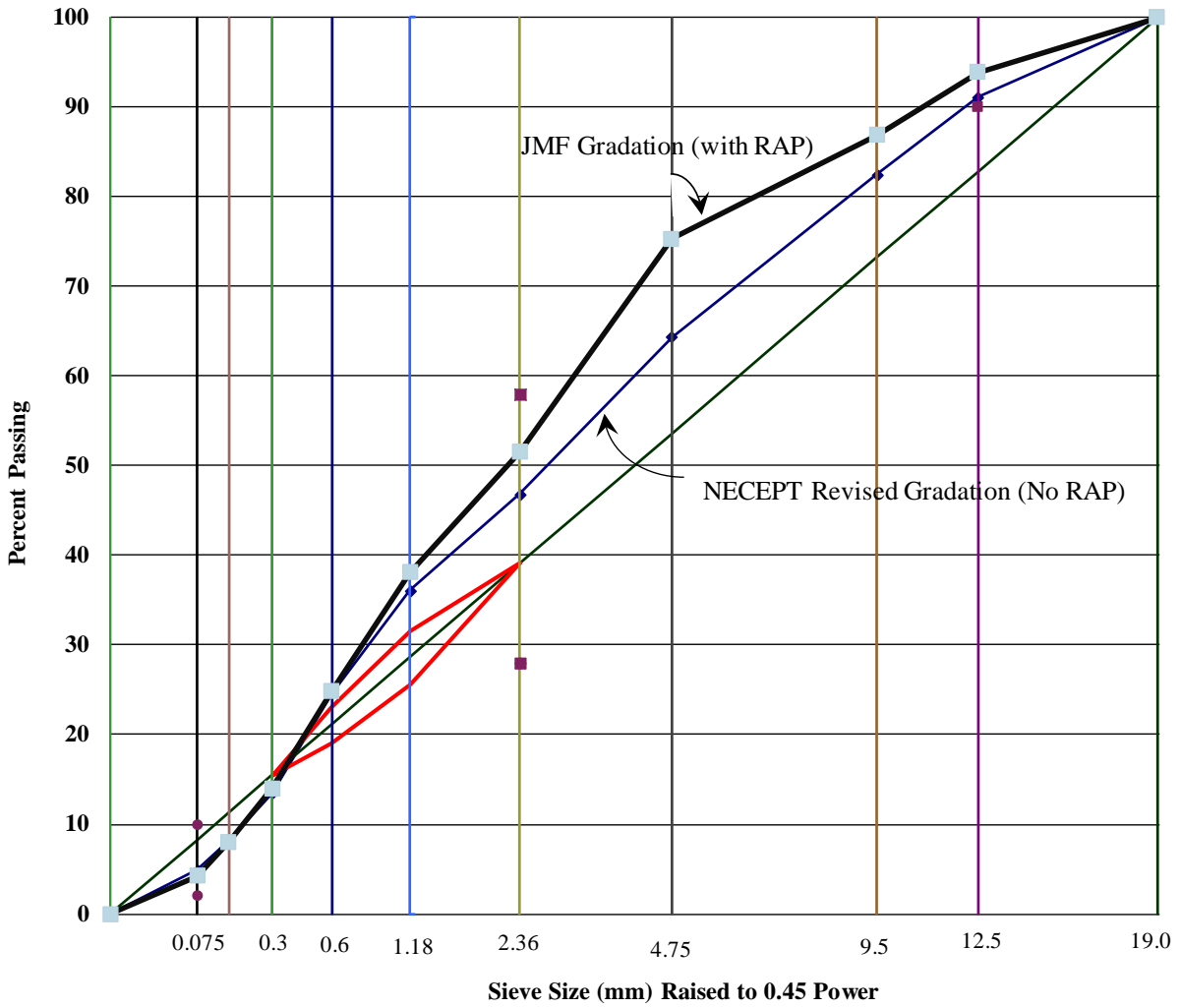
Waukesha, Design Gradation



Rock Springs, Design Gradation



Olsen, Design Gradation



APPENDIX B

Boil Test Report and Results

EXAMINATION OF EFFECT OF WATER ON ASPHALT MIX AND COATED AGGREGATE USING BOILING WATER

Objective

The objective of this experiment was to utilize the boil test for determining compatibility or incompatibility of the aggregate asphalt mixtures intended for this research study.

Scope of Work

The boil test was simply considered as an initial screening criterion and was conducted on loose asphalt mixtures made with different binders and aggregates. Sixteen different asphalt/aggregate mixtures, using four binders and four aggregate types, were prepared and subjected to the boil test. Comparison was made between the original mix and the boiled mix, and the results were reported as a qualitative rating of the level of stripping. Pictures were taken of the material before and after boiling for comparison. Finally, mass loss/gain of the material was determined and reported.

Introduction

The boil test is an old method of investigating asphalt/aggregate mixture susceptibility to moisture damage, and was approved by ASTM committee in 1977.¹ However, it continues to see somewhat widespread acceptance in academic papers for testing moisture sensitivity, mostly in combination with other testing methods.^{1,2,7} When testing loose asphalt/aggregate mixtures, the boil test is not the preferred adhesion properties test compared to more modern tests such as the rolling bottle test,³ but it is a valid testing method for moisture sensitivity.⁴ Boil testing is a subjective test, as assessment is based on visual observation of performance^{1,2,6}.

Boil testing continues to be used, due in large part to its simplicity and extremely low cost. It requires simple testing materials and equipment. Additionally, iterations can be done in rapid succession with minimal operator training. However, because testing only occurs on loose mix, as compared to compacted mix, the effect of many mix parameters on the moisture damage resistance is not considered. Binder-aggregate adhesion is the only variable tested in boil testing in a qualitative manner.⁹ Adhesion is a function of binder and aggregate physicochemical properties⁹, but those properties are not easy to quantify.

Stripping is defined as the physical separation of aggregate and binder.⁸ De-cohesion of binder to itself and de-adhesion of the binder to the aggregate is primarily caused by moisture effects via water or water vapor.⁶ In asphalt mix, stripping can be observed as aggregate becoming uncoated by binder and even separating from the bulk asphalt mix entirely. In boil testing, stripping is a result of de-cohesion and de-adhesion of the binder, dissolution of the binder in boiling water, and appearance of stripped binder on the surface of the water.⁶ The result of stripping in boil testing is most apparent on the resultant asphalt mix via lightening of the color of the asphalt mix.^{5,6}

Materials

Aggregates from the four sources were named: Waukesha, Menasha, Rock Springs, and Olsen. Four performance-grade binders were named: MTE 58S-28, 58-28F, 58-28WF, and 58-28. A full matrix of testing was used, delivering sixteen combinations. Graded material was used for each source to prepare the mixtures following proportions provided in the mix design. The blends were prepared at design binder content. A second set of boil tests were conducted on the coarse portion of the aggregate gradation (i.e., material retained on #4 sieve).

Experimental Procedure

Experimentation largely followed the “Standard Practice for Effect of Water on Bituminous-Coated Aggregate Using Boiling Water,” ASTM D3625/D3625M-12,¹ but small modifications were made to standard practice. In all, four binders and four aggregates of mixed sizes were tested, resulting in 16 total samples. Additionally, a secondary test was conducted with two samples of one-sized aggregate, 9.5 mm, and a single binder at two different binder ratios.

Next, asphalt mix samples were split into three separate sub-samples of approximately the same mass, about 300 grams. The sub-samples were massed and labeled. One of the sub-samples was boiled, one was submerged in room-temperature distilled water, and one did not undergo moisture testing. The boiled sample was heated to 95 °C in an oven for 30 minutes, then transferred to a 1000-mL beaker filled with 600 mL of boiling distilled water heated via propane torch (see Figure B-1). The water was brought back to a boil, and the asphalt mix was boiled for 10 minutes. Simultaneously, a control sample was put in a 500-mL beaker with 400 mL of room-temperature distilled water. After 10 minutes of boiling, the samples were allowed to cool for 45 minutes, stripped binder was skimmed off the surface of the water with cotton swabs, and the samples were drained of water. Finally, the samples were dried on Teflon paper overnight. The control sample was drained and allowed to dry overnight as well. Finally, the mass of the samples was measured again, and pictures of the samples were taken side-by-side with the sample which did not undergo moisture testing.



Figure B-1 Boil testing setup using propane fuel and handheld torch

Discussion of Findings

Table B-1 presents the average aggregate coating ratings based on three separate observers. For the individual scores of each observer, see Attachment 1. The rating system is based on a 0–10 system, where 0 represents complete stripping and 10 represents no stripping. In visual comparison of moisture effects, there were minute, but observable changes in color mostly. To view comparative photos, see Attachment 2. According to overall scores, it is difficult to categorically rate any of the combinations as being an incompatible matrix.

Table B-1 Average aggregate coating ratings, out of 10, derived from ratings of three observers

Average Aggregate Coating Rating				
Binder	Waukesha	Menasha	Rock Springs	Olsen
MTE 58S-28	9.5	9.4	8.93	8.6
58-28F	9.3	8.8	9.30	8.6
58-28WF	8.8	9.4	8.47	8.7
58-28	9.3	9.3	8.3	8.7

Table B-2 lists the samples' mass changes from before the boil test to after the boil test. To view initial and final masses of the samples, see Attachment 3. Overall, all of the boiled samples of asphalt mix gained an average of about 0.13 grams and all of the samples of asphalt mix immersed in cold water gained about 0.2 grams. The mass changes were on the order of $\frac{1}{1000}$ of the total mass of the sample and less than of $\frac{1}{10}$ of the initial mass of the binder. The loss in mass is due to stripping. The gain in mass is due to water absorption. Therefore, on average, the boiling water and cold water caused water absorption effects which were greater than the stripping effects, in terms of mass. Binder 58-28WF gained the most mass and binder 58-28F lost the most mass, on average.

Table B-2 Boil test mass changes, masses in grams

Boil Test Mass Change, grams								
Binder	Waukesha		Menasha		Rock Springs		Olsen	
	Boil	Cold Water	Boil	Cold Water	Boil	Cold Water	Boil	Cold Water
MTE 58S-28	0.2	0.1	0.6	0.2	-0.2	-0.2	0.1	0.3
58-28F	0.1	0	0.1	0.3	-0.9	0.4	0.6	0.3
58-28WF	0	0.4	0.4	-0.1	0	0.5	0.7	0.4
58-28	-0.2	0.2	0.2	0	0	-0.1	0.4	0.5

As the original results from the HWTD showed damage to the specimens, it was decided to rerun the boil tests using only the coarse aggregate portion for each source. The results indicated a higher level of stripping in the boil test when coarse aggregate was used compared to the mix aggregate gradation (Table B-3). The rating is on the scale of zero to 10, with increasing number indicative of less stripping potential.

Table B-3 Rating of Stripping Potential from Boil Test on Coarse Aggregate

	Binder/Additive	MTE 58S-28	58-28WF
Source	Menasha	7.5	8.0
	Waukesha	7.0	6.5
	Olsen	7.7	8.5
	Rock Springs	5.5	4.9

Conclusion

The conclusions are based on general qualitative assessment of boil test results. No apparent incompatibility could be observed based on the results from testing graded material. Comparing the initial and final mass, no strong pattern emerges. Mass changes in the primary boil test with full gradation mix displayed mass changes within a reasonable margin of error. In visual comparison and aggregate coating rating system of moisture effects, the differences were minute. Based on the testing on the coarse aggregate, the results indicated a higher level of stripping in the boil test when coarse aggregate was used compared to the mix aggregate gradation (Table B-3). The rating is on the scale of zero to 10, with increasing number indicative of less stripping potential.

References

1. ASTM D3625/D3625M-12 Standard Practice for Effect of Water on Bituminous-Coated Aggregate Using Boiling Water, ASTM International, West Conshohocken, PA, 2012, https://doi.org/10.1520/D3625_D3625M-12
2. Ahmad, Naveed. *Asphalt Mixture Moisture Sensitivity Evaluation Using Surface Energy Parameters*. University of Nottingham, 2011, *Asphalt Mixture Moisture Sensitivity Evaluation Using Surface Energy Parameters*.
3. Paliukaitė, Miglė, et al. “Evaluation of Different Test Methods for Bitumen Adhesion Properties.” *Transportation Research Procedia*, vol. 14, 21 Apr. 2016, pp. 724–731., doi:10.1016/j.trpro.2016.05.339.
4. Liu, Yawen, et al. “Examination of Moisture Sensitivity of Aggregate–Bitumen Bonding Strength Using Loose Asphalt Mixture and Physico-Chemical Surface Energy Property Tests.” *International Journal of Pavement Engineering*, vol. 15, no. 7, 2013, pp. 657–670., doi:10.1080/10298436.2013.855312.
5. Tayebali, Akhtarhusein A, et al. *Alternate Methods for Evaluation of Moisture Sensitivity of Asphalt Mixtures*. North Carolina Department of Transportation, 2017, pp. 1–82, *Alternate Methods for Evaluation of Moisture Sensitivity of Asphalt Mixtures*.
6. Kennedy, Thomas William, et al. *Texas Boiling Test for Evaluating Moisture Susceptibility of Asphalt Mixtures*. Center for Transportation Research, Bureau of Engineering Research, University of Texas at Austin, 1984, *Texas Boiling Test for Evaluating Moisture Susceptibility of Asphalt Mixtures*.
7. “Moisture Susceptibility.” *Pavement Interactive*, Pavia International, Inc, 2012, www.pavementinteractive.org/moisture-susceptibility/.
8. Taylor, Mark A, and N Paul Khosla. *Stripping of Asphalt Pavements: State of the Art*. Transportation Research Record 911.
9. Solaimanian, Mansour, et al. “Test Methods to Predict Moisture Sensitivity of Hot-Mix Asphalt Pavements.” *Moisture Sensitivity of Asphalt Pavements: A National Seminar*, Transportation Research Board of the National Academics, 6 Feb. 2003.

Attachment 1: Ratings by Individuals

Table B-4 Individual aggregate coating ratings, three observers

Observer #1				
	Waukesha	Menasha	Rock Springs	Olsen
MTE 58S-28	9.5	9.7	9.3	9.4
58-28F	9.5	9.4	9.4	9.2
58-28WF	9.5	9.7	9.4	9.5
58-28	9.9	9.9	9.8	9.7
Observer #2				
	Waukesha	Menasha	Rock Springs	Olsen
MTE 58S-28	9.5	9.5	8.5	8
58-28F	9.5	8	9	8
58-28WF	8	9	8	8
58-28	9	9	7	8
Observer #3				
	Waukesha	Menasha	Rock Springs	Olsen
MTE 58S-28	9.5	9	9	8.5
58-28F	9	9	9.5	8.5
58-28WF	9	9.5	8	8.5
58-28	9	9	8	8.5

Attachment 2: Before and after Photos



Figure B-2 Before and after boil testing: Waukesha aggregate with MTE 58S-28 binder



Figure B-3 Before and after boil testing: Waukesha aggregate with 58-28F binder



Figure B-4 Before and after boil testing: Waukesha aggregate with 58-28WF binder



Figure B-5 Before and after boil testing: Waukesha aggregate with 58-28 binder



Figure B-6 Before and after boil testing: Menasha aggregate with MTE 58S-28 binder



Figure B-7 Before and after boil testing: Menasha aggregate with 58-28F binder



Figure B-8 Before and after boil testing: Menasha aggregate with 58-28WF binder



Figure B-9 Before and after boil testing: Menasha aggregate with 58-28 binder



Figure B-10 Before and after boil testing: Rock Springs aggregate with MTE 58S-28 binder



Figure B-11 Before and after boil testing: Rock Springs aggregate with 58-28F binder



Figure B-12 Before and after boil testing: Rock Springs aggregate with 58-28WF binder



Figure B-13 Before and after boil testing: Rock Springs aggregate with 58-28 binder



Figure B-14 Before and after boil testing: Olsen aggregate with MTE 58S-28 binder



Figure B-15 Before and after boil testing: Olsen aggregate with 58-28F binder



Figure B-16 Before and after boil testing: Olsen aggregate with 58-28WF binder



Figure B-17 Before and after boil testing: Olsen aggregate with 58-28 binder

Attachment 3: Initial and Final Masses

Table B-5 Primary boil test, initial and final masses

	Waukesha				Menasha				Rock Springs				Olsen			
	Boil		Cold Water		Boil		Cold Water		Boil		Cold Water		Boil		Cold Water	
	Initial	Final	Initial	Final	Initial	Final	Initial	Final	Initial	Final	Initial	Final	Initial	Final	Initial	Final
MTE 58-28	300	300.2	300	300.1	300.3	300.9	298	298.2	300	299.8	300	299.8	300	300.1	299.9	300.2
58-28F	300	300.1	300	300	300	300.1	300	300.3	300	299.1	300	300.4	300	300.6	300	300.3
58-28WF	300	300	300	300.4	300	300.4	300	299.9	300	300	300	300.5	300	300.7	300	300.4
58S-28	300	299.8	300	300.2	300	300.2	300	300	300	300	300	299.9	300	300.4	300	300.5

APPENDIX C

Results from Indirect Tensile Tests on Dry and Conditioned Specimens

(Conditioned Based on AASHTO T 283 & MiST)

**Table C-1 Summary of Results from Indirect Tensile Test under Different Conditions
(Mix Source: Menasha)**

Condition of Specimen	Specimen ID	Strength (Peak Stress)		Strain at Peak Stress, %	Toughness (measured to peak), KJ/m ³
		KPa	PSI		
Dry 95-mm thick	MT3	569.3	82.6	2.64	9.33
	MT10	640.9	93.0	2.27	9.01
	MT19	789.9	114.6	2.17	11.13
	average	666.7	96.7	2.36	9.82
Wet/Freeze 95-mm thick	MT2	365.5	53.0	3.17	7.29
	MT7	442.0	64.1	2.93	8.28
	MT8	453.5	65.8	3.01	8.44
	average	420.3	61.0	3.04	8.00
Wet/No Freeze 95-mm thick	MT9	456.7	66.2	2.99	8.28
	MT17	544.8	79.0	2.64	9.11
	MT18	508.5	73.8	2.75	8.78
	average	503.3	73.0	2.79	8.72
Dry 60-mm thick	MT13	700.8	101.6	2.27	10.15
	MT14	765.9	111.1	2.35	11.22
	MT16	770.7	111.8	2.29	11.37
	average	745.8	108.2	2.30	10.91
Wet/Freeze 60-mm thick	MT11	496.0	71.9	2.56	7.92
	MT12	517.8	75.1	2.67	8.70
	MT15	493.9	71.6	2.53	7.96
	average	502.6	72.9	2.59	8.19

**Table C-2 Summary of Results from Indirect Tensile Test under Different Conditions
(Mix Source: Waukesha)**

Condition of Specimen	Specimen ID	Strength (Peak Stress)		Strain at Peak Stress, %	Toughness (measured to peak), KJ/m ³
		KPa	PSI		
Dry 95-mm thick	WT6	683.9	99.2	2.67	10.64
	WT8	627.5	91.0	2.40	9.15
	WT9	668.1	96.9	2.22	9.03
	average	659.8	95.7	2.43	9.61
Wet/Freeze 95-mm thick	WT2	420.3	61.0	3.23	8.13
	WT4	472.8	68.6	2.67	7.53
	WT10	468.2	67.9	2.56	7.50
	average	453.77	65.8	2.82	7.72
Wet/No Freeze 95-mm thick	WT3	483.5	70.1	2.80	7.67
	WT5	473.0	68.6	2.75	7.82
	WT7	505.7	73.3	2.64	7.80
	average	487.4	70.7	2.73	7.76
Dry 60-mm thick	WT14	750.1	108.8	2.19	10.73
	WT15	751.2	109.0	2.21	10.58
	WT16	757.0	109.8	2.24	10.73
	average	752.8	109.2	2.21	10.68
Wet/Freeze 60-mm thick	WT11	524.2	76.0	2.27	7.50
	WT12	575.4	83.5	2.24	7.87
	WT13	567.8	82.4	2.32	8.07
	average	555.8	80.6	2.28	7.81

**Table C-3 Summary of Results from Indirect Tensile Test under Different Conditions
(Mix Source: Rock Springs)**

Condition of Specimen	Specimen ID	Strength (Peak Stress)		Strain at Peak Stress, %	Toughness (measured to peak), KJ/m ³
		KPa	PSI		
Dry 95-mm thick	RT10	744.0	107.9	2.18	10.10
	RT11	779.4	113.0	2.07	10.04
	RT12	779.3	113.0	2.16	10.53
	average	767.6	111.3	2.14	10.22
Wet/Freeze 95-mm thick	RT14	447.2	64.9	2.22	6.08
	RT15	490.0	71.1	2.10	6.34
	RT16	553.2	80.2	2.10	7.06
	average	496.8	72.1	2.14	6.49
Wet/No Freeze 95-mm thick	RT8	628.0	91.1	1.81	7.22
	RT9	623.8	90.5	1.97	7.64
	RT13	647.4	93.9	1.86	7.69
	average	633.1	91.8	1.88	7.52
Dry 60-mm thick	RT2	816.1	118.4	2.03	10.36
	RT4	795.4	115.4	1.92	9.72
	RT6	889.9	129.1	1.91	10.97
	average	833.8	120.9	1.95	10.35
Wet/Freeze 60-mm thick	RT1	588.7	85.4	1.84	6.73
	RT3	601.2	87.2	1.79	6.86
	RT5	602.2	87.3	1.84	6.99
	average	597.37	86.6	1.82	6.86

**Table C-4 Summary of Results from Indirect Tensile Test under Different Conditions
(Mix Source: Olsen)**

Condition of Specimen	Specimen ID	Strength (Peak Stress)		Strain at Peak Stress, %	Toughness (measured to peak), KJ/m ³
		KPa	PSI		
Dry 95-mm thick	OT8	621.6	90.2	2.18	8.69
	OT0	621.9	90.2	2.51	9.94
	OT10	628.6	91.2	2.29	9.09
	average	624.0	90.5	2.33	9.24
Wet/Freeze 95-mm thick	OT2	394.8	57.3	2.80	7.08
	OT3	479.4	69.5	2.99	9.25
	OT5	499.6	72.5	2.77	8.69
	average	457.9	66.4	2.85	8.34
Wet/No Freeze 95-mm thick	OT4	403.5	58.5	3.12	8.03
	OT6	451.8	65.5	3.07	8.70
	OT7	460.6	66.8	2.75	8.02
	average	438.6	63.6	2.98	8.25
Dry 60-mm thick	OT11	623.4	90.4	2.40	9.71
	OT12	656.3	95.2	2.16	9.27
	OT14	674.3	97.8	2.21	9.55
	average	651.3	94.5	2.26	9.51
Wet/Freeze 60-mm thick	OT13	455.9	66.1	2.80	8.27
	OT15	509.3	73.9	2.64	8.73
	OT16	532.4	77.2	2.72	9.39
	average	499.2	72.4	2.72	8.80

Indirect Tensile Strength
for
Freeze-Thaw & MiST Conditioned Specimens
after
Completion of Dynamic Modulus Testing
(60-mm thick specimens)

Table C-5 Summary of Results from Indirect Tensile Test for Dynamic Modulus Specimens⁽¹⁾

Condition of Specimen	Specimen ID	Strength (Peak Stress)		Strain at Peak Stress, %	Toughness (measured to peak), KJ/m ³
		KPa	PSI		
Mix Source: Menasha					
after Freeze-Thaw Cycle 60-mm thick	M2	452.0	65.6	2.47	7.39
	M5	433.8	62.9	2.72	8.25
	M6	475.2	68.9	2.40	7.78
	average	453.7	65.80	2.53	7.81
after MiST 60-mm thick	M1	504.4	73.2	2.75	9.16
	M3	549.3	79.7	2.72	9.92
	M4	576.0	83.5	2.57	10.27
	average	543.23	78.80	2.68	9.78
Mix Source: Waukesha					
after Freeze-Thaw Cycle 60-mm thick	W1	529.0	76.7	2.57	9.07
	W5	570.1	82.7	2.45	9.41
	W6	581.3	84.3	2.32	9.17
	average	560.13	81.2	2.42	10.19
after MiST 60-mm thick	W2	575.2	83.4	2.32	9.16
	W3	635.2	92.1	2.62	11.35
	W4	631.9	91.7	2.32	10.05
	average	614.1	89.1	2.42	10.19

(1) These specimens were subject to dynamic modulus testing before and after moisture conditioning. After completion of the second dynamic modulus test, the specimens were subject to indirect tensile strength test for which the results are presented in this table.

Table C-6 Summary of Results from Indirect Tensile Test for Dynamic Modulus Specimens⁽¹⁾

Condition of Specimen	Specimen ID	Strength (Peak Stress)		Strain at Peak Stress, %	Toughness (measured to peak), KJ/m ³
		KPa	PSI		
Mix Source: Rock Springs					
after Freeze-Thaw Cycle 60-mm thick	R2	570.9	82.8	1.90	6.86
	R4	558.7	81.0	2.02	7.16
	R5	582.7	84.5	2.10	8.15
	average	570.8	82.8	2.01	7.39
after MiST 60-mm thick	R1	600.6	87.1	2.20	8.42
	R3	594.7	86.3	2.47	9.29
	R6	671.3	97.4	2.62	10.81
	average	622.2	90.3	2.43	9.51
Mix Source: Olsen					
after Freeze-Thaw Cycle 60-mm thick	O2	522.4	75.8	2.60	9.08
	O3	527.3	76.5	2.75	9.53
	O6	557.1	80.8	2.85	10.31
	average	535.6	77.7	2.73	9.64
after MiST 60-mm thick	O1	557.2	80.80	2.82	10.70
	O4	612.7	88.91	3.50	12.49
	O5	586.5	85.10	2.95	10.99
	average	585.5	84.9	3.09	11.39

(1) These specimens were subject to dynamic modulus testing before and after moisture conditioning. After completion of the second dynamic modulus test, the specimens were subject to indirect tensile strength test for which the results are presented in this table.

APPENDIX D

Results from Testing with Hamburg Wheel Tracking Device (HWTD)

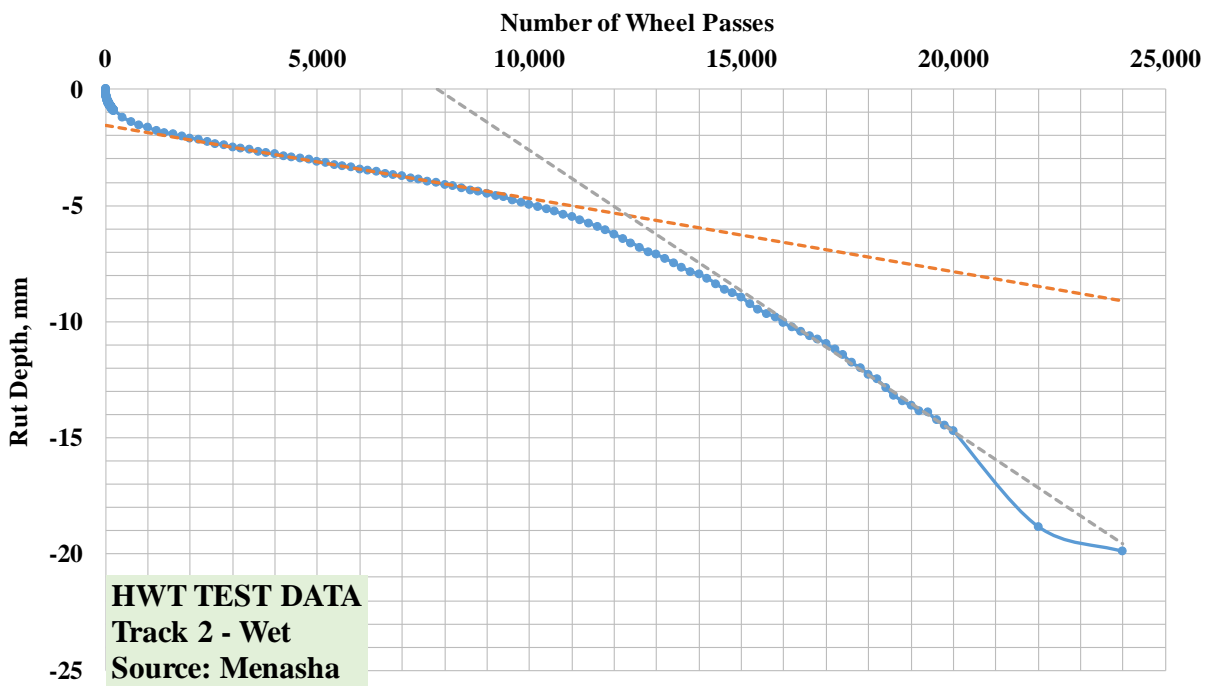
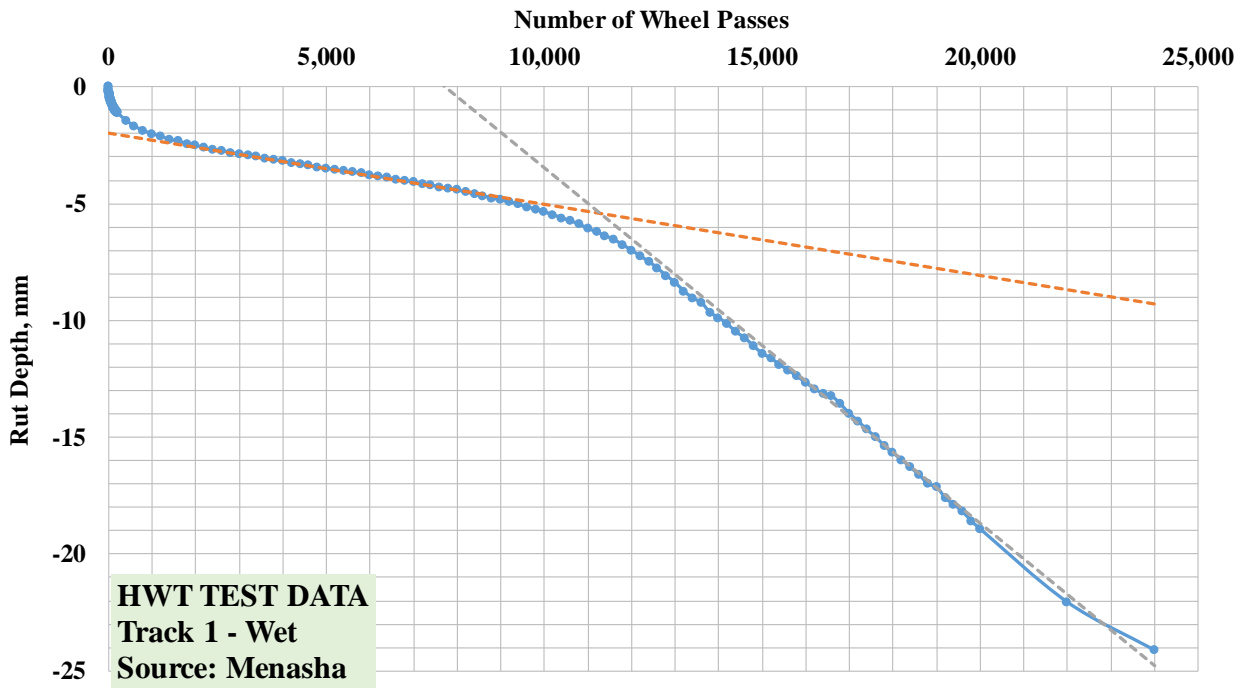
- 1. Submerged Condition**
- 2. Dry Condition**
- 3. Dry After MiST**
- 4. Moisture Damage Mitigation Study**

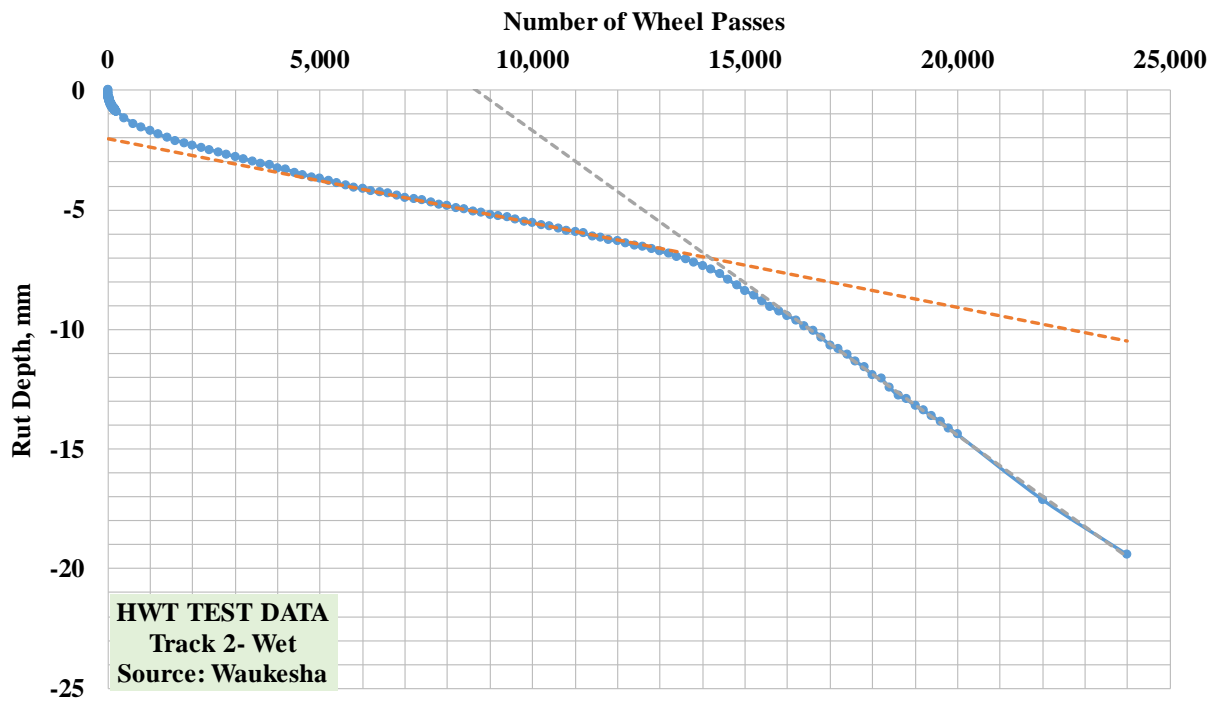
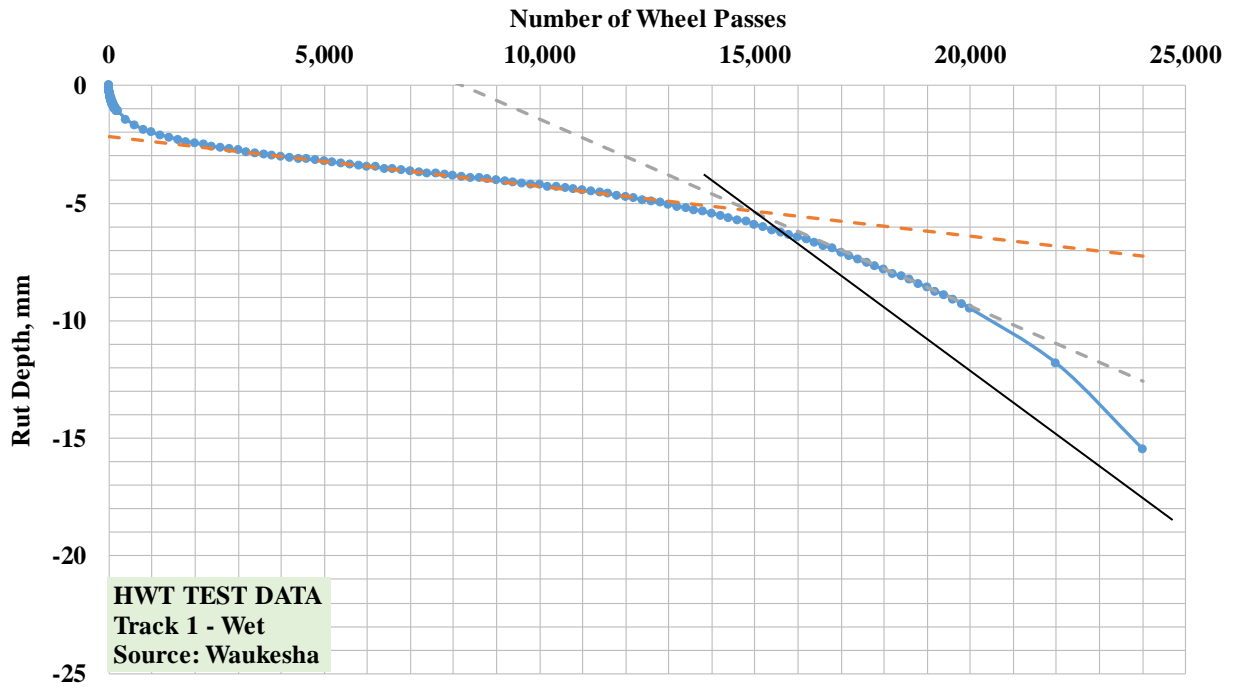
1. SUBMERGED CONDITION

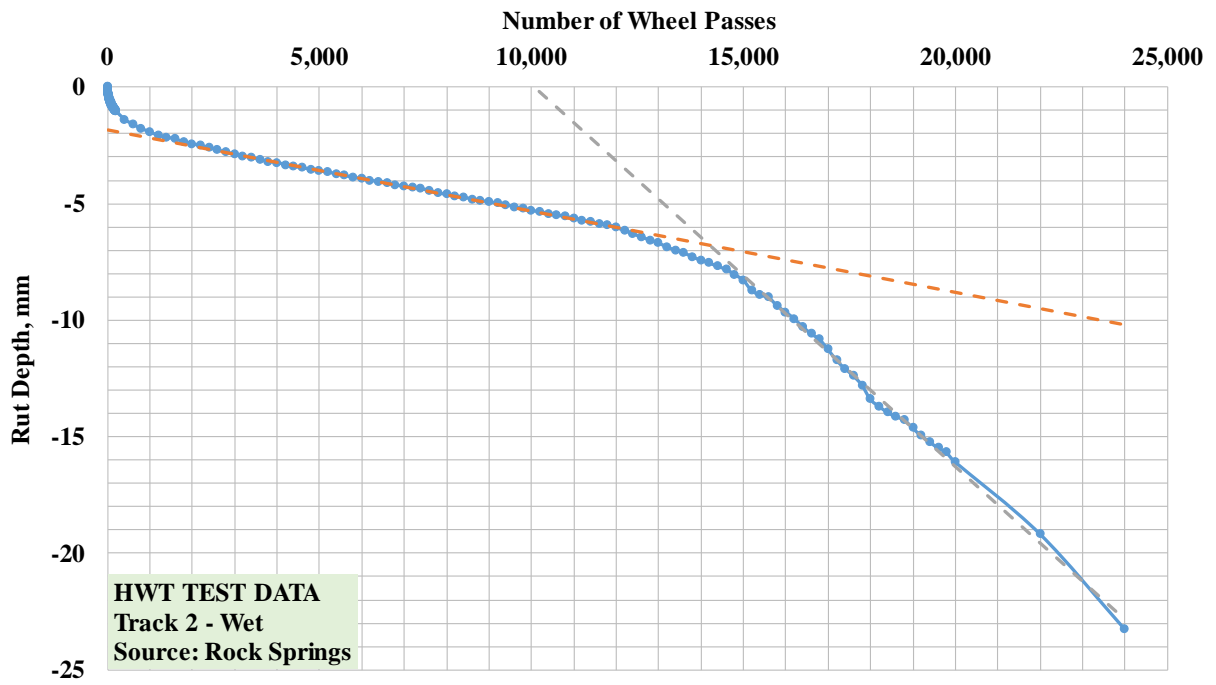
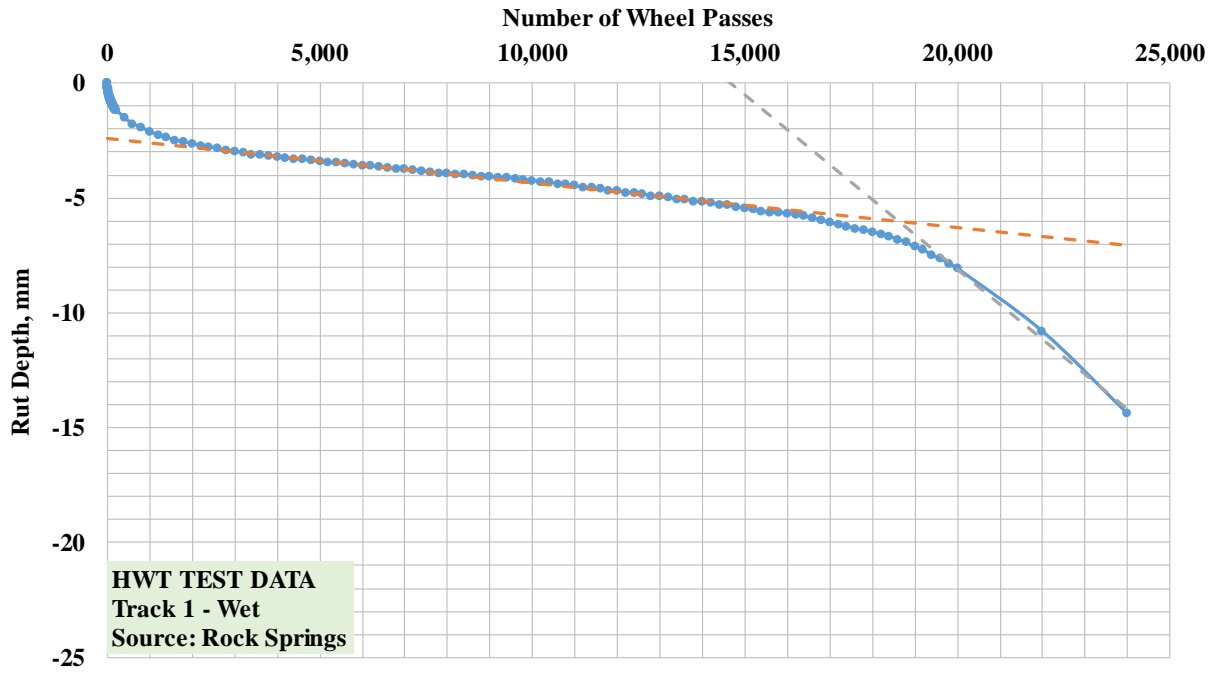
Table D-1 Air Void of Specimens Tested in HWTD under Submerged Condition

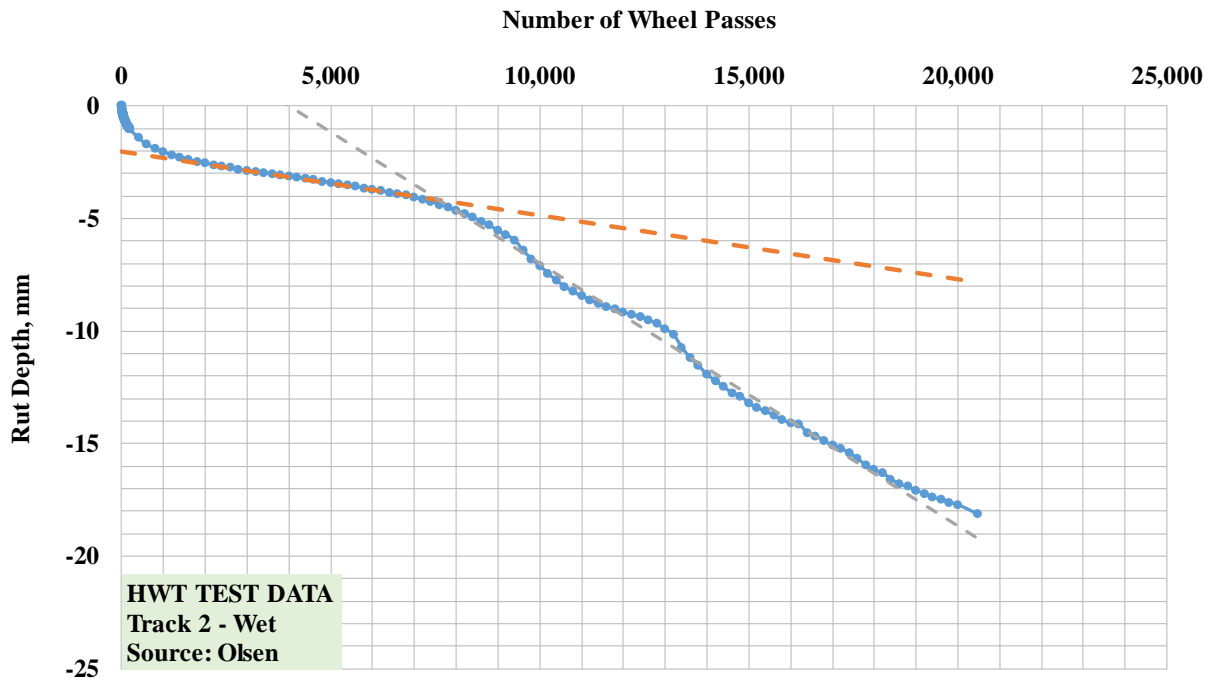
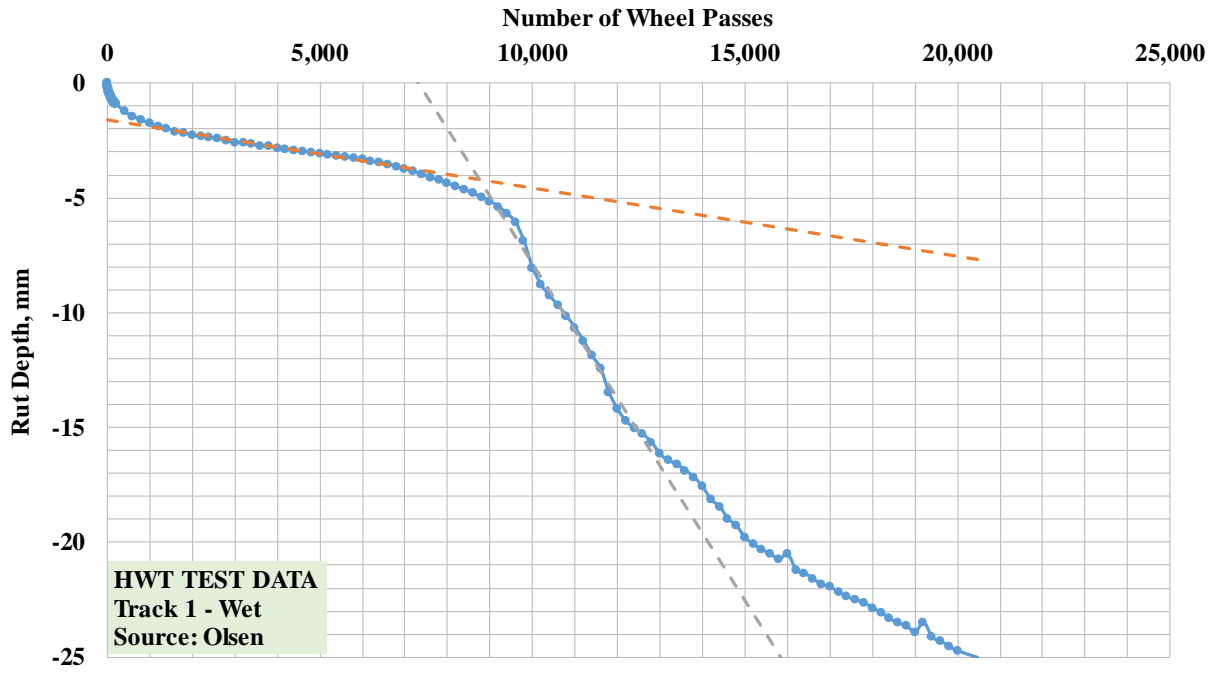
		Specimens of Track 1 (Right side)⁽¹⁾		Specimens of Track 2 (Left side)⁽¹⁾	
		Specimen 1	Specimen 2	Specimen 1	Specimen 2
Source	Menasha	6.5	6.4	7.0	6.8
	Waukesha	7.3	6.6	6.1	6.2
	Rock Springs	7.3	7.2	7.1	6.5
	Olsen	6.9	7.0	6.9	7.2

(1)Right and Left imply facing away from the machine







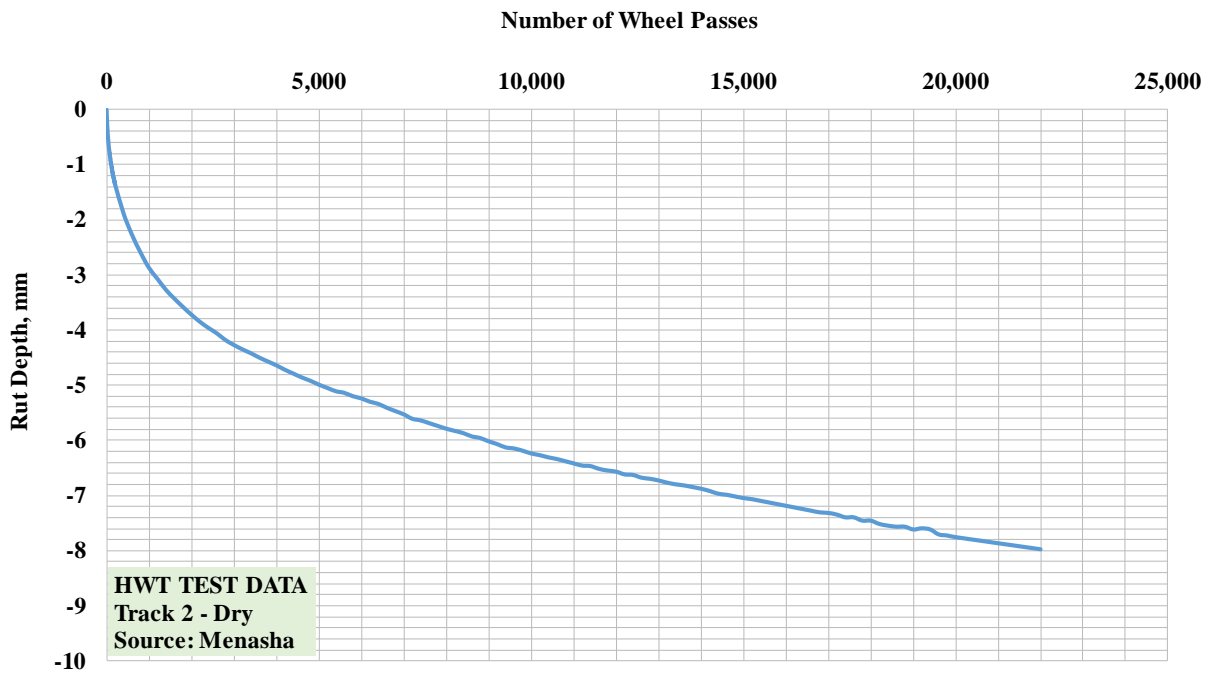
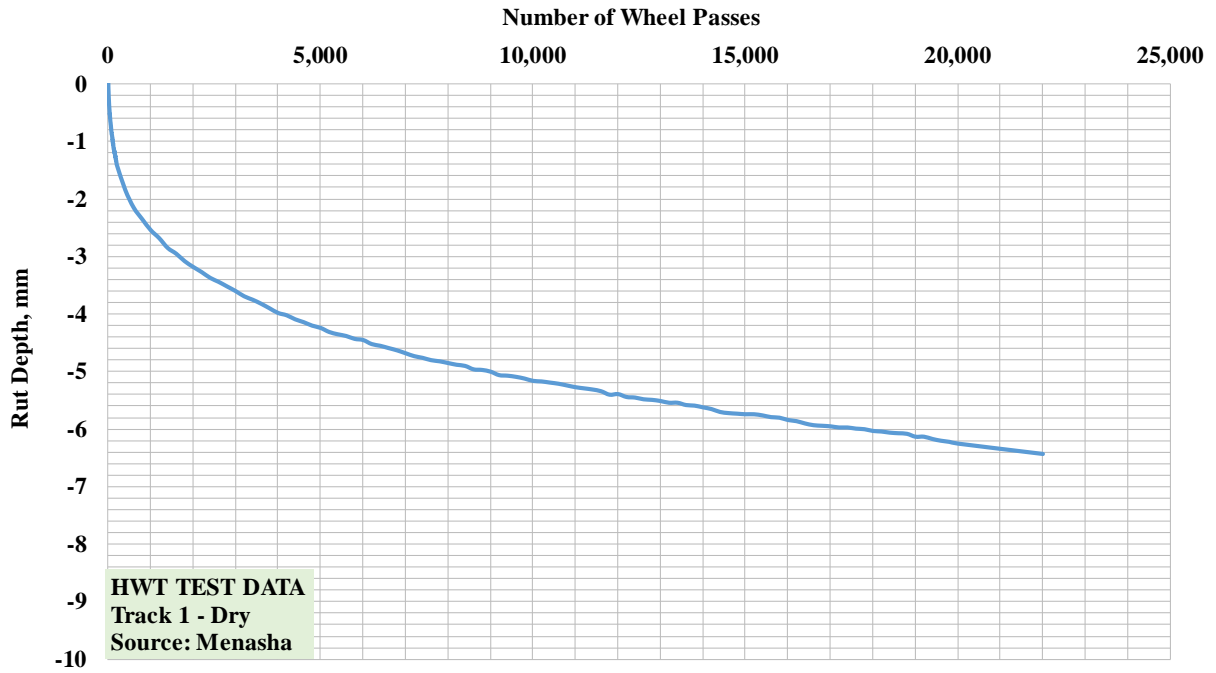


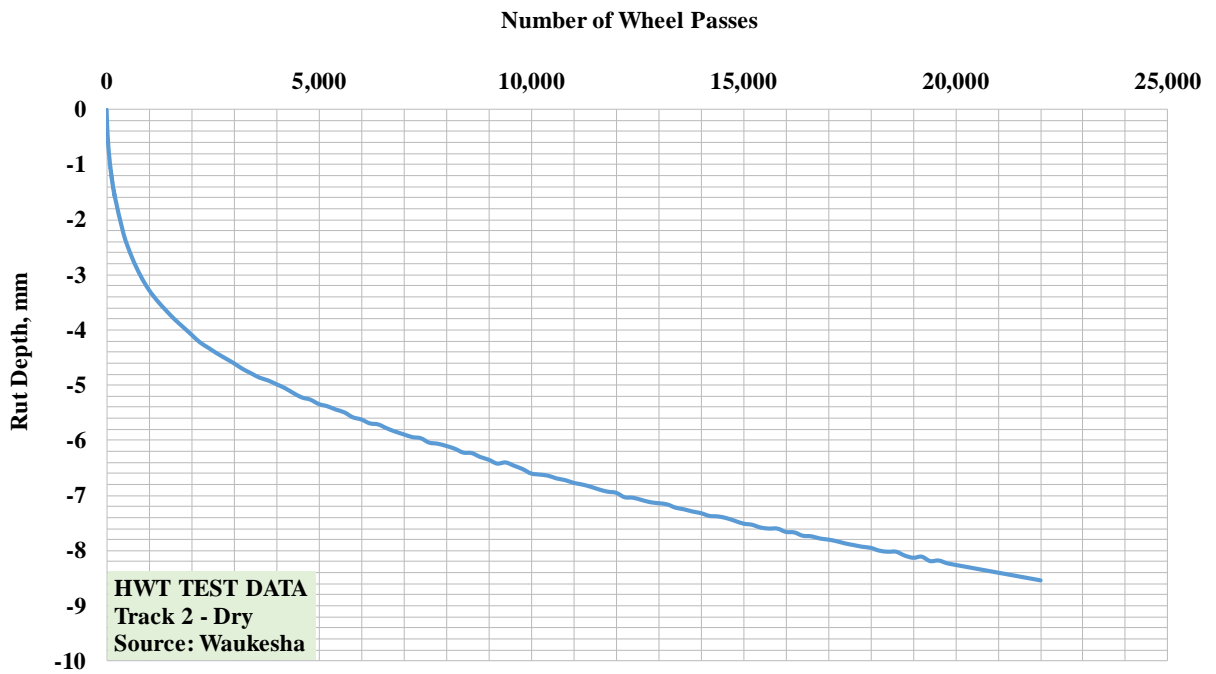
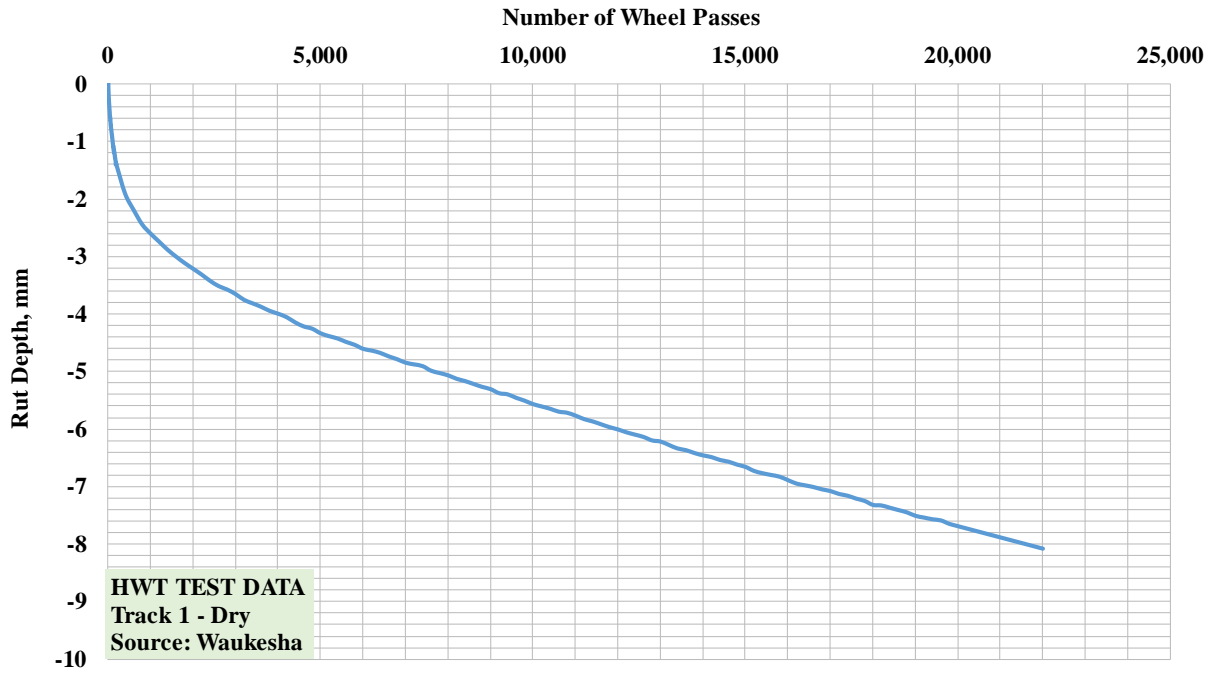
2. DRY CONDITION

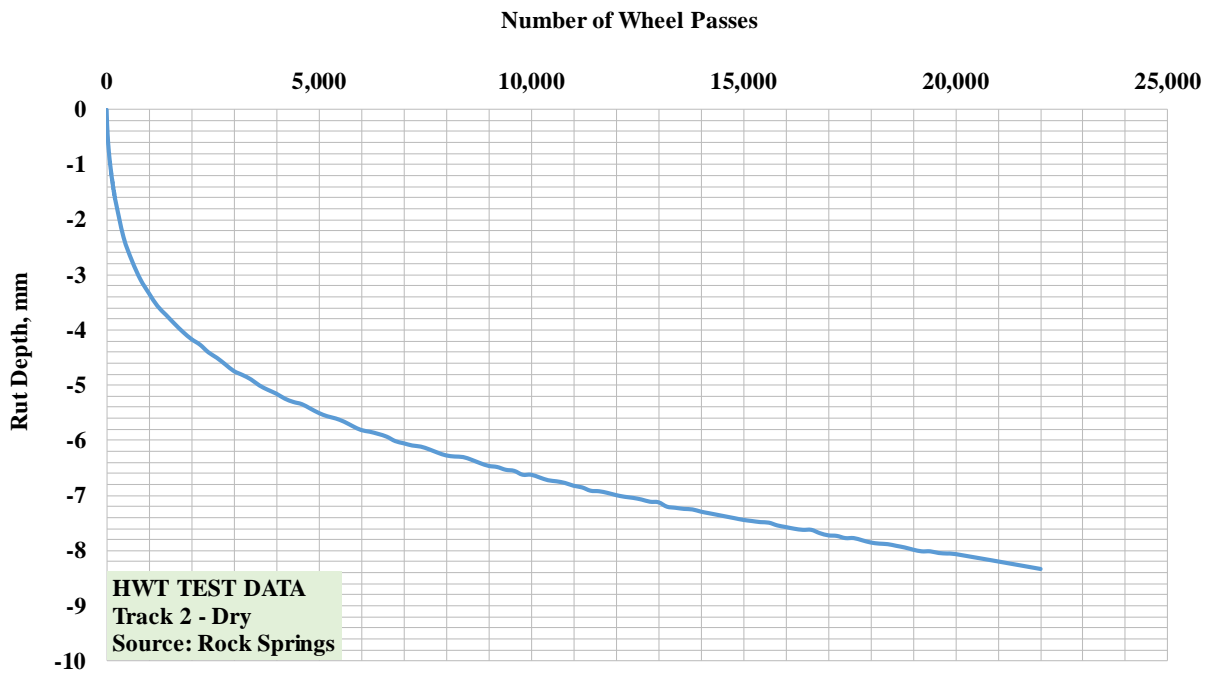
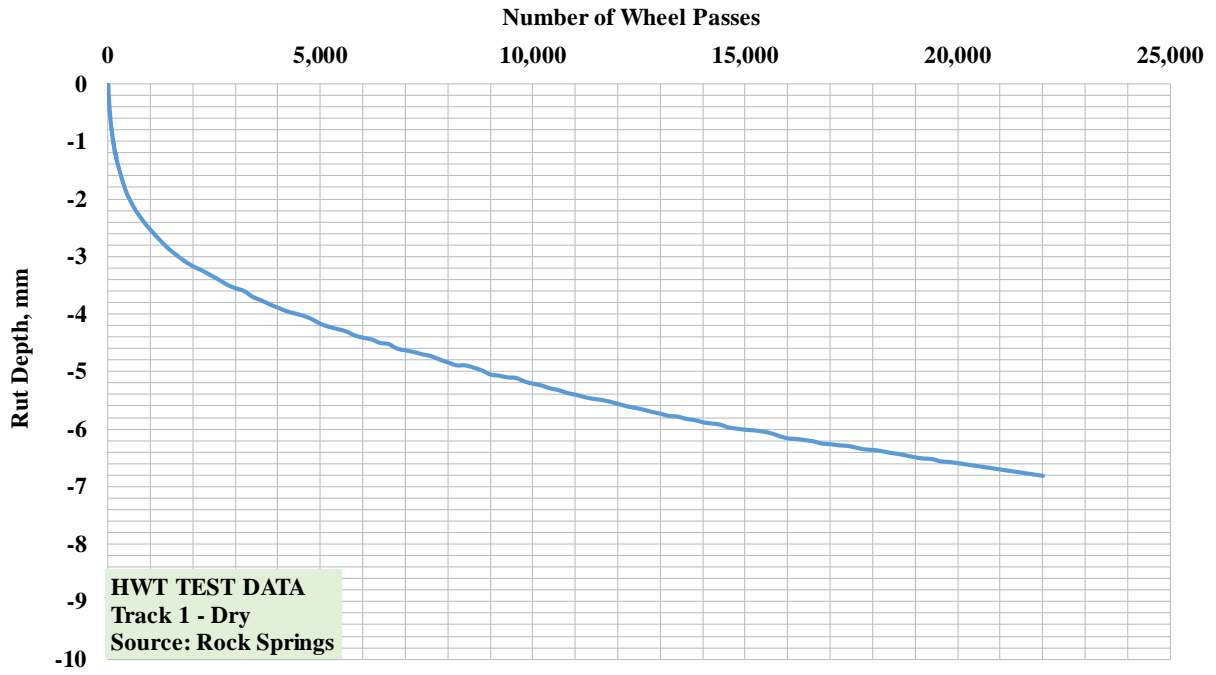
Table D-2 Air Void of Specimens Tested in HWTD under Dry Condition

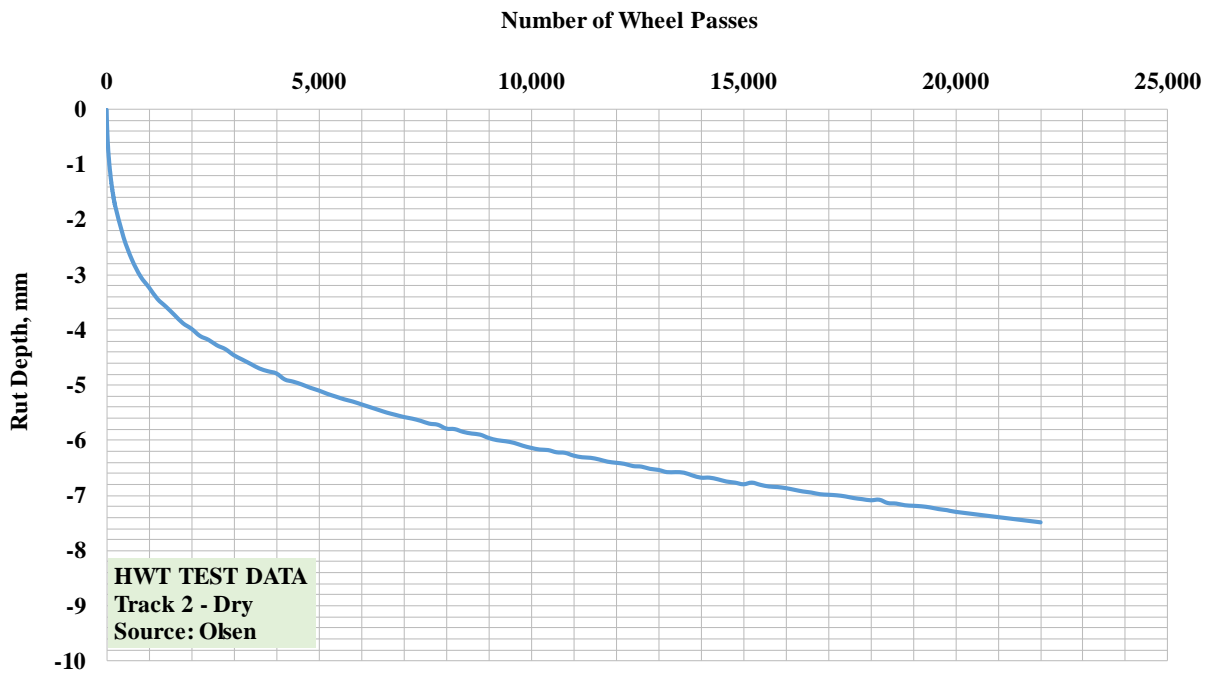
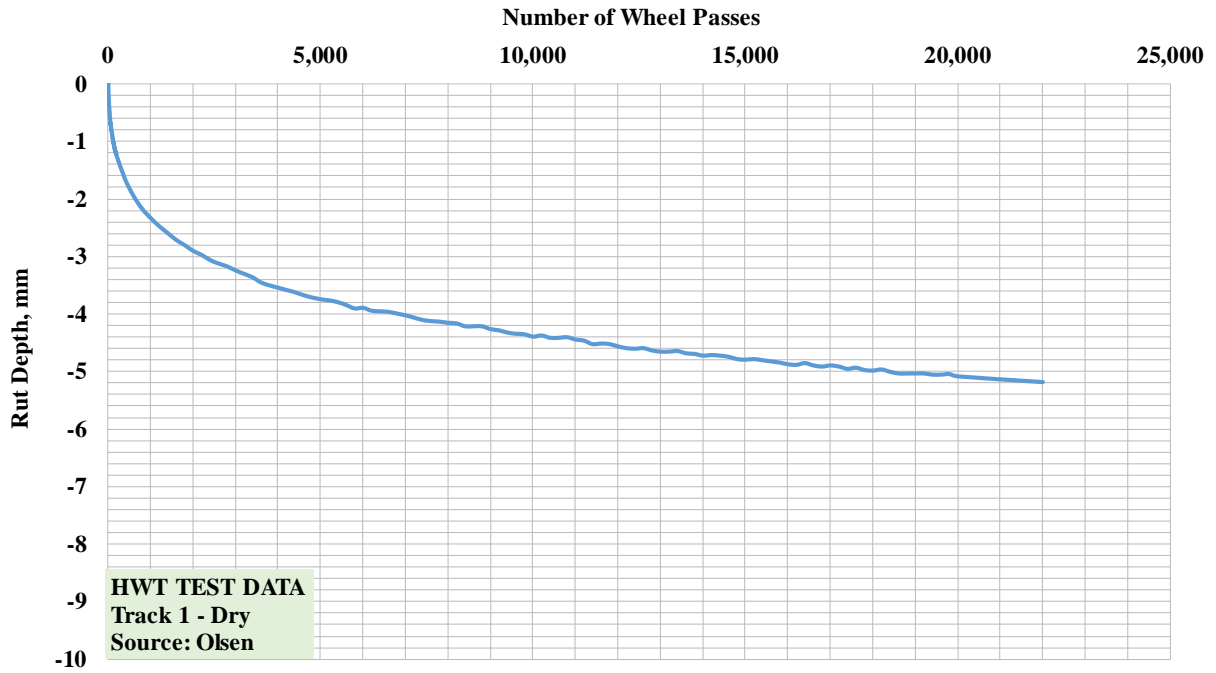
		Specimens of Track 1 (Right side) ⁽¹⁾		Specimens of Track 2 (Left side) ⁽¹⁾	
		Specimen 1	Specimen 2	Specimen 1	Specimen 2
Source	Menasha	7.6	7.2	6.9	7.2
	Waukesha	7.5	7.1	7.2	7.2
	Rock Springs	7.4	7.2	7.0	6.7
	Olsen	7.7	7.7	7.2	7.2

(1)Right and Left imply facing away from the machine







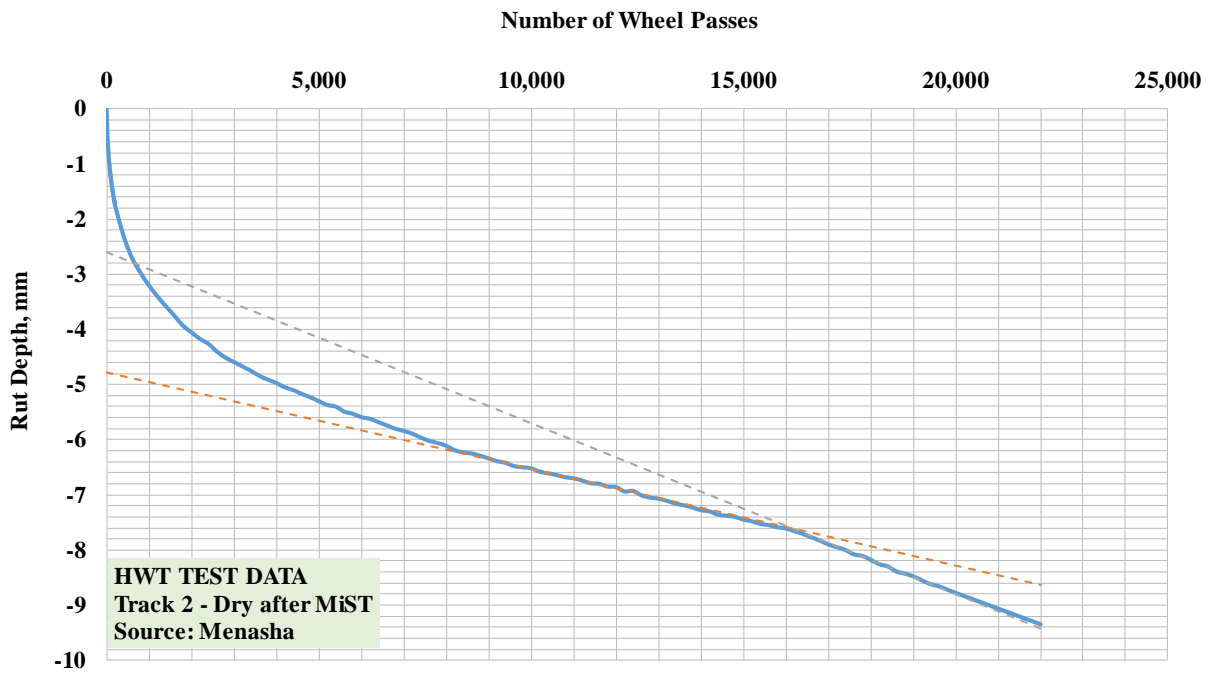
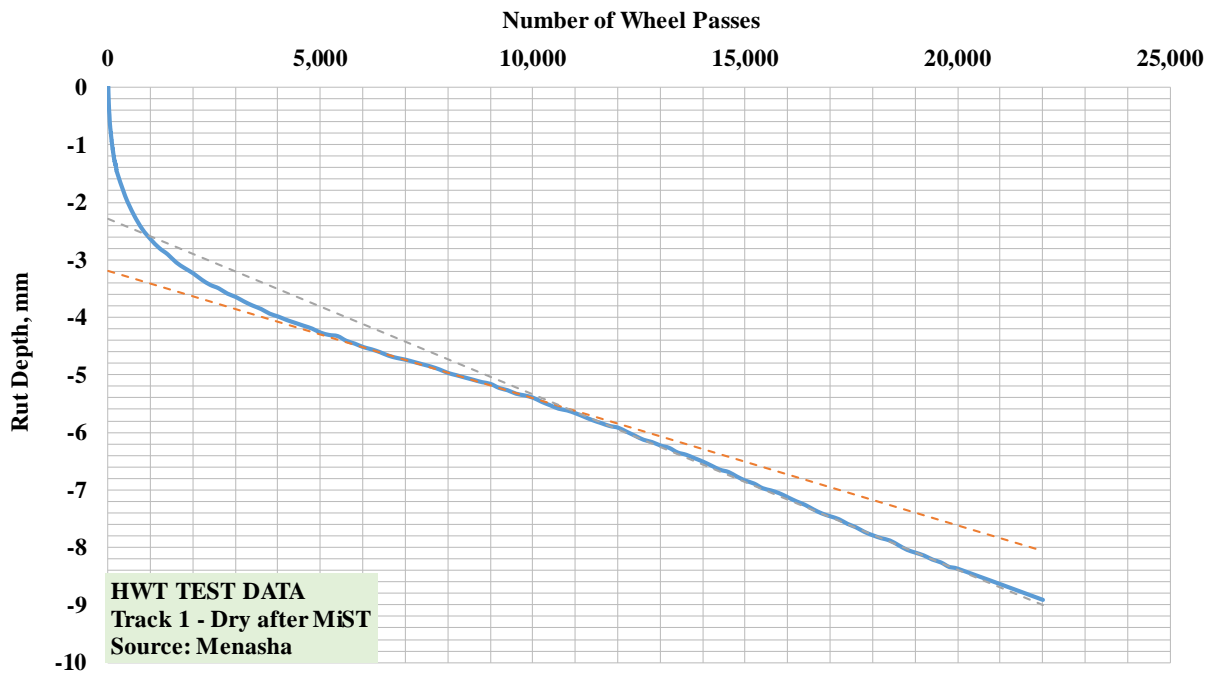


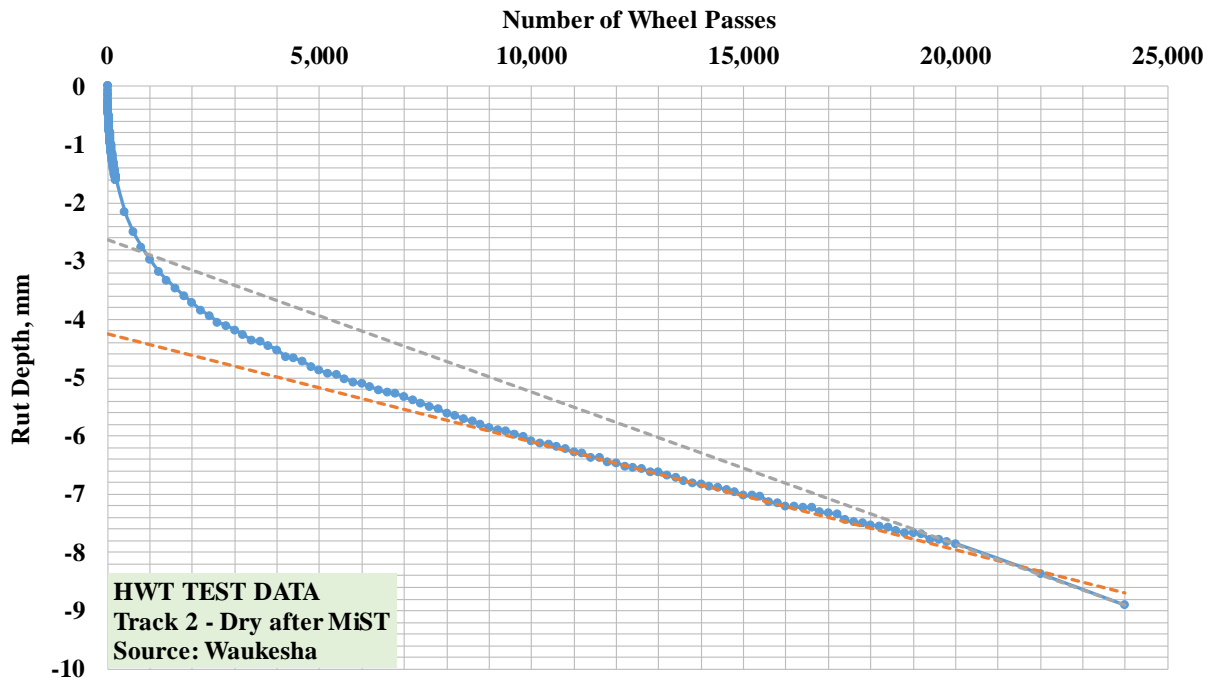
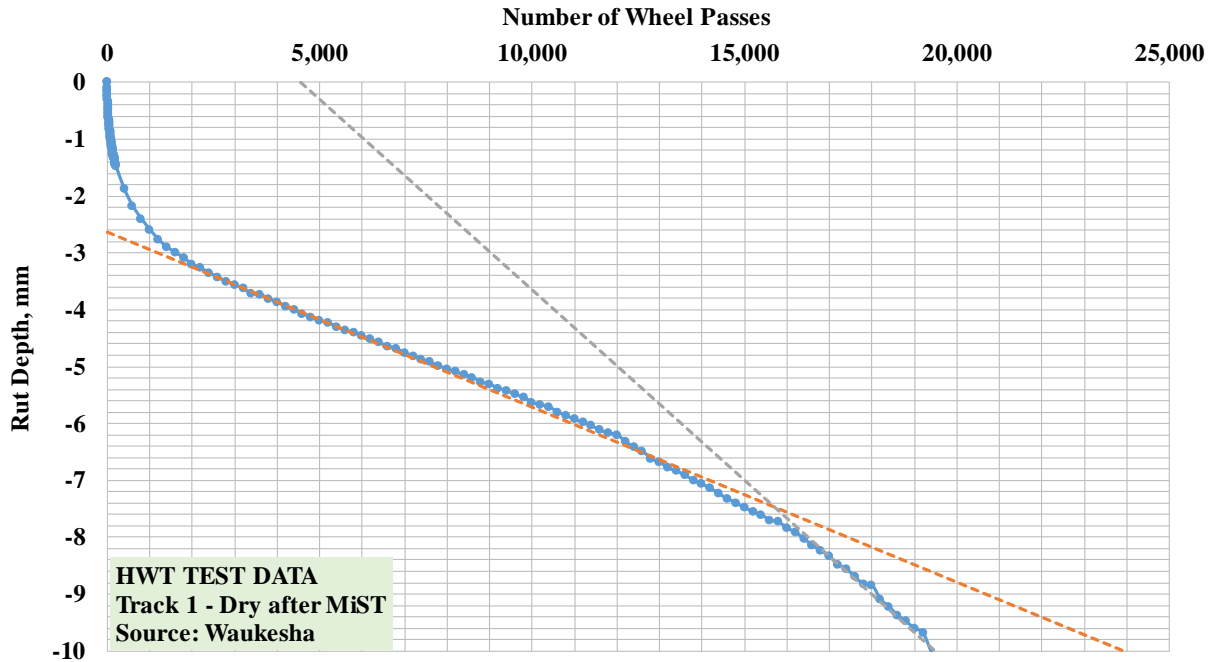
3. DRY AFER MiST CONDITIONING

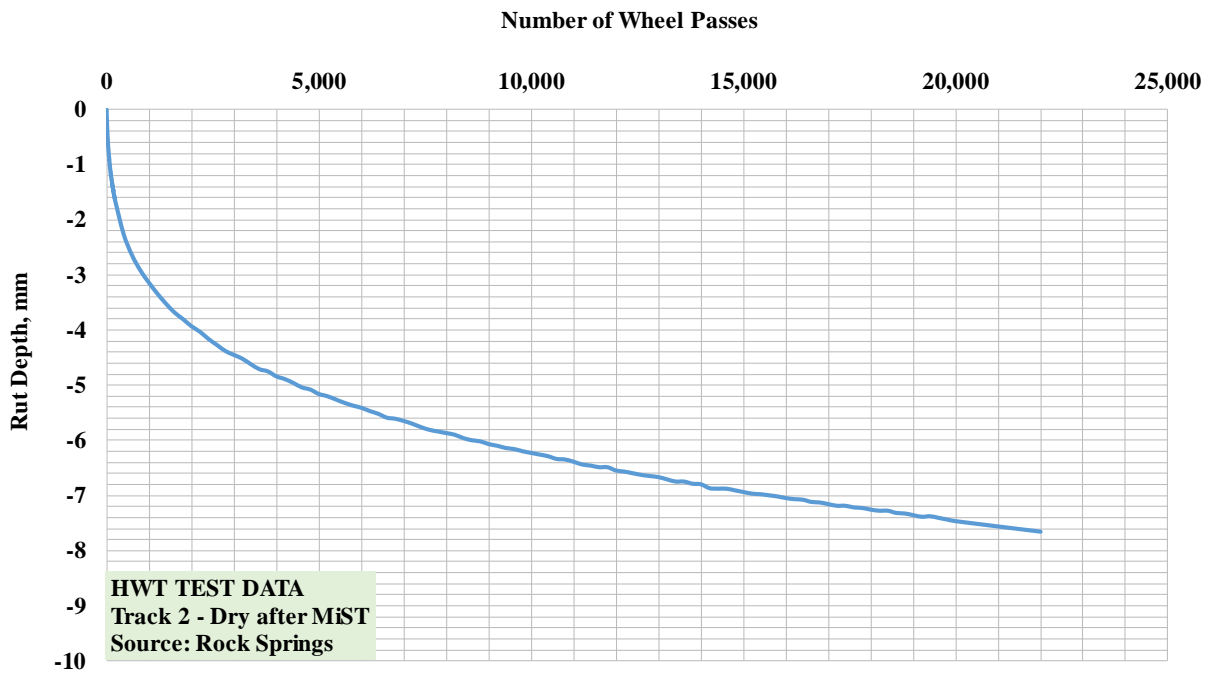
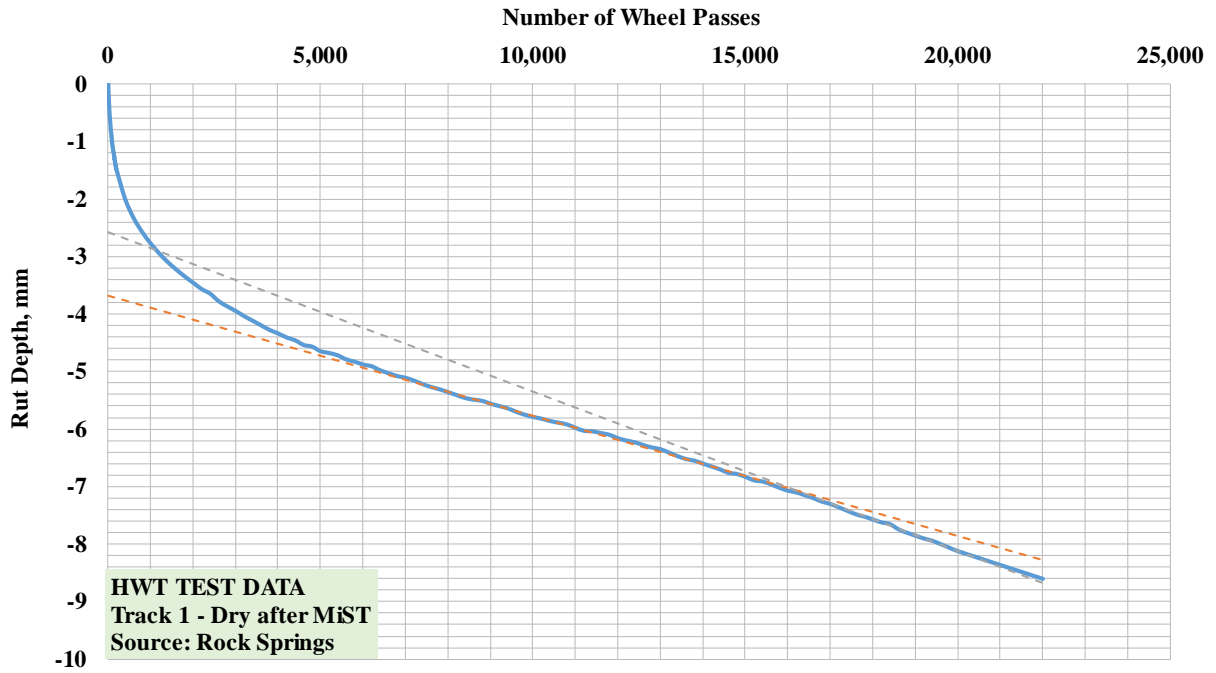
Table D-3 Air Void of Specimens Tested in HWTD after MiST Conditioning

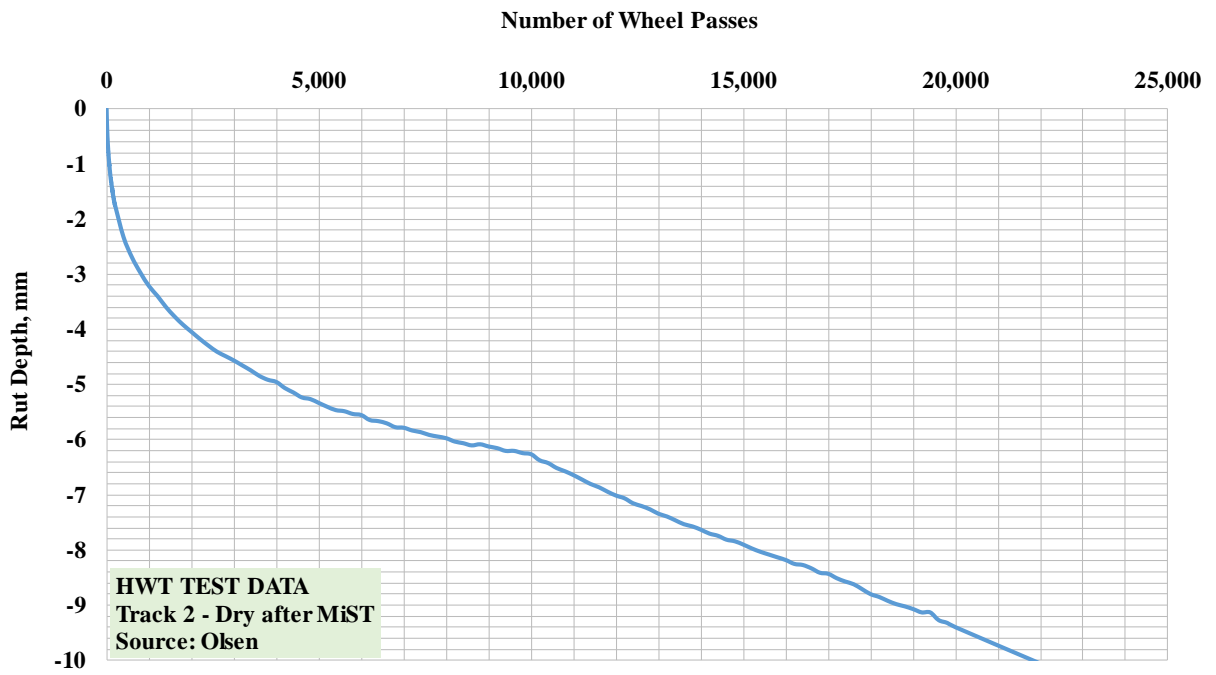
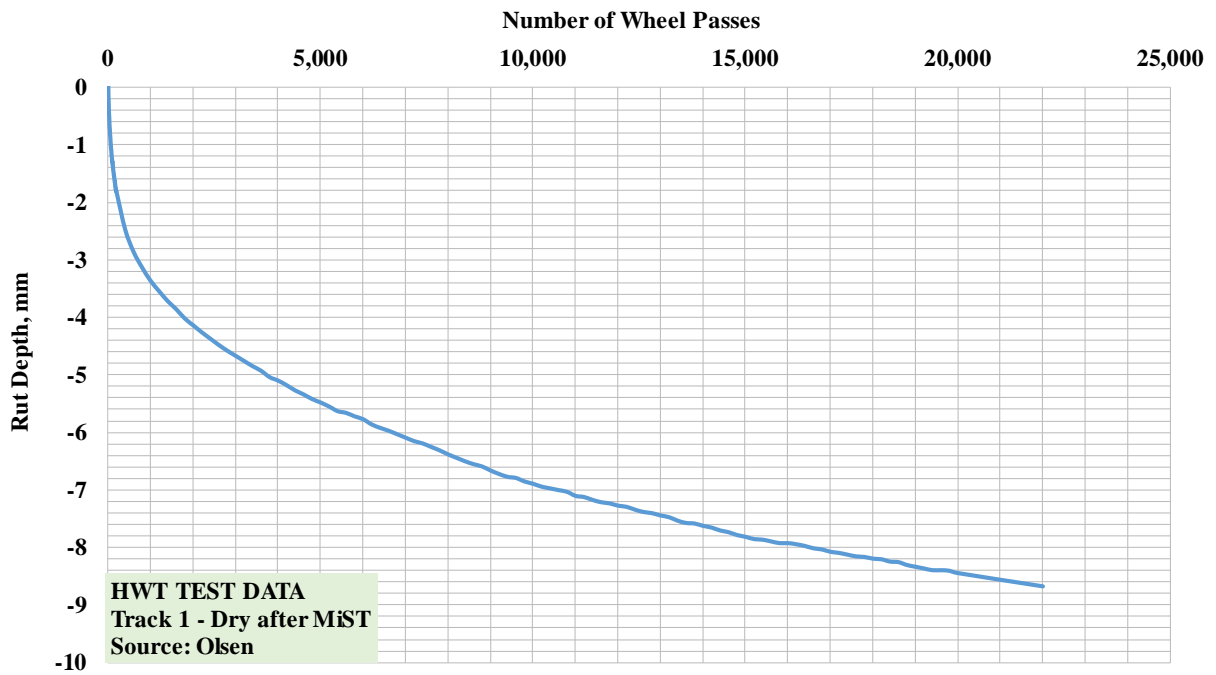
		Specimens of Track 1 (Right side)⁽¹⁾		Specimens of Track 2 (Left side)⁽¹⁾	
		Specimen 1	Specimen 2	Specimen 1	Specimen 2
Source	Menasha	6.6	6.1	6.4	6.6
	Waukesha	6.7	6.6	6.5	6.5
	Rock Springs	6.8	6.9	6.9	6.9
	Olsen	6.8	6.7	7.0	6.4

(1)Right and Left imply facing away from the machine

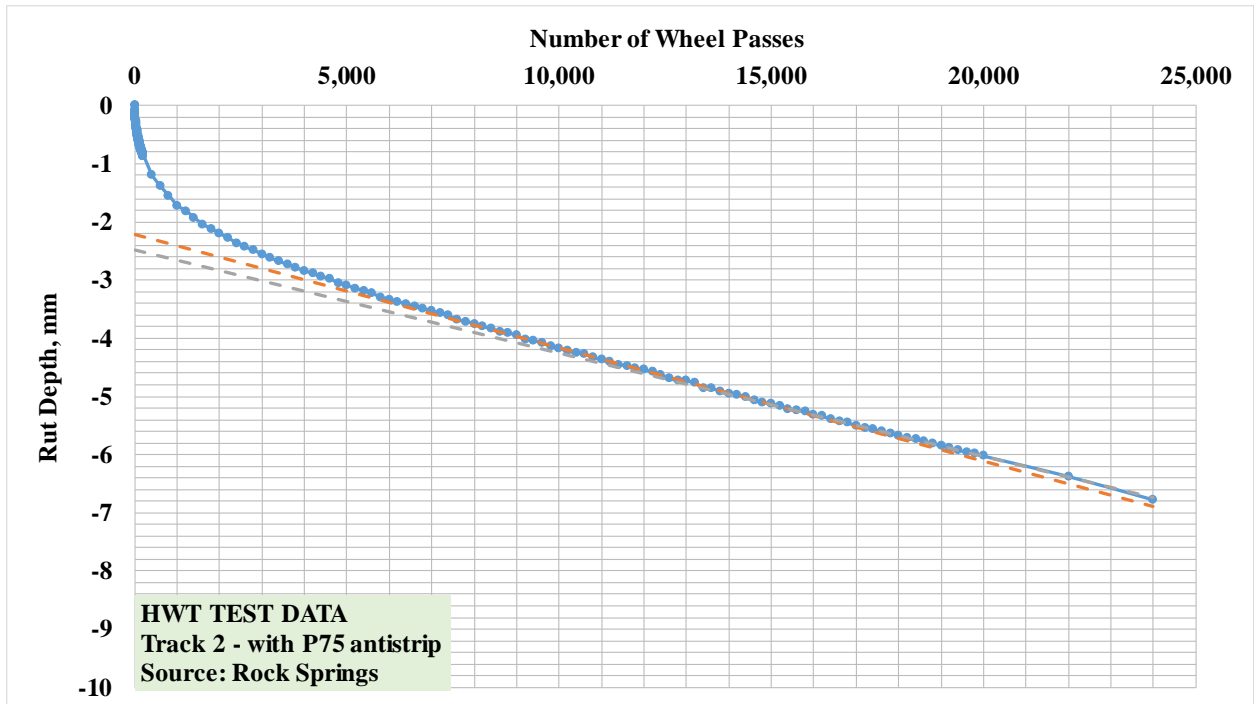
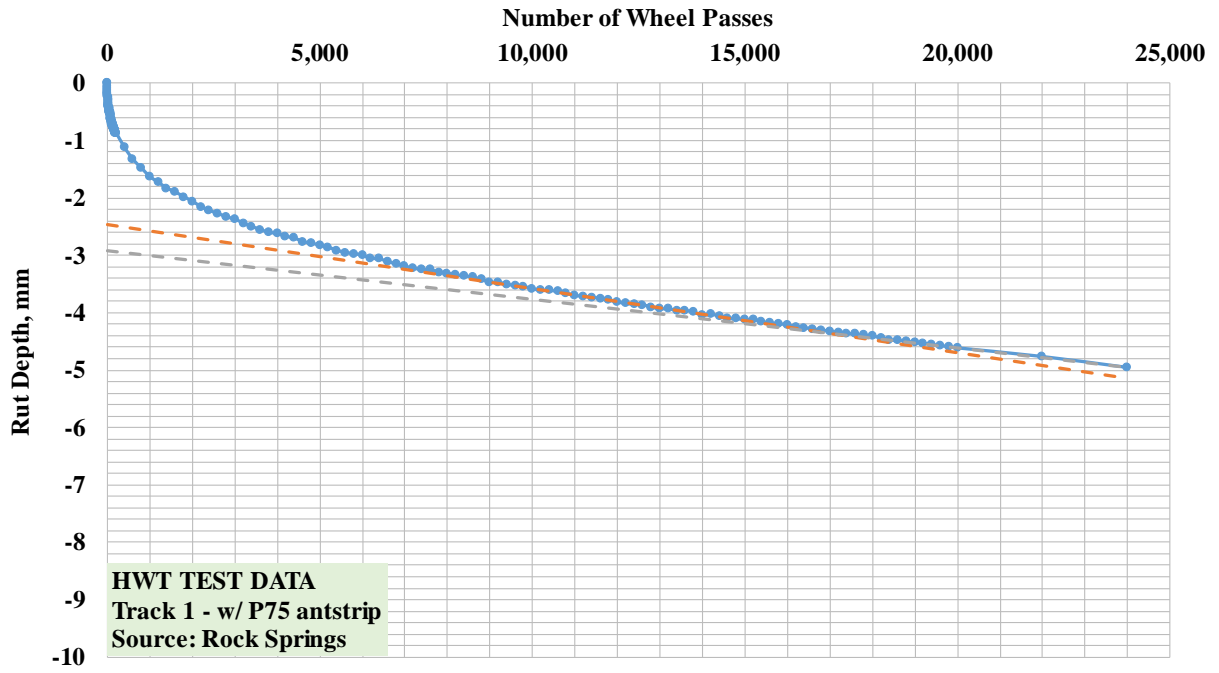


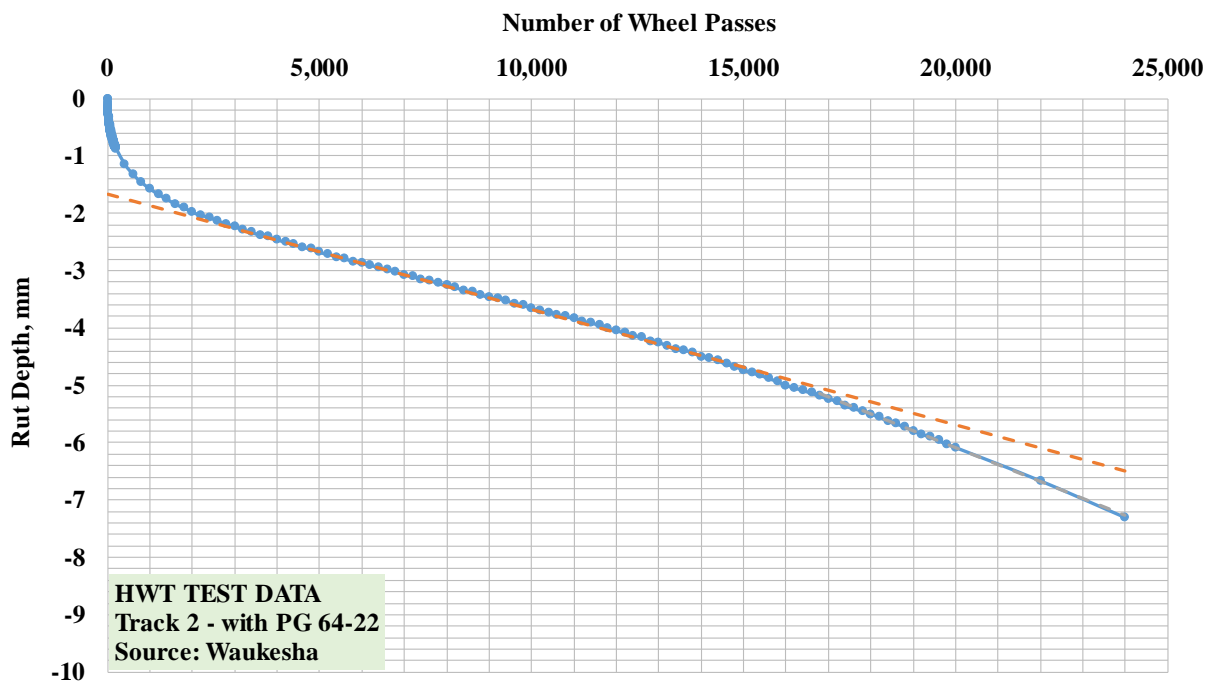
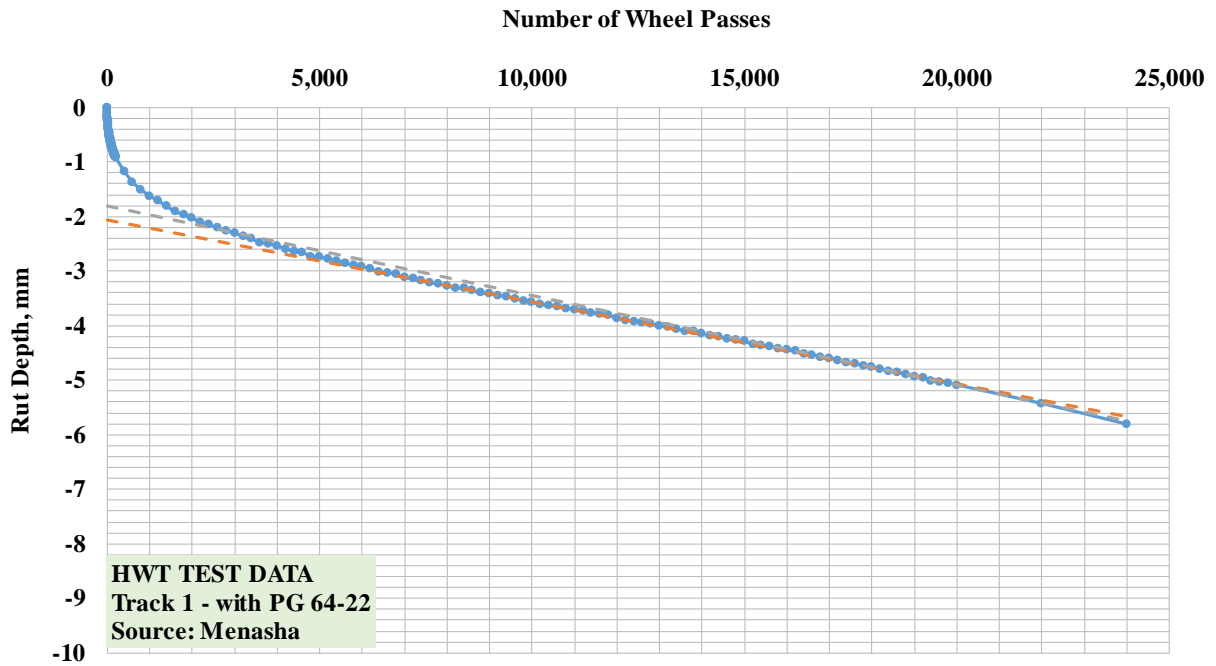


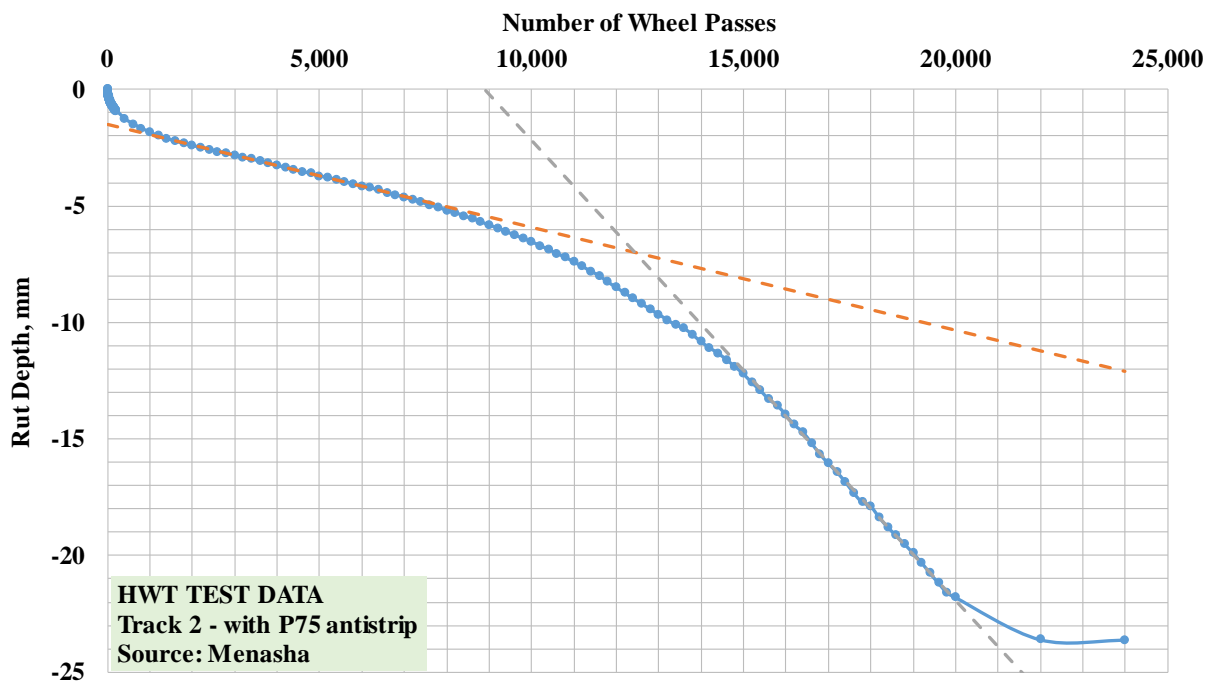
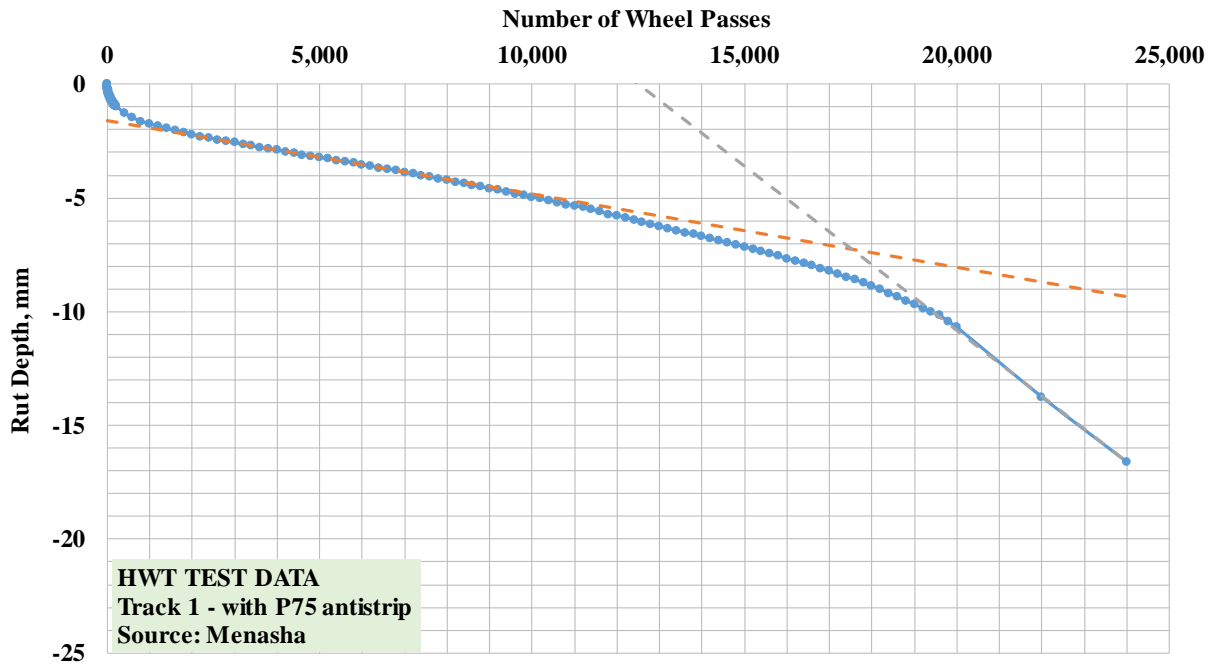


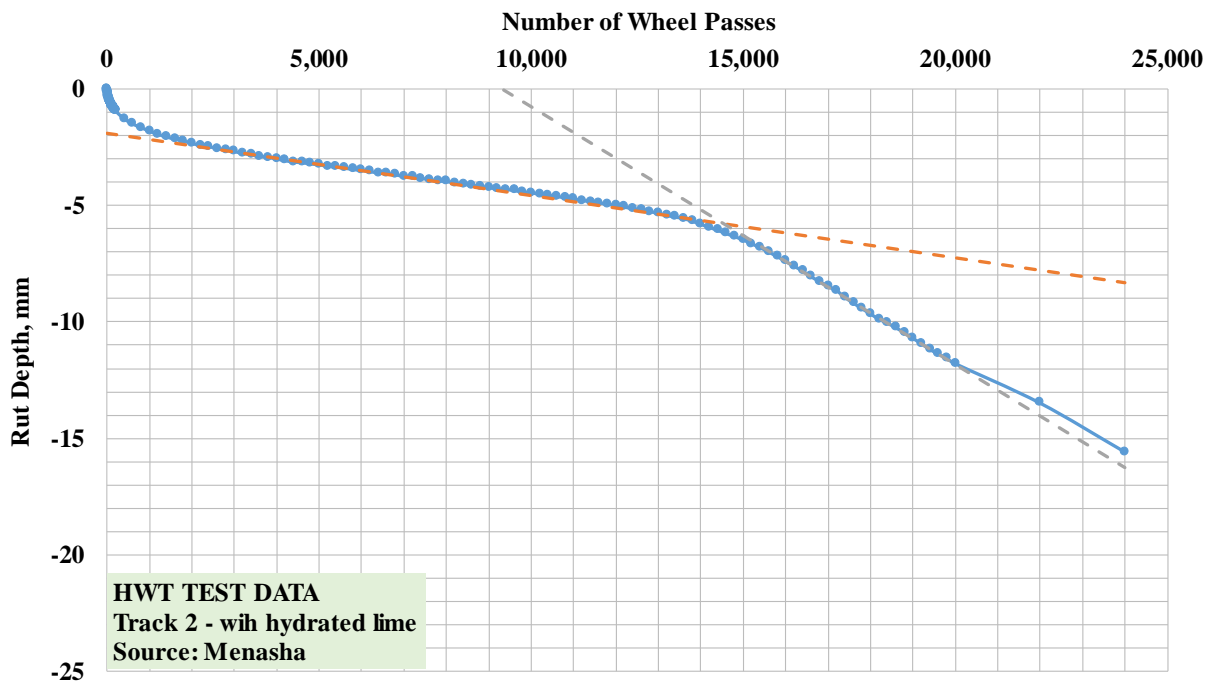
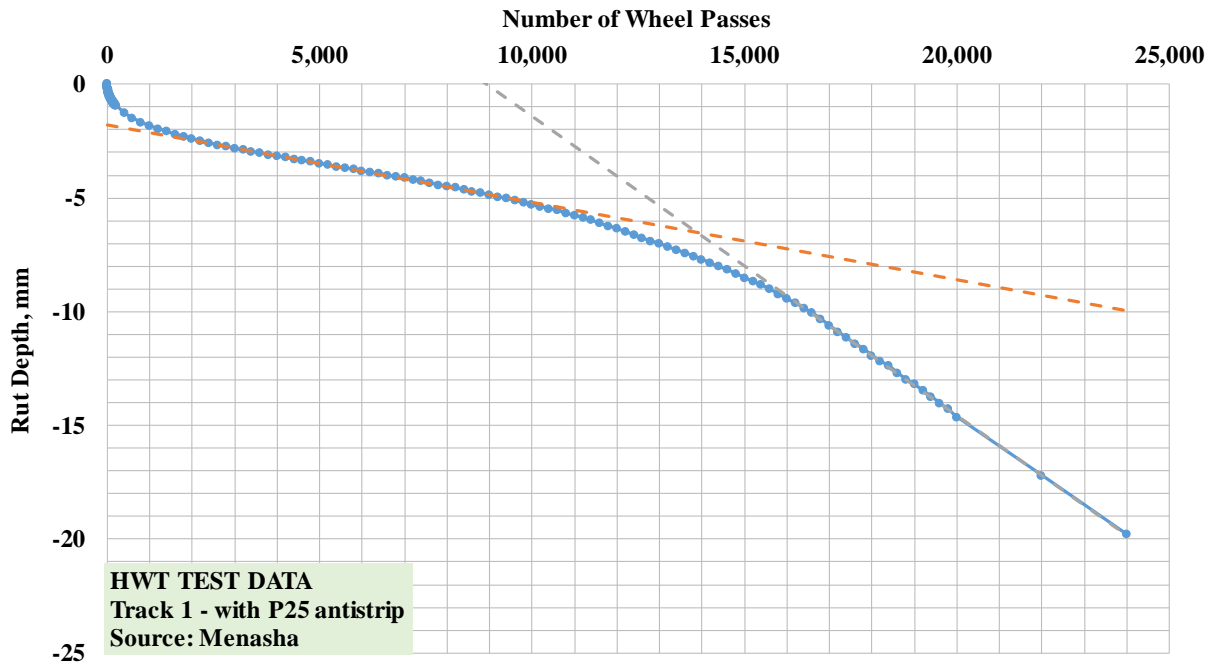


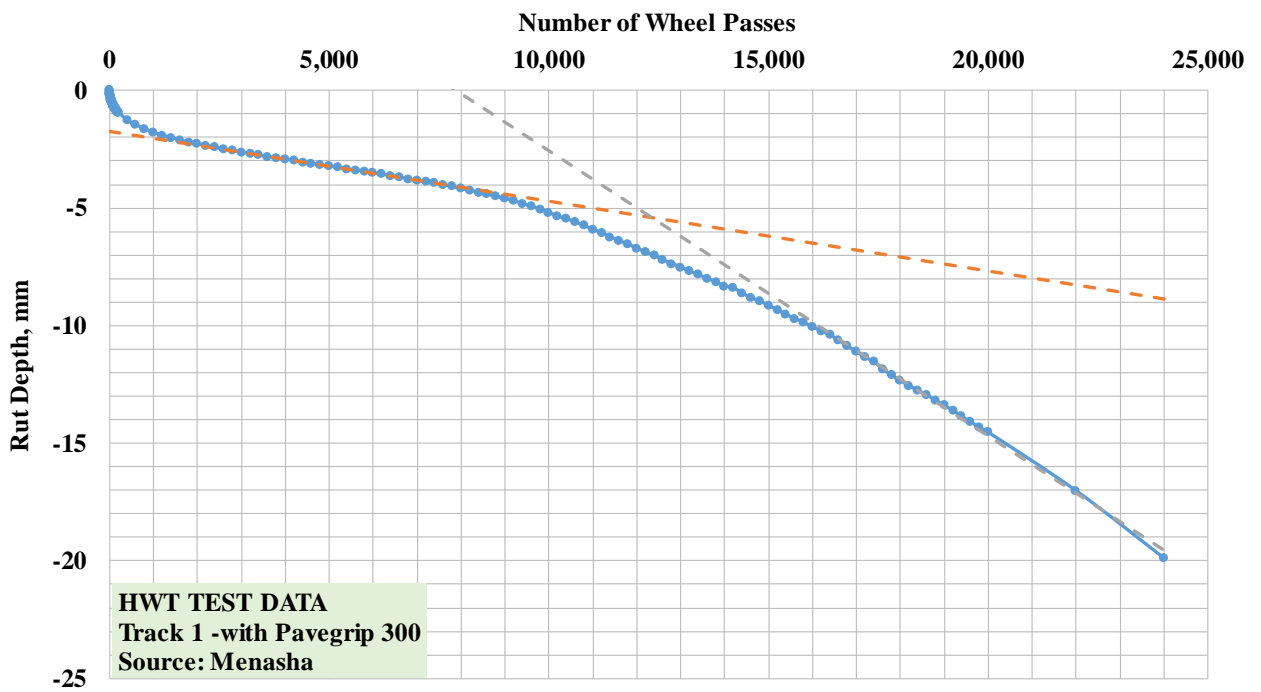
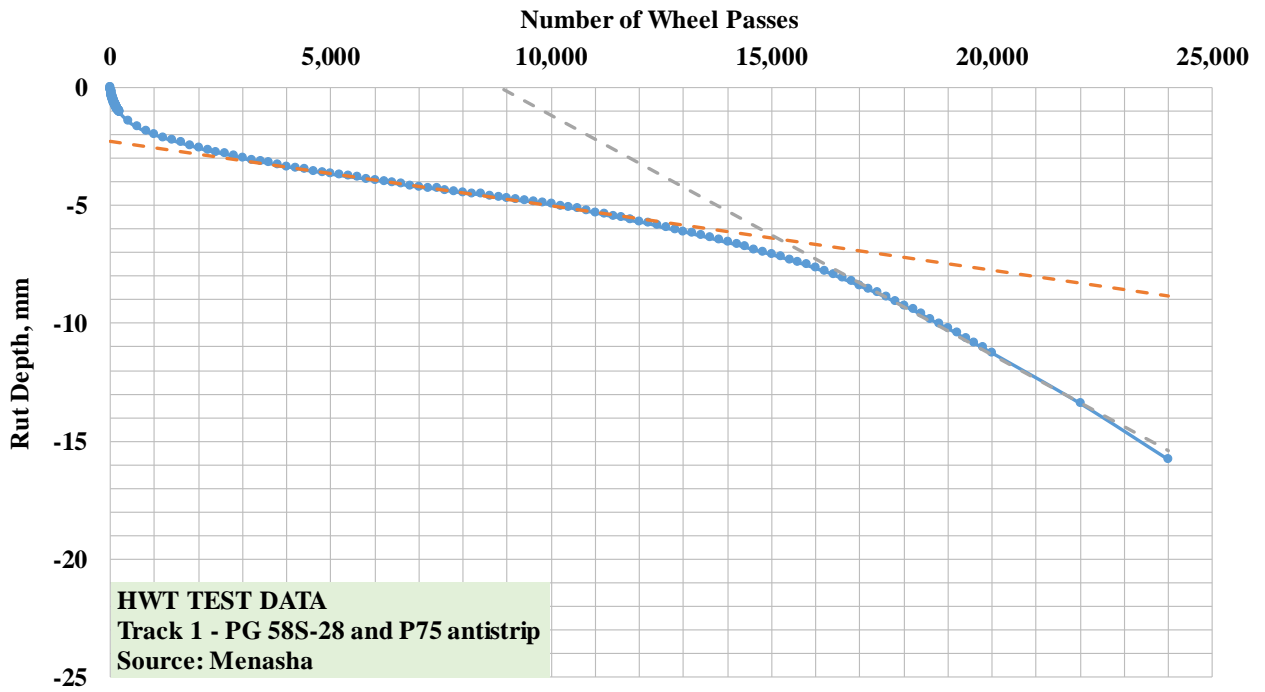
4. MOISTURE DAMAGE MITIGATION STUDY - SUBMERGED TESTING

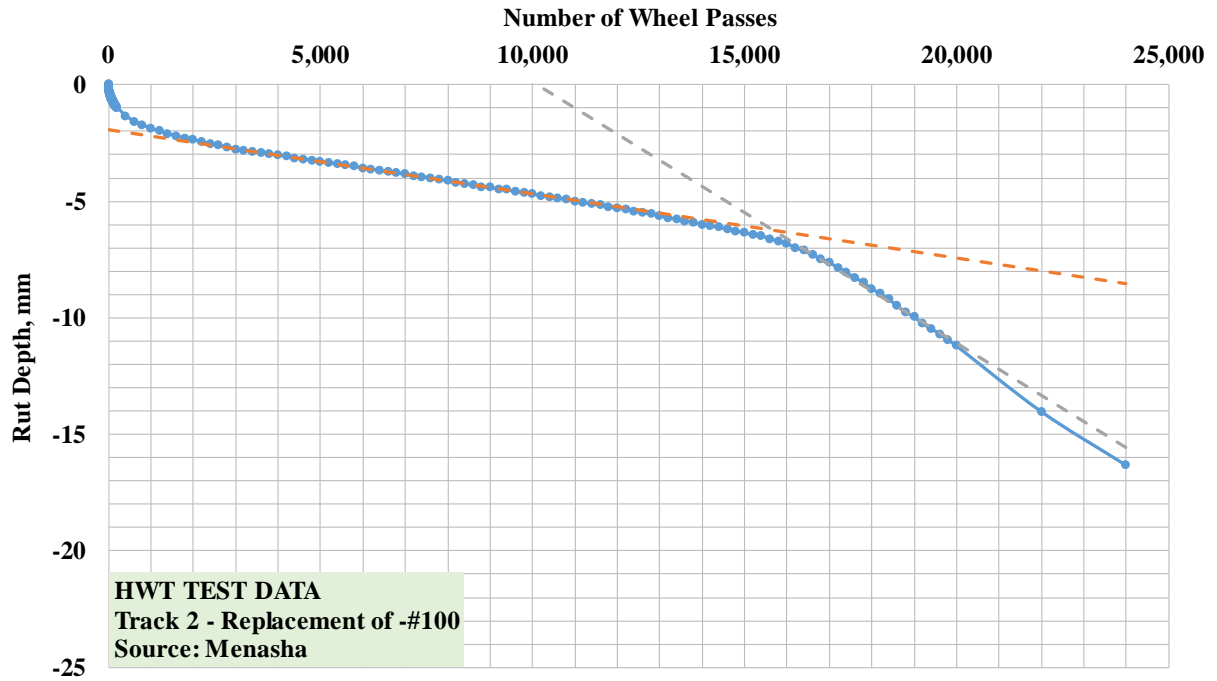












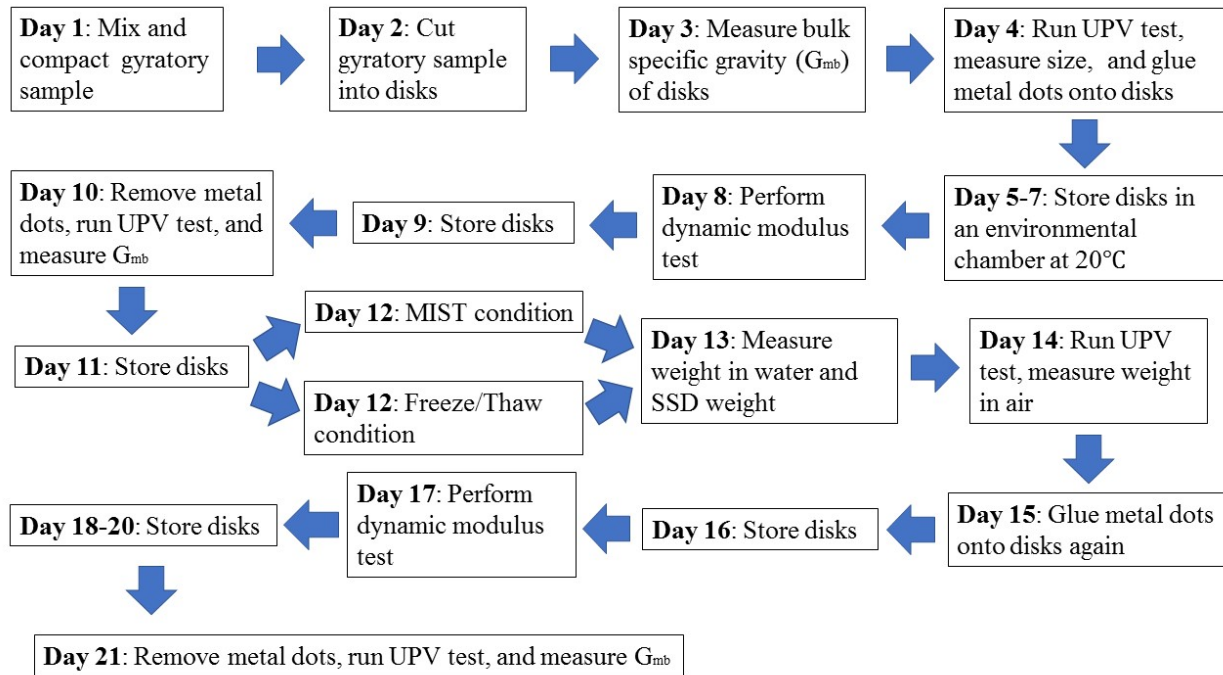
APPENDIX E

Results from Indirect Tensile Dynamic Modulus Tests (Modified AASHTO TP 131-18)

Notes on Legends in Graphs:

- **DM: Dynamic Modulus**
- **F/T: Freeze Thaw**
- **MR: Modulus Ratio**

FLOW CHART OF SPECIMEN PREPARATION AND TEST SCHEDULE FOR INDIRECT TENSILE DYNAMIC MODULUS TESTING



Note: UPV = Ultrasonic Pulse Velocity, SSD = Saturated Surface Dry

Table E-1 Summary of Modulus Values

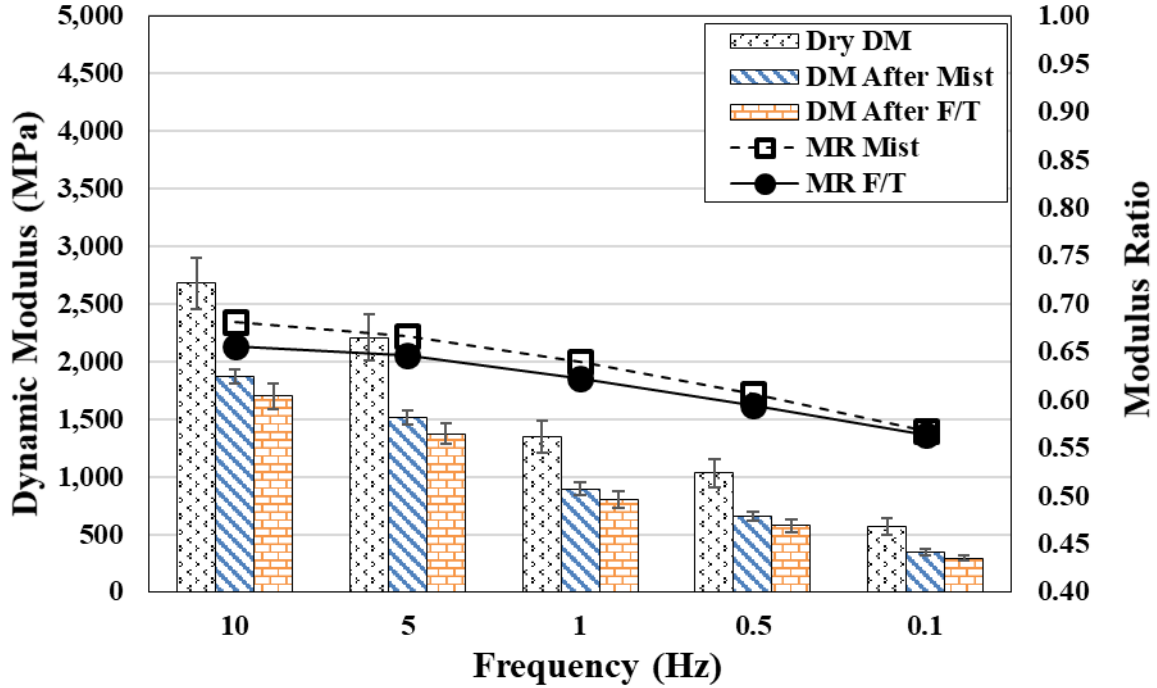
	Parameter	Condition	Material Source				
			Menasha	Waukesha	Rock Springs	Olsen	
Results from Indirect Tensile Dynamic Modulus Test	Modulus ⁽¹⁾ , MPa	Dry	2680	3414	3805	3341	
		after Freeze Thaw	1700	2490	2896	2325	
		after MiST	1874	2548	2306	2390	
	Modulus Ratio ⁽²⁾	after Freeze Thaw	0.66	0.71	0.74	0.70	
		after MiST	0.68	0.76	0.63	0.72	
Results from UPV Test	Modulus, MPa	Dry	15,935	17,598	19,733	19,621	
		after Freeze Thaw ⁽³⁾	13,486	15,786	19,882	16,505	
		after MiST ⁽³⁾	14,564	16,592	17,998	17,949	
	Modulus Ratio	after Freeze Thaw					
		after MiST					

(1) Only Modulus from 10 Hz frequency is reported in this table.

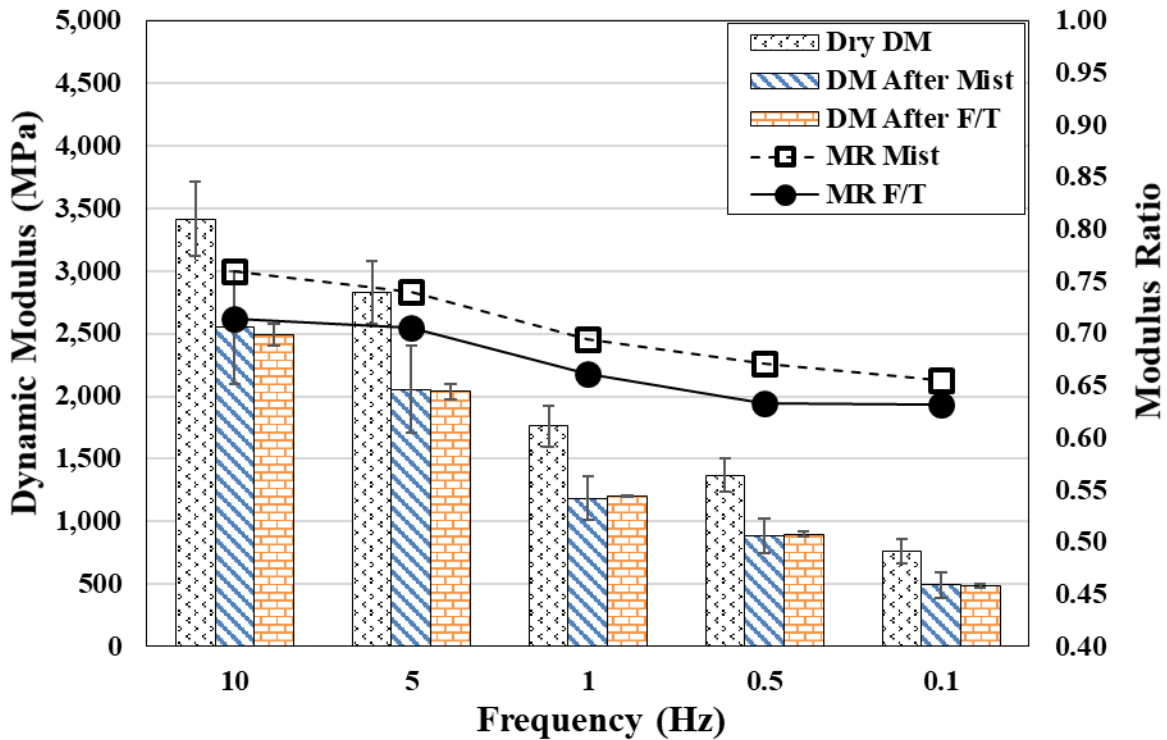
(2) Modulus ratio is calculated separately for each of three specimens, and then averaged.

1. PRESENTATION OF RESULTS BASED ON CALCULATED AVERAGE
FROM 3 REPLICATE SPECIMENS

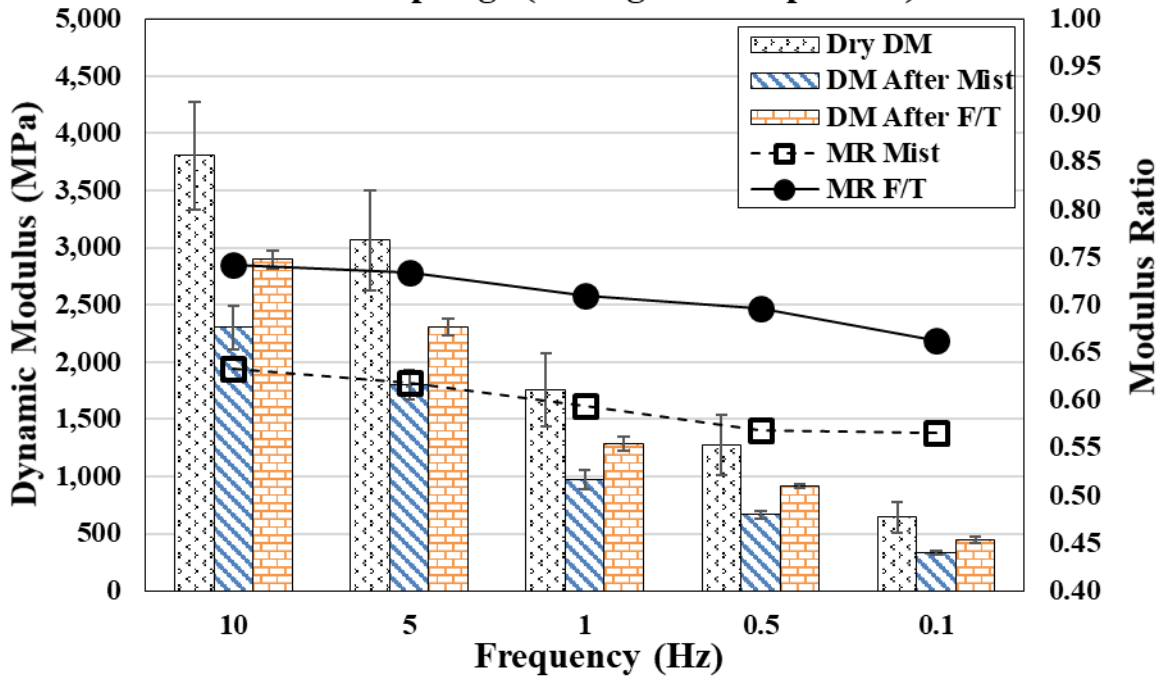
Menasha (Average of 3 Replicates)



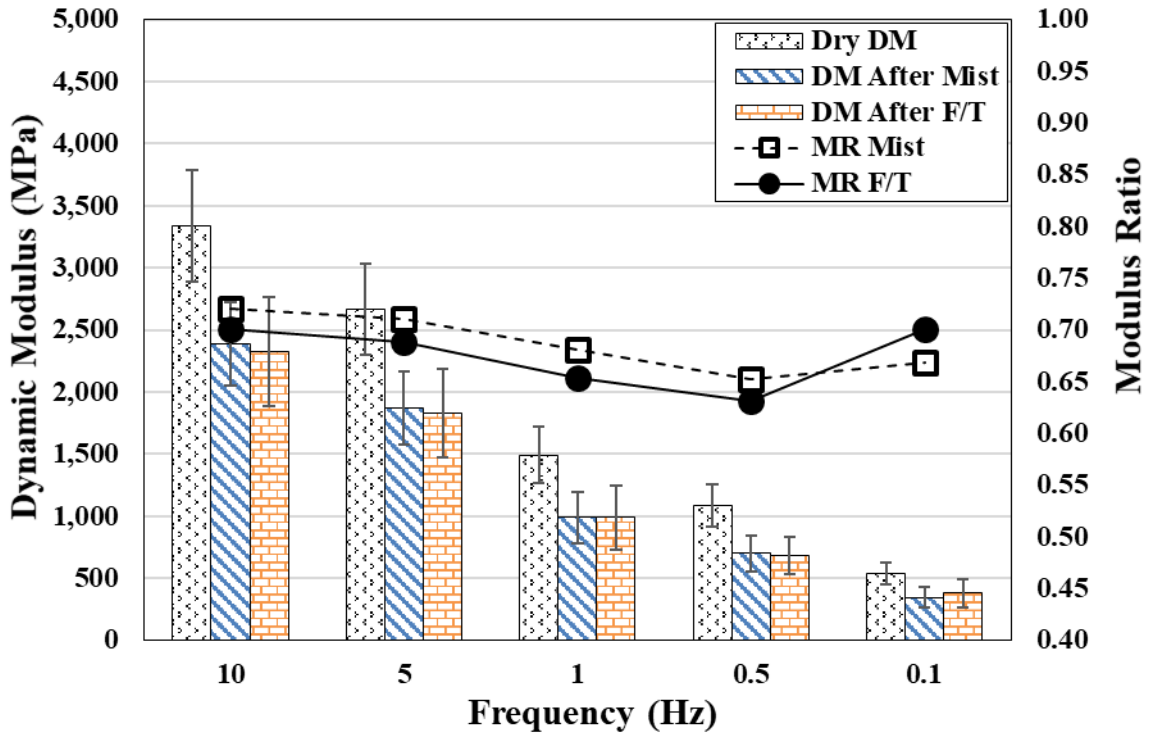
Waukesha (Average of 3 Replicates)



Rock Springs (Average of 3 Replicates)

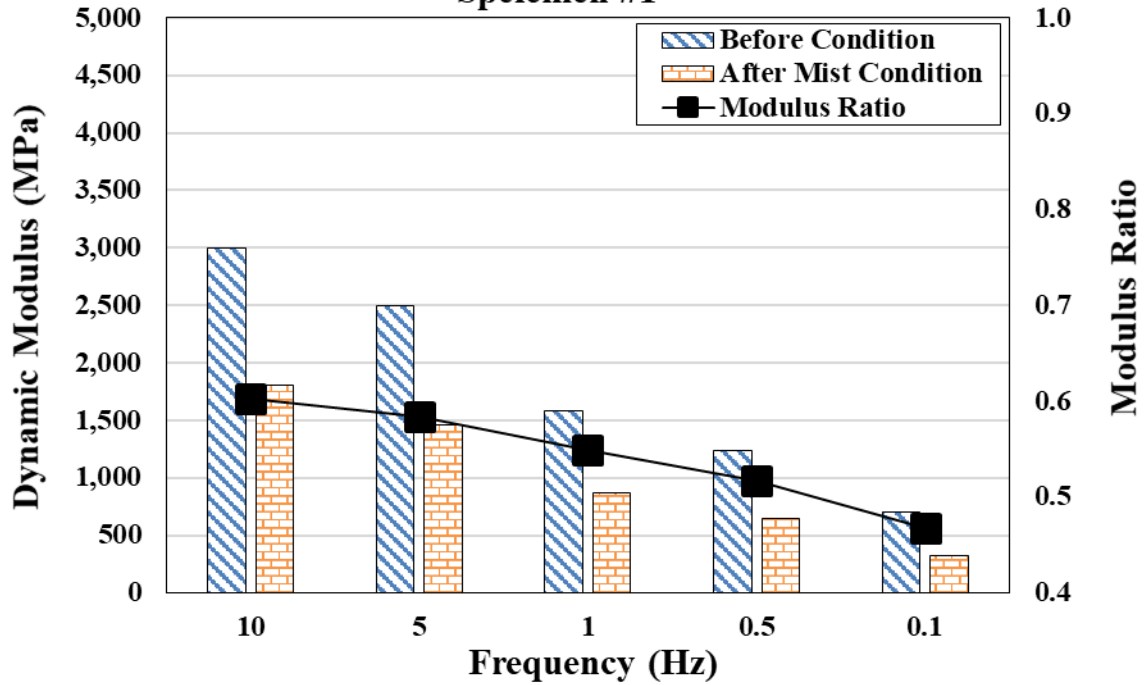


Olsen (Average of 3 Replicates)

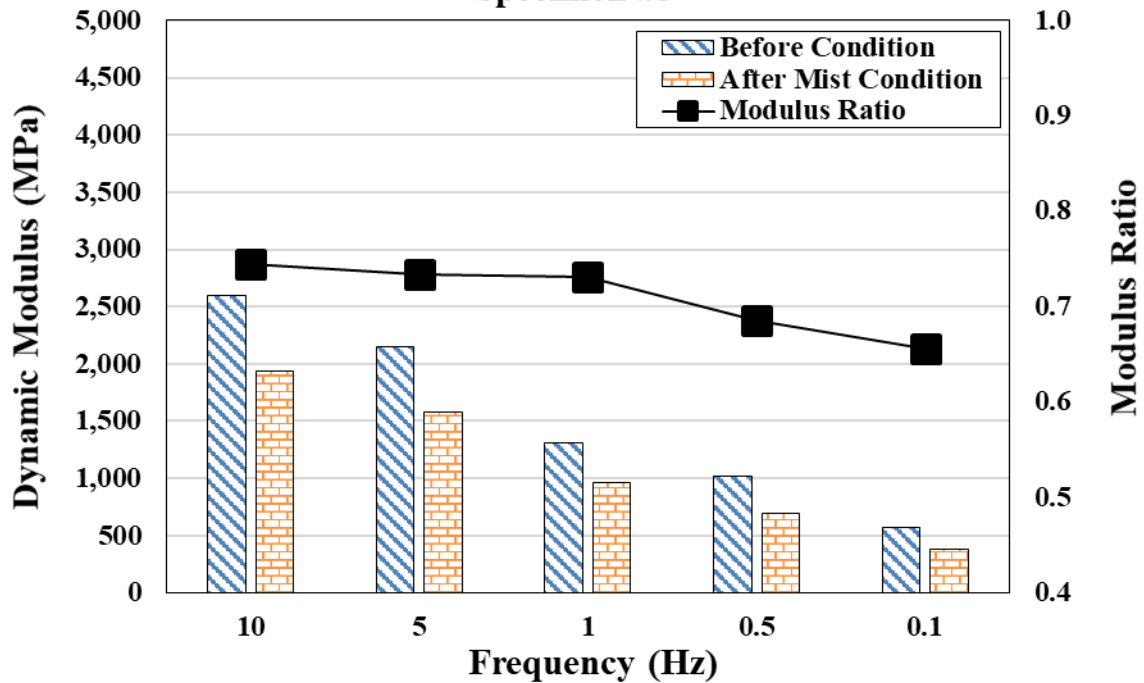


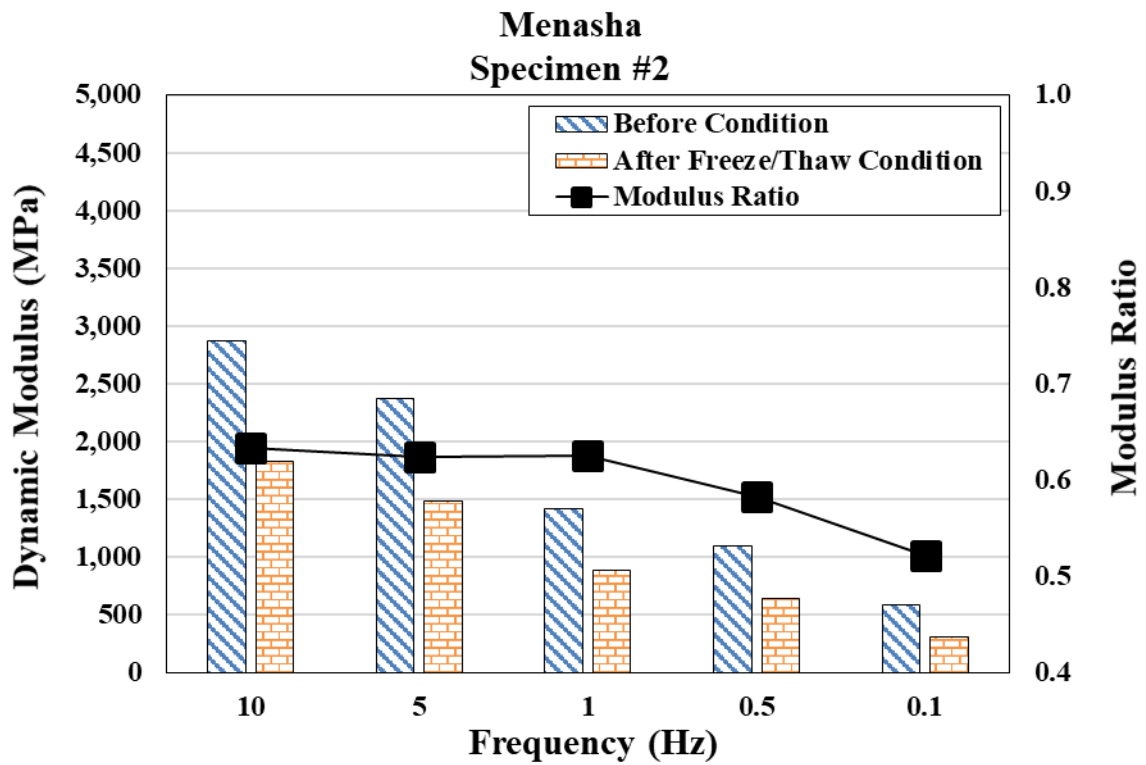
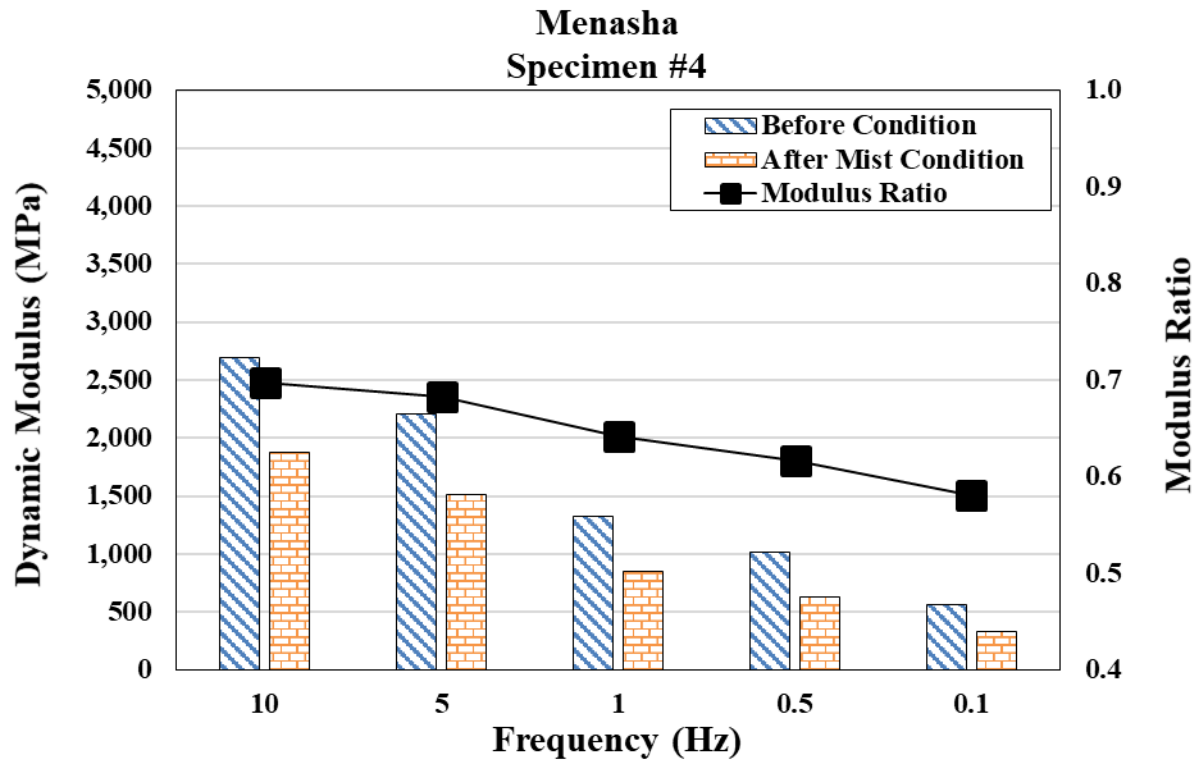
2. PRESENTATION OF RESULTS FOR EACH SPECIMEN

**Menasha
Speicmen #1**

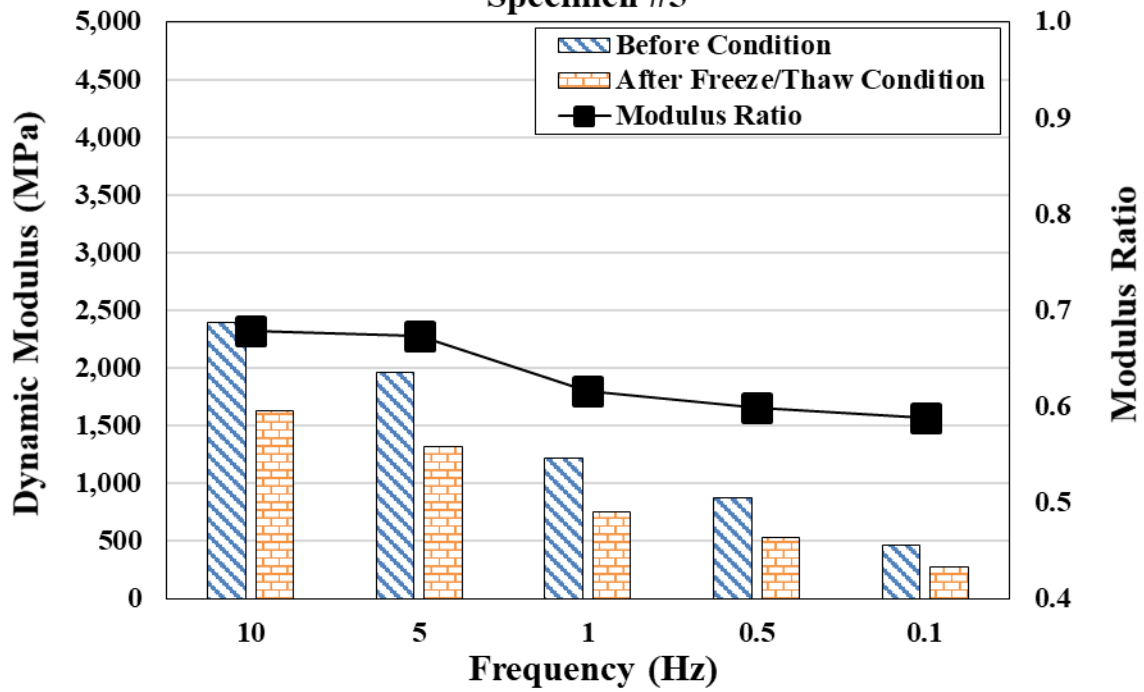


**Menasha
Specimen #3**

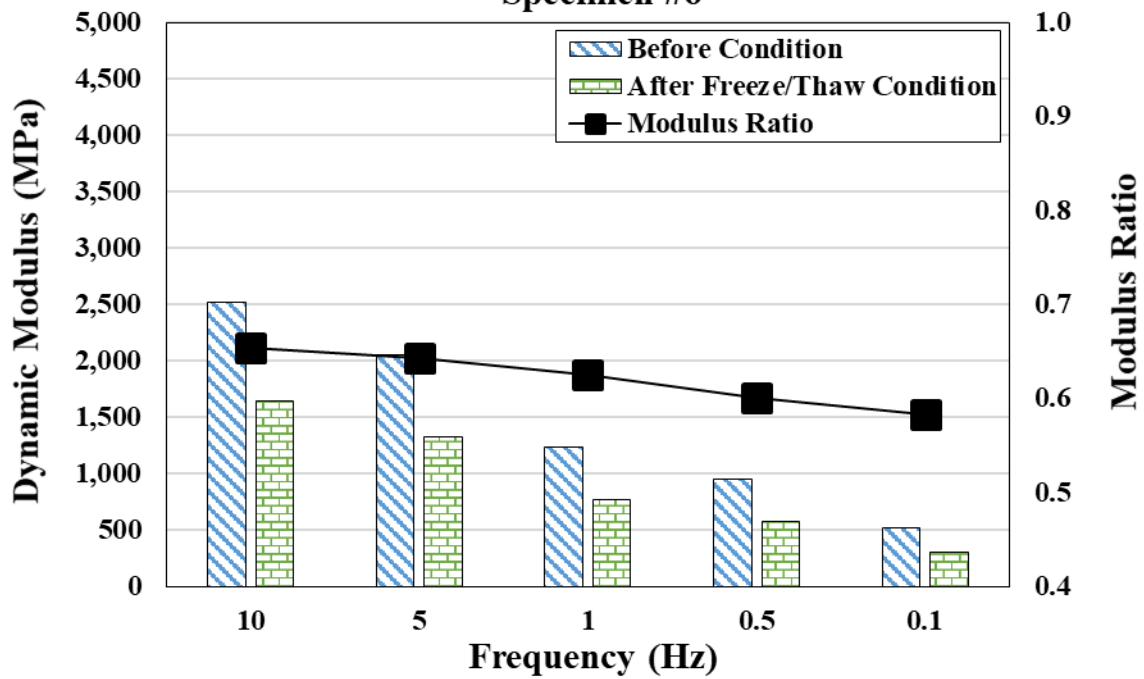




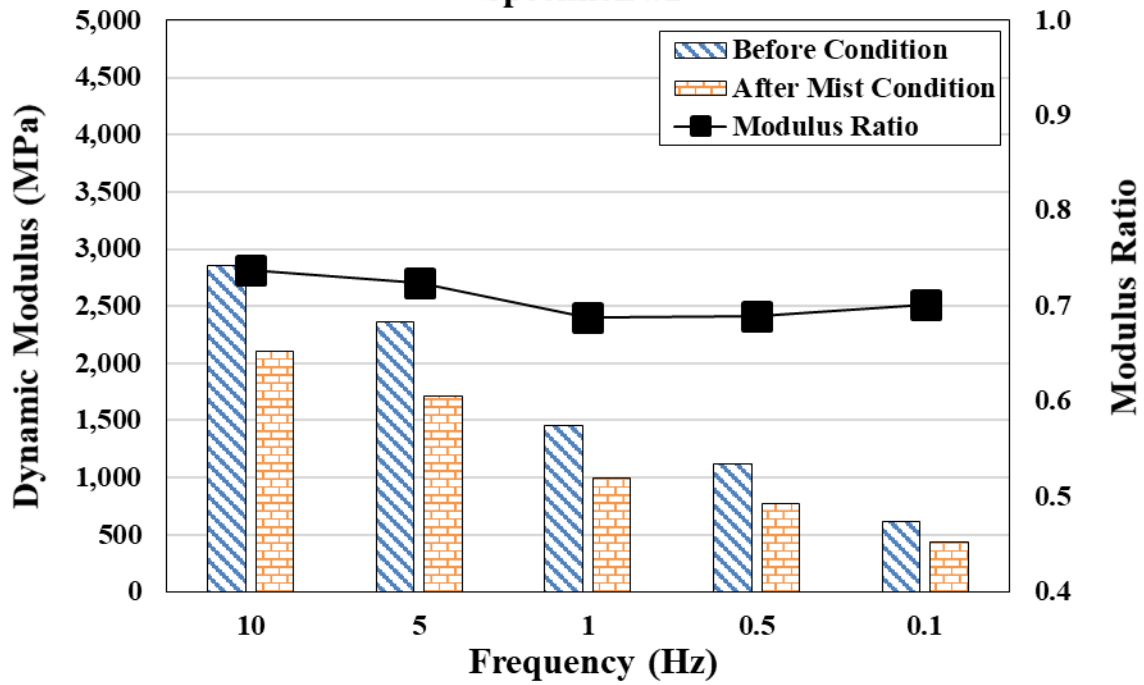
**Menasha
Specimen #5**



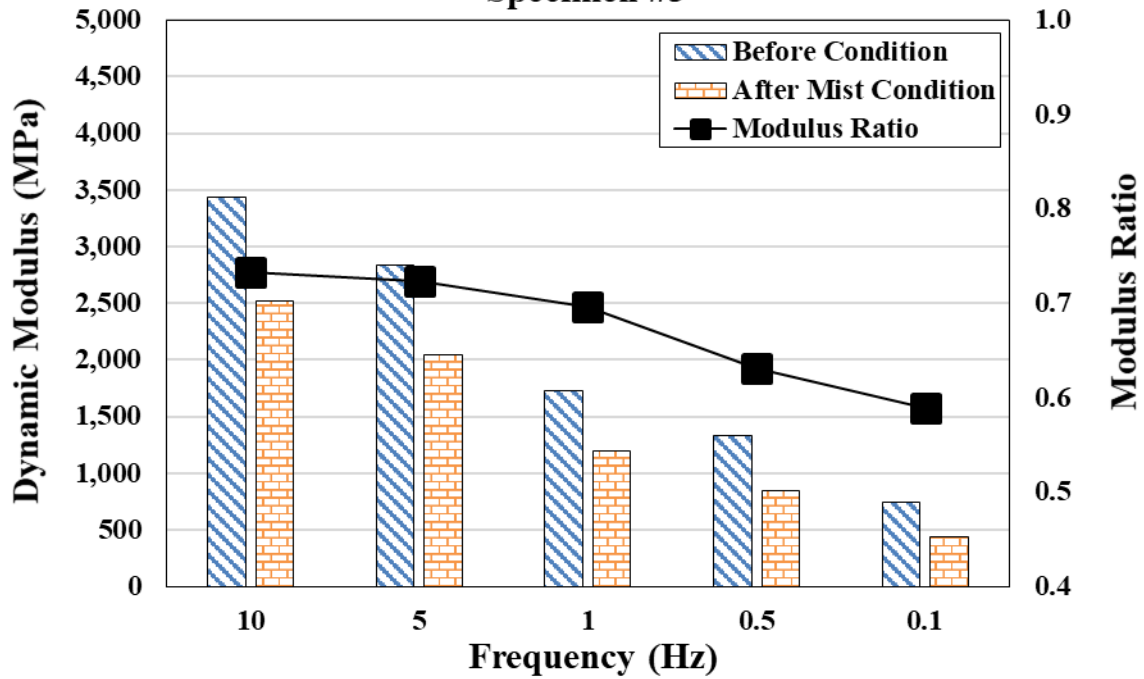
**Menasha
Specimen #6**



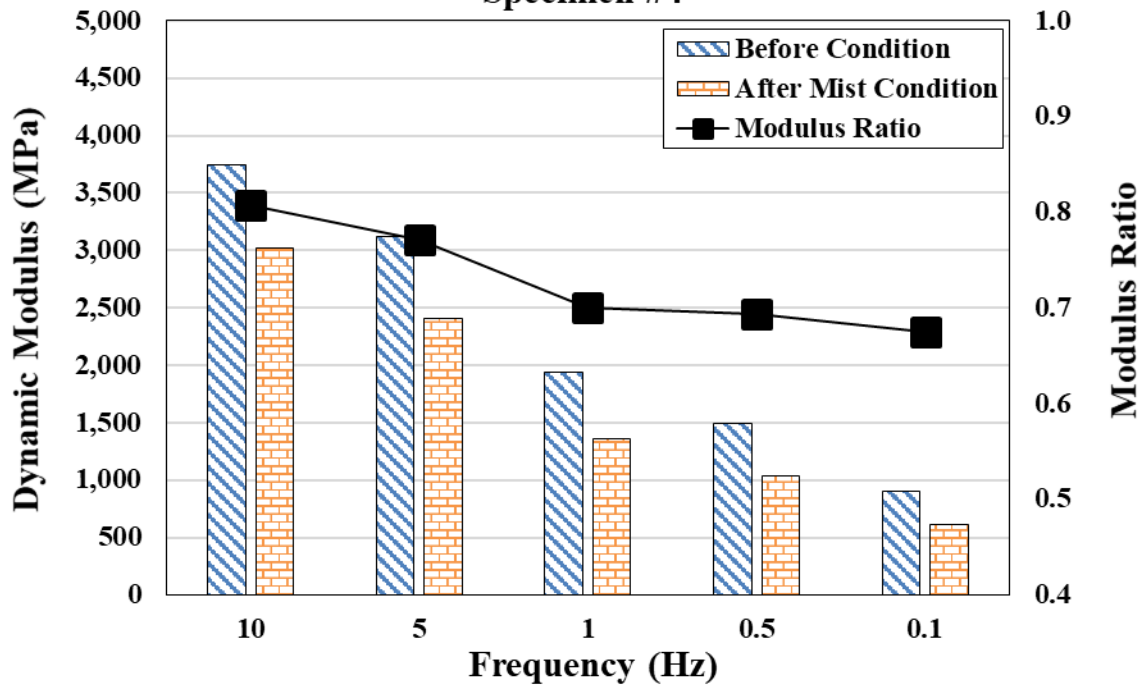
Waukesha Specimen #2



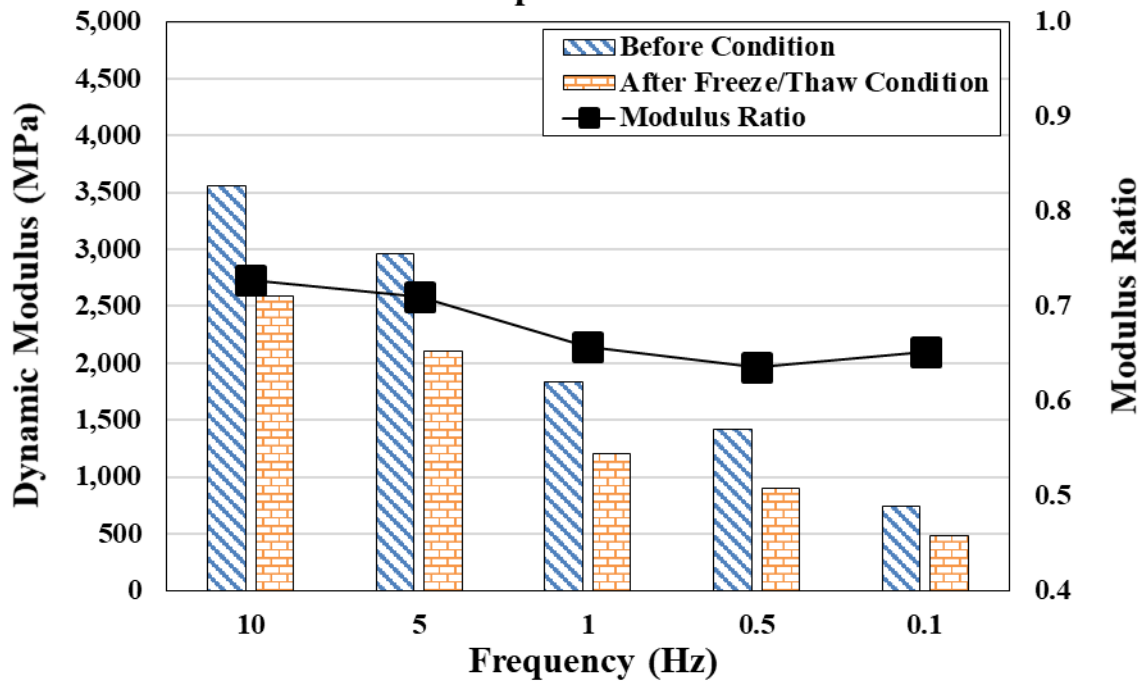
Waukesha Specimen #3



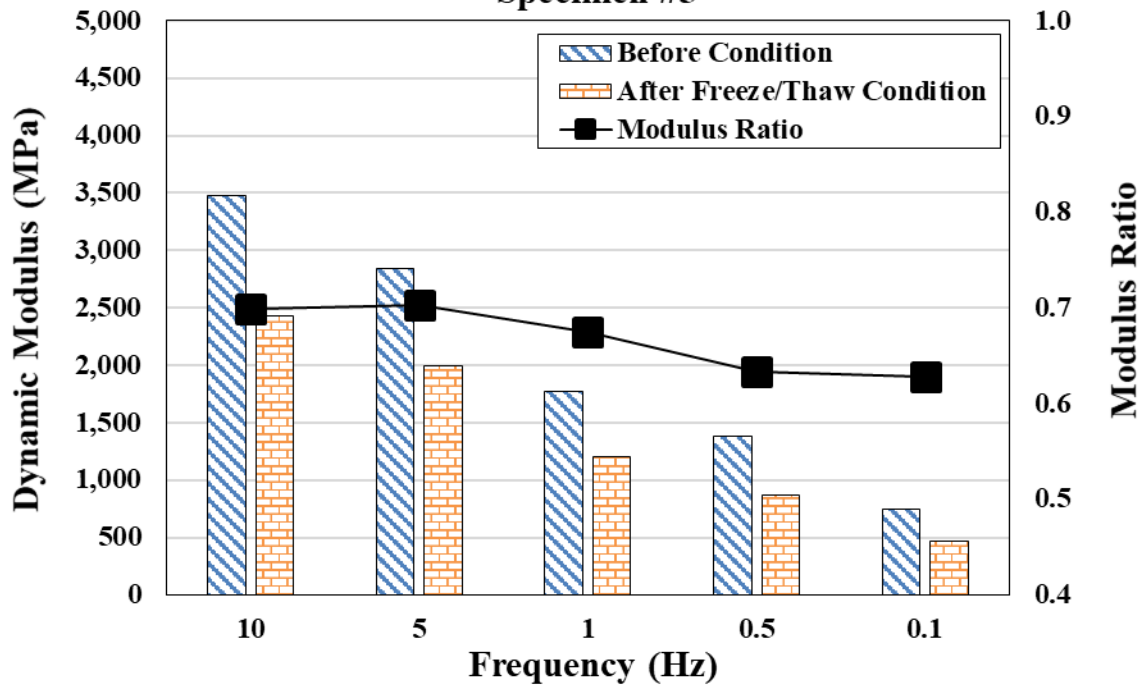
**Waukesha
Specimen #4**



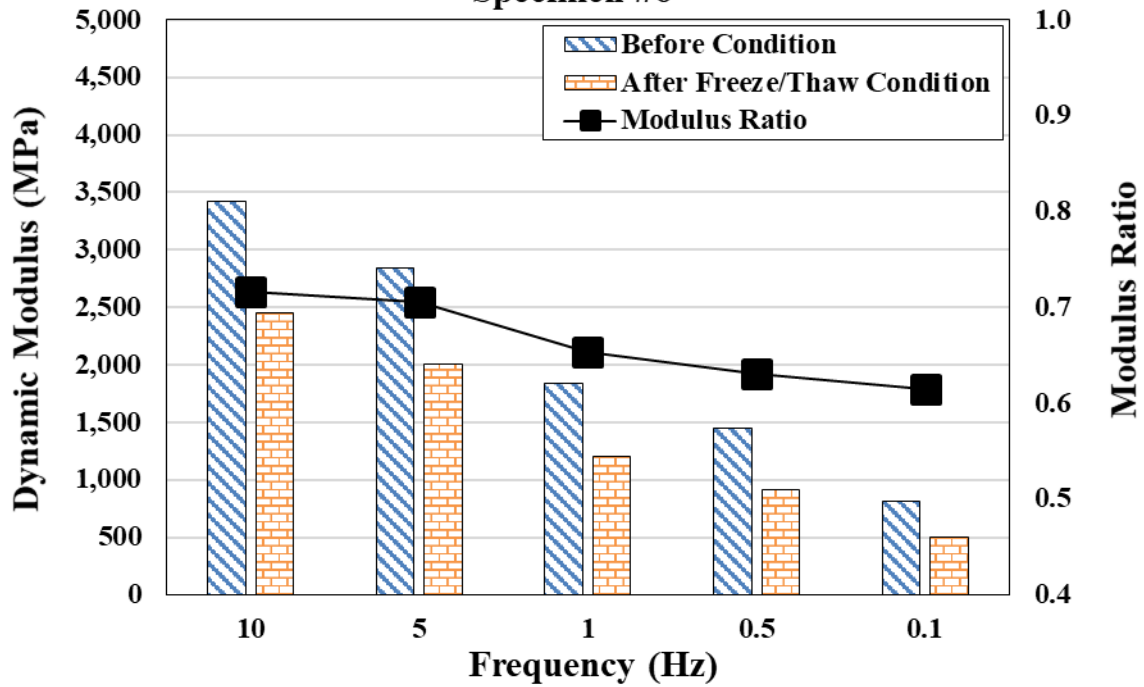
**Waukesha
Specimen #1**



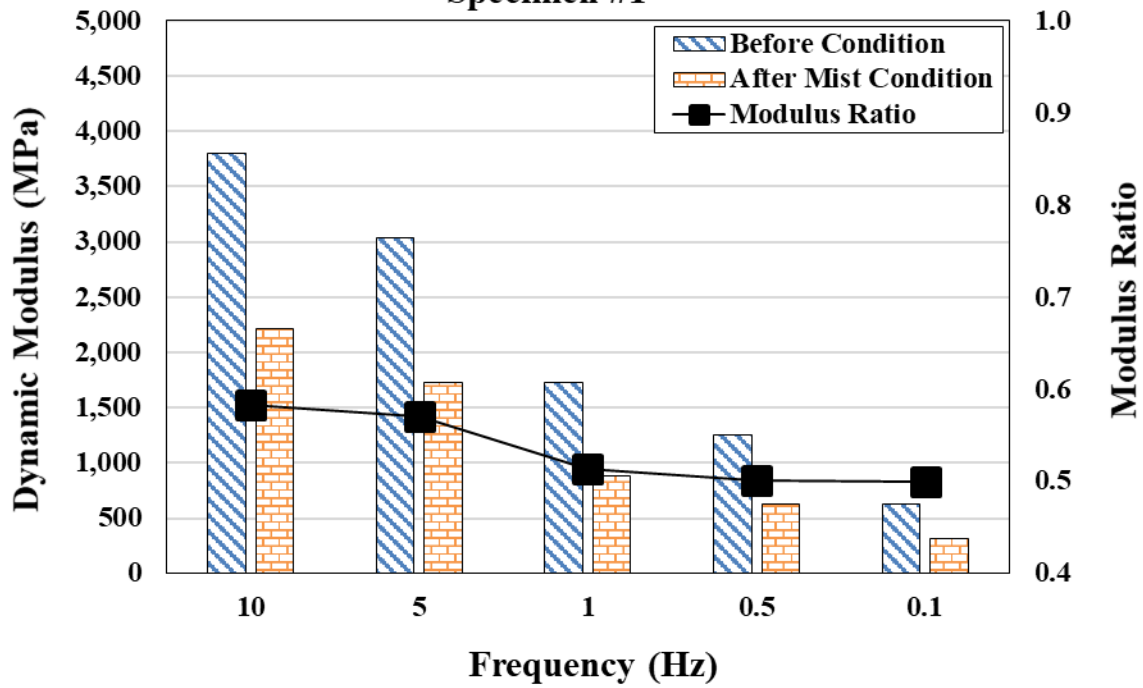
Waukesha Specimen #5



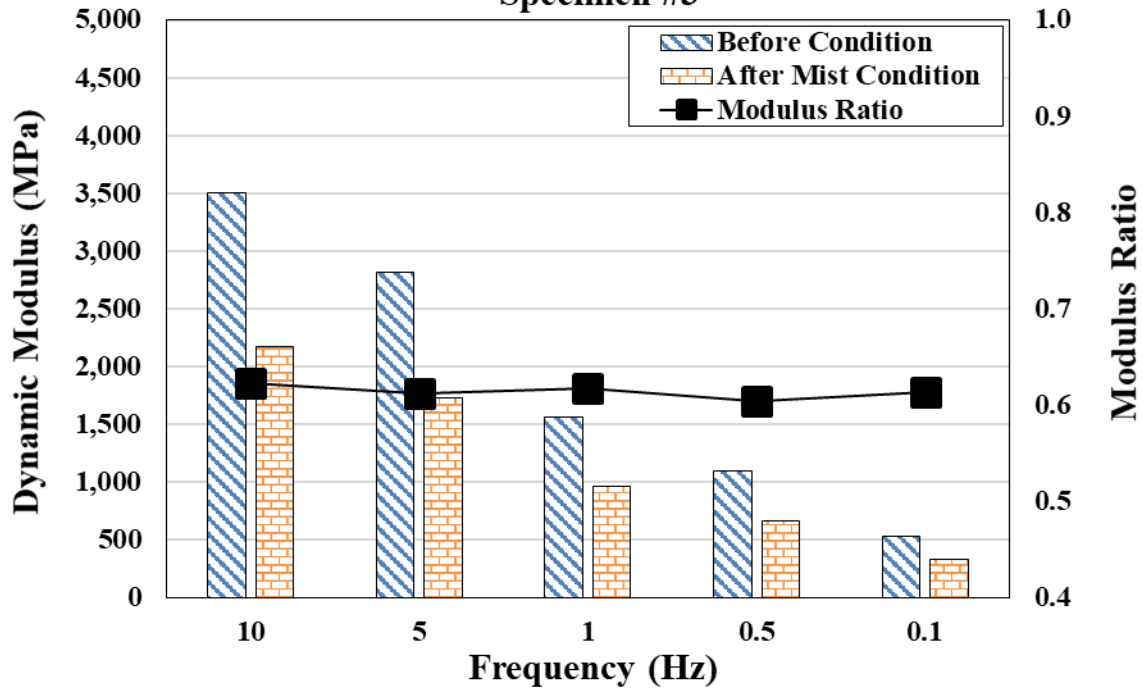
Waukesha Specimen #6



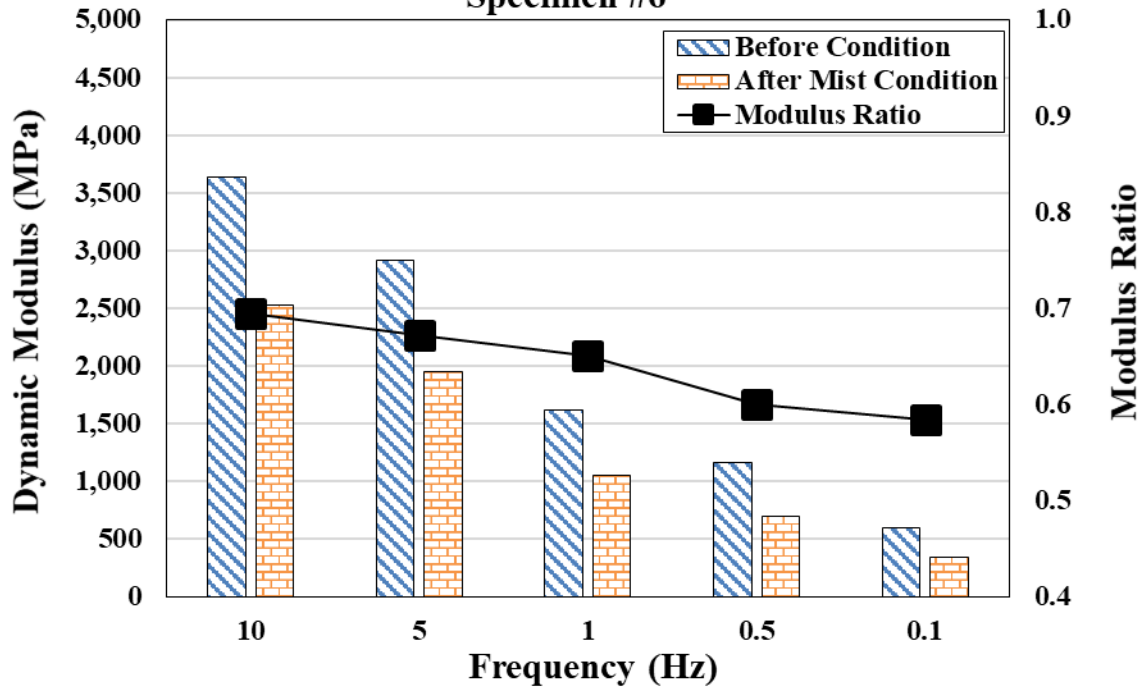
Rock Springs Specimen #1



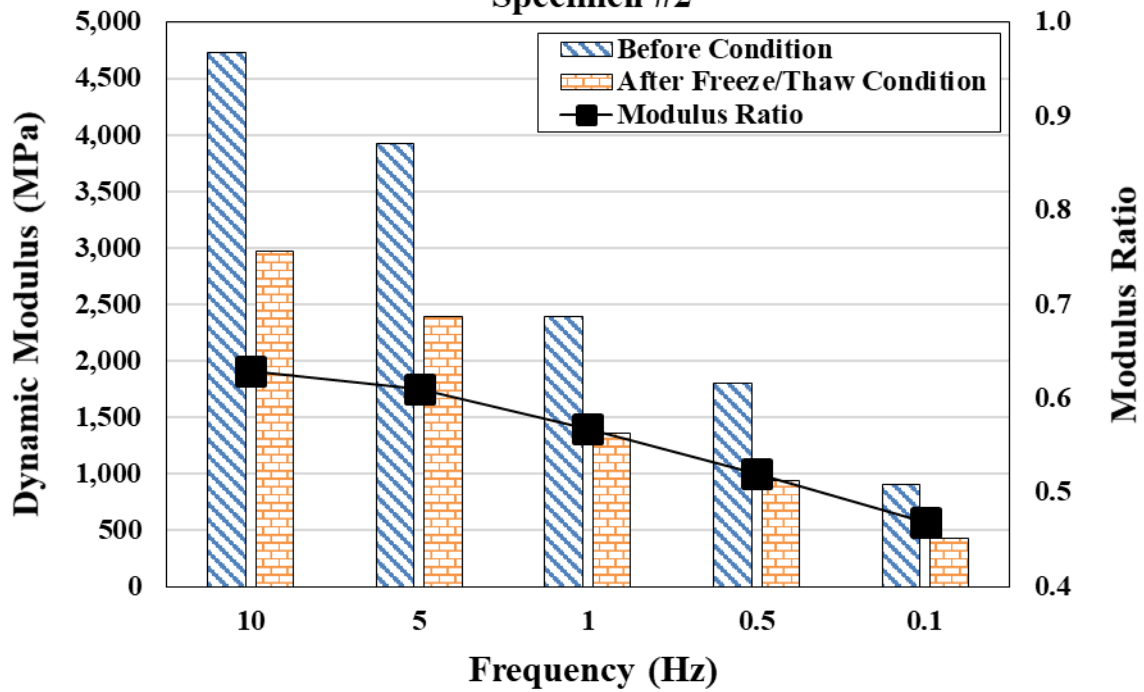
Rock Springs Specimen #3



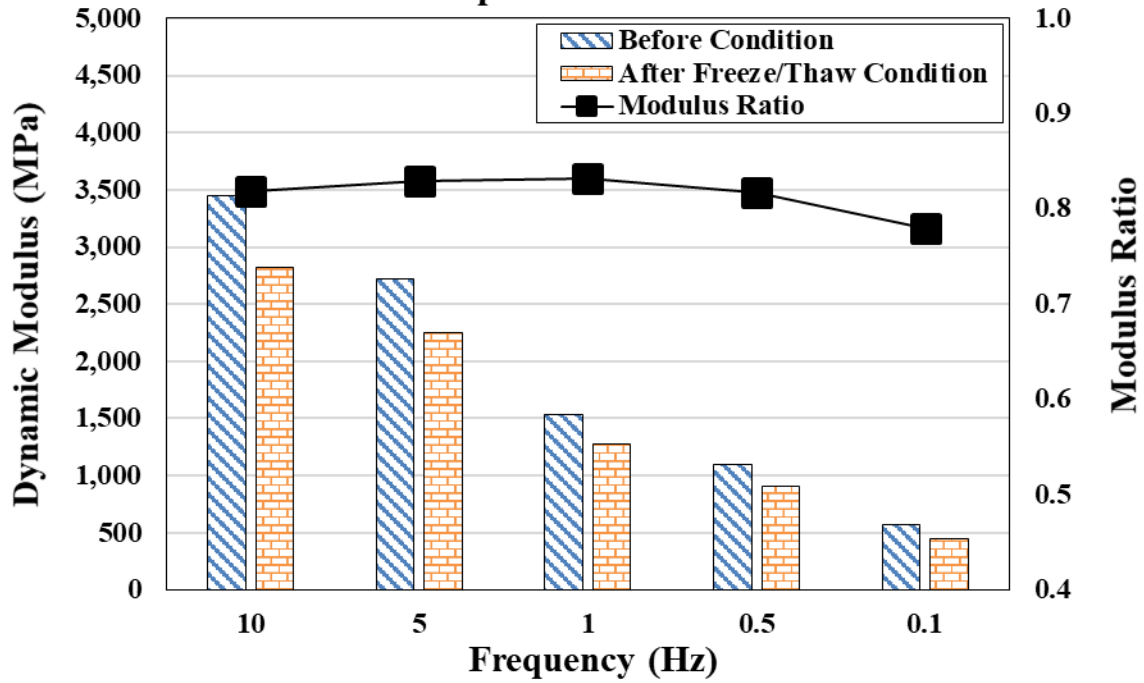
Rock Springs Specimen #6



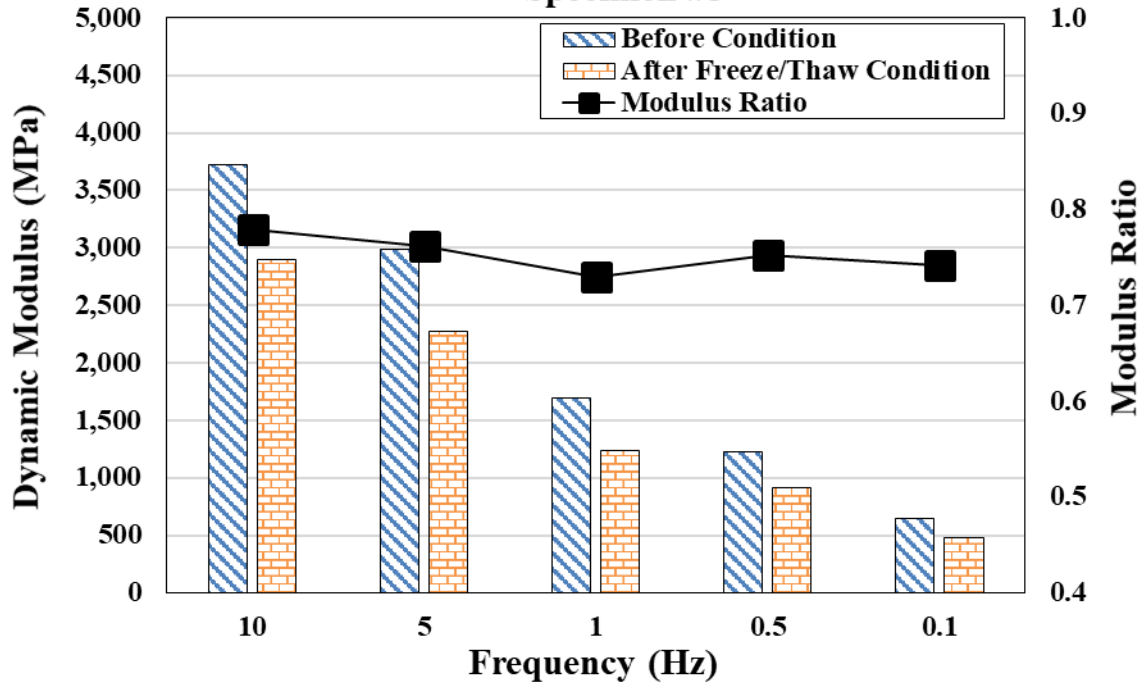
Rock Springs Specimen #2



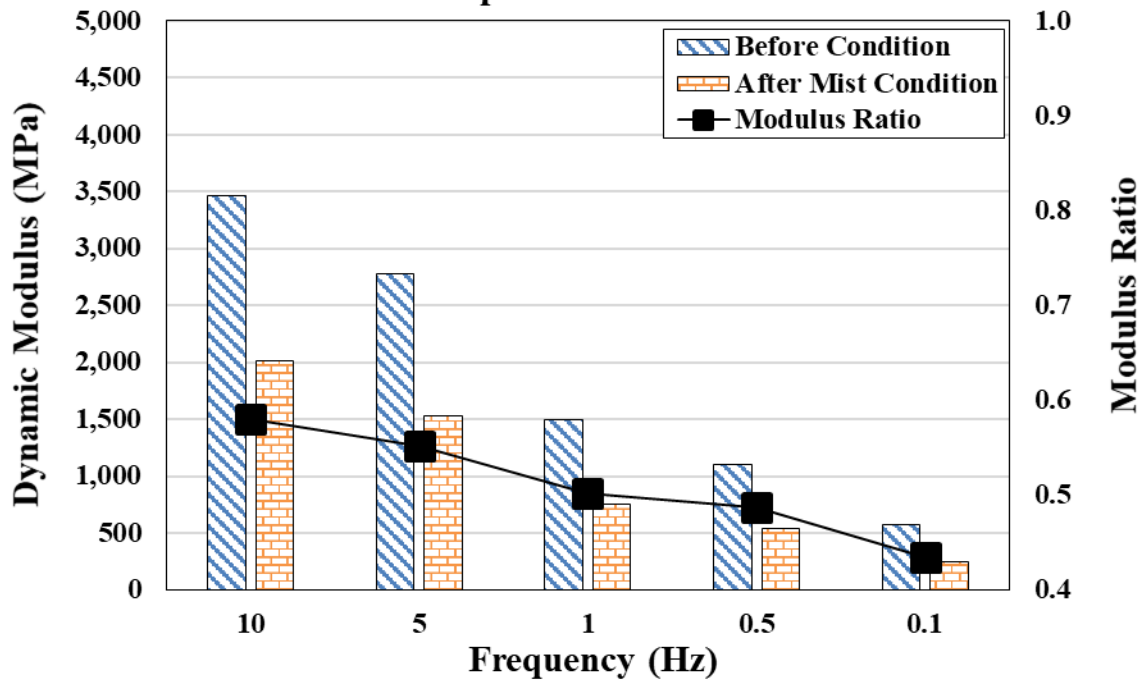
Rock Springs Specimen #4



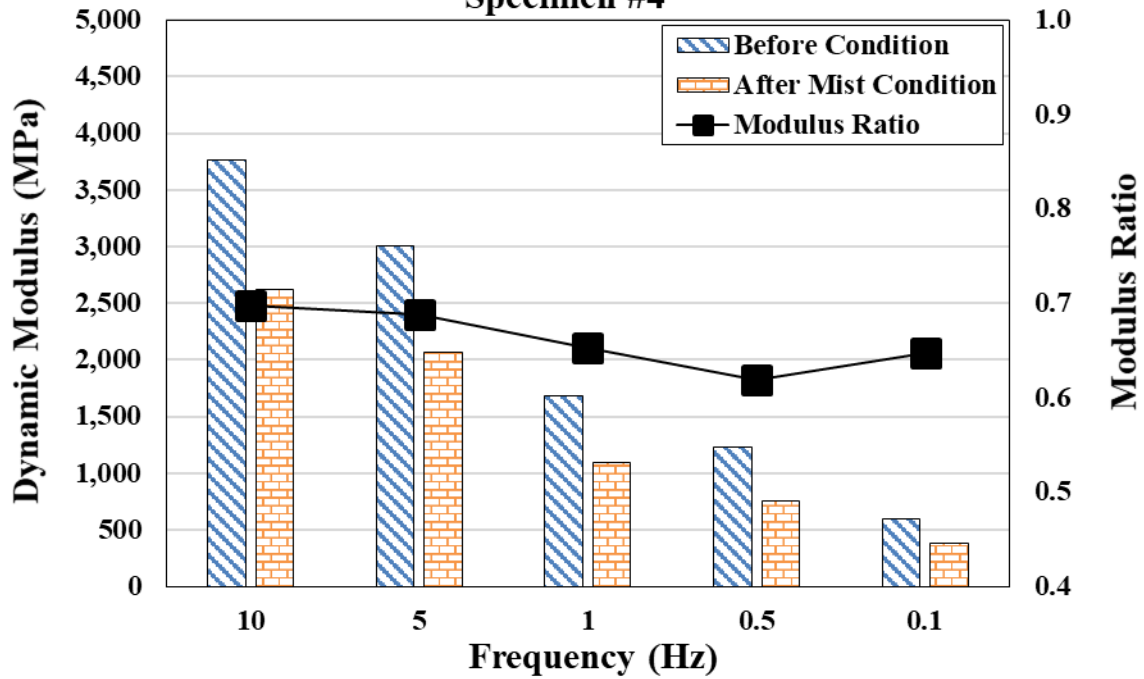
Rock Springs Specimen #5

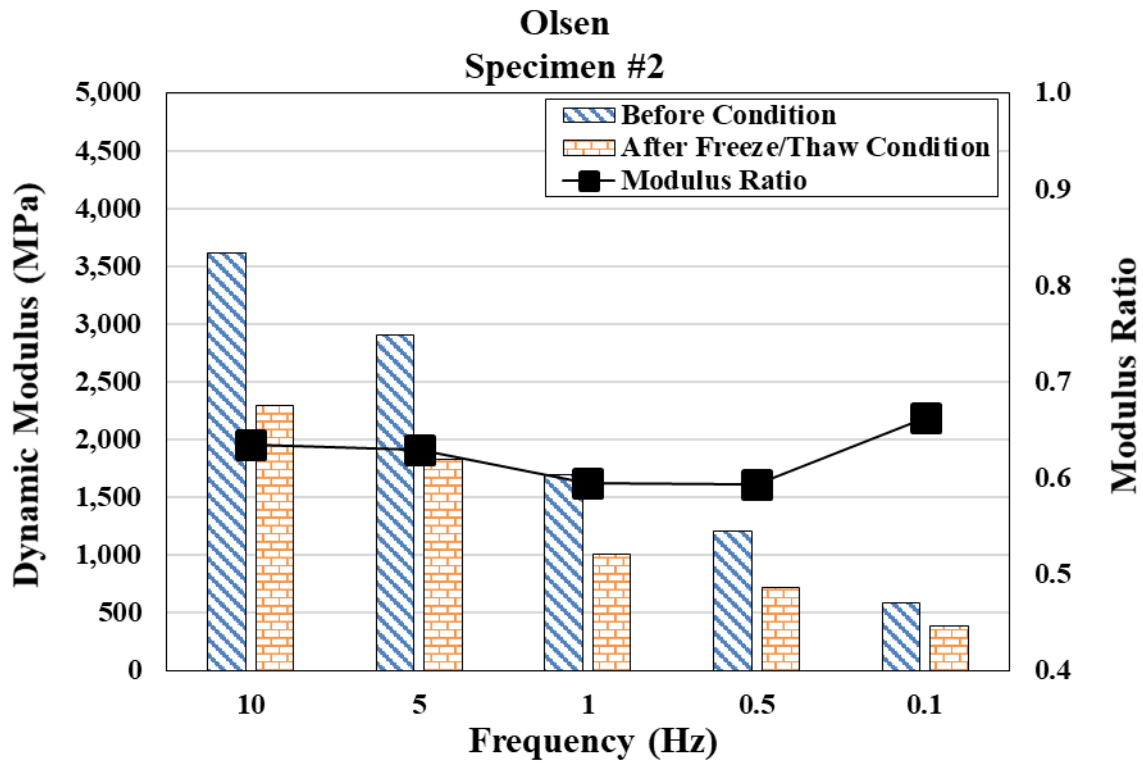
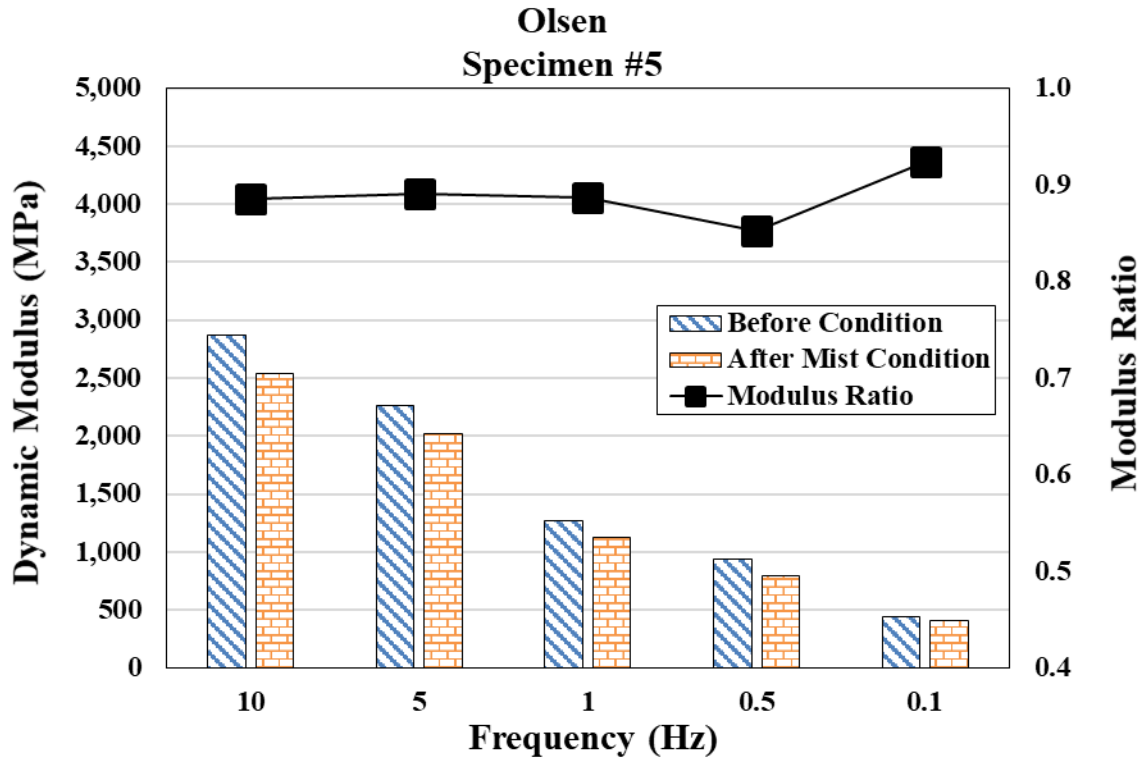


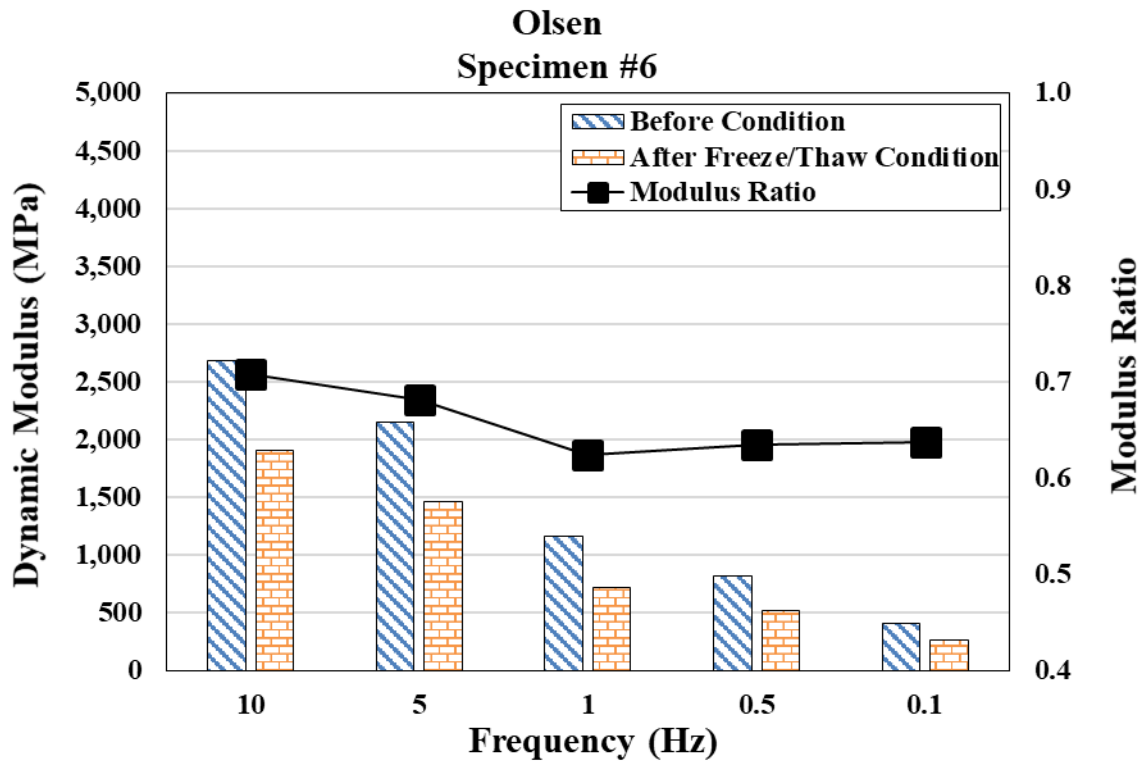
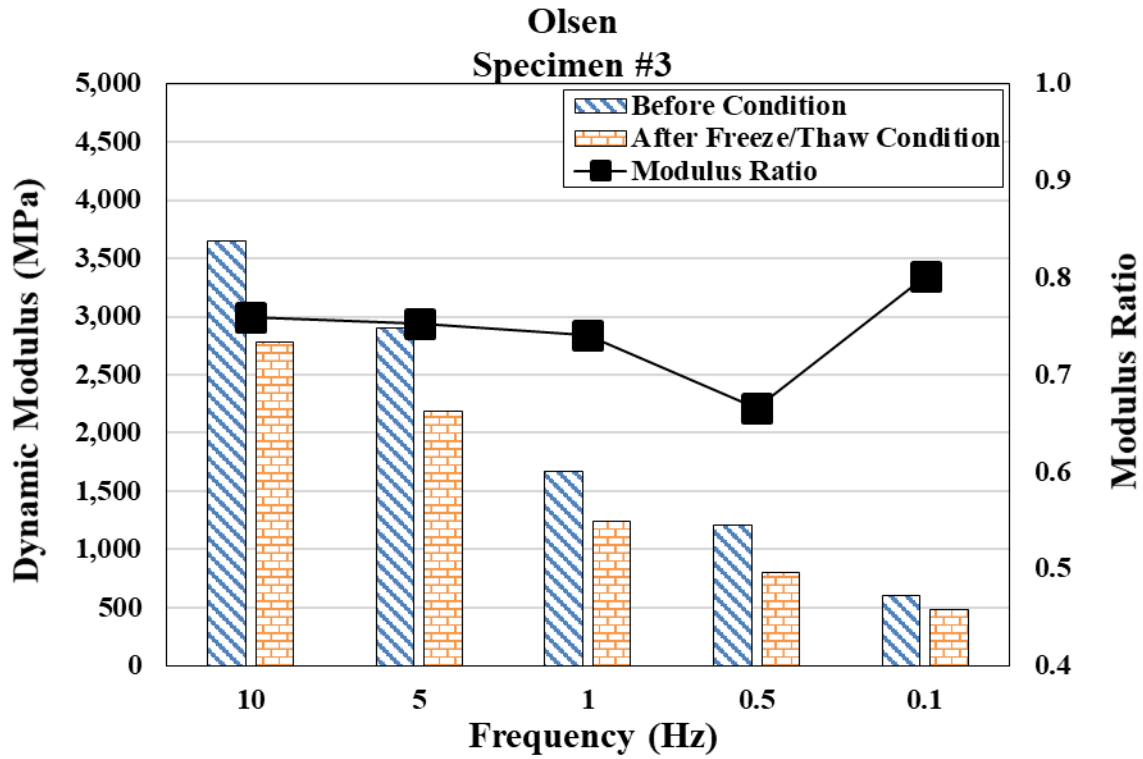
Olsen
Specimen #1



Olsen
Specimen #4

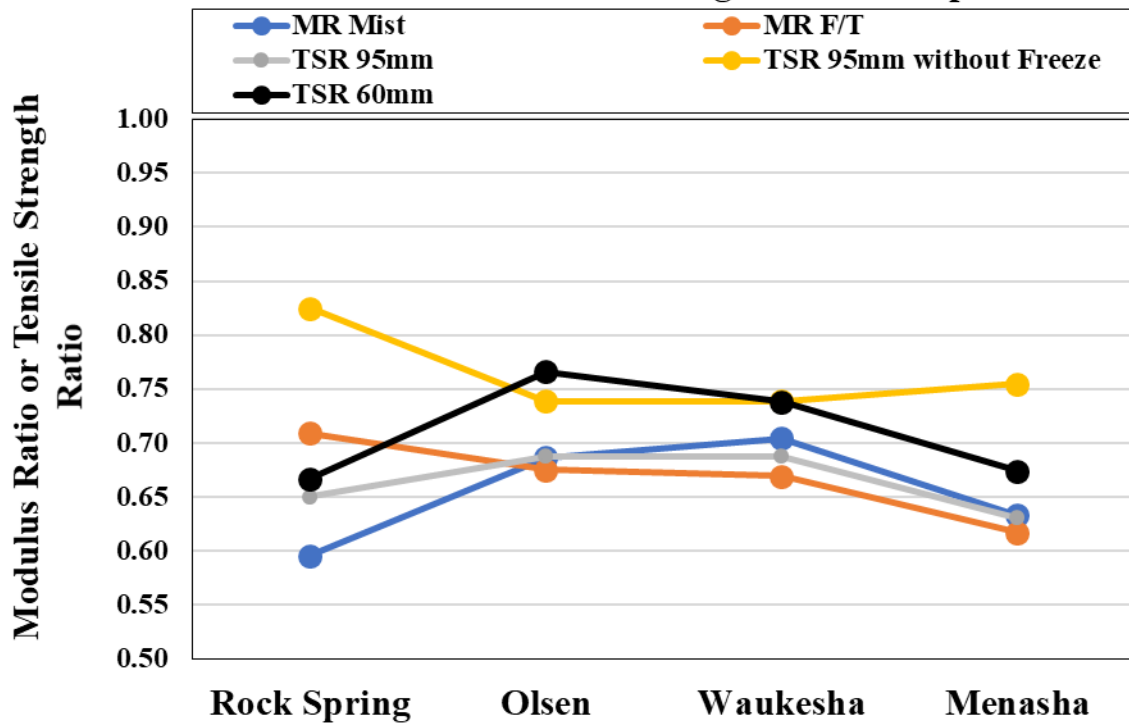




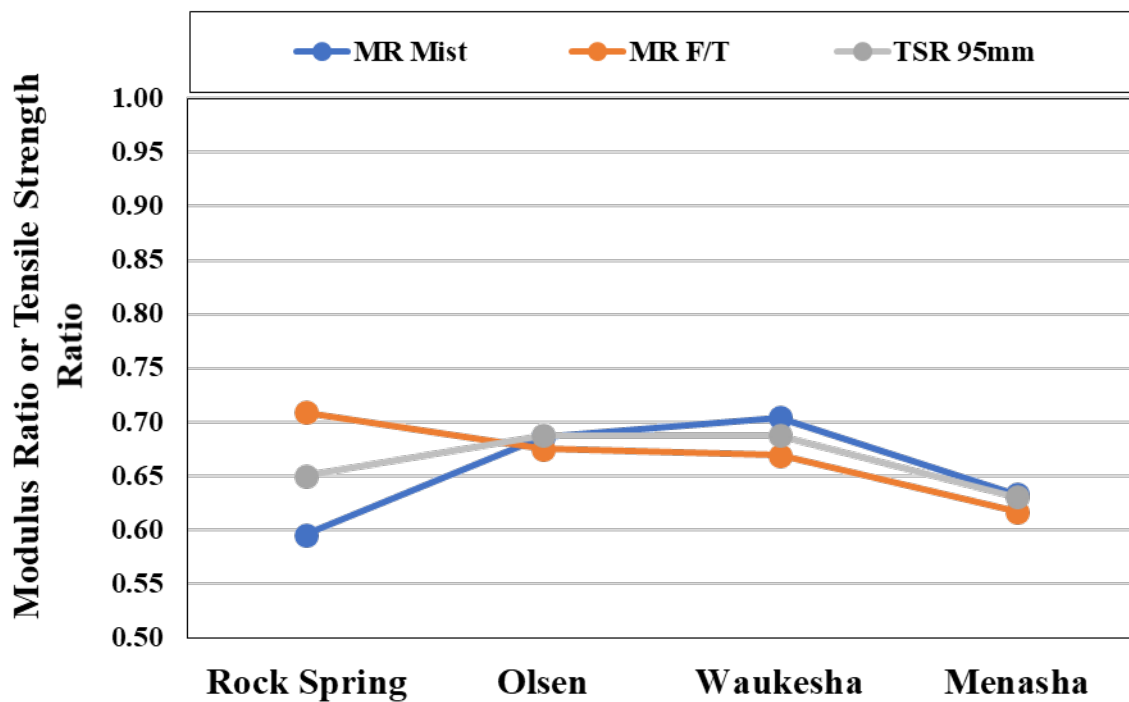


3. COMPARISON OF DYNAMIC MODULUS RATIO AND TENSILE STRENGTH RATIO

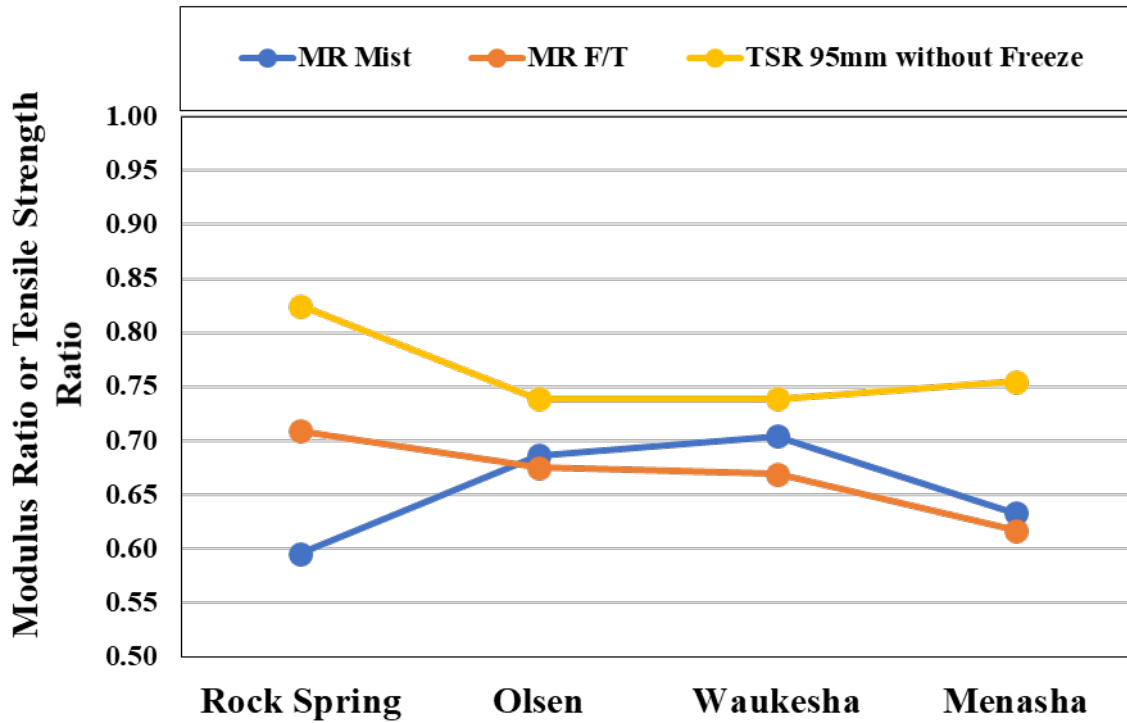
Modulus Ratio and Tensile Strength Ratio Comparison



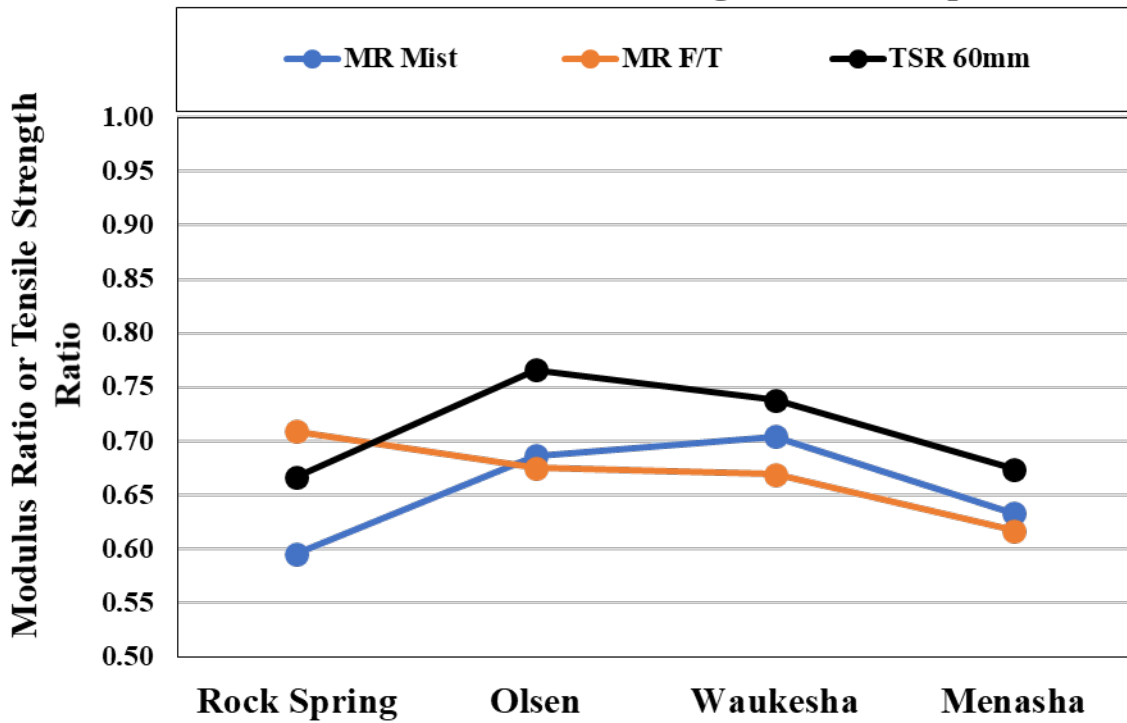
Modulus Ratio and Tensile Strength Ratio Comparison



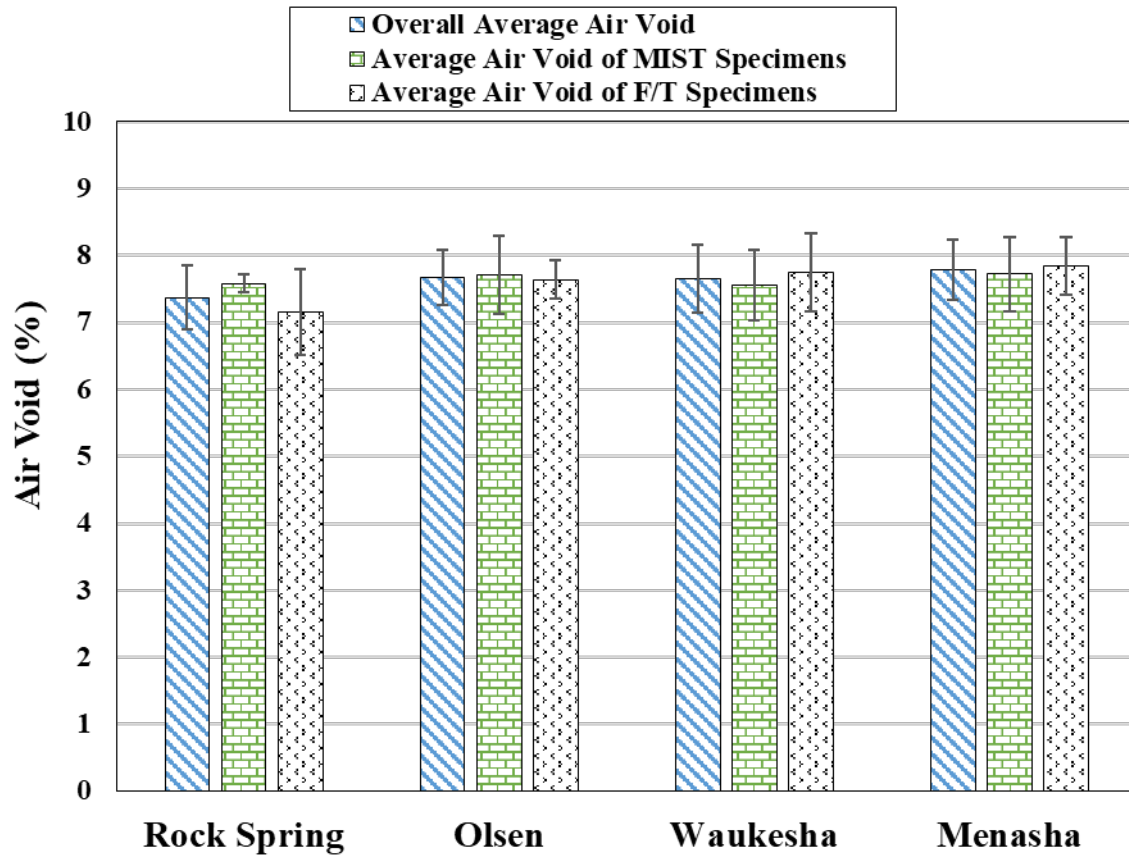
Modulus Ratio and Tensile Strength Ratio Comparison



Modulus Ratio and Tensile Strength Ratio Comparison



Air Void Distribution of Specimens Used in Dynamic Modulus Testing



APPENDIX F

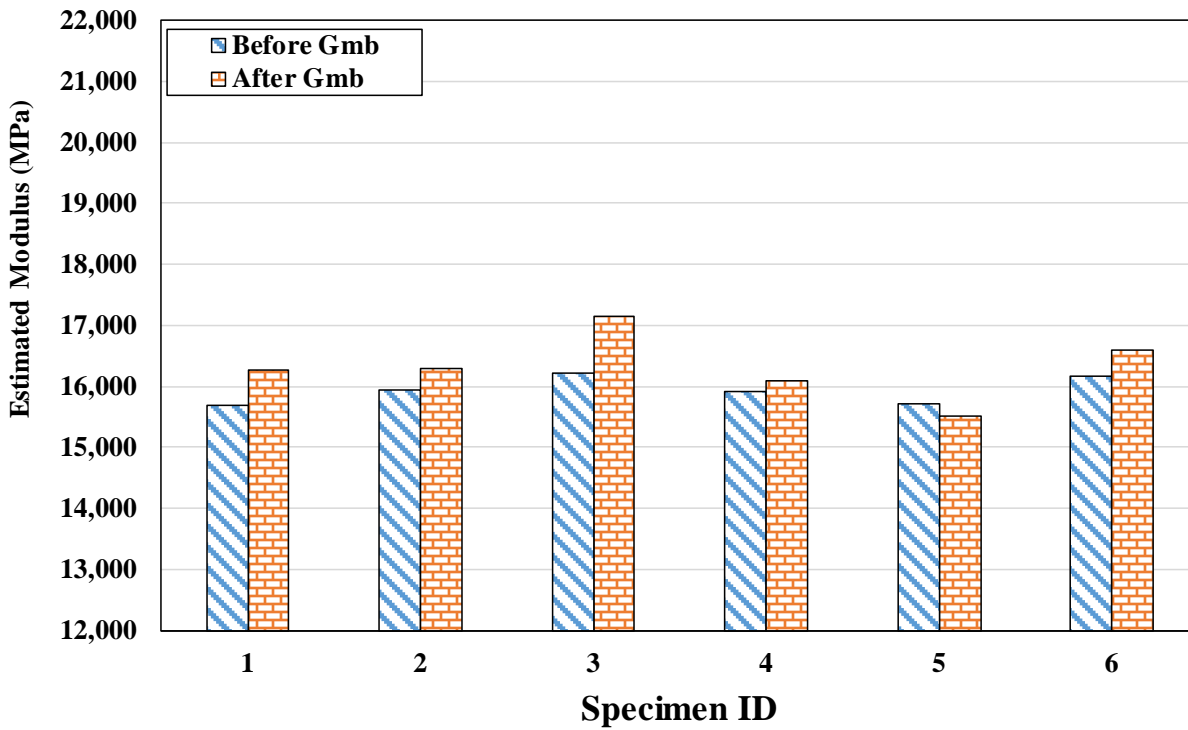
Results from Ultrasonic Pulse Velocity (UPV) Test

Notes on Legends in Graphs

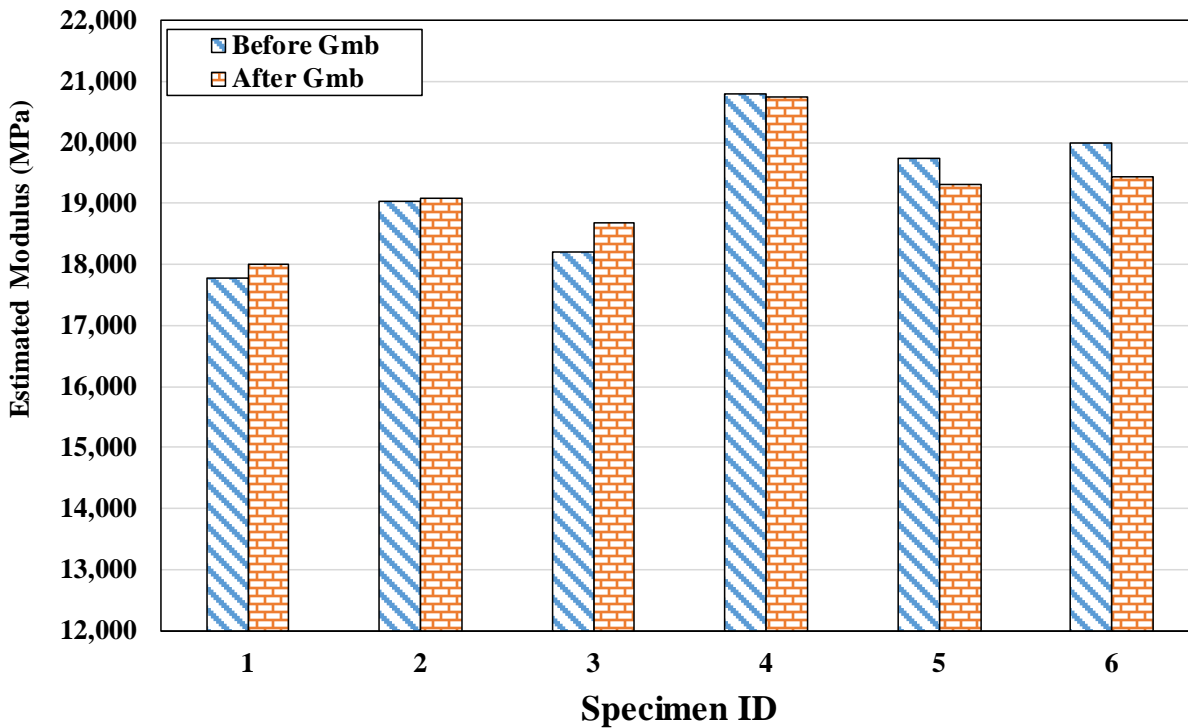
- **Before Gmb: Dry samples after compaction**
- **After Gmb: SSD samples after AASHTO T-166**
- **After first IDT DM: Unconditioned and dry samples after the first IDT Dynamic Modulus (DM) test**
- **After F/T: Samples after Freeze/Thaw conditioning**
- **After MiST: Samples after Mist Conditioning**
- **After second IDT DM: Samples with reduced water content (partially dried)**

1. EFFECT OF ABSORBED WATER DURING AASHTO T-166
(DETERMINATION OF AIR VOID RATIO AND BULK SPECIFIC
GRAVITY) ON UPV ESTIMATED MODULI

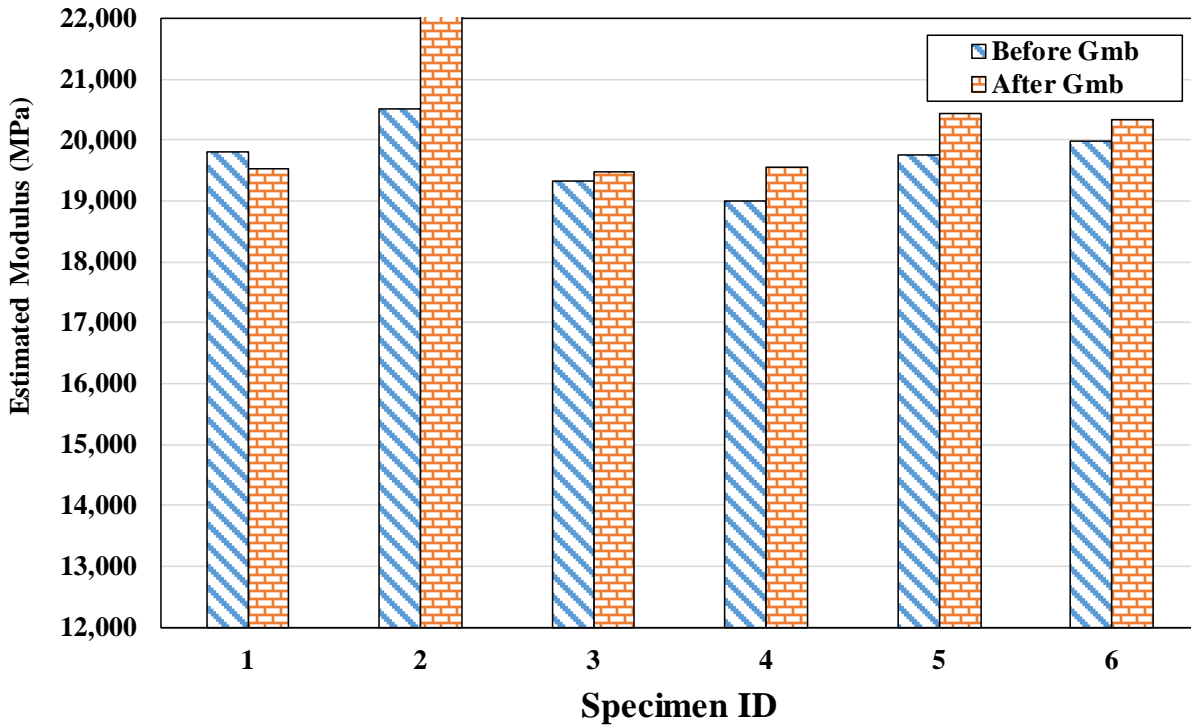
Menasha



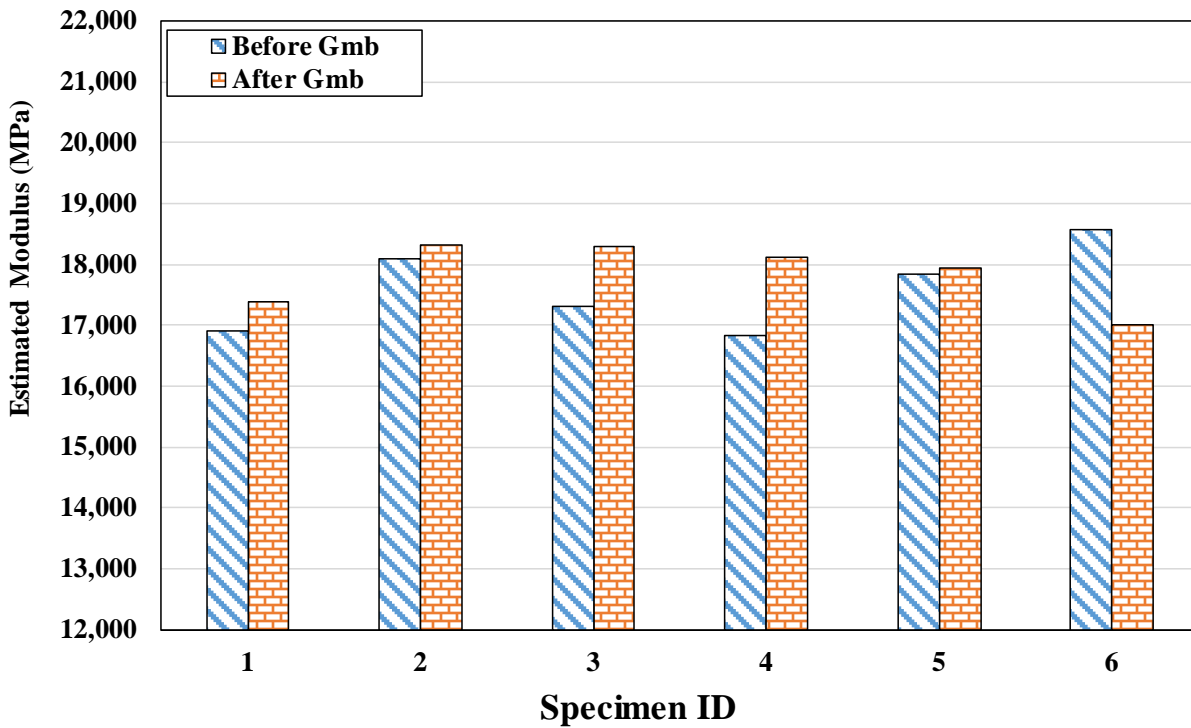
Olsen



Rock Springs

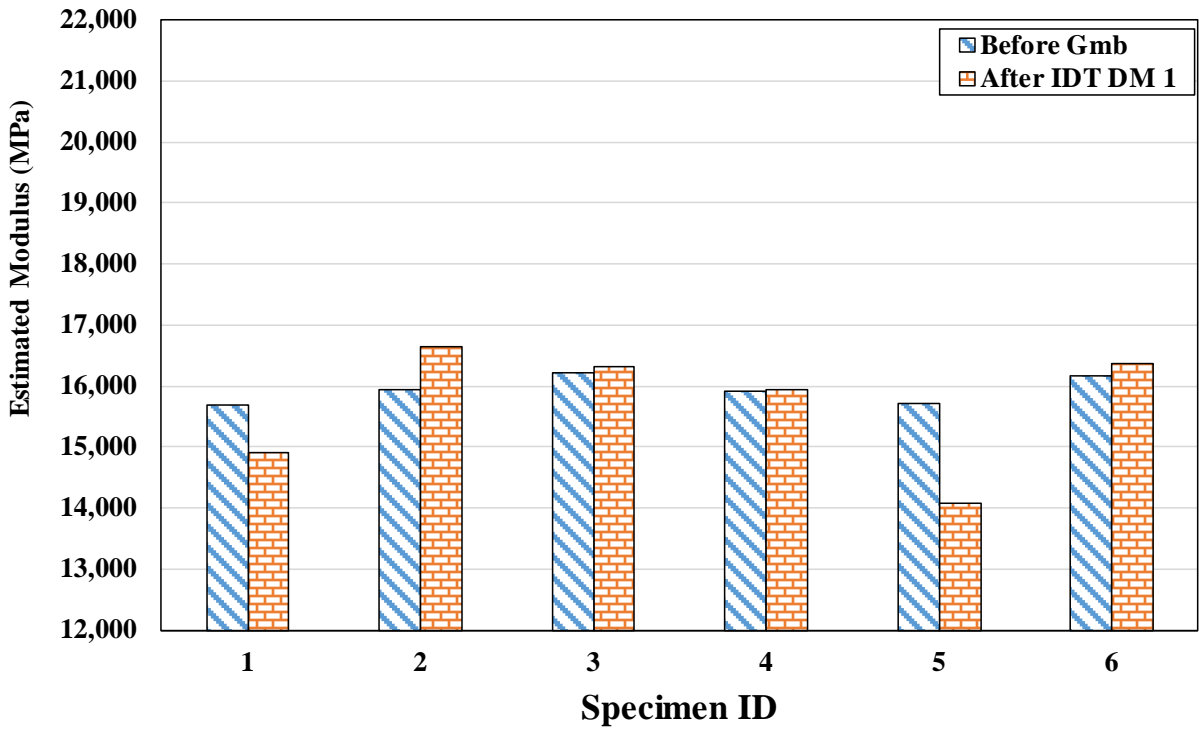


Waukesha

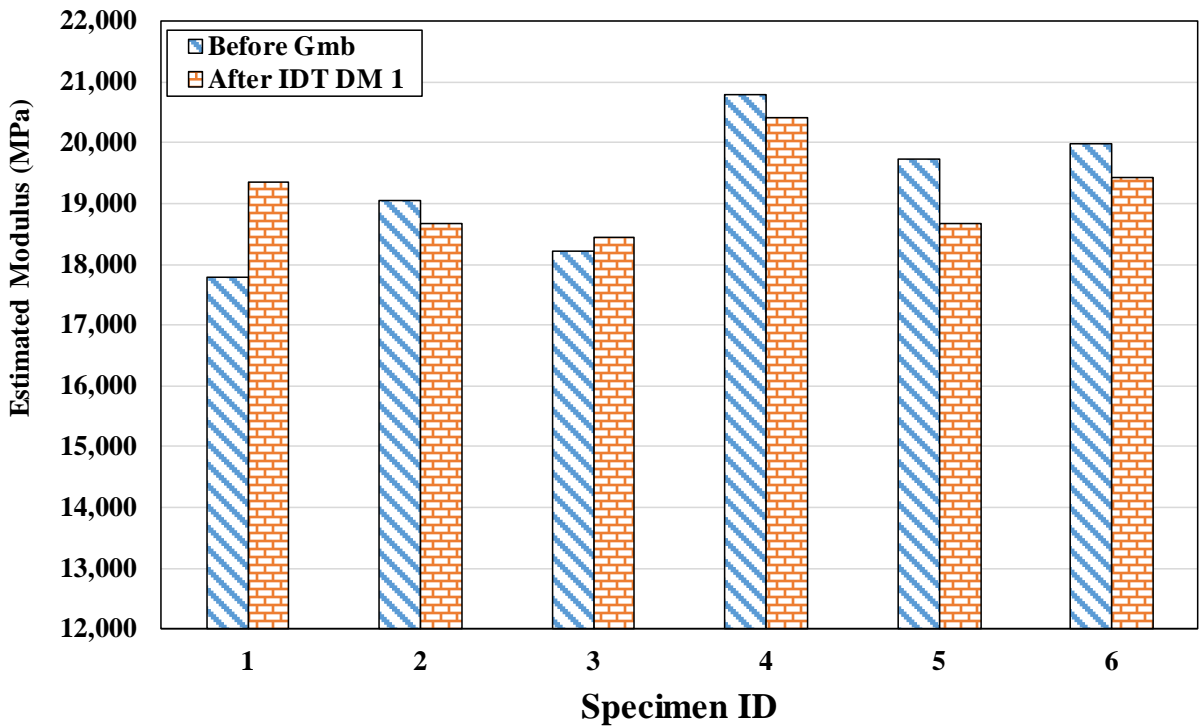


2. EFFECT OF THE FIRST IDT DM TEST ON UPV ESTIMATED MODULI OF UNCONDITIONED SAMPLES

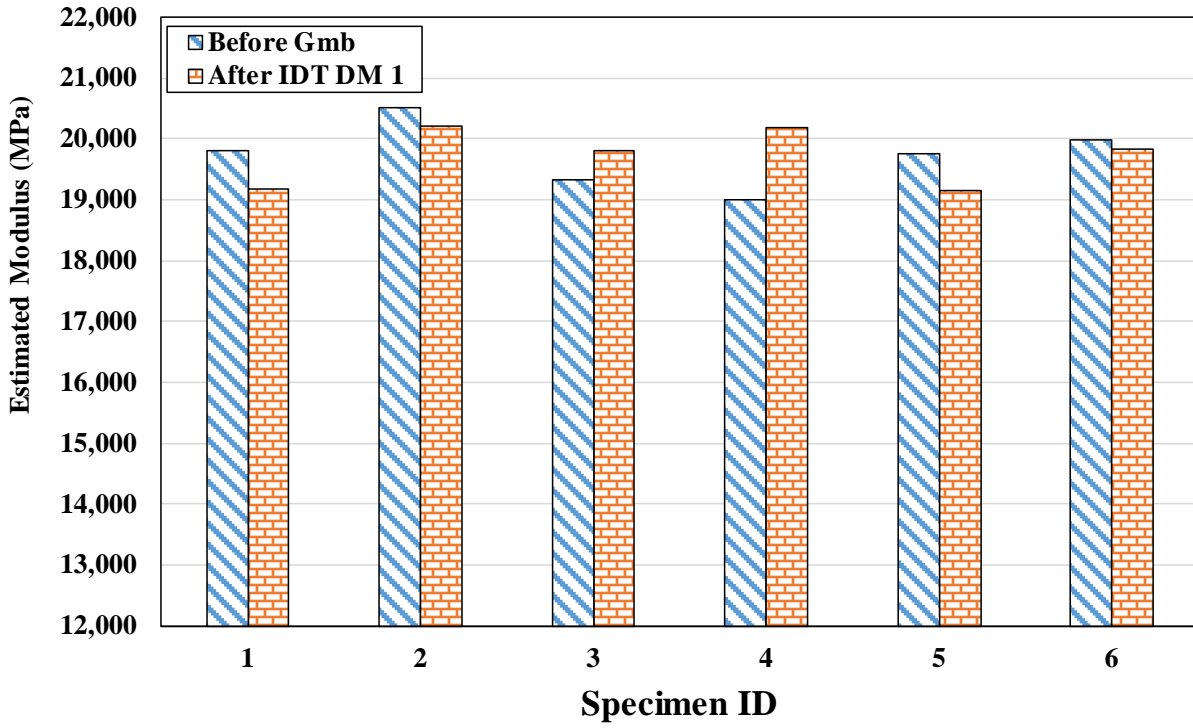
Menasha



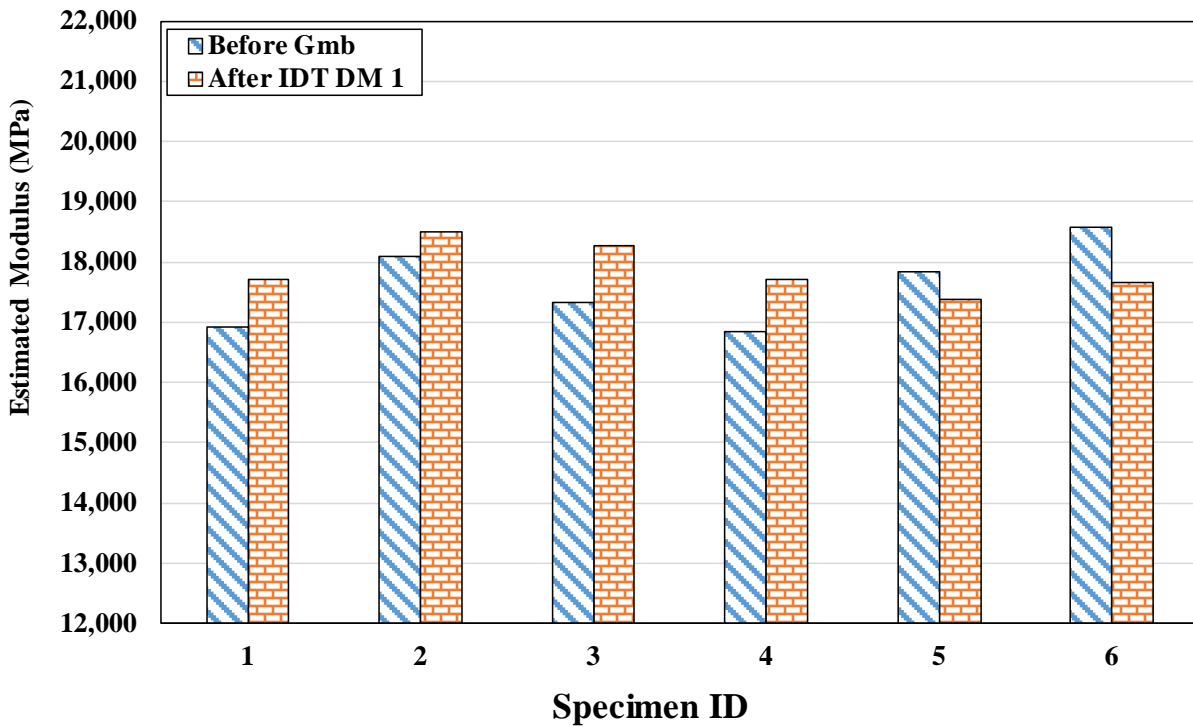
Olsen



Rock Springs

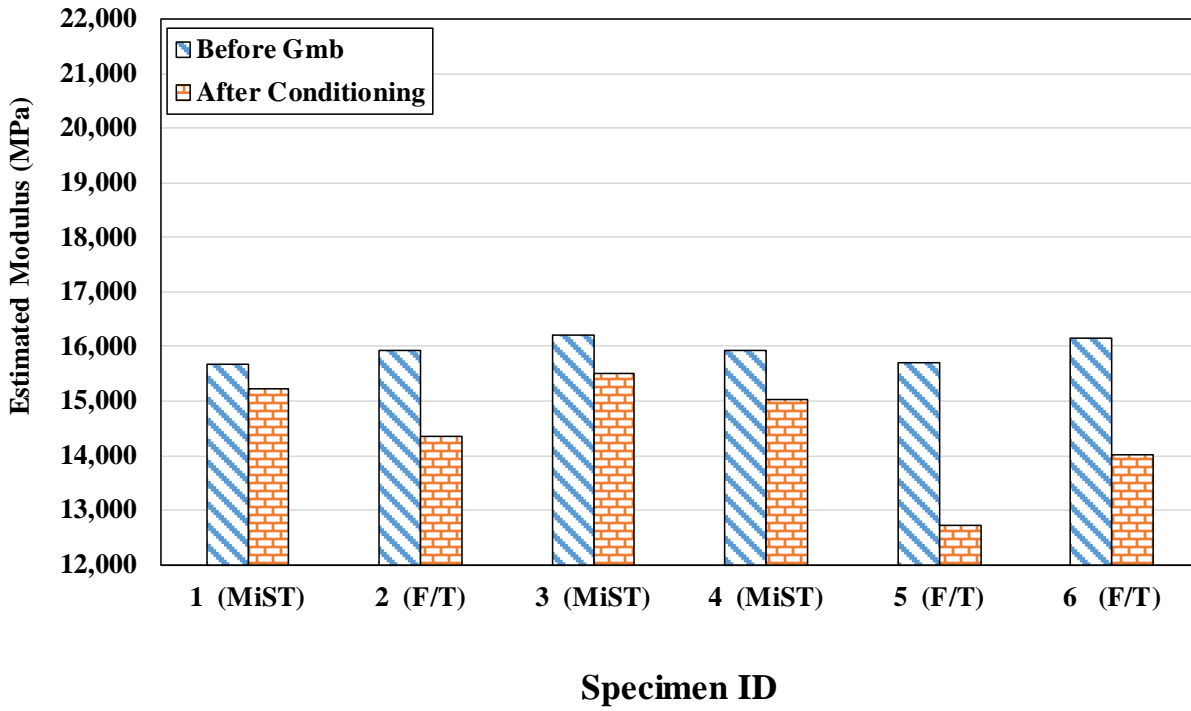


Waukesha

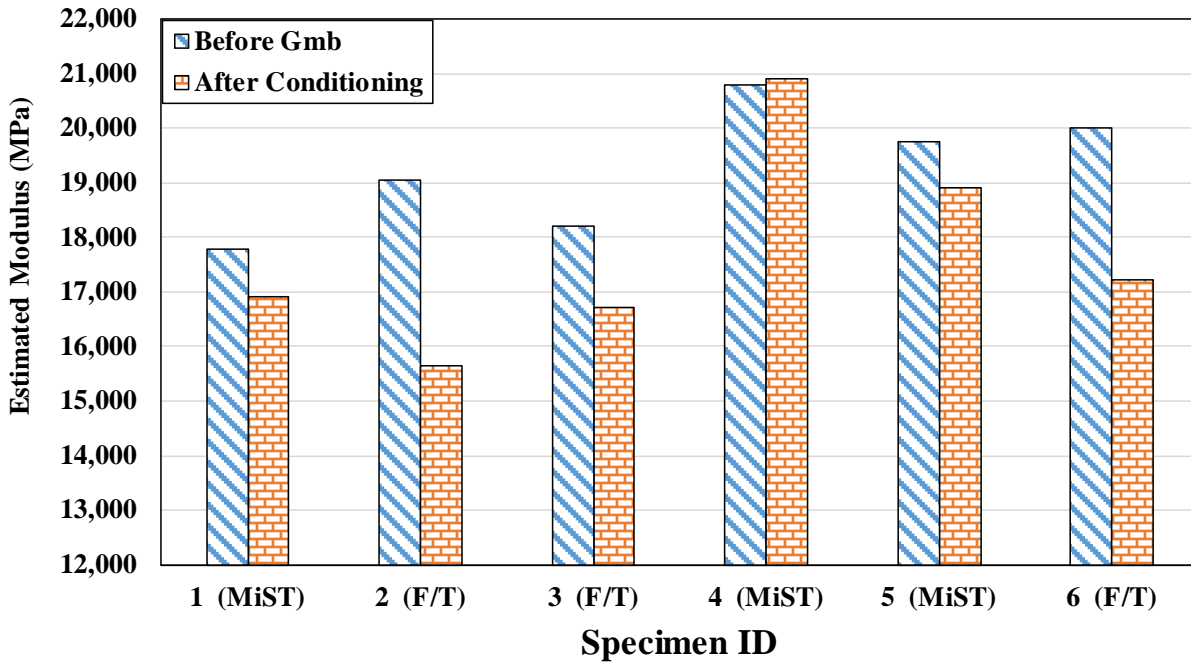


3. EFFECT OF THE FREEZE/THAW AND MIST CONDITIONING ON UPV ESTIMATED MODULI

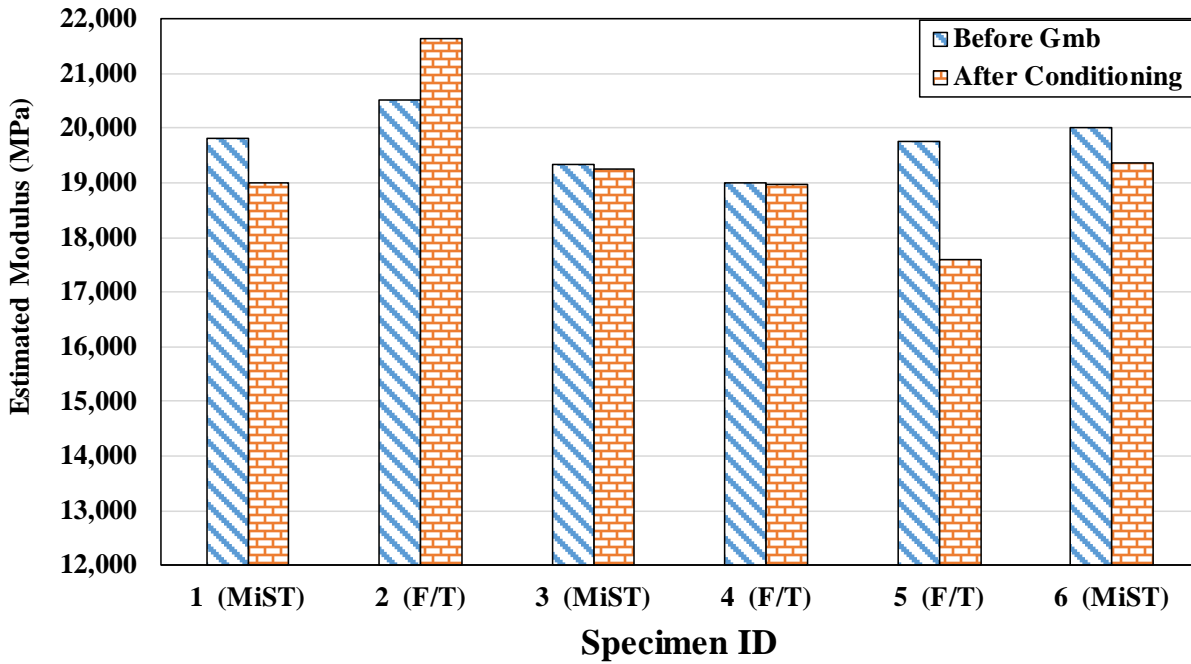
Menasha



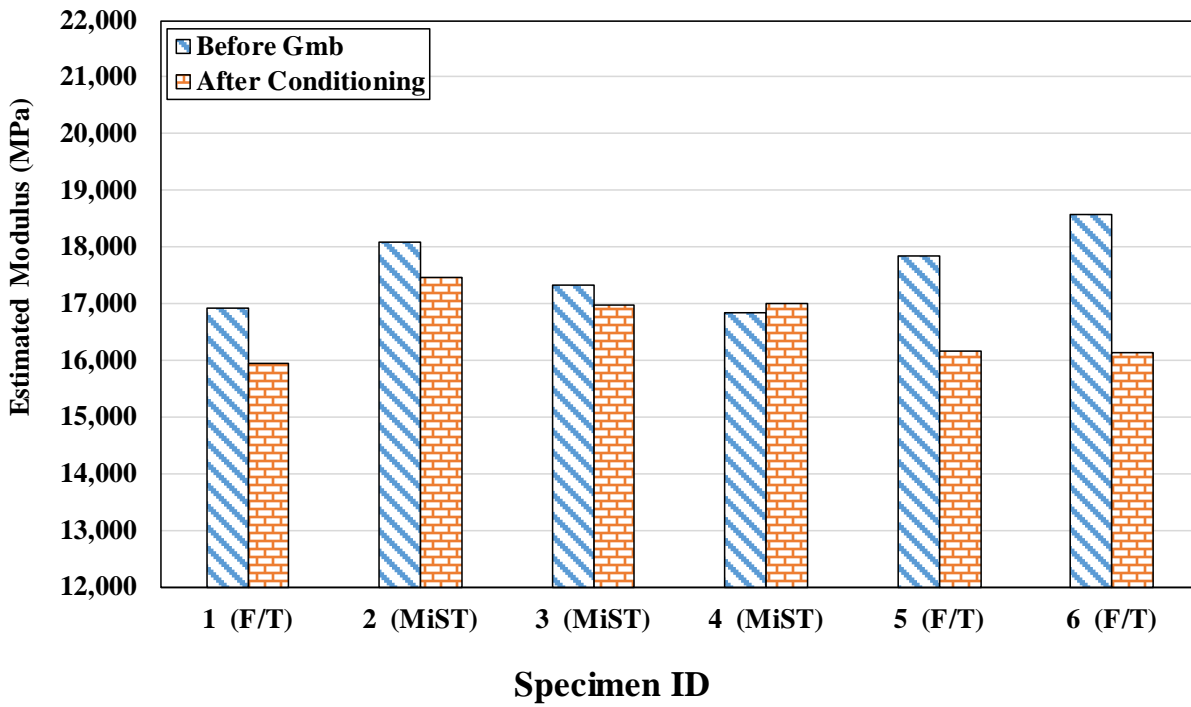
Olsen



Rock Springs

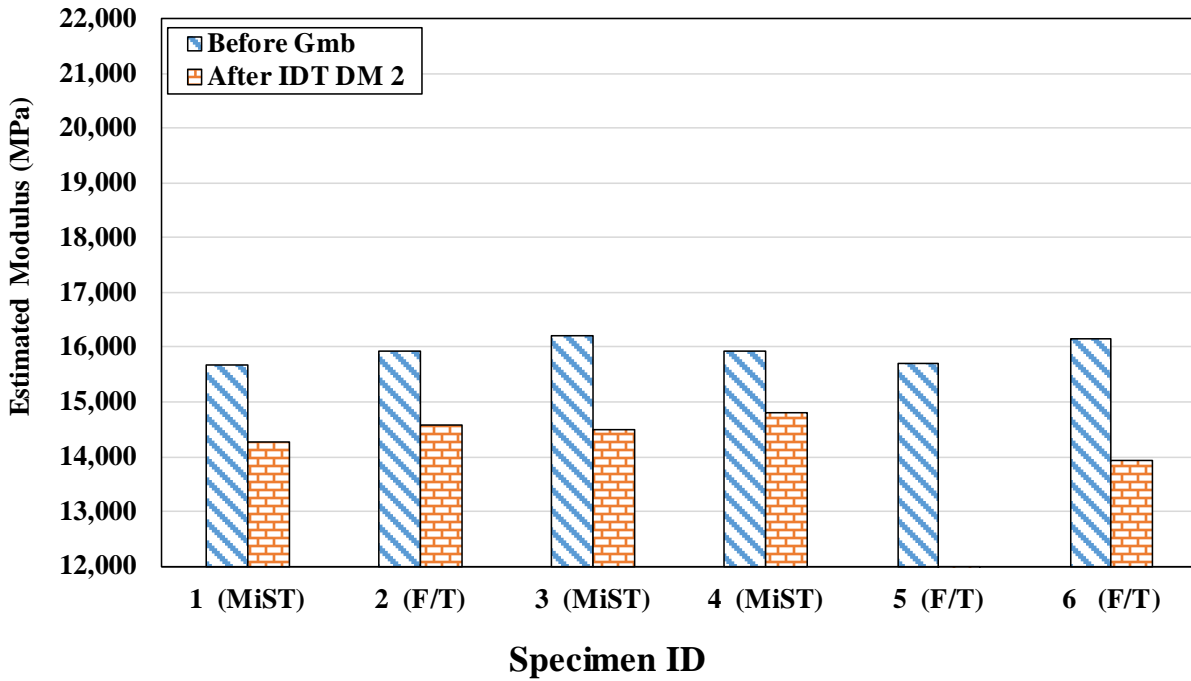


Waukesha

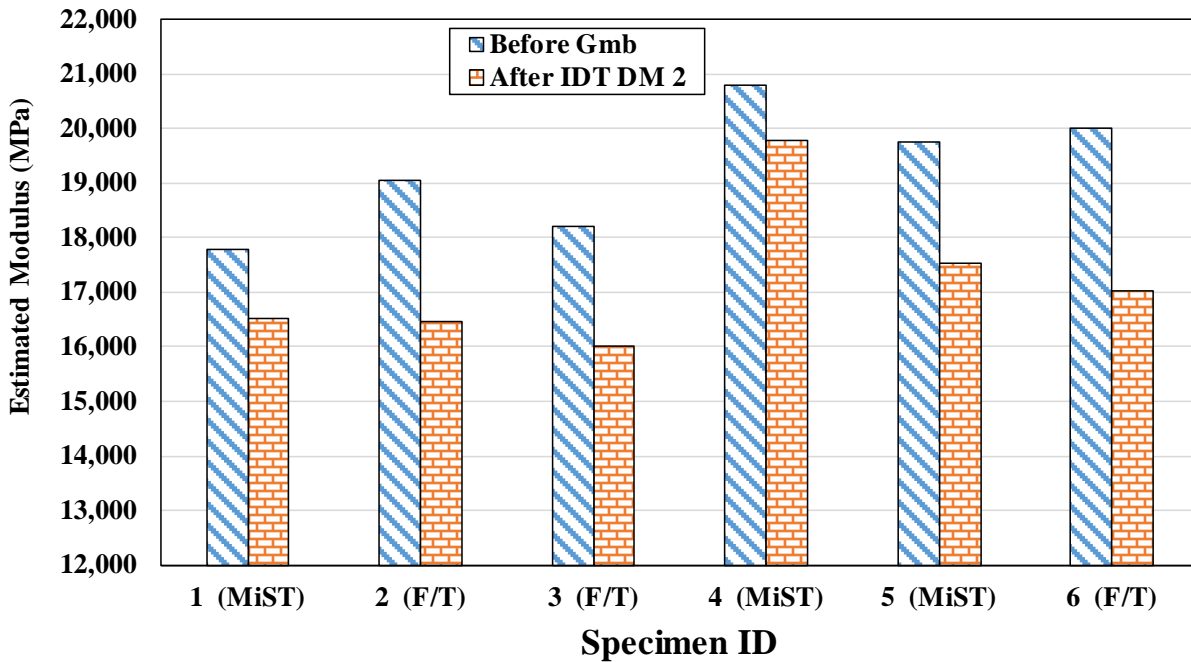


4. EFFECT OF THE SECOND IDT DM TEST ON UPV ESTIMATED MODULI OF CONDITIONED SAMPLES

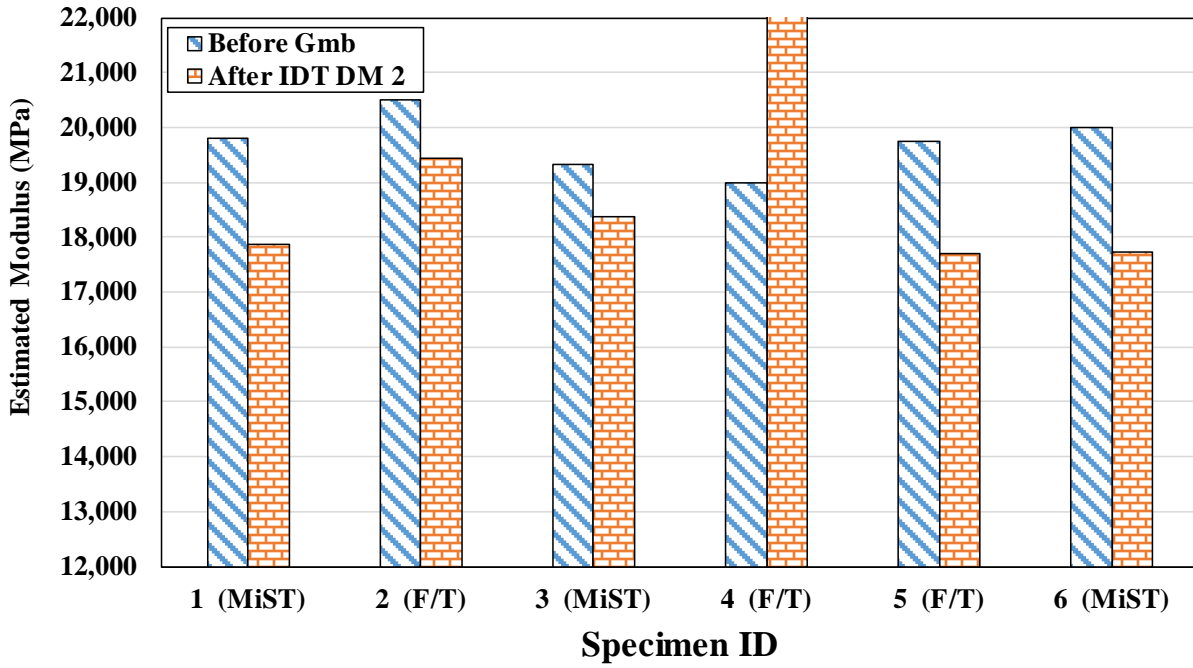
Menasha



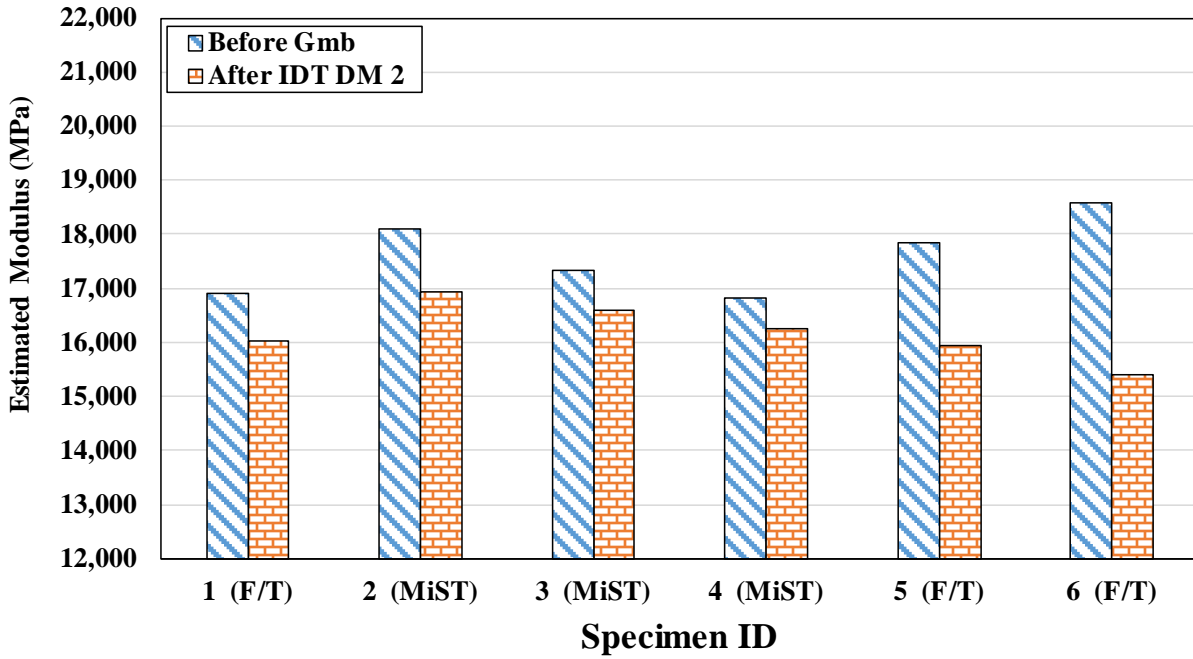
Olsen



Rock Springs

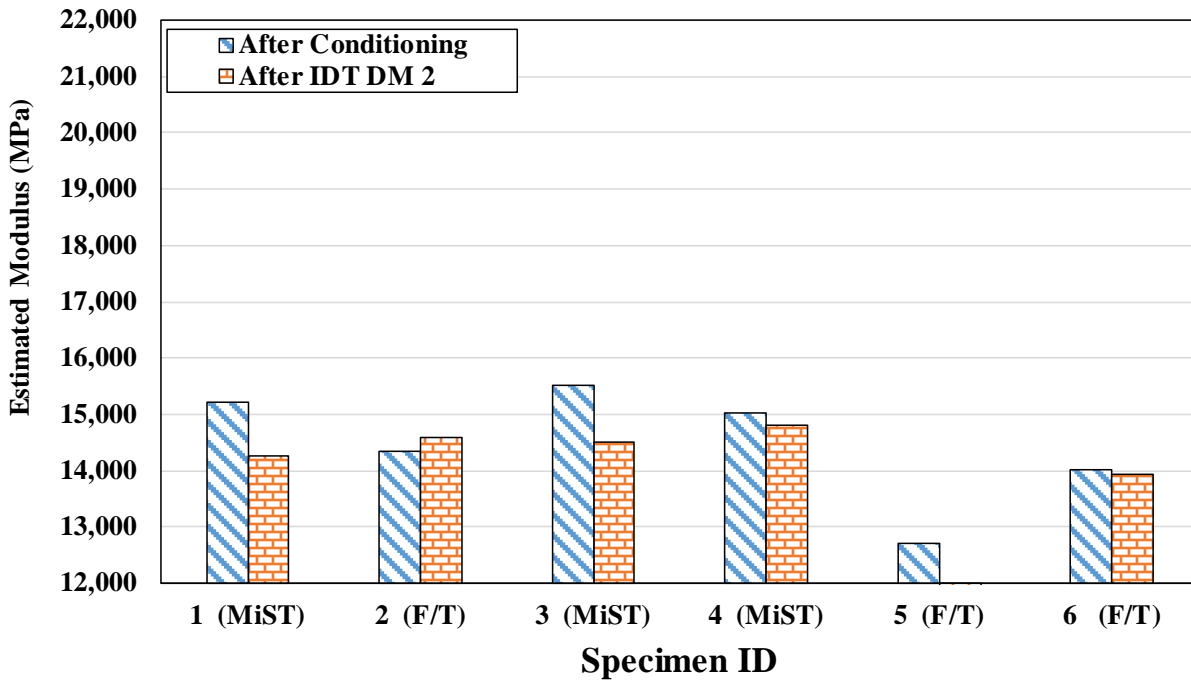


Waukesha

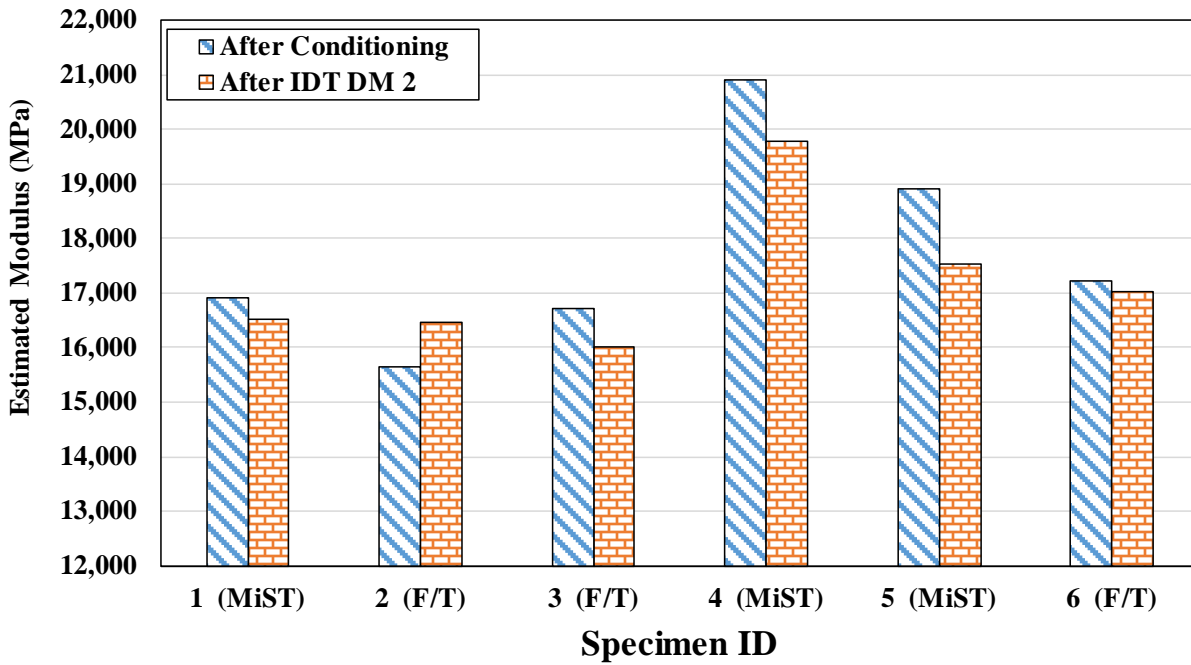


5. EFFECT OF REMOVAL OF WATER FROM CONDITIONED SAMPLES
ON UPV ESTIMATED MODULI

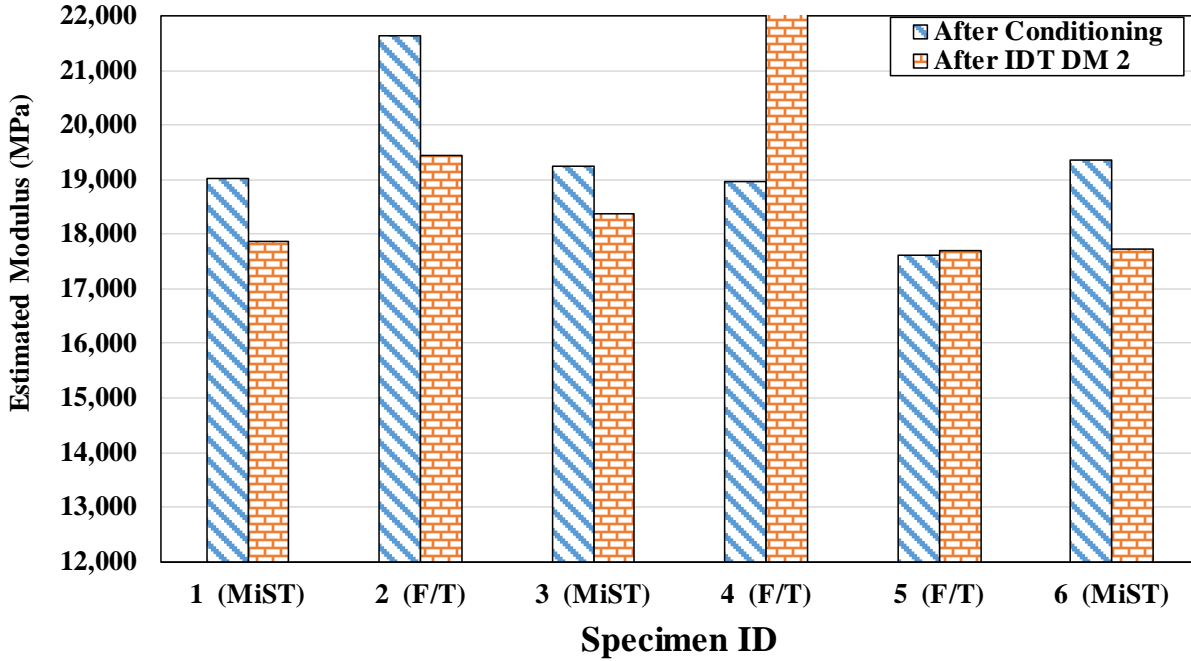
Menasha



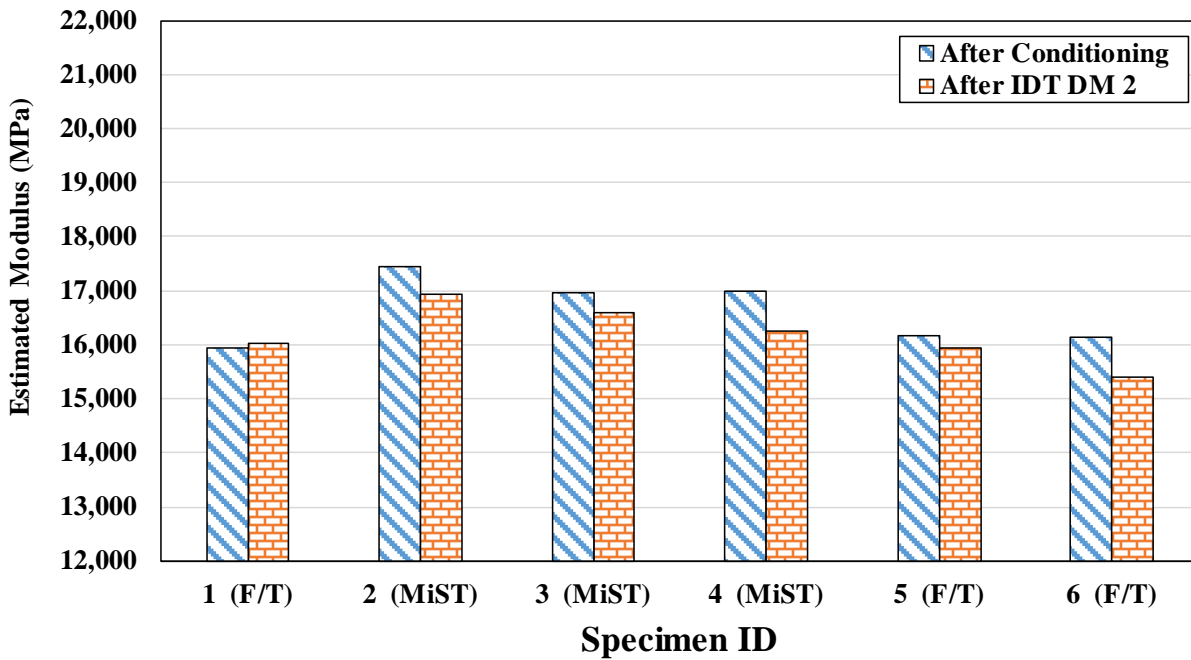
Olsen



Rock Springs



Waukesha



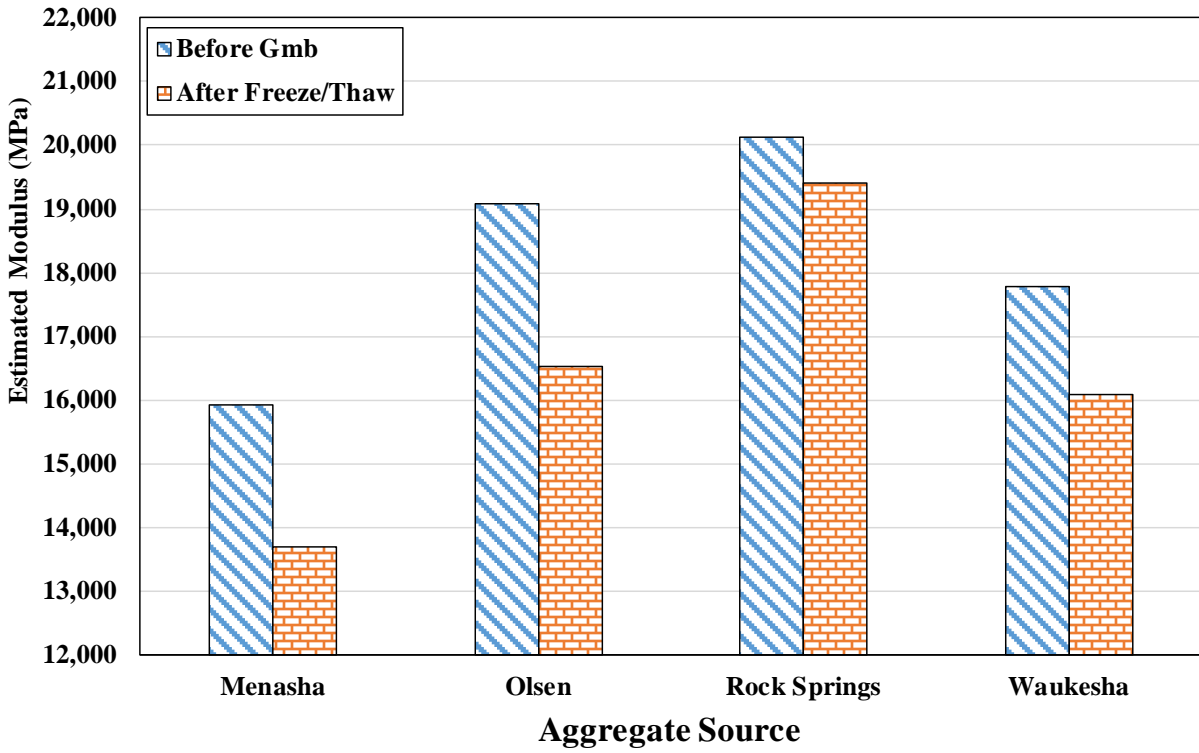
6. EFFECT OF CONDITIONING ON THE AVERAGE ESTIMATED MODULI FROM UPV TEST

NOTE:

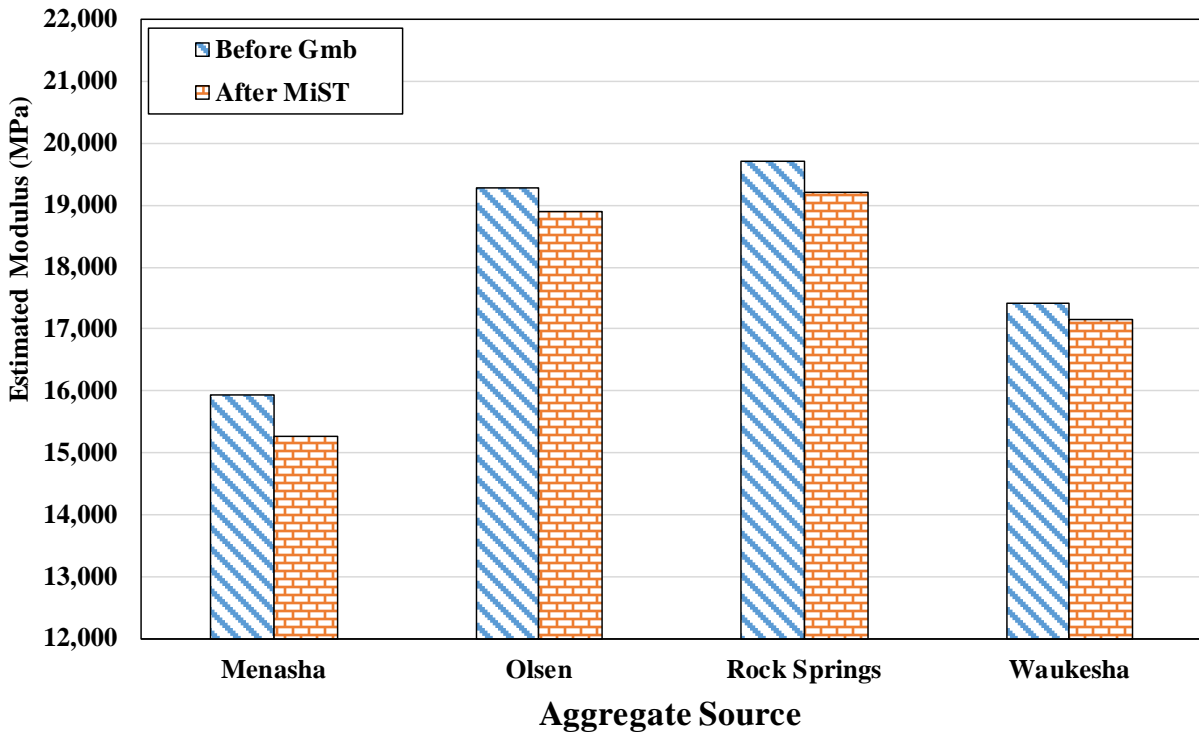
Saturated samples refer to specimens that were subject to freeze-thaw conditioning or MiST conditioning, and immediately after conditioning they were subject to UPV testing. The term “saturated” simply implies that water was retained in the specimen at the time of UPV testing. It does not mean that the specimens were fully saturated.

Dried samples refer to specimens that were subject to freeze-thaw conditioning or MiST conditioning, and water was removed from the specimens to a very large extent before the specimens were subject to UPV testing. The term “dry” does not mean complete dryness of the specimens. However, it does indicate that little water is in the specimen at the time of UPV testing compared with the water content after completion of conditioning.

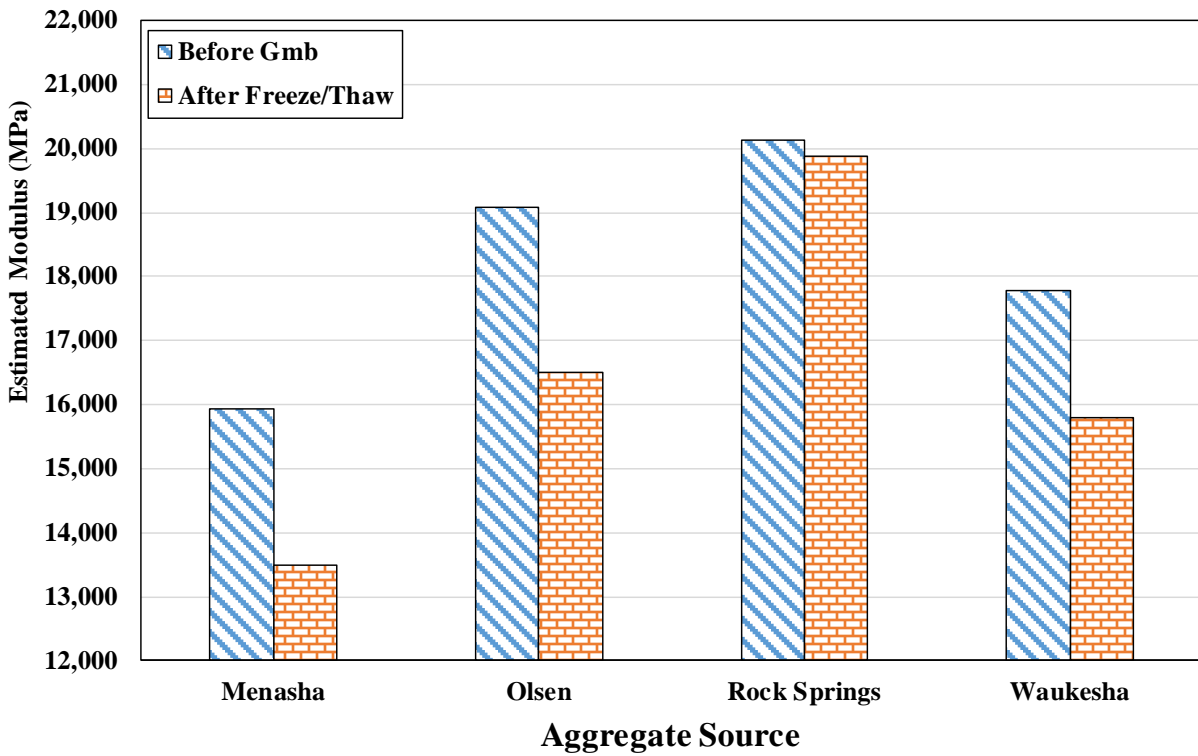
Saturated Samples



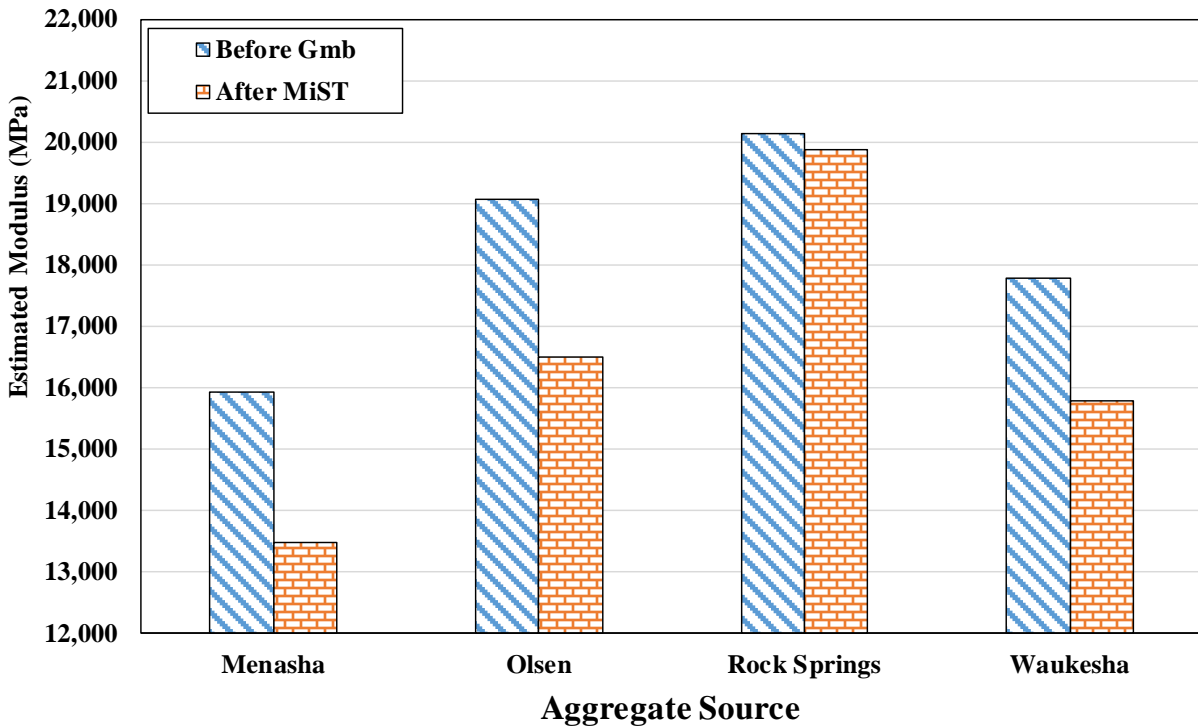
Saturated Samples



Dried Samples

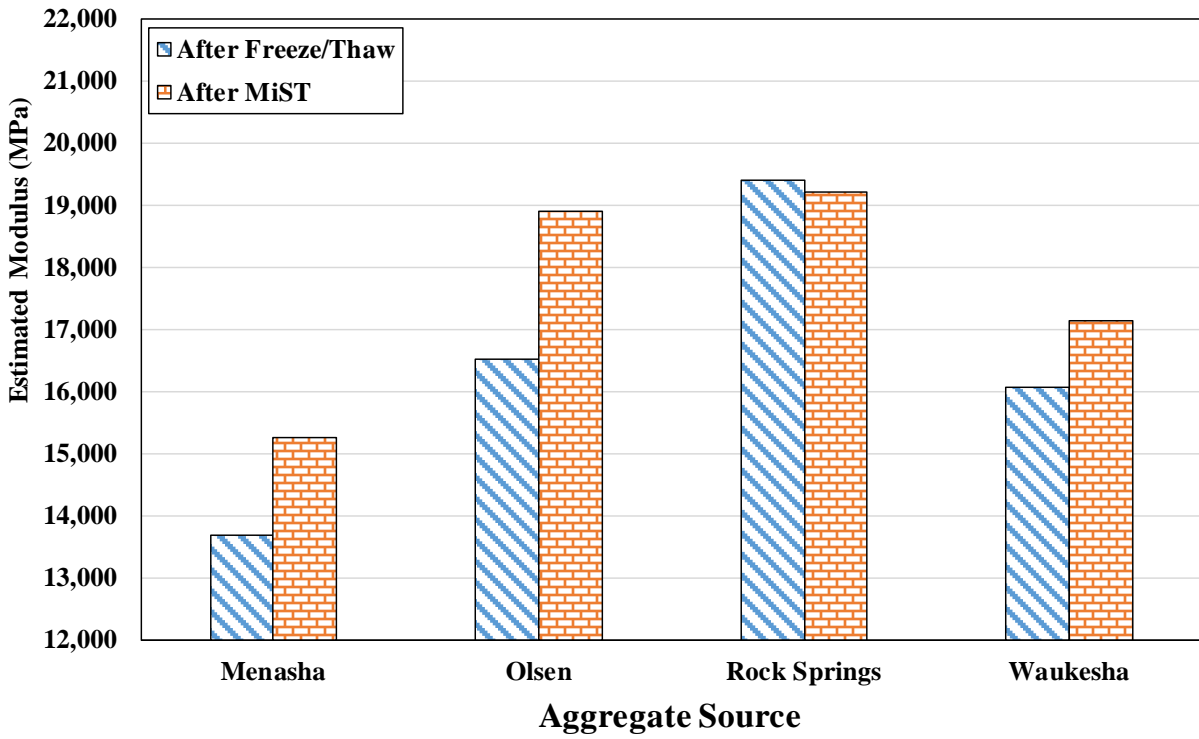


Dried Samples

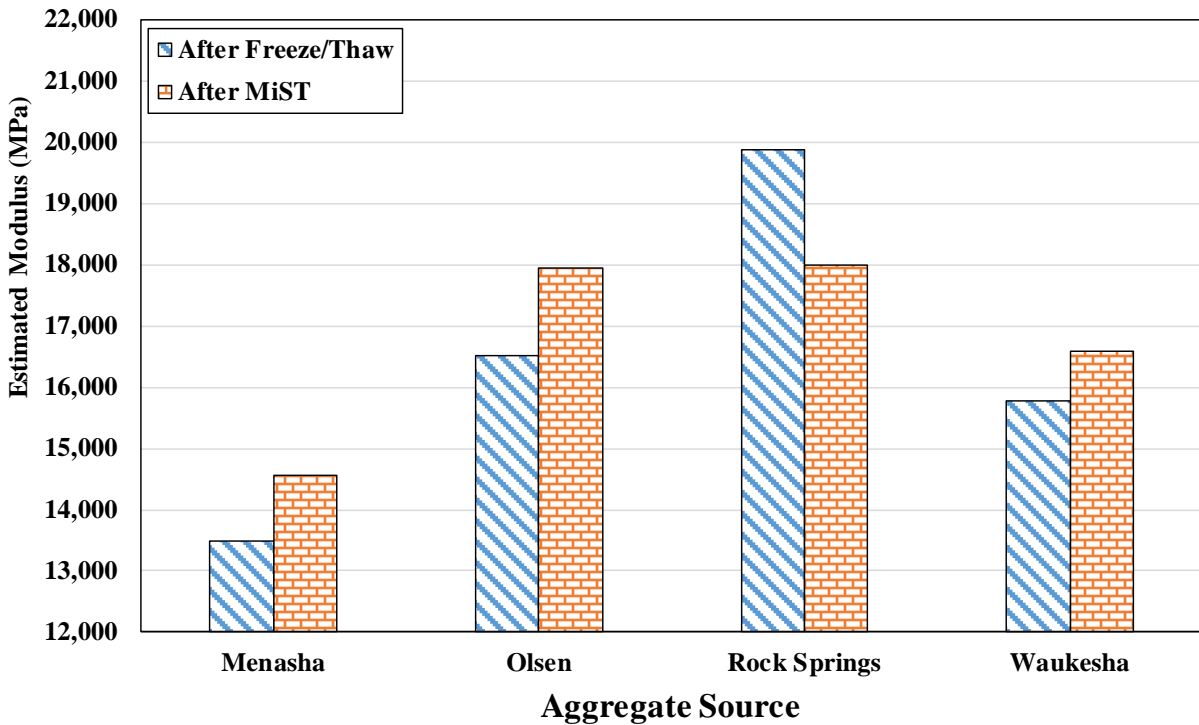


**7. COMPARING THE EFFECT OF CONDITIONING TECHNIQUE ON
THE AVERAGE ESTIMATED MODULI FROM UPV TEST**

Saturated Samples

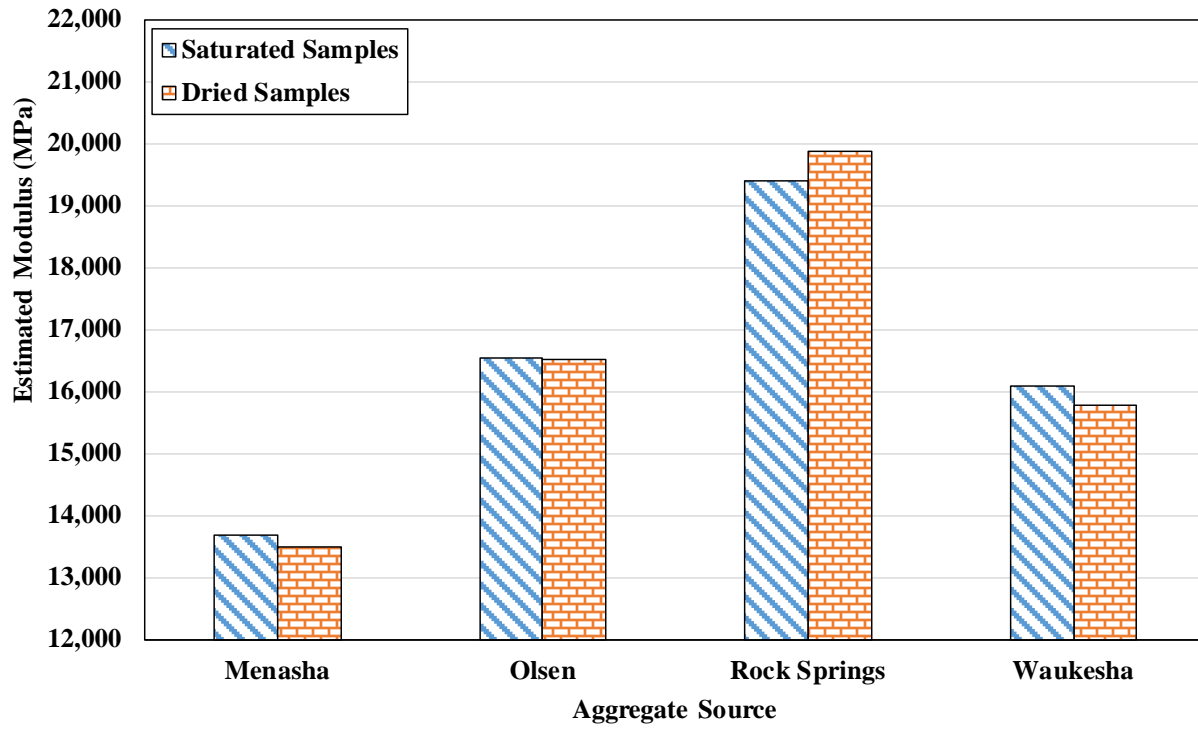


Dried Samples

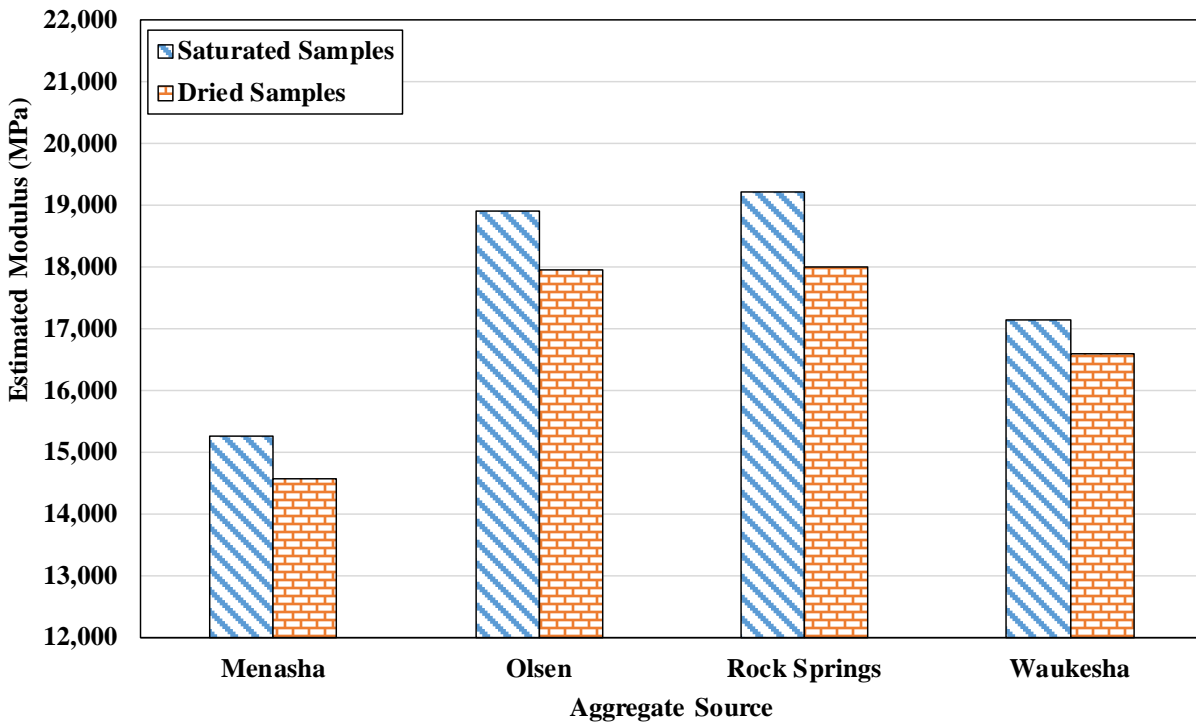


8. EFFECT OF REMOVING OF WATER ON ESTIMATED MODULI OF CONDITIONED SAMPLES

Freeze/Thaw Conditioned Samples

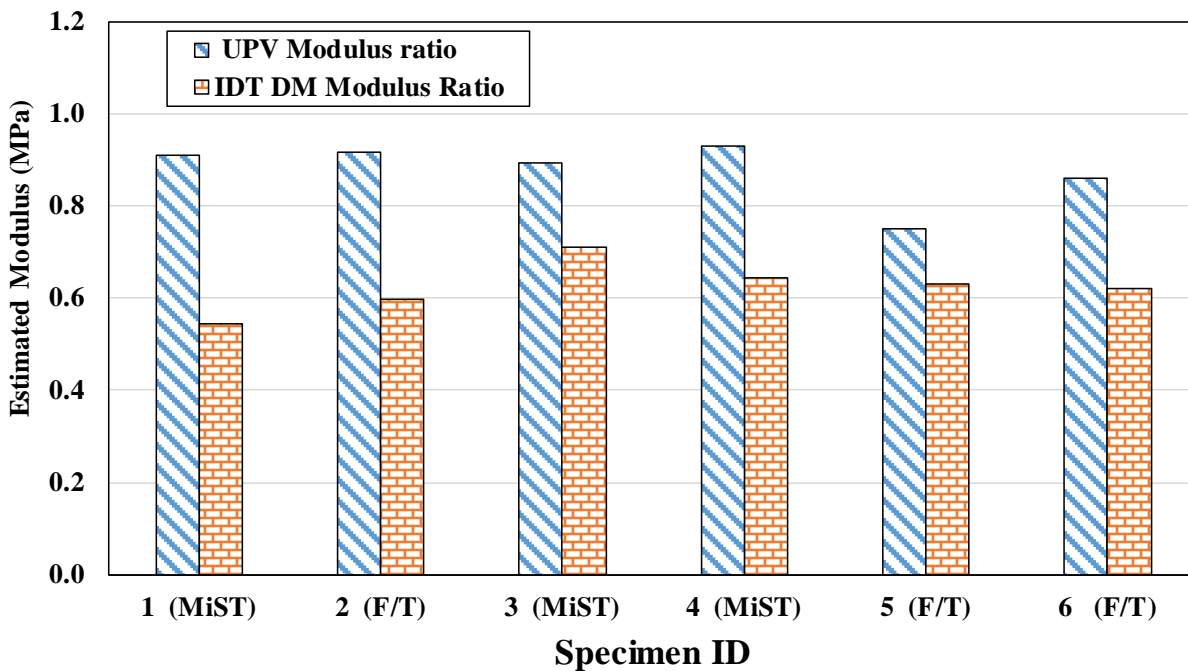


MiST Conditioned Samples

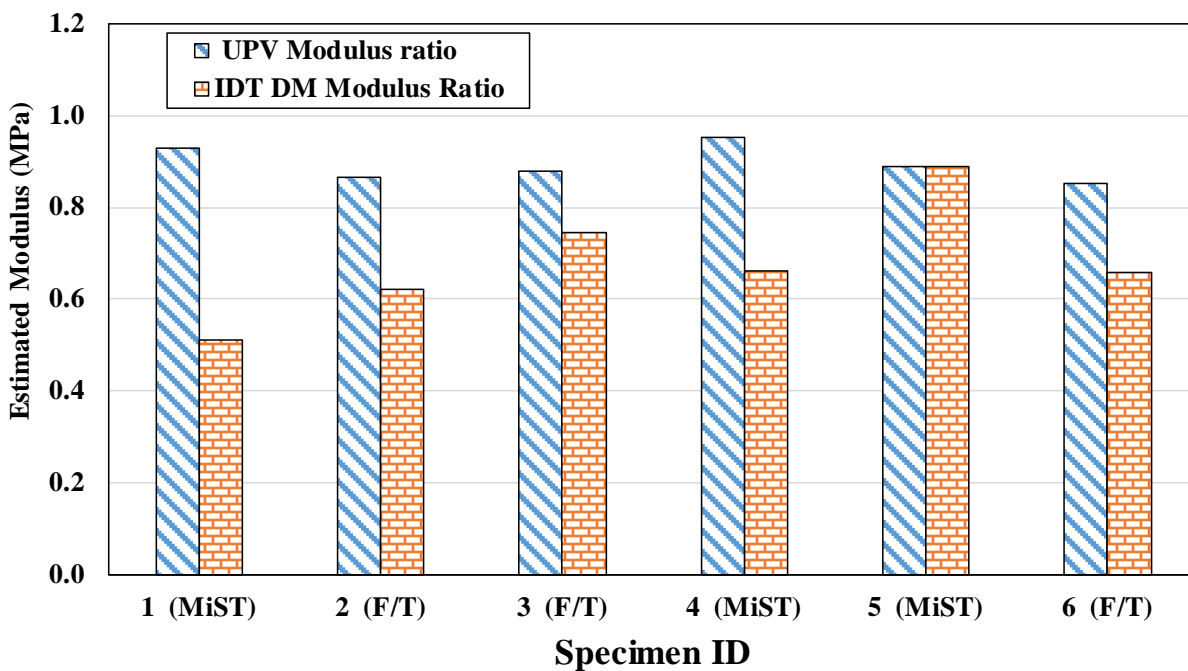


9. COMPARING THE ESTIMATED CHANGE IN MODULI DUE TO
CONDITIONING (MODULUS RATIO) BETWEEN UPV AND IDT DM
TESTING

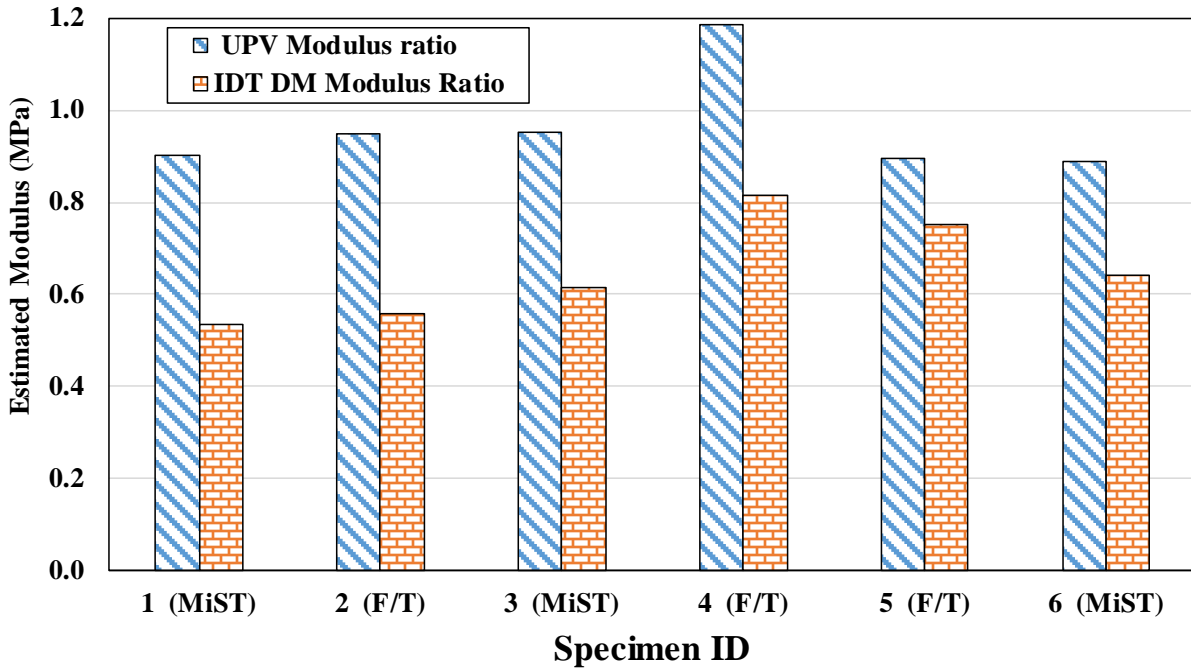
Conditioned Samples after Drying (Menasha)



Conditioned Samples after Drying (Olsen)



Conditioned Samples after Drying (Rock Springs)



Conditioned Samples after Drying (Waukesha)

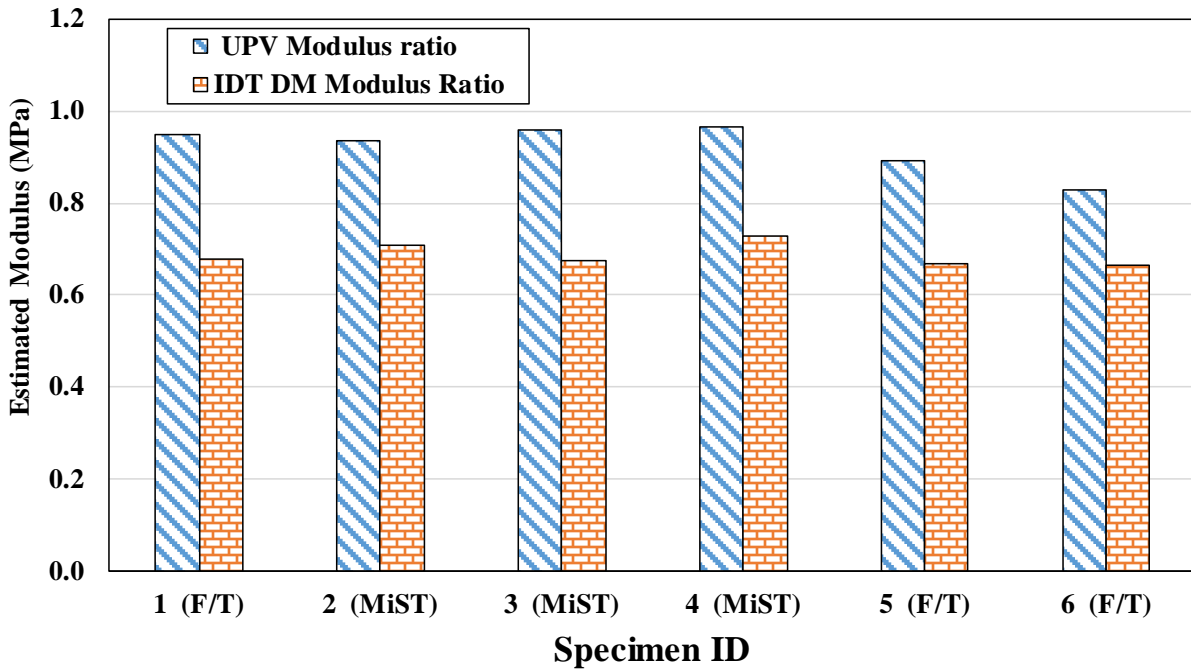


Table F-1 Summary of estimated compressional wave (p-wave) and shear wave (s-wave) velocities for the samples from the four aggregate sizes

Source	Sample ID	Before SSD		After SSD		After IDT 1		After Conditioning		After IDT 2	
		V_P (m/s)	V_S (m/s)	V_P (m/s)	V_S (m/s)	V_P (m/s)	V_S (m/s)	V_P (m/s)	V_S (m/s)	V_P (m/s)	V_S (m/s)
Menasha	MI1	3223.9	1436.5	3266.7	1433.0	3208.8	1373.9	3228.9	1373.9	3285.5	1319.4
	MI2	3229.7	1433.0	3229.1	1457.4	3224.1	1461.0	3210.8	1282.7	3193.1	1293.7
	MI3	3323.6	1422.8	3380.9	1475.4	3393.9	1436.5	3293.1	1380.2	3321.8	1316.5
	MI4	3276.2	1436.5	3341.8	1475.4	3279.5	1457.4	3190.6	1399.5	3195.7	1349.1
	MI5	3081.5	1380.2	3121.0	1358.3	3104.8	1334.1	3117.8	1222.4	3104.5	1200.4
	MI6	3322.7	1439.9	3368.0	1464.5	3326.7	1464.5	3296.7	1305.0	3261.6	1279.9
Olson	OI1	3560.7	1501.3	3606.0	1535.9	3619.9	1568.1	3535.1	1433.0	3545.3	1412.7
	OI2	3523.0	1505.0	3543.9	1539.8	3529.6	1520.3	3392.3	1367.6	3462.4	1406.1
	OI3	3370.1	1512.6	3397.9	1543.8	3420.3	1512.6	3307.7	1383.4	3281.7	1416.1
	OI4	3487.3	1539.8	3463.7	1564.0	3503.5	1508.8	3456.9	1535.9	3441.4	1468.1
	OI5	3591.4	1520.3	3572.9	1588.9	3633.3	1524.2	3483.1	1508.8	3530.9	1453.9
	OI6	3488.5	1539.8	3553.3	1580.5	3492.3	1547.8	3377.3	1443.4	3418.5	1446.9
Rock Springs	RI1	3547.4	1547.8	3503.9	1605.9	3489.0	1532.0	3393.2	1516.5	3377.3	1497.5
	RI2	3674.5	1632.2	3592.8	1641.1	3636.4	1627.7	3581.2	1524.2	3573.7	1532.0
	RI3	3492.2	1547.8	3515.2	1588.9	3546.7	1601.6	3424.9	1547.8	3439.4	1493.8
	RI4	3484.6	1580.5	3528.2	1614.6	3558.9	1584.7	3423.7	1516.5	3375.2	1497.5
	RI5	3497.7	1593.1	3542.0	1614.6	3588.7	1568.1	3385.3	1490.0	3445.1	1490.0
	RI6	3556.4	1618.9	3629.5	1636.6	3632.2	1605.9	3431.7	1524.2	3482.4	1493.8
Waukesha	WI1	3432.5	1479.0	3322.4	1512.6	3415.6	1512.6	3351.1	1399.5	3350.8	1393.0
	WI2	3445.3	1528.1	3437.6	1551.8	3428.1	1543.8	3360.1	1475.4	3437.2	1429.6
	WI3	3483.8	1475.4	3508.9	1532.0	3479.4	1516.5	3381.6	1436.5	3449.4	1389.8
	WI4	3488.0	1464.5	3516.1	1512.6	3466.6	1501.3	3466.7	1443.4	3426.1	1402.8
	WI5	3457.3	1501.3	3473.2	1520.3	3426.3	1493.8	3365.7	1399.5	3424.9	1380.2
	WI6	3405.3	1528.1	3424.1	1457.4	3416.2	1524.2	3424.3	1399.5	3414.0	1367.6